ISSN 0236-2945

LIGHT & ENGINEERING

Volume 27, Number 6, 2019

Editorial of Journal
"Light & Engineering" (Svetotekhnika), Moscow

The purpose and content of «Light & Engineering» is to develop the science of light within the framework of ray, photometric concepts and the application of results for a comfortable light environment, as well as for visual and non-visual light technologies, including medicine. The light engineering science is a field of science and technology and its subject is the development of methods for generation and spatial redistribution of optical radiation, as well as its conversion to other forms of energy and use for various purposes.

The scope of journal includes articles in the following areas:

- Sources of light;
- Light field theory;
- Photometry, colorimetry and radiometry of optical radiation;
- Visual and non-visual effects of radiation on humans;
- Control and regulation devices for light sources;
- Light devices, their design and production technology;
- Light devices for the efficient distribution and transportation of the light energy: hollow light guides, optical fibers;
- Lighting and irradiation installations;
- Light signaling and light communication;
- Light remote sensing;
- Mathematical modelling of light devices and installations;
- Energy savings in light installation;
- Innovative light design solutions;
- Photobiology, including problems of using light in medicine;
- Disinfection of premises, drinking water and smell elimination by UV radiation technology;
- Light transfer in the ocean, space and other mediums;
- Light and engineering marketing;
- Legal providing and regulation of energy effective lighting;
- Light conversion to other forms of energy;
- Standardization in field of lighting;
- Light in art and architecture design;
- Education in field of light and engineering.

Journal "Light & Engineering" had been founded by Prof. Julian B. Aizenberg in 1993

LIGHT & ENGINEERING

СВЕТОТЕХНИКА

Editorial of Journal "Light & Engineering/Svetotekhnika"

Moscow, 2019

Editorial Office:

Russia, VNISI, Rooms 327 and 334
106 Prospekt Mira, Moscow 129626

Tel: +7.495.682.26.54
Tel./Fax: +7.495.682.58.46
E-mail: lights-nr@inbox.ru
http://www.l-e-journal.com

Light & Engineering" is an international scientific Journal subscribed to by readers in many different countries. It is the English edition of the journal "Svetotekhnika" the oldest scientific publication in Russia, established in 1932.

Establishing the English edition "Light and Engineering" in 1993 allowed Russian illumination science to be presented the colleagues abroad. It attracted the attention of experts and a new generation of scientists from different countries to Russian domestic achievements in light and engineering science. It also introduced the results of international research and their industrial application on the Russian lighting market.

The scope of our publication is to present the most current results of fundamental research in the field of illumination science. This includes theoretical bases of light source development, physiological optics, lighting technology, photometry, colorimetry, radiometry and metrology, visual perception, health and hazard, energy efficiency, semiconductor sources of light and many others related directions. The journal also aims to cover the application illumination science in technology of light sources, lighting devices, lighting installations, control systems, standards, lighting art and design, and so on.

"Light & Engineering" is well known by its brand and design in the field of light and illumination. Each annual volume has six issues, with about 80–120 pages per issue. Each paper is reviewed by recognized world experts.

CONTENTS

VOLUME 27 NUMBER 6 2019

LIGHT & ENGINEERING

Light & Engineering
Vol. 27, No. 6, pp. 4–15, 2019 *https://doi.org/10.333383/2019-002*

STATUS OF LIGHTING TECHNOLOGIES IN NEPAL

Diwakar Bista[1,2], Ashish Shrestha[1,2], Georges Zissis[3], Pramod Bhusal[4], Frangiskos V. Topalis[5], and Bhupendra B. Chhetri[6]

[1]*Department of Electrical and Electronics Engineering, Kathmandu University, Nepal*
[2]*Center for Electric Power Engineering (CEPE), Kathmandu University, Nepal*
[3]*Laboratory of Plasma and Conversion of Energy (LAPLACE), Paul Sabatier University, Toulouse, France*
[4]*Aalto University, Department of Electrical Engineering and Automation, Finland*
[5]*National Technical University of Athens, Athens, Greece*
[6]*School of Engineering, Kathmandu University, Nepal*
E-mail: diwakarbista@ku.edu.np

ABSTRACT

Lighting is a thoughtful application of lighting source to get visibility and accomplish a specific task during the darkness by providing desirable illumination. In present context, there are numerous light sources and lighting technologies. But, with the advancement of technologies, traditional lighting technique is being gradually replaced by efficient lighting system with specific purpose and application. This study presents current status of lighting technologies, applications, challenges, policies and impacts in Nepalese scenario. This study also presents some statistic outcome, drawn from a survey of 250 sample size including different five target group. From this study, it is found that the people and government are moving toward the efficient and clean lighting technologies from traditional one. These activities on the implementation of efficient lighting technologies help the people in different sectors, such as education, health, security, economy etc., and in the improvement of living standard.

Keywords: lighting system, lighting design, lighting issues

1. INTRODUCTION

Light has a big role in the lives of all living beings. Starting from the food chain it contributes to provide all necessities required to live, such as nutrition, healthy atmosphere etc. Similarly, most of the living beings require light to see and conduct their routine tasks. In other words, light is a means to communicate in-between members of a group, and as such it is hard to survive without the presence of light [1]. From the ancient age, when people lived in caves and used fire as the source of light after blackout, the importance of lighting has increased day by day with the progression of human evolution. The light and lighting technologies, one of the routine amenities, affects human living profoundly. With the development of electric lighting, the lighting approach has become easier and initiate numerous scopes and applications [2]. Nowadays, lighting has become an essential kit in human's perception on their life style. In-house lighting helps in conducting the regular tasks and improve the effectively during night. But in current context, it is used for other special aspects of room's interior designing, work space etc., and provides opportunities to set ideal working environment [3]. Like fresh food, air and other necessities, good illumina-

a) *b)*

Fig.1. People using fuel-based lighting for study, cooking and other activities [5,6]

tion helps to improve the health, self-empower, and efficiency of individuals [2].

In this study, the current status of lighting technologies, scopes, impacts etc. in Nepalese scenario are discussed. It is mainly focused on the current practices, implementation of illumination engineering in different sectors of Nepal. Also, the impacts of lighting system in people's daily lives have been discussed. This study first introduces the issues and importance of lighting in human life. Section 2 presents the overview of lighting technologies existing in Nepalese market and their applicable areas. Section 3 presents the governmental policies and the standard related with lighting and renewable energy technologies in brief. In section 4, requirements and effects after implementation of lighting technologies in rural and urban communities of Nepal has been discussed. Section 5 presents some data on current practice and consumer's perceptions. Finally, in section 6, conclusions have been drawn and presented.

2. OVERVIEW OF LIGHTING TECHNOLOGIES AND SCOPE

The use of light and the lighting system began in ancient age in Nepal similar to the rest of the world, when the ancient people used fire as a light source. Later, people used fuel-based inflammable (fossil fuelled) lighting system. This type of lamps was made up of metallic bottle body, and fuelled with animal and/or vegetable fats. Currently, the modified version of this lamp is used in the rural community of Nepal, where the lamps are made up of metallic can or glass body, and fuelled with a petroleum product such as kerosene, diesel, bio-oil etc. The candle is another type of flamable lighting technology. Fig.1 (a, b) show the samples of tradetional lamp (tukki in local language) used in rural Nepal. As per the data provided by Central Bureau of Statistics (CBS) in 2011, 67.26 % (94.11 % in urban and 60.84 % in rural) of household uses electricity as the source of lighting and 18.28 % (4.04 % in urban and 21.68 % in rural) of household uses kerosene as the source of lighting. Other types of sources are negligible in the case of urban area, but in rural area, 0.26 % of household uses biogas, 9.16 % uses solar and 7.41 % uses other sources for lighting [4].

In the modern age, people are using different types of lighting technologies as per their comfort. The trend of change in lighting technologies and their source type can be observed in Fig. 2. In 2001, kerosene was the major source of lightning, where

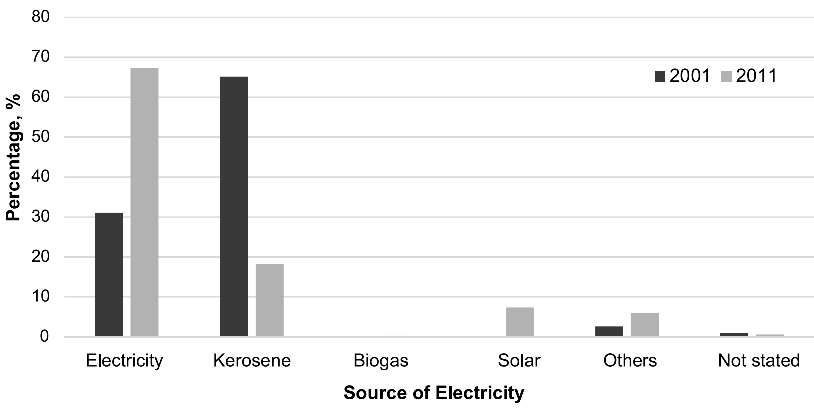

Fig. 2. Percentage of household using different sources of lighting in 2001 and 2011 AD [4]

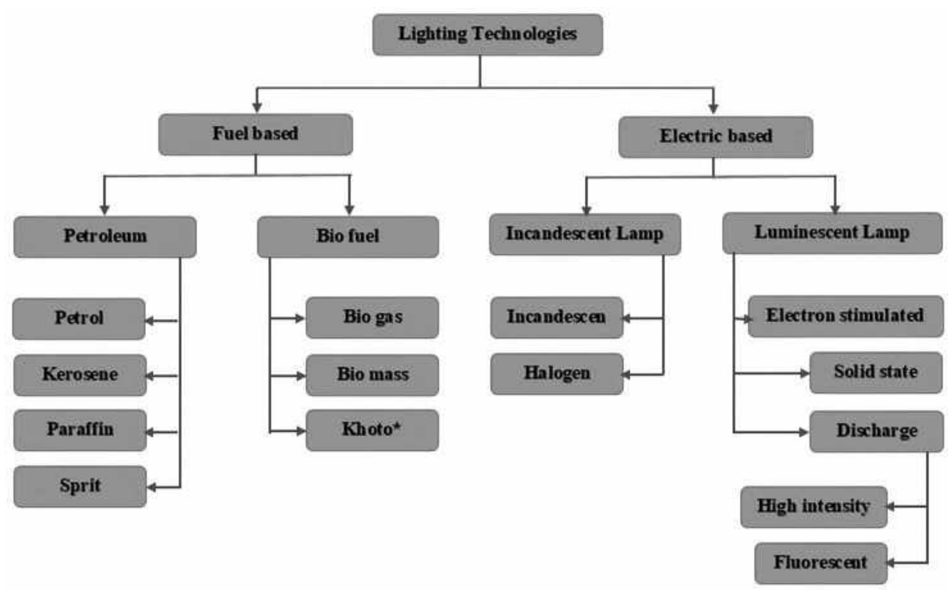

Fig. 3. Source and lighting technologies adopted in Nepal (* Khoto is the local name of turpentine extracted from pine resin)

as in 2011, electric lighting technologies covered the major proportion. In the past decade, the incandescent lamps were very popular in major cities where electricity supply was available. But in present context they are only found in some remote area due to lack of awareness, and in some hotels and museums because of their high colour rendering ability and warmth. Fluorescent lamps are one of the popular types of lighting scheme in the Nepalese market, because of its efficiency, and are found in commercialized buildings as well. The major proportion of indoor and outdoor lighting in the present context is covered with compact fluorescent lamps (CFLs) and light emitting diode (LED), whereas halogen lamps are very popular for flood lighting. Over time, different shaped and coloured lighting technologies are available in the market for specific applications. The general overview of different lighting technologies and the fuels adopted in Nepal is shown in Fig. 3. Some of the important applications of lighting noticed in Nepal are discussed below.

2.1. Indoor Lighting

Lighting is the thoughtful application of light to accomplish a specific task during the darkness by providing desirable illumination. The major requirement of lighting is aiding in in-house activities such as in home, office, industries, underground parking, shops, malls, hotels, restaurants, museums etc., and the major objectives are to provide desirable lighting and improve attractiveness of space and objects. Lighting has different provisions and purposes as per their applications, and can also be an essential component of living. Household use normal lighting to conduct their activities during night time, and the illumination design and varieties may differ as per the specific functional requirements, whereas the industries, shop and hotel use the lighting design with specific characteristics to meet their requirements. Based on the purpose, the illumination level, intensity, diffusion types and forms of lighting vary. Fig. 4 (a) shows the indoor lighting utilized in ho-

a) *b)*

Fig. 4. Lighting system in hotel/ restaurant (a), and in museums (b) to highlight the ancient objects

Fig. 5. Lighting system used in heritage sites of Nepal

tels to provide attractive environment with desirable illuminations, and Fig. 4 (b) shows the lighting system used in museums to highlight the ancient objects.

2.2. Street and Road Lighting

Over the last decade, the street and road lighting have been blooming and is being implemented as one of the fundamental requirements in the growing cities of Nepal. In the past, most of the streets and roads were being lighted by utility based incandescent lamps, which were later replaced by fluorescent lamps. With the advancement of technologies, the previous lighting techniques are being replaced by solar-based isolated lighting system containing white light emitting diodes (WLED). The configuration of solar street light system must be designed to be robust and must be good enough to withstand the harsh environmental condition. The solar street lighting installation shall not damage aesthetic of the existing city or street plan; rather it shall add beauty to the existing roadway. The main objectives of the road and street lighting are to provide brighter light during the night and improve the road and street conditions as well as to minimize the security issues such as sexual harassment, theft, accident etc. Further, it helps to increase the active working period of the people resulting in positive contribution to the nation's economy.

2.3. Heritage Lighting

Currently, state-of-the-art lighting systems have been used to present and express the culture and history of Nepal highlighting their existence and importance, Fig.5.

Different lighting designs have been introduced on the cultural heritage site via the development of variety of concepts and materials. One of the major contributors in Nepal's economy is the tourism industry. Nepal has a wide cultural and natural diversity that attracts tourists from all over the world. Apart from international tourists, domestic tourism also contributes largely to the tourism associated economy. The major tourist attractions of Nepal are natural beauties, biodiversity, adventure activities, trekking and mountaineering in the mid-hill to high mountains, and diverse heritage area present across the country. Focused on the heritage sites, the major cities of Nepal are very rich and attracts tourist from all over the world. Unfortunately, most of the tourist attractions or tourist residing vicinities seem to be improperly and inadequately lighted. In the present context, there are no facilities to visit the heritage site at night due to the absence of illumination. Even in the important and popular heritage sites, there are no lighting mechanisms, nor are there proper illuminating systems. This has hindered the heritages' beauty and shortened the visiting duration of tourists. Fig. 5 show some of the existing lightings at the heritage site of Bhaktapur and Kathmandu, Nepal, which are not properly designed. Recently, concerned people have been working at few important sites (Tripura Sundari Temple, Patan Durbar Square site and Bhaktapur Durbar Square site) on illumination task to increase their beauty during dark, and bolster the tourist flow at night period, thus increasing the economic activities there as well.

Table 1. Types of Solar Street Lighting Adopted in Nepal [11]

Type	Lamp power, W	Min. peak PV module power, W	Min. battery capacity for Lead, Ah	Min. battery capacity for Lithium, Ah	Min. charge controller, A	Pole height, m	Right of way, m
Type 1	10	50	40	30	5	7	< 4
Type 2	20	100	60	45	10	7	4–6
Type 3	30	150	80	60	12	7	6–10
Type 4	40	200	100	75	15	8/ 9	10–14
Type 5	60	300	150	115	25	8/9	14–20
Type 6	80	400	200	150	30	10	20–30
Type 7	100	500	250	180	40	10	> 30

2.4. Automotive Lighting

Automotive lighting includes the lamps used in--front (headlights) and back-front (tail lights) of the vehicle to provide the necessary illuminations during traveling at night. The vehicle also includes some specific lighting system for a specific task such as an indication of different parameters, illumination of the interior part, decoration etc. In most of the modern vehicles, the lighting is replaced with LED technologies. Basically, two types of front lights are available in Nepalese vehicles: white and yellow (basically halogen, Xenon and/ or LED types); white for normal condition, whereas yellow for foggy environments. Similarly, red and white lamps are present in back-front; red for breaking indication and white for illuminating the upcoming status during the back-mode operation. LEDs today are mainly used for secondary functions such as dashboard lighting, turn signals and side-markers of the vehicles, but with the development in high brightness LED, they are now also being used as headlamp in automobile.

2.5. Other

Although spending on digital approaching, different sectors have been escalating at the expenditure of traditional techniques. Today's digital advertisement is one of the major examples of lighting application. Majority of spaces in big cities and highways are displayed with some big advertisements. Similarly, with the increase of traffic flow, automated traffic lights are used in most of the busy centres, digital noticeboard are placed in-front of institutions, digital information boards are showing the contents etc. These are all some of the major applications of lighting system follow in Nepal. There are various other applications like machine vision lighting, lighting for medical and dental observation, lighting in indoor sport hall and stadium, phototherapy lighting, marine, portable torch lights and airport signalling etc. The application field is no doubt going to increase because lights are now being used in all areas and have become one of the fundamental demands in human life.

3. POLICIES AND INCENTIVES

In Nepal, there is no clear policy on lighting technologies directly, although some incentives on clean energy associated with lighting existed. A standalone solar photovoltaic street lighting system is an outdoor lighting unit used for illuminating a street or an open area. The PV powered street light utilizing LED has become a wide spread practice. Alternative Energy Promotion Centre (AEPC) in collaboration with different municipalities has been installing Solar Power LED Street Light with specific purpose. AEPC provide subsidy to renewable energy based technologies to secure the socio-economic development of communities by utilizing the available natural resources with best technology. It is expected to provide 40 % of subsidy in total cost of the solar based energy system in metro and sub-metro municipality, where 30 % cost will be covered by the beneficiaries and 30 % coming from credit [7]. Similarly, 70 % of project cost is subsidized in the rural municipality and 60 % in the municipality by AEPC [7,8]. As per the data provided by AEPC, in the fiscal years of 2016/17, 2017/18 and 2018/19, a total of 1622, 1357 and 1060 street light systems are implemented under AEPC in different communities all over the

Table 2. Technical Specification of Solar PV Module [11]

Description	Specification
Module capacity	Capacity must be selected as per type of solar street light
Module type	Mono or Poly Crystalline or Thin Film
Operating voltage w.r.t. output power	Crystalline: 34Vmp for each 24V and 17 Vmp for each 12V module Thin Film: At least 40 % higher than system voltage
Min. module efficiency	Crystalline: 14 % Thin Film: 10 %
Junction box	IP 65 or above
Tilt angle and Direction	Towards due south around local latitude
Fasteners	Stainless Steel or Hot deep Galvanized
Design standards	IEC61215, IEC61646
Safety standard	IEC61730
Certification	RETS Certified

countries. The specified specification and types of solar street light supported by AEPC is listed in Table 1, and that of solar PV module is presented in Table 2. On the other hand, Nepal Electricity Authority (NEA) had installed 1600 street light with lamps of 30W, 40W and 60W within Kathmandu Valley at various locations. Some innovative concepts that links business and lighting just implementing, in which private company owned street lighting system with advertisement display as source of revenue. In past few years, more than 2000 lamps of 30W and 40W had been installed in such business oriented concept. Further, different NGOs and INGOs are providing small scale solar system, lantern and torch light for the rural communities untouched with national grid.

NEA had launched an energy efficient lighting project to decrease the application of incandescent lamps. In 2014, this program distributed 750,000 efficient CFL in the support of Asian Development Bank (ADB) in different part of the country [9]. NEA also conducted an awareness campaign “Bright Nepal, Prosperous Nepal”, focused on the proper demand side management by displacing the inefficient incandescent lamps by LED, so that the peak demand can be clipped by a certain amount [10].

As per the registered data provided by Renewable Energy Test Station (RETS), 5218 samples of WLED with different ratings have been tested within the last 5 years, and more than 2,568,222 lamps were approved for sale. Among these 5 years, the highest numbers of WLED were imported in 2014 AD. The required specification of lighting sources (LEDs) is given in Table 3. Nepal Academy of Science and Technology (NAST) is also working to develop a testing and standardization section in Nepal, so that the product imported from other countries or developed within the country can be monitored and maintain the quality.

In addition, informative audio and visual materials on energy efficient lighting are disseminated through televisions, radios and newspapers. Big hotels and commercial buildings, government organization are using CFL or LED lamps, and have occupancy sensors to promote the energy efficient lighting programs. Proper training for the use of energy efficient lighting and courses at universities are delivered to speed up the energy efficient lighting initiatives.

4. SOCIO-ECONOMIC IMPACT OF THE LIGHTING SYSTEM

More than 9.3 % of Nepalese population (22.513 % rural and 3.1 % urban) are out of reach of electricity, and even the people connected with the national grid are unable to get reliable and sufficient electricity supply [12]. One of the main reason behind it is the mountainous geography of the country, where more than 60 % of the population are living in the hilly area, where it is quite difficult to transmit the electricity through the national grid [9,13]. These people are forced to use fuel-based lighting system leaving female and children in danger. The energy sources are techno-e-

Table 3. Technical Specification of Lighting Sources for Street Lighting [11]

Description	Specification
Type	Light Emitting Diode (LED)
LED light source	The capacity of light must be selected as per the type of solar street light
Luminous efficacy	≥ 100 lm/W
LED illumination	Street lamp should have illumination not less than 0.5 lx/W perpendiculars from the height of 9 m. The illumination should be uniform without dark rashes on the ground
View angle	Equal or greater than 2 * 50 angular degree
Colour Rendering Index (CRI)	CRI of individual WLED must not be less than 60 and the correlated colour temperature must be in the range of (5000–6000) K
Lamp Rated Total Power	The capacity of light capacity must be selected as per the type of solar street light
Control Function	Must have Automatic dusk to dawn function. Also include at least two stage of dimming function. First stage-system should function at 100 % load for six hours and second stage: system should function at 50 % load for next 6 hours
Driver Circuit	Must have Driver circuit Charge Controller with not less than 85 % efficiency
Protection	The lamp must be protected against reverse polarity
Certification	Must submit IP65 or above Compliance Certificate and RETS Certified
Expected Life	Minimum 50,000 hours

conomically as well as environmentally unfeasible to human life. Improved technologies should be interfaced to reduce the cost and the emission produced from the system, which will have a significant impact on the targeted group as well as the host countries. Different techniques and pilot projects have been installed in recent years to provide access to clean energy to the targeted groups for their sustainable development pertaining to health, education, security, economic activities, etc. Solar lanterns, small-scale solar system, solar street lights, community-based distributed energy systems, and grid-connected lighting systems are some of the examples of the initiatives of the energy providing system. It is assumed that such technologies help them to light their household and residence area after dusk, and increase their effective working hours. Based on this assumption, the relief activity is focused on the product-based research and implementation of foreign products, which provide an immediate solution, but not sustainable. Similarly, such type of energy system is not techno-economically feasible for the middle-long period. Further, in an urban area the lighting system has important impacts on service mains, security issues, economic activities and promotional activities of cultural heritage and business-oriented components. The detailed impacts and role of the lighting system in socio-economic advancement of the people are explained below.

4.1. Impact of the Lighting System in Rural Nepal

A big proportion of rural Nepalese population is using the conventional source of lighting such as fossil fuel, biomass etc. which are not clean, sustainable, and techno-economically unfeasible, leaving female and children in danger [14]. Most of the developing countries including Nepal face a big challenge in education, health, security and economic activities because of those unreliable energy supply. People are forced to use conventional fuel sources to increase their active working hour per day [15]. The people now attempt to conduct their daily work activities such as cooking and other works associated with rural home, and children attempt to conduct their academic activities with the help of small kerosene lamps, solar lanterns or other proper lighting systems in the grid-connected area to provide proper lighting [15]. Fig. 1 shows the situations, where people are dependent on the fuel-based lighting technologies. Beside the difficulties to conduct the task and comfort zone for specific age group (to study for children, cooking for adult, and other basic activities for all), using conventional fuel source for lighting has various impacts on the human health, such as pneumonia, stroke, ischemic heart disease, chronic obstructive pulmonary disease (COPD), lung cancer [16]. Most of the traditional lighting lamps are responsible for dangerous and toxic impurities in environment that are in the range of values higher than the standard of World Health Organization (WHO) guideline. It is reported that, there may be unique emissions or hazards from wicks as well from some of the lighting fuels made with lead cores and lantern mantles with radioactive thorium [17]. In the study [18], it is found that the chance of Nepalese women using kerosene to get TB was nine times greater than those using electric light. Among all age groups, female and children are in higher risk of danger, since they spend majority of their time performing in indoor activities [17]. Similarly, use traditional lighting contributes to a number of accidental events such as fire hazard for non-electric domestic appliances. It is reported that, the burns are the second most (5 % of overall disabilities) common injury in rural Nepal, where 20 % of the cases in a total of 237 burn accidents were caused from the fire hazard via traditional lamp accidents [19, 20]. These burn cases lead physical as well as financial disadvantages to the people of Nepal, since it damages the public health, houses, industries, farms etc. Sexual harassment during the night in the absence of proper lighting, cases of theft, wild animal attack, and snake bite are some major issues occurred in the rural area [13].

The government of Nepal, with the assistance of different development bodies has been working to provide electricity access, so that the people are being safe from the problems associated with the fuel-based lighting technologies. It is assumed that the under-developing strategy on lighting technology helps to improve the education, health, security, economic factors in rural communities in Nepal [21]. A study stated that, the health-related issues can be significantly reduced by replacing the fuel-based lighting system by clean renewable energy system [18]. An empirical study [22], reported the health and safety problems of 500 households associated with a fuel-based lighting system and the relief response after replacing them with the solar system. The health and injury issues of kerosene lanterns were completely eliminated with the displacement of kerosene lamp. Similarly, the implementation of renewable energy based lighting system helps to improve the education of rural area by providing the comfort as well as allowing practice of the latest methodologies of teaching via the Internet, computer, projector, printer, photocopy etc. [18]. On the other hand, the intervention of lighting system helps to increase the economy of the rural community by increasing their daily active hours as well as by providing much-needed energy that powers local industries [23]. Further, in the presence of a proper lighting system, the rate of sexual harassment, theft, wild animal attack has been reduced significantly.

4.2. Impacts of the Lighting System in Urban Nepal

Although only 3.1 % of the urban population is unreached to the electricity supply, proper lighting plays important role in their daily life [12]. Basically, the lighting is associated with the education, safety, cultural and economic activities in urban reason. Proper lighting in the streets or squares and facilities such as restaurants, shops, hotels, monuments, etc. definitely would be liked by the tourists and should contribute to the tourism economy greatly. The total contribution of travel and tourism in gross domestic product (GDP) of Nepal was 7.8 % in 2017 with 1.02 million job creation [24]. Attractive lights at the restaurants results in increased preference to dine there, and proper lighting at monuments and heritage sites means enhanced beauty and more visitors. Similarly, proper lighting at the shops means customers have a better view of goods at the display and a better chance of buying, etc. It also helps to increase the people's activity at night increasing the efficiency and economy of people. Proper lighting at the streets or pathways and squares means increased sense of security and tendency to spend more time there, and further helps to reduce the crime significantly. Sexual harassment is one of the big risk for females, and also supposed to be disturbingly dominant in the cities around the world [25]. Figs 4 and 5 can define the positive impacts of lighting on the public lifestyle and the communities in urban Nepal.

5. CURRENT PRACTICES ON LIGHTING

As per the report [26], 43.50 % of energy was consumed by domestic, 3.11 % by non-commercial, 7.38 % by commercial, 37.53 % by industrial, 8.43 % by others and 0.05 % was exported to India in 2018. Those data show that majority of Nepalese electricity is consumed due to residential loads. As per the load data of NEA, the peak de-

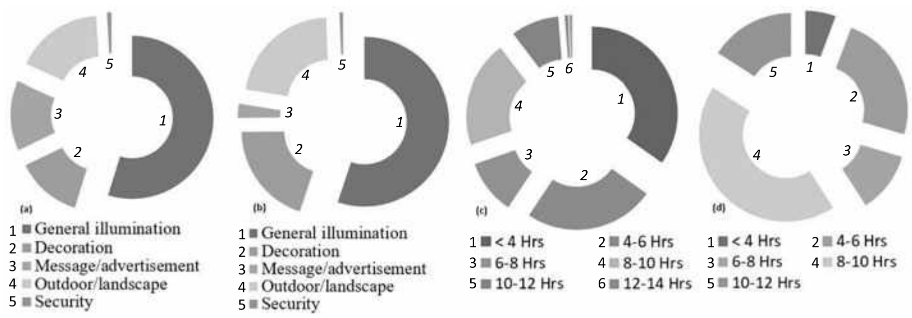

Fig. 6. Purpose of artificial lighting at workspace and residence (a, b); hours of use of artificial lighting at workspace and residence (c, d)

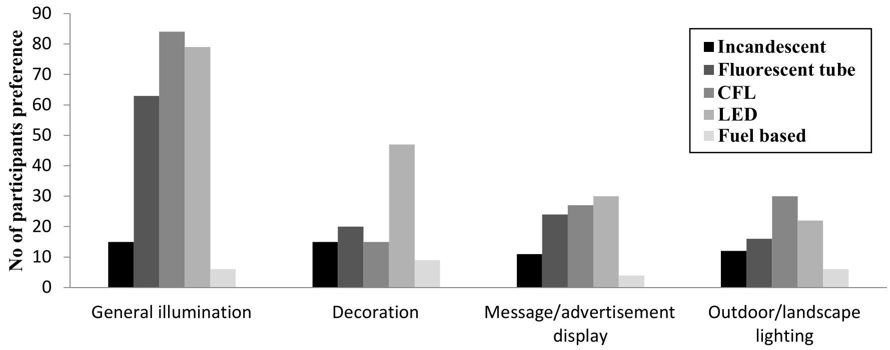

Fig. 7. Types of luminaries being used for various purposes

mand of electricity in Nepal occurred at evening hours and lighting has a major impact [26]. A study showed that about 60 % energy used in Kathmandu can be saved by using LED lamps [27]. Thus, the energy efficient lighting is considered to be preferred to maintain the demand and supply ratio. A team including the authors conducted a survey on necessity of lighting education by developing the questionnaires for different five groups: employers, university graduates, students, teachers and consumers [28]. The survey includes 250 samples (20 employers, 30 graduates, 98 students, 57 teachers and 45 consumers) from different groups. From the survey it was found that all types of participant use artificial lighting either at workspace or home for general illumination along with some other purposes depending upon their need. The digit for application of artificial lighting for workplace and residence are presented in Fig. 6 (a, b), showing the proportions of various habits of artificial lighting. The use proportion of lighting for general purpose is more than 50 % in both of the cases, and that for security and message/advertisement is very less. Similarly, the hours of use of artificial lighting at workplace and residence are depicted in Fig. 6 (c, d), presenting most of the participants are using lighting for more than 8 hours at residence, while that was less than 6 hours at workplace for general purpose lighting.

In current scenario, various types of luminaries are used in the Nepal's market and users have their own preferences as per the cost, purpose of use and efficiency. CFL is more dominant in the Nepal compared to incandescent lamp, fluorescent tube lamp, LED lamps or others. Fig. 7 presents the different types of luminaries being used for various purposes by the participants. For general purpose LED lamps, CFLs and fluorescent tube lamps are used in equal proportions throughout Nepal. For decoration and display, LED lamps are being used significantly high now days compared to other lamps, and for outdoor or landscape lighting CFL and LED lamps are being preferred. The major challenges in adoption of efficient lighting are found to be lack of knowledge and awareness, lack of skilled manpower, high initial cost and low quality of available product within the market. As shown in Fig. 8(a), the participants claimed that the lack of knowledge and high initial cost of efficient technologies are the main challenges in the adoption of efficient lighting technologies. During the survey, most of the participants were found to be familiar with efficient lighting technologies, where 72 % of the graduates and 97 % of teachers stated that they were aware of energy efficient lighting management. Fig. 8(b) shows that 63 % of the participants in the survey prefer LED lamps among all the luminaries available, whereas, Fig. 8(c) presents the reasons of preference of luminaries by the different participants; 25 % of participants prefer high efficiency luminaries, 28 % prefer luminaries with longer life and 21 % participants prefer luminaries of least cost.

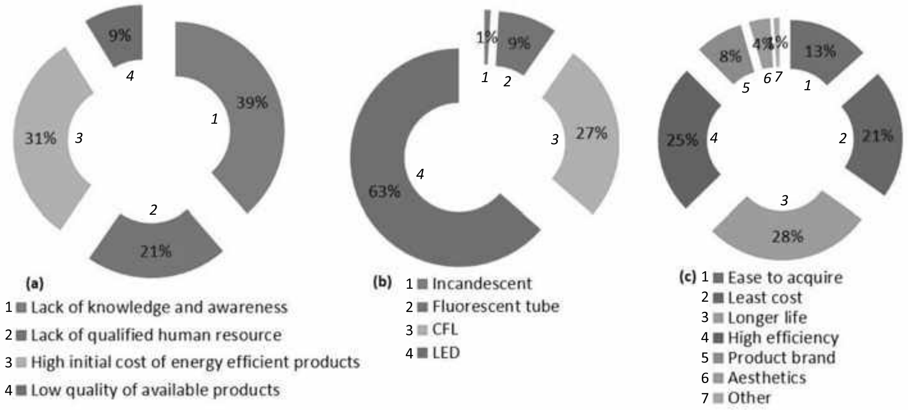

Fig. 8. Challenges of adaptation of energy efficient lighting (a), preference of luminaries for lighting (b), and reasons for preference of luminaries for lighting (c)

6. CONCLUSION

The demand of electrical power is increasing day to day and the supply requirement in most of the developing country cannot be met due to the high capital cost of generation and transmission. Lighting is one of the major loads for residential sector and contributes for the peak demand in the evening hours for most of the developing countries like Nepal. The use of energy efficient lighting would help to decrease the electrical power demand and would thus help to minimize the difference between demand and supply of electrical power. Lighting in most of the residential as well as commercial buildings use incandescent lamps, or florescent tube lamps which are less efficient compared to the today available CFLs and LEDs. Despite of several initiatives form the government, the use of inefficient lamp has not stopped. The quality of LED lamps available, high initial cost of efficient product and the lack of awareness in users are the major drawbacks.

Energy efficient lighting is concerned with the use of luminaries which consumes less energy and which has high efficiency compared to other luminaries available. These lighting maintains the lighting quality with less power consumption. Hence, the people and government are moving toward the efficient and clean lighting technologies from traditional one. The implementation of efficient and clean lighting technologies helps the people to improve their living standards.

ACKNOWLEDGMENT

This study is supported by the Centre for Electric Power Engineering, Kathmandu University under the funding of Royal Norwegian Embassy at Nepal, and ELNAB Project co-funded by the Erasmus+ programme of the European Union. The authors would like to acknowledge Mr. Bashanta Dhakal and Mr. Madan Oli from RETS, Chaitanya P. Chaudhary from AEPC for their kind support during the data collection required in this study. The author also thankful to the Ministry of Finance, Nepal, Mr. Ramesh Maharjan and Mr. Kshitiz Khanal for their kind support during the whole period of this study.

REFERENCES

1. Reference*. *Why Is Light so Important to Us?* Available: https://www.reference.com/science/light-important-38b176ddab4c448c

2. NREL, "Vision 2020 The Lighting Technology Roadmap," in "A 20-year Industry Plan for Lighting Technology," U.S. DEPARTMENT OF ENERGY FOR MORE INFORMATION, United State2018, Available: https://www.nrel.gov/docs/fy00osti/27996.pdf.

3. ANJ. (2018). *Importance of Lighting*. Available: https://anj.co.in/idea-at-anj/importance-of-lighting/

4. CBS, "National Population and Housing Census 2011 (National Report)," Central Bureau of Statistics, Government of Nepal, Kathmandu, Nepal2011, Available: https://unstats.un.org/unsd/demographic-social/census/documents/Nepal/Nepal-Census-2011-Vol1.pdf.

5. A. Vagianos and D. Hahlen. (2016, December 30). *50 Captivating Photos of Girls Going to School Around the World: Gender should not be a factor in education* Available: https://www.huffingtonpost.com/entry/50-captivating-photos-of-girls-going-to-school-around-the-world_us_56d61a7de4b0871f60ed1fce

6. "Leaf-nosed bat," in *Encyclopædia Britannica*, ed: Encyclopædia Britannica Online, 2009.

7. AEPC, "Urban Solar Energy System & Soft Loan Operation Manual," in "Urban Solar Energy System Subsidy and Loan Mobilization Directives-2072," Ministry of Science, Technology and Environment, Lalitpur, Nepal2016, Available: https://www.aepc.gov.np/urbansolar/downloadfile/URBAN%20SOLAR%20ENERGY%20

SYSTEM%20&%20SOFT%20LOAN%20OPERATIONAL%20MANUAL_1467103507.pdf.

8. AEPC, "Renewable Energy Subsidy Policy, 2073 BS (Unofficial translation)," Ministry of Population and Environment, Lalitpur, Nepal2016, Available: https://www.aepc.gov.np/uploads/docs/2018–06–19_RE%20 Subsidy%20Policy,%202073 %20(English).pdf.

9. NEA, "Annual Report," Nepal Electricity Authority, Kathmandu, Nepal2017, Available: file:///C:/Users/user/Downloads/87757284.pdf.

10. NEA, "Terms of Reference for Promotion of High Efficiency Light Emitting Diode (LED) Lamps ", ed. Kathmandu, Nepal: Nepal Electricity Authority, 2015.

11. AEPC, "Technical Guideline for Solar Street Light Project," in "Technical Specification," Alternative Energy Promotion Center, Lalitpur, Nepal2018, Available: https://www.aepc.gov.np/uploads/docs/2018–06–19_Technical%20Standard%20for%20Solar%20Street%20Light%20System,%202072.pdf.

12. SE4ALL. (2018). *Access to electricity (% of population)*. Available: https://data.worldbank.org/indicator/EG.ELC.ACCS.UR.ZS

13. B. Raj Upreti, S. KC, R. Mallett, and B. Babajanian, "Livelihoods, basic services and social protection in Nepal," Nepal Center of Contemporary Research, 111 Westminster Bridge Road, London, UK2012, Available: https://www.odi.org/sites/odi.org.uk/files/odi-assets/publications-opinion-files/7784.pdf.

14. H. Kobayashi, H. Zhang, P. Manandhar, A. Jude, and K. Yokoyama, "NEPAL ENERGY SECTOR ASSESSMENT, STRATEGY, AND ROAD MAP," Asian Development Bank, 6 ADB Avenue, Mandaluyong City, 1550 Metro Manila, Philippines2017, Available: https://www.adb.org/sites/default/files/publication/356466/nepal-energy-assessment-road-map.pdf.

15.] N. Shrestha, "Enabling children to study after sunset," in "Nepal: Light for Hope," SUMAR- LAKHANI FOUNDATION: FOSTERING UNIQUE VISIONS TO TACKLES THE WORLD'S TOUGHEST PROBLEMS2017, Available: http://www.sumarlakhanifoundation.org/nepal-solar-lamps/.

16. WHO. (2018, December 30). *Household air pollution and health*. Available: https://www.who.int/news-room/fact-sheets/detail/household-air-pollution-and-health

17. J. Seftel, "Profile: Irene Pepperberg & Alex," in *NOVA Science Video Podcast*, N. d. G. Tyson, Ed., ed. Boston: WGBH, 2011.

18. E. Mills, "Health impacts of fuel-based lighting," in *3rd International Off-Grid Lighting Conference, Dakar, Senegal*, 2012, pp. 13–15.

19.] E. Liu, B. Khatri, Y. Shakya, and B. Richard, "A 3 year prospective audit of burns patients treated at the Western Regional Hospital of Nepal," *Burns,* vol. 24, no. 2, pp. 129–133, 1998.

20. C. Mock *et al.*, "A WHO Plan for Burn Prevention and Care," Geneva, Switzerland 2018, Available: http://apps.who.int/iris/bitstream/handle/10665/97852/9789241596299_eng.pdf; jsessionid=E347ED36E3460C39E41BED35CCB5A936?sequence=1.

21. A. Sapkota, Z. Lu, H. Yang, and J. Wang, "Role of renewable energy technologies in rural communities' adaptation to climate change in Nepal," *Renewable Energy,* vol. 68, pp. 793–800, 2014.

22. S. Thatcher, "An empirical Study into the benefits of relieving energy poverty in the developing world," *2pp. Retrieved from http://www. pfpi. org/pdf/empiricalStudy_energy_poverty. pdf [Accessed July 23, 2014], plus data files (personal communication,* 2012.

23. U. Basnet. (2014, December 30). *Renewable Energy Powers Rural Nepal Into the Future*. Available: http://www.worldbank.org/en/news/feature/2014/02/05/renewable-energy-powers-rural-nepal-into-the-future

24. R. Turner, "Travel & Tourism Economic Impact 2018: Nepal," in "Travel & Tourism Economic Impact 2018," World Travel & Tourism Council2018, Available: https://www.wttc.org/-/media/files/reports/economic-impact-research/countries-2018/nepal2018.pdf.

25. "EXPERT SURVEY: GIRLS' SAFETY IN CITIES ACROSS THE WORLD," Plan international2018, Available: https://plan-international.org/publications/expert-survey-girls-safety-cities#download-options.

26. NEA, "NEA Annual Report 2074/75," in "NEA Annual Report," Nepal Electricity Authority, Kathmandu2018, Available: http://www.nea.org.np/annual_report.

27. S. R. Timilsina and S.R. Shakya, "The Status of Energy Efficient Bulbs and the Potential Energy Savings in the Kathmandu Valley," presented at the IOE Graduate Conference, Pulchowk, Lalitpur, 2013. Available: http://conference.ioe.edu.np/ioegc2014/papers/IOE-CONF-2014–57.pdf

28. ELNAB, "National Need Assessment Report Nepal," Kathmandu University, Nepal Engineering College and Sagarmatha Engineering College2017.

Divakar Bista,

M. Sc. He graduated from Katmandu University, Nepal, in 2005. At present, he is Assistant Professor and Head of the Chair at the same university. His scientific interests are the control systems, in-door and out-door LED illumination, photoelectrical lighting systems

Ashish Shrestha,
M. Sc. He graduated from School of Engineering, Kathmandu University, Nepal in 2014. At present, he is a lecture at the same university. His scientific interests are design and exploitation of energy systems, renewable energy sources, energy installations

Georges Zissis,
Ph.D**.** He has graduated in 1986 from Physics department of University of Crete in general physics. He got his M. Sc. and Ph.D. in Plasma Science in 1987 and 1990 from Toulouse 3 University (France). He is today full Professor in Toulouse 3 University (France). His primary area of work is in the field of Light Sources Science and Technology. He is especially interested in the physics of electrical discharges used as light sources; system and metrology issues for solid-state lighting systems; normalization and quality issues for light sources; impact of lighting to energy, environment, quality of life, health and security; interaction between light source and associated power supply; illumination and lighting. He is director of "Light & Matter" research group of LAPLACE that enrols 20 researchers. He won in December 2006 the 1st Award of the International Electrotechnical Committee (IEC) Centenary Challenge for his work on normalization for urban lighting systems (in conjunction with IEEE, IET and the Observer). In 2009, he won the Energy Globe Award for France and he got the Fresnel Medal from the French Illuminating Engineering Society. In 2011, he has been named Professor Honoris Causa at Saint Petersburg State University (Russian Federation) and he is President IEEE Industrial Application Society for the period 2019–2020

Promod Bhusal,
Dr. of Sc. He graduated from Kathmandu University, Nepal in 2000. At present, he is in staff of Aalto University in Finland

Frangiskos V. Topalis,
Dipl. Eng, Ph.D. He has got degree in mechanical and electrical engineering from the National Technical University of Athens in 1979 and the Ph. D. degree in 1990. At present, he is the Professor at the School of Electrical and Computer Engineering of the National Technical University of Athens (NTUA). His scientific interests are illumination design, rational energy use in buildings

Bhupendra Bimal Chhetri,
D. Eng. He has graduated from Kyushu Institute of Technology, Japan, as a post graduate student in 2003. At present, he is Visiting Professor at Kathmandu University. His scientific interests are optical communication, lighting, renewable energy sources, and holography

Light & Engineering
Vol. 27, No. 6, pp. 16–26, 2019 *https://doi.org/10.33383/2018-079*

RENEWING STREET LIGHTING WITH LED TECHNOLOGY: A SINGLE CASE STUDY IN CASARABONELA

Rosa María Morillas and José Ramón de Andrés

School of Industrial Engineering, Universidad de Málaga, Spain
E-mails: rmmorillas@uma.es; deandres@ctima.uma.es

ABSTRACT

In 2015, the ecological, economic and social necessity of increasing energy efficiency contributed to street lighting renewal in the Spanish municipality of Casarabonela. Considering fixed operating and maintenance costs, it was a significant, long term investment with high impact for the community. Technicians chose LED light sources after studying technical and economic proposals submitted. Measurements of light levels, energy consumption and costs were carried out before and after the renovation. Once the chosen proposal was implemented, follow up surveys from technicians, maintenance workers and final users were collected. This case study aims to describe steps taken in the process of luminaires replacement. It has been estimated savings, expected and actual together with the return period on investment. This case may well serve as a prototype for a subsequent multiple case study which aims to validate a list of indicators obtained in a previous research.

Highlights:

- When valuing a luminaire, there may not be one that is the best in all parameters;
- Illuminance is not the only important indicator for final user satisfaction, correlated colour temperature and uniformity must be also considered;
- Indicators evaluated must be required in bids;
- Final savings can be greater than first estimated.

Keywords: LED lighting, municipalities, energy efficiency, indicator, street lighting, and sustainability

1. INTRODUCTION

Since the Spanish economic crisis started in 2007, public administrations in general and municipalities in particular have seen their budgets significantly reduced. Moreover, the progressive increase of energy costs and carbon footprint generated by energy consumption has forced local governments to study and optimize their consumption sources to comply with environmental objectives established by the European Union [1].

Between 2007 and 2010, the local government developed the Energy Optimization Plans (POE) with the objective of elaborating an inventory of every source of energy consumption in the municipality (public lighting, municipal buildings, etc.) as an indicator of residential activity, socio-economic factors, and even to estimate GDP and CO_2 emissions [2]. These plans also proposed specific measures to increase efficiency.

Conclusions of these plans most often showed the need to optimize and reduce consumption in public lighting installations. In 2009, Casarabonela power consumption percentage of street lighting compared with total electricity consumption was 47 %, almost half of the municipal electricity costs [3].

What's more, the recent development of new alternatives to traditional light sources LEDs, Micro LEDs, (Light Emitting Diodes much more efficient in theory) has also led municipal technicians to study a multitude of options that sometimes do not contain enough information or are not sufficiently detailed to be properly assessed. This new situation may create discrepancies about the proposals that are submitted to them, as to whether or not they will meet with the legislation and the specific needs of the municipality.

In 2015, a study was conducted by the authors of this paper [4] that aimed to identify a set of indicators whose assessment could help technicians in decision making. As Polzin et al indicated: "Municipal representatives often fail to evaluate the market for LED lighting" [5]. The study identified a series of indicators that could predict the suitability of a street lighting system. In order to verify their results, the authors will use this case study to initiate the validation in practice of their indicators.

In order to achieve this purpose, a single case study has been carried out in the municipality of Casarabonela. It has intended to check, considering the information collected, if decisions taken match with the result of indicator assessment.

2. BACKGROUND

Casarabonela is located geographically on the western edge of the Guadalhorce River Valley, south of the Ronda region, province of Malaga. It has been declared a Biosphere Reserve by UNESCO and classified as zone E1 according to CIE126–1997 [6]. 70 % of the municipality population resides in the city centre and the overall population has been slightly decreasing from 2009 to 2015 [7].

Provincial Government of Málaga elaborated Casarabonela Municipality's POE in 2009, Fig.1. This study, revised in 2012, showed the power consumption due to public lighting increased by almost 30 % in 2012 as compared to 2009. This power consumption represented 42 % of the total energy consumed and 36 % of the total electricity costs in the municipality.

POE conclusions reflected a "saving opportunity" [8]. Moreover, the new legislative requirements of the EU Regulation Commission Nº 245/2009 [9] prohibited the use of mercury lamps as of 2015. These two events forced the municipality to find alternatives to traditional lighting sources, a "more ecological and sustainable image of common outdoor areas" [10].

3. METHODS

A descriptive single case study [11] has been carried out to illustrate the whole renovation process. The data were collected in three stages.

The stage one is before the execution of the renewal actions:

• Update Casarabonela urban lighting inventory;

• Develop a renovation project and begin the contracting procedure of planned actions in the project;

• Examine the proposals presented for project execution;

• Measure of lighting levels in a sample of streets.

The second stage is after the execution of the renewal actions:

• Repeat lighting level measurements;

• Interview with municipal mayor, technicians and politicians;

• Interview with municipal maintenance staff;

• Interview with residents;

• Elaborate a comparative analysis of electric costs;

• Calculate the economic investment and the return period on investment (ROI).

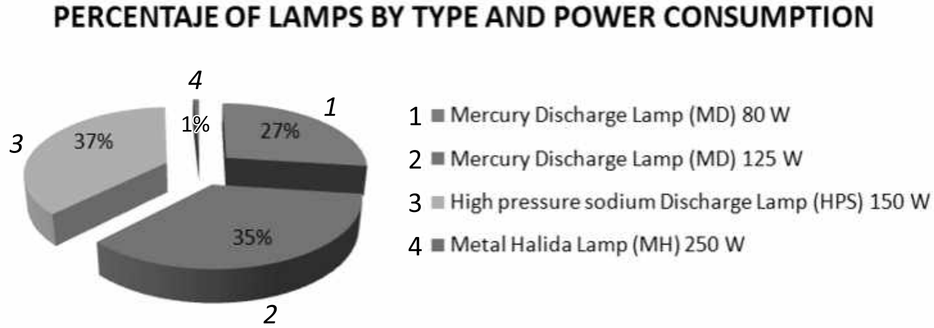

Fig. 1. Casarabonela urban lighting inventory (source: Casarabonela's POE)

Table 1. Casarabonela Inventory (Source: Provincial Government of Málaga)

Summary of required actions	Units
New Villa luminaire located in city centre streets and squares	365
New Fernandino LED module (LED Lamp + Gear Power) to install inside existing luminaires	40
Luminaire to install on a passage way ceiling	1
Cast aluminium bracket, of (0.6–0.7) m length	170
Cast column of 3.95 m high	71

Table 2. Bid Technical Requirements (Source: Provincial Government of Málaga)

Requirements	Values
Luminaire Material	Cast Aluminium
Luminaire Protecting Rate	IP65
Light Source	LED
Useful Life (Light Source)	≥ 90,000 h.
Heat dissipation elements in the light source	Yes
Light Source Luminous Flux	≥ 3,800 lumens
System Power (driver + light source)	≤ 38 W.
Correlated Colour Temperature	3,000 K (Warm White)
Upward light output ratio (ULOR)	≤ 1 %
Optic	Asymmetrical Distribution
Optical Unit Protection	IP54
Over Load Protection	Yes
Over Voltage Protection	≥ 10 KV.
Driver (Gear Power)	Electronic/Individual
Regulation	5 Steps Programmable Driver
Price	420 € (luminaire)/ 289 € (LED Module)

The third stage assesses presented proposals using the indicators.

4. DATA COLLECTED AND RESULTS

4.1. Updating of Casarabonela Urban Lighting Inventory

In November 2013, the public lighting inventory was updated by street and type of luminary to quantify the necessary technical and economical actions, Table 1.

Technicians also included the relocation or installation of new light points in areas that had shown a lack of quality of the lighting parameters during the inventory review. They increased the number of light points in some areas to increase the perception of safety and facilitate the use of public spaces for citizens [12]. Consequently energy consumption per capita increased in some areas [13, 14].

The diagnosis was completed with the inclusion of the renewal of three deteriorated electrical panels that didn't comply with the electrical safety current regulations [15].

4.2. Develop a Renovation Project and Begin the Contracting Procedure of Planned Actions in the Project

Technicians elaborated a project for the implementation of the inventory recommendations that finally amounted to 169,100 €. The contracting procedure was carried out by the City Council itself according to the state administrative regulations in force [16]. Several companies presented offers, of which only two completed the technical

Table 3. Comparative of Luminaires Offered

Mismatched Parameters *	BIDDER1	BIDDER2
System Power (driver + light source)	38 W	30 W
Luminaire Luminous Flux	3,328 lm	3,000 lm
Upward light Output Ratio (ULOR) (%)	< 1 %	0.74 %
Luminaire Efficiency	79 %	NP*
Luminaire Protecting Rate	IP44	IP65
Luminaire Price	420 €	386 €
Light Source Power	35 W	28 W
Led Module Luminous Flux	4,350 lm	4,000 lm
Colour Rendering Index	NP	>75
Led Module Working Current	500 mA	350 mA
Led Module Useful Life	68,000 hours	90,000 hours
LED Module Price	289 €	266 €

* *Not providing information, value, certification or required document*

and economic documentation required in the bid specifications.

The technical criteria for valuation of the offers included in the bid specifications are presented in Table 2.

The two final bidders were invited to install their luminaires as a test in several streets of the urban nucleus, as recommended by Polzin [5] with three purposes: to verify luminaires offered, to measure illumination levels provided by installed luminaires, and to follow up by assessing the degree of satisfaction for end users/residents.

4.3. Examine the Proposals Presented for Project Execution

An initial evaluation of submitted documentation by the bidders was carried out, according to the document "Technical requirements for luminaires with LED technology" of Energy, Tourism and Digital Agenda [17]. Subsequently, technical files and certificates provided were studied. Table 3 describes the parameters evaluated in which the bidders differed.

If bidder technical parameters are compared with technical requirements (Table 2), it can be deduced that Bidder 1 did not comply with "Luminaire Protecting Rate" nor "LED Module Useful Life" parameters. Both bidders failed to comply with "Correlated Colour Temperature" parameter, but municipal technicians accepted a value of 4,000 K.

4.4. Measurement of Lighting Levels in a Sample of Streets

A series of measurements were carried out on an example of five street roadways where the renovation was to take place.

The selected roadways were classified according to CIE and CEN / TR13201–1 "Road Lighting Part 1: Selection of Lighting Classes" [18] and UNE13201–2 "Road Lighting – Part 2: Performance Requirements" [19]; according to CIE126–1997 [6] all roads were classified as an E3 protection zone, because they were located in a residential area within the urban area, considered as a medium brightness or medium luminosity area, Table 4.

Measurements were always completed on the same streets and between the same luminaires. Identical inter-distances and measurement conditions were guaranteed at three different times:

1. The first series of measurements with the existing luminaires, before any action took place in the installation (in March 2014);
2. The second measurements with the test luminaires installed in the selected streets by the two final bidders (between March 2014 and January 2015);
3. A third series of measurements in the streets with Bidder 1's luminaires, replaced for Bidder 2's luminaires, which were ultimately selected by the municipality (during first semester of June 2015).

Table 4. Roadway Classification

Roadway Classification*	Type	Project Situation	Lighting Class	E_m, lx	E_{min}, lx
{1}Juan XXIII Avenue	D	D3-D4	S1	15.0–22.5	5
{2}Cantarraijana Street	E	E1	S2	10–15	3
{3}Saldaña Street	E	E1	S2	10–15	3
{4}Real Street	D	D3-D4	S1	15.0–22.5	5
{5}Francisco Herrera St.	D	D3-D4	S1	15.0–22.5	5

* *Real Decreto 1890/2008 [20]*

Measurements were obtained on windless nights without any other adverse weather conditions. The inter-distances chosen did not have any other light sources nearby (local, luminous signs, etc.) that might have interfered with measurements. Traffic was not cut off at any time, the technicians merely waited for the cars' light interference to disappear. A digital luxmeter, Grossen model Mavolux 50328 USB, provided a direct reading for each measurement.

The drawings are outlines of point grids selected by street, with measurements points, as well as the results of the mean and minimum illuminance and overall uniformity values obtained of each measurement carried out are presented in Table 5.

As the type of lamps is LEDs, a Maintenance Factor value of 0.85 can be considered for efficiency calculations [21]. This value corresponds to a cleaning interval of 3 years and a intermediate degree of contamination. The obtained results of the Road Energy Efficiency Class calculations, according Real Decreto 1890/2008 [20], showed a classification of "A" in all the streets.

4.5. Interview with Municipal Mayor, Technicians and Politicians

To get impressions about the whole process, the municipal technician who had witnessed the entire selection and renewal process, was interviewed. With regard to the bid selection, installation and subsequent start up period, he indicated that he had not detected any anomalies, difficulties or complaints. However, he did note that the selected luminaires were not of the highest quality although in his opinion they were technically sufficient. In addition, the mayor was interviewed and noted the opinions of his technicians and as well as of neighbours.

4.6. Interview with Municipal Maintenance Staff

One of the two municipal electricians was interviewed. He has been employed in the City Council for 20 years and was responsible for trouble shooting any incidents that occur in the daily operation of street lighting installation. The interviewee offered his experience and impressions about this particular case. During the selection phase, the electrician did not indicate anything worthy of mention.

During the execution phase, he remembered that at first the neighbours protested, perceiving a lack of adequate lighting that made their walks less pleasant [22]. One of the motives for the complaints was that the front of buildings were not lit, however, none of these initial complaints lasted over time. There was also another incident, the driver deprogramming of all luminaires belonging to one circuit, which the manufacturer solved satisfactorily. He also indicated that currently, during the maintenance and warranty phase, he did not carry out any preventive or maintenance activities; he only attended to occasional incidents.

During the last months of the test period the installation suffered several problems: some drivers in one of the circuits failed due to over voltage failures in power line and some luminary screws fell out and several luminaires had to be repaired.

The awardees, as agreed, were collaborating and were going to analyze the damaged equipment. In addition, the company was checking for possible alterations or defects in power supply lines. These small repairs incurred expenses of approximately 600 € to the municipality.

The town electrician stated that the whole process of substitution, from the beginning to the present, was on the whole adequate, but he did con-

Table 5. Road Drawn Measurements and Results

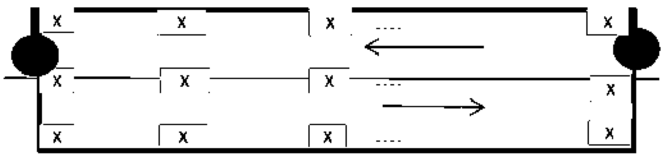

{1} Luminaire layout	Measure Number	Light Source	Power, W	Bidder	Dates	Em, lx	Emin, lx	Uo
Heigh: 4m	1° (39)	MD	80		mar-14	6.6	2.9	0.4
Road width: 5 m.	2ª (66)	LED	30	2	jan-15	14.5	5.0	0.3
Interdistance: 24 m.	-	-	-	-	-	-	-	-

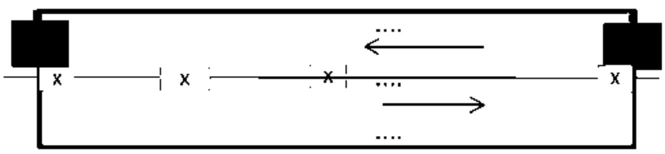

Luminaire layout	Measure Number	Light Source	Power, W	Bidder	Dates	Em, lx	Emin, lx	Uo
{2} Heigh: 3m	1° (12)	MD	80		mar-14	8.8	5.3	0.6
Road width: 2 m.	2° (11)	LED	30	2	jan-15	60.8	35.0	0.5
Interdistance: 17 m.	-	-	-	-	-	-	-	-
{3} Heigh: 3m	1° (15)	MD	125		mar-14	3.9	1.8	0.5
Road width: 3 m.	2° (15)	LED	30	2	jan-15	45.2	20.0	0.4
Interdistance: 19 m.	-	-	-	-	-	-	-	-
{4} Heigh: 3m	1° (12)	MD	80		mar-14	4.7	1.2	0.3
Road width: 3 m.	2° (12)	LED	38	1	jan-15	25.5	8.3	0.3
Interdistance: 19 m.	3° (17)	LED	30	2	jun-15	30.4	3.9	0.1
{5} Heigh: 3m	1° (11)	MD	80		mar-14	4.2	0.9	0.2
Road width: 3 m.	2° (11)	LED	38	1	jan-15	27.4	12.0	0.4
Interdistance: 21 m.	3° (17)	LED	30	2	jun-15	31.6	8.0	0.3

sider that some narrow streets were less illuminated, or had significant shadows.

4.7. Interview with Residents

Based on a small sample, residents living in the municipality have not been excessively positive regarding the renovation. They have noticed a change in the colour of the light, but they could not be sure if the perceived illumination had resulted in a higher quality. Although there were no specific complaints in historic centre, some neighbours did perceive a lack of lighting in residential areas when walking. They described totally dark areas between lamp posts. During the interview, when indicated that luminary renovation process had resulted in an electric bill saving, interviewed neighbours understood that the action was justified, but would have preferred that the lighting conditions had not diminished in some areas.

4.8. Elaborate a Comparative Analysis of Electric Costs

A comparative study of municipal electric consumption in public lighting supplies was carried out to check if there was any saving during last 12-month period (July-2015 to June 2016) since the renovation in relation to electric consumption study carried out in 2012, Table 6.

According to obtained values, the annual energy saving (154,709 kWh) represented a saving percentage of 50 %, equivalent to 62t CO_2 equivalent, while economic savings, represented 48 % of annual costs.

4.9. Calculate the Economic Investment and Period of Return on Investment (ROI)

The amount to be used exclusively for the replacement of luminaires of total renovation budget was of 110, 460 €.

Table 6. Comparative Consumptions 2012–2015

Consumption and Costs Differences	Results
Number of Electrical Panel Studied	4
Costs 2012, €	46,027
Costs 2015, €	23,817
Difference, €	- 22,210
Power Consumption 2012, kWh	310,931
Power Consumption 2015, kWh	156,222
Difference, kWh	-154,709

Table 7. Return on Investment Period and Energy Consumption Cost Calculations

Cost Calculations	Results
Initial Investment, €	110,460
Maintenance Costs, €/2015	600
Reduction of Energy Consumption Costs, €/2015	22,210
Total Reduction, €/year	21,610
Return of Investment, years	5

Table 8. Light Evaluation Indicators and Associated Parameters

Indicator	Associated parameters	
Luminaire Design	Photometry Protecting Rate Mechanical Impact Protecting Code	Luminaire Efficiency Over Voltage Over Load Protection
Light Source Power	LED Module Power LED Module Working Current	LED Module Luminous Flux Useful Life
Spectral distribution of light source	Minimum wavelength [6] Correlated Colour Temperature	Colour Rendering Index
Regulation possibility		
Luminaire Cost		

With prices and technical characteristics of awardees' luminaire, a preliminary study of the period of return on investment was carried out and the results showed a return on investment period between 6 and 7 years. Taking into account that the warranty usually covers the first 5 years of installation [1] this theoretical return on investment period is too high, Table 7.

From later tariff study, it was observed that the renovation produced a significant real saving (around 50 %) of the energy consumption and public lighting supply costs in its first year. The reason was the efficiency of existing luminaries was very small compared to the luminaires installed. With the real data of consumptions, the return on investment period reduced at least 1–2 years. If real savings obtained in the first year were maintained, it would greatly increase the investment profitability.

4.10. Assess Presented Proposals Using the Indicators

The conclusions of the study carried out by the authors in 2015 [4] were used as selection of a luminaire indicators list [23] that could help municipal technicians in decision making about street lighting renewal.

A total of 5 luminaire indicators were obtained. However, once contrasted in practice, an additional parameter was found to be necessary such as the cost of the light source. This new indicator allowed us to elaborate the cost calculations and periods of return on investment.

A review of these results was carried out in two ways. First, by associating some parameters to each luminaire indicator, the authors were able to quantify indicators such as "Design of the Luminaire." This indicator also includes parameters such as efficiency, degree of protection against external elements, IP or IK grade. Second, the authors eliminated any indicators that were common to all proposals as they would not influence the results, for example "Road Classification", "Operation Hours" and "Extent of Illuminated Areas", Table 8. At the same time, any indicators, which value could only be obtained after installation, were also not considered [24].

The valuation was carried out once the indicators were associated with quantitative parameters, because the qualitative nature of some of them could distort their assessment. Qualitative assessment will transform quantitative data in results [25].

The luminaire parameter values provided by only the two final bidders were used. In order to as-

Table 9. Bidder Scores

VALUATION	BID TECHNICAL REQUREMENTS	BIDDER1		BIDDER2	
		VALUE	SCORE	VALUE	SCORE
1. Luminaire Design					
Photometry	Asymmetric	Asymmetric		Asymmetric	
Protecting Rate (IP)	IP65	IP44		IP65	A
Mechanical Impact Protecting Code (IK)	-	-		-	
Luminaire Efficiency,%	-	79 %	A	-	
Over Voltage/Over Load Protection, kV	10	Have it		Have it	
2. Light Source Power					
LED Module Power, W	38	38		30	A
LED Module Working Current, mA	-	500		350	A
LED Module Luminous Flux, lm	3,800	4,350	A	4,000	
Useful Life, hours	90,000	68,000		90,000	A
3. Spectral distribution of light source					
Minimum wavelength, μ	-	-		-	
Correlated Colour Temperature, K	3,000	4,000		4,000	
Colour Rendering Index	-	-		>75	A
4. Regulation possibility	5 Steps	Have it		Have it	
5. Luminaire/Led Module Costs, €	420/289 €	420/289 €		386/266 €	A

Notes: Don't provide information. A: Advantage over the other bidder.

sign to each one the score corresponding to the indicator, the parameters on which one was superior to the other were reflected as ADVANTAGE, (A). In case of a tie, none obtained ADVANTAGE, (A). The Table 9 shows obtained values.

5. DISCUSSION

Without a doubt, data collection has been complex given the diverse areas considered to obtain a complete picture of actions carried out in the municipality. There have been economic, technical as well as social implications.

Economically, it might seem that the price of the luminaire was the main indicator that City Council technicians ultimately used to make a decision, although it should be noted that only the bidders who justified the technical requirements were considered viable by the technical assessment. In relation to the economic results, the offer presented by Bidder 2 was the most beneficial for the City Council. This offer resulted in a real return on investment of 5 years, the same or less than the warranty period, considering the first year of the installation.

Clearly luminaire price and technical requirements compliance were the decisive factors in the final decision of the municipal technicians. It can be construed that the municipal technicians based their decision on the similar indicators because of the 15 technical specifications of the Bid, 8 of them coincided with the indicators evaluated.

Technically, both bidders provided practically all the technical documentation required, with the exception of the Mechanical Impact Protecting Code of luminaires and certificates of some UNE standards. In addition, to complying with the Bidding Technical Requirements, Bidder 2 provided the most complete and detailed technical information. Several luminaire parameters presented by Bidder 2 were also superior (for example, "LED Module Working Current" value, "Luminaire Protection Rate", and "Useful Life of Light Source").

The two bidders met energy efficiency parameters, obtaining both the Class A. However, the average illuminance levels measured for the selected roadways exceeded the established illumination levels (S1 or S2) by more than 50 %. Bidder 2's results did show one exception (Juan XXIII Avenue). In addition, there is a sample where the road average illuminance level is five times higher than the pre-existing levels (Cantarraijana Street) measured on that street.

The results obtained, regarding minimum illuminance levels, are slightly better in Bidder 1 in relation to Bidder 2 and both meet the established levels, except Bidder 2 in one street. Regarding overall uniformity levels, both proposals showed worse or equal results in all streets except one where both improved (Francisco Herrera Street). Illumination levels measurements would have been carried out systematically according to UNE-13201–3 [26]. However, this case has not considered them.

Maintenance staff interviewed indicated that they were satisfied, as they were not required to perform periodic maintenance. But the street lighting installation had suffered mechanical breakdowns and failures in luminaires that should not have occurred during the first year of operation. The town electrician was also satisfied with the response that the Bidder had given to these failures, although the municipality had to make payments during the first year guarantee.

Socially, an overview of neighbours' opinions showed that initially their complaints were due to a feeling of lack of uniformity in some residential areas near the historic centre. Despite increasing illuminace levels, measurements also confirmed the existence of new shadow zones like "bright and dark patches" [27]. This assessment contrasted with the fact that some of the new luminaires had been installed to eliminate poorly lit areas. The new luminaire, installed in the same places as the previous installation, in most cases, generated new shadow zones as corroborated by Valentová and Quicheron's study [28].

Although the measurement results showed an increase of illuminance levels in all the roads studied and an improvement of minimum illuminance levels in the majority of them, these changes were not uniform and people interviewed did not identify any significant improvements in the daily use that they made of the street lighting installation, In addition, light source colour temperatures were not measured, as light spectral characteristics may have an impact in the design and appearance of public lightings [29] and colour difference may modify people's opinion [30]. The bid technical requirements only included a parameter related to the spectral distribution of the light source, the "Correlated Colour Temperature". As a result, the bidders have not provided enough information, so this indicator probably wasn't evaluated satisfactorily.

Using a list of indicators preselected in a previous study, the assessment of two bidders has been done in a straight forward way. One bid has result advantageous over the other in one parameter without taking into account the degree of improvement that this difference in value contributed to the luminaire. In consequence, every parameter defined by the indicator had the same weight. As there were only two bidders with one luminaire each, this difference in value has not been relevant.

The result of the evaluation of the indicators coincided with the decision made by the municipal technicians and validated 53 % of the indicators. Indicators list assess technical and economic aspects, but they do not assess residents' opinions of installation once renewed. Residents' opinions without a doubt have effectively detected a lack of uniformity and this need to be considered before the final project implementation. Clearly a small sample installation allows for a more complete overview of the renewal project before carrying out the full execution.

6. CONCLUSION AND POLICY IMPLICATIONS

The objective of this case study has been to evaluate the actions carried out in 2015 to replace street lighting installation in municipality of Casarabonela. At the same time, the authors have revised the conclusions of an earlier study with the aim of using the indicators selected in that study. The goal has been to verify if the municipal technicians would have chosen the same offered luminaire if they had used these new indicators.

Results indicated that the best bidder in technical characteristics, luminaire lower price and LED Module lower power value, is the one that got the best score in the indicator assessment and coincided with the option chosen by technicians. On the other hand, the bidder who obtained better results in the light levels measurement, failed to obtain the contract, mainly due to the price of the luminaire and some technical parameters in which the bid was overcome by the opponent. Clearly when assessing a proposal, all parameters play a role and there may not be one bidder who is best in all areas.

Street lighting execution project met the technical requirements. The levels of illuminance increased but the overall luminance uniformity worsened. Annual savings of 48 % (22,210 €/year) and a decrease of 50 % (62t CO_2 equivalent) in CO_2 emissions per year were finally obtained with a Return of Investment of 5 years.

This case study has also been used to justify the addition and elimination of some indicators from a previous study. The parameter assignment to the indicators allowed for a better assessment procedure to quantify qualitative indicators. The luminaire price indicator has been added, as an essential parameter in the valuation of the contracts signed by Public Administration.

Although results indicated proposed indicators are correct, a uniformity indicator would be include. More cases that contain a greater number of bidders and type of luminaires would corroborate or refute the conclusions obtained, and demonstrate the convenience of weighing the evaluation parameters or indicators.

ACKNOWLEDGEMENTS

The authors would like to thank Casarabonela residents, Mayor, technicians and maintenance staff, transfer their gratitude to the Provincial Government of Málaga, and Raul Cremades from Málaga University. This research did not receive any specific grant from funding agencies in the public, commercial, or not-for-profit sectors.

REFERENCES

1. Papagiannis G., Dagoumas A., Lettas N., Dokopoulos P. Economic and environmental impacts from the implementation of an intelligent demand side management system at the European level. Energy Policy, 2008. V36, pp.163–180. doi: 10.1016/j.enpol.20007.09.005.

2. Lu H., Liu G. Spatial effects of carbon dioxide emissions from residential energy consumption: A county-level study using enhanced nocturnal lighting. Applied Energy, 2014. V131, pp.297–306. http://dx.doi.org/10.1016/j.aperegy.2014.06.036.

3. Fiaschi D., Bandinelli R., Conti S. A case study for energy issues of public buildings and utilities in a small municipality: Investigation of possible improvements and integration with renewables. Applied Energy, 2012. V97, pp.101–114. http://dx.doi.org/10.1016/j.aperegy.2012.03.008.

4. Morillas R.M., de Andrés J.M. Identificación de Indicadores para la toma de decisiones en las instalaciones de Alumbrado Exterior de un municipio. In: 6ª Forum of Urban Intelligence and Sustainability Greencities, Málaga, 2015. pp.24.

5. Polzin F., von Floton P., Nolden C. Modes of governance for municipal energy efficiency services- The case of LED street lighting in Germany. Journal of Cleaner Production, 2016. V139, pp.133–145.

6. International Commission on Illumination. CIE126–1997 Guidelines for minimizing sky glow.

7. Spanish Statistical National Institute, INE. Demography and Population, http://www.ine.es/dyngs/INEbase/es/categoria.htm?c=Estadistica_P&cid=1254734710990 [accessed 03.15.17].

8. Jollands N., Waide P., Ellis M., et al. The 25 IEA energy efficiency policy recommendations to the G8 Gleneagles Plan of Action. Energy Policy, 2010. V38, pp.6409–6418. doi: 10.1016/j.enpol.2009.11.090.

9. European Parliament. COMMISSION REGULATION (EC) No 245/2009 of 18 March 2009 implementing Directive 2005/32/EC of the European Parliament and of the Council with regard to eco-design requirements for fluorescent lamps without integrated ballast, for high intensity discharge lamps, and for ballasts and luminaires able to operate such lamps, and repealing Directive 2000/55/EC of the European Parliament and of the Council.

10. Radulovic D., Skok S., Kirincic V. Energy efficiency public lighting management in the cities. Energy, 2011. V36, pp.1908–1915. ISSN: 0360–5442.

11. Yin R.K. Case Study Research. Design and Methods. 4th ed. SAGE Publications Inc, 2009.

12. Heath G.W., Parra D.C., Sarmiento O.L., et al. Evidence-based intervention in physical activity: lessons from around the world. The Lancet, 2012. V380, 9838, pp.272–281. doi: 10.1016/S0140–6736(12)60816–2.

13. Rutter P., Keirstead J. A brief history and the possible future of urban energy systems. Energy Policy, 2012. V50, pp.72–80. http://dx.doi.org/10.1016/j.enpol.2012.03.072.

14. Herring H. Does energy efficiency save energy? The debate and its consequences. Applied Energy, 1999. V63, pp.209–226. ISSN: 0306–2619.

15. Ministry of Science and Innovation. Real Decreto 842/2002, de 2 de agosto, por el que se aprueba el Reglamento Electrotécnico para Baja Tensión.

16. Ministry of Finance and Civil Service. Real Decreto legislativo 3/2011 de 14 de noviembre, por el que se aprueba el texto refundido de la Ley de Contratos de las Administraciones Públicas.

17. Ministry of Energy, Tourism and the Digital Agenda, Instituto para la Diversificación y la Energía,

Comité Español de Iluminación. Requerimientos técnicos exigibles para luminarias con tecnología Led, 2011.

18. European Committee for Standardization. CEN/TR13201–1 “Road Lighting Part 1: Selection of lighting classes”.

19. European Committee for Standardization. UNE-EN13201–2 “Road lighting – Part 2: Performance requirements”.

20. Ministry of Energy, Tourism and the Digital Agenda. Real Decreto 1890/2008, de 14 de noviembre, por el que se aprueba el Reglamento de Eficiencia Energética en Instalaciones de Alumbrado Exterior.

21. European Committee for Standardization. UNE-EN13201–5:2015. “Road Lighting – Part 5: Energy performance Indicators”.

22. Clark M.I., Berry T.R., Spence J.C., et al. Key stakeholder perspectives on the development of walkable neighborhoods. Health & Place, 2010. V16, 1, pp.43–50. doi: 10.1016/j.healthplace.2009.08.001.

23. Jägerbrand A.K. New Framework of Sustainable Indicators for Outdoor LED (Light Emitting Diodes) Lighting and SSL (Solid State Lighting). Sustainability, 2015. V7, pp.1028–1063. doi: 10.3390/su7011028.

24. Budak, V.P., Ilyina, E. Choosing luminaire efficiency parameters during development for external illumination. Light & Engineering, 2013. V21, 2, pp.13–20.

25. Patton, M.Q. Two Decades of Developments in Quality Inquiry. Qualitative Social Work, 2009. V1, pp.261–283.

26. European Committee for Standardization. UNE-EN13201–3:2016. “Road Lighting – Part 3: Calculation of performance”.

27. Kostic M., Djokicb L. Recommendations for energy efficient and visually acceptable street lighting. Energy, 2009. V34, 10, pp.1565–1572.

28. Valentová M., Quicheron M. LED projects and economic test cases in Europe. International Journal of Green Energy, 2015. V12, 8, pp.843–851. doi: 10.1080/15435075.2014.887568.

29. Habel J., Zak P. The future of public lighting. PrzegladElektrotechniczny, 2011. V87, 4, pp.50–52. ISSN: 0033–2097.

30. Knight C. Field surveys of the effect of lamp spectrum on the perception of safety and comfort at night. Lighting Research &Technology, 2010.V42, 3, pp.313–329. doi: 10.1177/1477153510376794.

Rosa Maria Morillas,
M. Sc. and M. Eng. She has a M. Sc. in Industrial Engineering, a M. Sc. in Electrical Engineering from the Universidad de Málaga (Spain) and a M. Sc. in Occupational Health and Safety at the Workplace from the University of San Pablo Ceus (Spain). She completed her Master’s thesis at Skövde University (Sweden) in 2012. For the last seven years, she has been working as an electric engineer for the Ministry of Public Works in Málaga, Spain. Her research interests include Project Management and Lighting

José Ramon de Andrés
received an Industrial Engineering degree from the University of Comillas (ICAI), and his Ph.D. degree from the University of Málaga Spain, in 1989 and 1998 respectively. Currently he is an Associate Professor at the Department of Graphical Expression, Design and Projects at the University of Málaga. His research interests include Product Design, LCA, Project Management and Lighting

Light & Engineering
Vol. 27, No. 6, pp. 27–33, 2019
https://doi.org/10.33383/2019-014

SELECTION OF THE AREA OF WINDOW OPENINGS OF RESIDENTIAL BUILDINGS IN CONDITIONS OF MONSOON CLIMATE OF THE FAR EAST OF THE RUSSIAN FEDERATION AND NORTHERN AREAS OF CHINA

Alexei K. Solovyov and Bi Guofu

Moscow State National Research University of Civil Engineering, Moscow
E-mails: agpz@mgsu.ru, biguofu16@gmail.com

ABSTRACT

The term "window" in architecture usually stands for an opening in a wall or roof for penetration of natural light, sunrays and fresh air in premises. Recently, the requirement of contact with environment is added to this condition. It is especially relevant for residential buildings where rooms are considered residential if they have windows. The energy consumption of a building depends on sizes, form and location of windows. In winter, windows cause huge heat losses, in summer, on the other hand, large heat enters a building via the windows and is required to be removed by means of air conditioning. Moreover, windows are used for penetration of natural light in premises, which assists in saving of large amounts of power for artificial illumination. This article discusses partial solving the problem of the energy efficiency of residential buildings by determining the most efficient area of windows in terms of energy spending for compensation of heat losses via windows in winter, elimination of heat penetration through them in summer and energy losses for artificial lighting throughout the year. The analysis of the results of calculation of power consumption for residential premises in conditions of monsoon climate of the Russian Far East and Northern areas of China (PRC) is provided.

Keywords: window area, energy efficiency, natural and artificial illumination, heat losses, heat gain, critical illuminance, power consumption

1. INTRODUCTION

The area of windows of residential premises is set by means of standardised values of daylight factor (DLF). However, DLF characterises only physical conditions of natural illumination of premises. In Russia, it is considered that the premises is perceived as saturated with natural light with DLF of 0.5 % on the floor at a distance of 1 m from the wall opposite to the windows, but the standards in other countries may be different. For instance, in Germany it is considered that saturation of the premises with natural light is reached at DLF = 0.5 % in the middle of the premises on the level of working surface (i.e. 0.8 m above the floor) at distance of 1 m from the side wall of the premises [1]. In this article, the Russian standards are used [2].

Windows are the weakest point of the thermal envelope of a building. In winter, the largest heat losses are caused through them. For instance, the standards [3] require to reach the value of heat transmission resistance of about 3 $(m^2 \cdot °C)/W$ in Moscow whereas ordinary windows do not even provide 1 $(m^2 \cdot °C)/W$. It means that three times as much heat is lost via windows as via blank walls in winter, which causes additional losses for heating. On the other hand, a lot of solar heat is gained through the windows in summer, which causes overheating of premises and increased losses of power for its cooling by means of air conditioning.

NIISF RAASN developed the method of energy evaluation of the system of natural illumi-

Table 1. Average Monthly Temperatures, Taken Temperatures and Some Data for Winter Period

City	Average ambient air temperature, °C												Annual indicators					
	I	II	III	IV	V	VI	VII	VIII	IX	X	XI	XII	Average annual temperature, °C	Absolute minimum temperature, °C	Absolute maximum temperature, °C	t_1*, °C	t_{OT}**, °C	Z_{OT}, days
Khabarovsk	-22.3	-17.2	-8.5	3.1	11.1	17.4	21.1	20.0	13.9	4.7	-8.1	-18.5	1.4	-43	40	-34	-10.1	205
Harbin	-23.1	-18.7	-8.8	8.4	8.4	15	18.3	16.7	8.9	0.6	-9.6	-19.1	4.9	-38.1	36.8	-33	-10	176

* Taken minimal ambient temperature in the cold period.
** Average ambient temperature during the heating period.

nation of buildings with consideration of power consumption for electrical illumination, compensation of winter heat losses via the windows and energy losses for air conditioning in summer [4]. The authors of the article updated this method a little with consideration of the new types of air conditioners (split systems) by simplifying the calculation of air conditioner operational period and took the new provisions of energy efficiency of natural illumination according to SR (Set of Rules) [5] into account.

2. MONSOON CLIMATE CONDITIONS OF THE RUSSIAN FAR EAST AND NORTH-EASTERN AREAS OF PRC

Khabarovsk (Russia) and Harbin (PRC) are characteristic and similar cities of the Far East of Russia and the Northeastern part of PRC in terms of climate. Their climate is characterised by a large amount of clear and half-clear days with high solar radiation both in winter and in summer. For instance, in Khabarovsk, the diffuse and total illuminance are 13.8 klx and 28.6 klx at noon in January and 29.3 klx and 56.5 klx in July, whereas in Moscow the same values are 7.0 klx and 9.2 klx in January and 28.3 klx and 47.8 klx in July. Proportions of these values at noon in Khabarovsk: 1:2.07 in January and 1:1.92 in July and in Moscow: 1:1.31 in January and 1:1.69 in July. This means that there are twice as many sunny and half-clear days as dismal days in Khabarovsk and there are significantly less clear and half-clear days in Moscow, especially in winter. The number of clear and half-clear (with open Sun) days in Harbin is approximately the same as in Khabarovsk. The thermal cycle in both cities is approximately the same too (Table 1). Table 2 shows that both cities may be considered identical for summer period when artificial cooling of air by means of air conditioning is rather rarely but still required too.

There is data of temperature frequency for the cities of Russia [6] including Khabarovsk krai, where frequency of temperatures higher than 28 °C is just 16 hours per year (i.e. air conditioning (cooling) of premises oriented to the North is required for 16 hours per year). It is negligible and the power consumption for cooling of premises oriented to the South, West and East may be calculated only based on the conditions of overheating by solar radiation.

Table 2. Climatic Data for Summer Period in Khabarovsk and Harbin

City	Temperature, °C								Maximum rhumb wind velocity in June, m/s
	V	VI	VII	VIII	IX	Absolute maximum air temperature	Average maximum air temperature	Prevailing wind direction in July and August	
Khabarovsk	11.1	17.4	21.1	20.0	13.9	40.0	25.7	SW	4.6
Harbin	8.4	15	18.3	16.7	8.9	36.8	26.4		1.71

3. METHOD OF CALCULATION OF POWER CONSUMPTION FOR NATURAL ILLUMINATION

The systems of natural illumination may be assessed using two methods: 1) evaluation on the basis of reduced costs for installation of natural and artificial illumination and its operations (in roubles per m^2 of the area of premises per year); 2) evaluation of power consumption of illumination, compensation of heat losses via the lighting openings and elimination of heat gains through them (in kg of reference fuel per 1 m^2 of the area of premises per year). The first method is well suited for economical evaluation of a specific project in the course of cost calculation with consideration of corresponding current prices and tariffs but it is not well suited for common evaluation since it is almost impossible to account for future price changes. For this purpose, the second method suits better as it provides assessment of the system in terms of power consumption, more objective and long-term one.

Annual specific heat energy consumption for heating $W_{T.OT}$ (GJ/m^2/year) is determined as follows:

$$W_{\text{T.OT}} = 10^{-6} \cdot 1.1 \cdot 3.6 \cdot 1.3 \cdot \left(\frac{1}{R_{\text{ск}}} - \frac{1}{R_{\text{о}}}\right) \times$$
$$\times\ (t_{\text{в}} - t_{\text{от}}) \cdot 8760 \cdot Z_{\text{OT}} \cdot b \cdot \frac{A_{\text{ск}}}{365 \cdot A_{\text{п}}},$$

where 10^{-6} is J to GJ transfer ratio; 1.1 is the ratio considering useless heat losses of heating systems; 3.6 is the unit recalculation ratio, kG/W×h; 1.3 is the ratio considering heat losses for heating of external air by ventilation of the premises; $R_{ск}$ and $R_о$ are heat transmission resistance values of the window and the wall respectively, (m^2·°C)/W; 8760 is the number of hours per year; $t_{от}$ and Z_{OT} are average temperature, °C and duration of heating season, days; $t_в$ is the temperature of inner air of the building; b is the ratio of window area to the area of the translucent structure of the wall; $A_{ск}$ and $A_п$ is the area of the windows and the floor respectively, m^2; 365 is the number of days per year [4].

Power consumption for compensation of heat losses via windows with $R_{ск}$ of 0.7 (m^2 · °C)/W and $R_о$ of 2.12 (m^2 · °C)/W will be equal to 0.026 GJ/m^2/year. Calculated as 1 kg of reference fuel, it will be equal to 1.07 kg/m^2/year (41.2 kg/GJ×0.026 GJ/m^2/year).

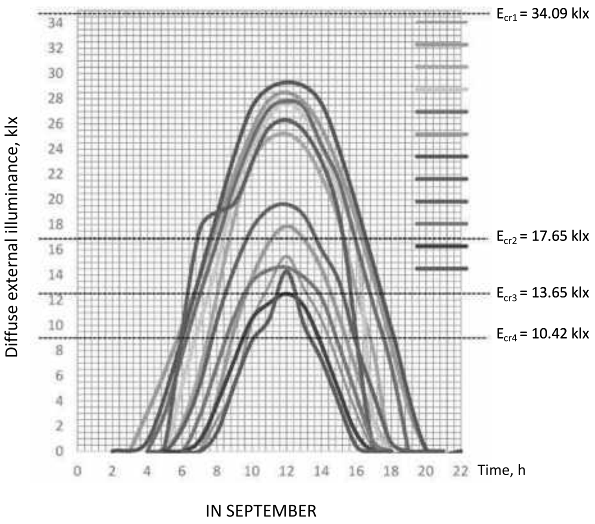

Fig. 1. The graphs of natural illuminance in Khabarovsk

Annual specific (per 1 m^2 of area) power consumption for artificial illumination of the premises $W_{s.p.c.}$ (kWh/m^2/year) is calculated in accordance with [4]:

$$W_{\text{spc}} = 10^{-3} \cdot E_i^{norm} \cdot Z \cdot \alpha \cdot P_l \cdot (1+\beta) \times \times T_p / [(u_{\text{св}} \cdot MF) \cdot \Phi_l], \quad (1)$$

where E_{i}^{norm} is the standardised artificial illuminance in residential rooms, equal to 150 lx; *MF* is the operating factor for artificial illumination luminaires [2] taken equal to 0.71; *Z* is the ratio considering irregularity of illuminance (rather high for residential premises, approximately equal to 1.3 [2]); α is the ratio considering power losses of control gear, which may be taken equal to 1.2 for FL and LED lamps; β is the ratio considering power losses in the grid (equal to 0.03 if IL, FL or LED lamps are used); P_l and Φ_1 are total power and luminous flux of the lamps, W and lm; $u_{\text{св}}$ is the operation factor of the luminaire equal to 44 with the premises index i = 0.8 [7]; T_p is the period of using the artificial illumination determined on the basis of critical illuminance E_{cr} and the graphs of natural illuminance in Khabarovsk (Fig.1).

With the above-mentioned parameters of the premises and the window opening, the calculated value of DLF *e* is 0.84 % at distance of 1 m from the back wall, therefore

$$E_{cr} = \frac{E_i^{\text{norm}} \cdot 100}{e} = 17{,}65 \text{ [klx]}.$$

Fig. 1 shows that the standardised value of 150 lx is complied with in the design point for at least 105 h (3.5×30) in September, 186 h (6.0×31) in March, 217.6 h in April, 232.5 h in May, 240.0 h in June, 258.23 h in July and 217.0 h in August. Annual period of natural light use is equal to 1238.73 h. T_{p} is the difference between the total number of hours per year excluding 8 h of sleep per day and the period of natural light use: 4578.9 h [(16×30.3·12 = 5817.6) – 1238.7]. According to formula (1), $W_{s.p.c.}$ is equal to 8.586 kWh/m^2/year. Calculated as consumption of reference fuel, $W_{s.p.c.}^{eq}$ is the equivalent of 2.833 kg/m^2/year (0.33×8.586). We take that consumption of reference fuel in common use power plants per 1 GJ of heat energy A_1 is equal to 41.2 kg/GJ, and consumption of electric power A_2 is equal to 0.33 kg/kWh [4].

Therefore, consumption of reference fuel for compensation of heat losses through windows and for artificial illumination of the studied room W_{eq} calculated as

$$W_{eq} = W_{\text{T.OT}} \cdot A_1 + W_{\text{s.p.c.}} \cdot A_2,$$

is equal to 2.54 + 2.83 = 5.37 [kg/m^2/year].

Consumption of reference fuel for compensation of heat losses through the window in winter is directly proportional to the area of the window, i.e. the value of $W_{\text{T.OT}}$ of 2.54 kg/m^2 for windows with other dimensions may be changed proportionally to the area. Similar recalculation of consumption of reference fuel for artificial illumination cannot be done as it depends on T_p.

T_p depends on E_{cr} and is determined on the basis of Fig. 1. To determine E_{cr}, *e* should be calculated in design point of the premises with the above-men-

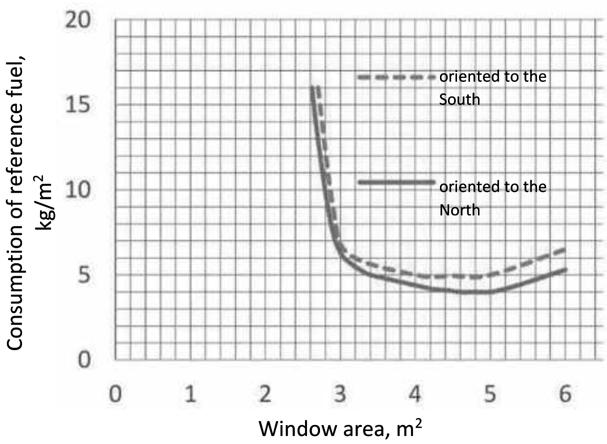

Fig. 2. The graphs of consumption of reference fuel for window operation (compensation of winter heat losses, artificial illumination and summer cooling)

Table 3. Consumption of reference fuel for operation of the windows per year

No.	Window type (dimensions), m	Window area, m²	$W_{т.от}$, kg/m²	$W_{s.p.c.}$, kg/m²	$W_{eq} = W_{т.от} + W_{s.p.c.}$, kg/m²
1	1.5 × 1.8	2.7	2.18	13.29	15.47
2	1.5 × 2.1	3.15	2.54	2.835	5.37
3	1.7 × 2.5	4.25	3.43	1.626	5.056
4	1.7 × 3.5	5.95	4.8	1.22	6.02

tioned dimensions of the premises and other considered size of the window.

4. STUDY OF ENERGY EFFICIENCY OF WINDOWS WITH DIFFERENT SIZES IN THE MONSOON CLIMATE OF THE SOUTHERN FAR EAST OF RUSSIA AND NORTH-EASTERN PART OF PRC

For this study, the residential premises with dimensions of (4×6) m and height between the floor and the ceiling of 3 m on one of the middle floors of a multi-floor building with no building located opposite to it were choosed. The type of glazing is described above.

Four types of windows were studied: a standard one with height of 1.5 m and width of 2.1 m; a large one with height of 1.7 m and width of 2.5 m; a small-size window, 1.5×1.8 m; a window with height of 1.7 m and width almost equal to the width of the room: 3.5 m.

The results of calculation are listed in Table 3 and shown in Fig. 2 which witnesses that the least power consumption for compensation of heat losses and for artificial illumination of the studied premises in kg of reference fuel occur with window area ranging between 3 and 5.0–5.5 m². With less dimensions of the windows, power consumption for electric illumination increases dramatically. In case of windows with area of 5.5 m², power consumption for compensation of heat losses via the windows will prevail increasing total power consumption.

It is worth noting that this conclusion is relevant only for the premises oriented to the North, North-North-West and North-North-East. For Southern orientations, heating of the premises by means of solar energy penetrating the windows should be taken into account. In this case, the premises may require air-cooling by means of air conditioners with high power consumption.

Specific power consumption for cooling $W_{s.p.c.c.}$ should be determined in accordance with [4] using the following formula

$$W_{s.p.c.c.} = L_{\text{o}} \cdot N_{\text{x}} \cdot T_{\text{x}}, \qquad (2)$$

where N_{x} is power consumption for cooling of air by means of an air conditioner (kWh/m³); T_{x} is duration of operation of the cooling system, h; L_{o} is performance of the conditioner ventilation system (m³/h) per 1 m² of the floor area with consideration of average heat retention of the premises calculated as follows

$$L_{\text{o}} = \frac{3,6 \cdot 0,7 \cdot q_{rad}^{\max}}{c \cdot \rho \cdot (t_{\text{пр.А}} - t_{\text{р.А}})}, \qquad (3)$$

where 3.6 is unit recalculation ratio, kJ/Wh; 0.7 is consideration of air heating in pipelines; c = 1 kJ/kg/°C is air specific heat; ρ = 1.2 kg/m³ is air density; $t_{n\text{р.А}} - t_{\text{р.А}}$ is the difference between summer design input temperature of air and the temperature of air in the premises taken equal to 3 or 5 °C depending on heat load density of the premises [8]; $q_{rad}^{\max}$ is the largest value of radiant heat gain in the premises, W/m², determined by maximum value of heat gain by total solar radiation reaching the surface of the window during a day and calculated using the following formula

$$q_{rad}^{\max} = (Q_{\text{dir.h.g.}}^{\max} + Q_{\text{dif.h.g.}}^{\max}) \times \\ \times \tau_e \cdot \tau_2 \cdot MF \cdot \beta_{c.з} \cdot b \cdot A_{cк} / A_{\text{п}}, \qquad (4)$$

where $Q_{\text{dir.h.g.}}^{\max}$ and $Q_{dif.h.g.}^{\max}$ are the maximum values of the direct and diffuse heat gains by solar radiation on the vertical surface of the window with relevant orientation (W/m²) with clear sky defined in accordance with SNiP [6] (for Khabarovsk (N48°), with orientation to SE $Q_{\text{dir.h.g.}}^{\max} + Q_{dif.h.g.}^{\max}$ = 473 W/m²); τ_{e} is the transmittance of translucent filler of the opening for solar radiation equal to 0.57 [5]; τ_2 is the ratio considering light losses on window sashes [2] taken equal to 0.9; MF is the ra-

Table 4. Consumption of Reference Fuel for Operation of Windows with Southern (SW) and, by Comparison, Northern Orientation of the Premises

No.	Window type (dimensions), m	Window area, m^2	W_{eq}, kg/m^2, northern side	W_{eq}, kg/m^2, southern side	$W_{s.p.c.c/}$, kg/m^2
1	1.5 × 1.8	2.7	15.47	16.042	0.0572
2	1.5 × 2.1	3.15	5.37	6.038	0.668
3	1.7 × 2.5	4.25	5.056	5.957	0.901
4	1.7 × 3.5	5.95	6.02	7.281	1.261

tio considering glass fouling in the course of operation [2] taken equal to 0.71; $\beta_{c3} = \tau_4 = 1$ (no solar protection is available); $b = 1$.

In the formula (2):

– T_x is determined in accordance with SNiP [6, table External air temperature frequency in hours] for external temperature of $t_н = 25$ °C, taken with a little reserve considering heat retention of the structures of the premises. For Khabarovsk, T_x=66 h;

– For determination of N_x (in accordance with [9]), it is necessary to calculate excess heat of the premises (Q) which comprises heat of the solar radiation penetrating the windows (Q_1), domestic appliances heat (Q_2) and heat generated by people (Q_3). $Q_1 = V{\cdot}q$ where V is the volume of the premises (in our case, 76 m^3, (4×6×3) m^3); q is specific heat gained by the premises via the South-West-oriented windows taken equal to 30 W/m^3; Q_1 = 2160 W; Q_2 = 500 W (TV set, PC); Q_3 = (100 W/person)×3 persons = 300 W; Q = 2960 W.

On the basis of these results, we are taking the contemporary household air conditioner by *Samsung* with refrigeration capacity of 3.2 kW. Its air capacity is P = 900 m^3/h. Then power consumption for cooling of air using this air conditioner is $N_x = Q/P$ = 3.23 Wh/m^3.

Then the multiplier $L_о$ in formula (2) is calculated using formulas (3) and (4) and reference data [6] for calculation of $W_{s.p.c.cool}$ and for its transformation into kilograms of reference fuel per 1 m^2, this value should be multiplied by conversion factor A_2 = 0.33 kg/kWh.

The consumption of reference fuel for compensation of fuel losses through the windows in winter, for artificial illumination and for cooling in summer for the studied windows of the room with the area of 4×6 m^2 oriented to the South-West (SW) with a household conditioner used for summer cooling is given in Table 4.

In Fig. 2, the graphs of changing of consumption of reference fuel for operation of light openings with different area in the residential premises oriented to the North and to the South are given provided that at $t_н$ > +25 °C the *Samsung* household air conditioner is activated in the room oriented to the South. Heat gains through the window in winter are not considered.

It is worth noting once more that the least consumption of reference fuel occurs with window area ranging between 3 and 5.0–5.5 m^2 both with orientation to the South and to the North (Fig. 2).

We would also like to note that the values of Q_1, Q_2 and Q_3 were taken in accordance with [9] and although the specific power consumption for cooling may change after changing these values, it does not affect the results of this study.

CONCLUSIONS

The research for Khabarovsk climatic conditions has shown that the areas of windows ranging between 3 and 5.0–5.5 m^2 in residential rooms with dimensions of 6 m are the most energy-efficient. In Harbin, where the climatic conditions are similar, the windows of the same area are the most energy efficient. Of course, shadowing by surrounding buildings should be considered in each specific case but such recommendations may be considered common for typical development.

REFERENCES

1. DIN5034–3–1994 Daylight in interiors. Calculation.

2. SR 52.13330.2016 Daylighting and artificial lighting. The updated version of SNiP 23–05–95*.

3. SR 23–101–2000 Designing of thermal protection of buildings.

4. NIISF of the Gosstroy of USSR. Handbook for calculation and designing of natural, artificial and combine illumination (to SNiP II-4–79) / NIISF Moscow, Stroyizdat, 1985.

5. SR 367.1325800.2017 Residential and public buildings. Daylighting design.

6. SNiP II-A.6–72 Construction Climatology and Geophysics.

7. Electric Lighting Design Handbook [Spravochnaia kniga dlia proektirovaniia elektricheskogo osveshcheniia] / Edited by G.M. Knorring. Leningrad: Energiya, 1976, 384 p.

8. Designer's Handbook. Internal Sanitary and Technical Equipment in 2 Parts [Spravochnik proektirovshchika. Vnutrennie sanitarno-tekhnicheskie ustroistva v 2 chastiakh] / Edited by I.G. Staroverov. Part 2. Ventilation and Air Conditioning [Chast 2. Ventiliatsiia i konditsionirovanie vozdukha]. Moscow: Stroyizdat, 1978.

9. Split systems data sheets (courtesy of *SAMSUNG*)

Alexei K. Solovyov,
Prof., Dr. of technical sciences. He graduated from Moscow Institute named after V.V. Kuibyshev in 1965. At present, he is the Professor of the department "Design of buildings and structures" (former department of "Architecture of civil and industrial buildings") of the NRU "MGSU". He is a Member of the European Academy of Sciences and Arts and the editorial board of the "Lighting Engineering" and "Svetotekhnika", has the titles of "Honorary Builder of the Russian Federation" and "Honoured Worker of the Higher School of Russia"

***Bi Guofu*,**
Bachelor and Master Degree (Industrial and Civil Construction speciality). Graduated from Bachelor's programme of the Heilongjiang University in 2013 and from the Master's programme of NIU MGSU in 2016. At present, he is the 3rd year postgraduate student of NIU MGSU

Light & Engineering
Vol. 27, No. 6, pp. 34–40, 2019 *https://doi.org/10.33383/2019-019*

RESEARCH INTO LUMINANCE CHARACTERISTICS OF OBJECTS WITH ARCHITECTURAL LIGHTING OF CENTRAL STREETS OF TULA

Svetlana V. Kolgushkina, Nataliya V. Bystryantseva, and Victor T. Prokopenko

ITMO University, Saint Petersburg, RF
E-mails: svkolgushkina@corp.ifmo.ru; kolgushkinasv@gmail.com

ABSTRACT

The study of luminance distribution over the facades with architectural lighting allows us to estimate the perception of architectural objects, to analyse the quality of light solutions. The relevance of luminance characteristics estimation in night-time urban conditions has been increasing over the years, in particular, for cities where the development direction of lighting environment aims at increase of the number of illuminated objects and where there is no developed strategy of lighting environment development. Using the example of 11 central streets of Tula, the article describes the comprehensive approach to analysis of the quality of architectural lighting. Using a CCD matrix-based luminance meter, the luminance characteristics of facades were estimated.

Keywords: architectural lighting, luminance distribution, lighting environment, luminance measurements, lighting quality

1. INTRODUCTION

Nowadays, the lighting environment of Russian cities has been forming spontaneously, without taking the hierarchy of objects in the urban environment into account [1–3]. The luminance characteristics of applied lighting installations are often overestimated, which causes negative impact on visual perception [1–3]. Increase of the number of architectural lighting solutions based on local lighting method causes visual destruction of perception integrity of buildings, in most cases, the relations between minimal and maximum illuminance values do not comply with the requirements of SP 52.13330.2016 and exceed 1:30 [4].

The lighting composition of an evening city should be based on compliance of all elements of lighting environment in the entire solution. The requirements imposed on architectural lighting are: identification of building mass, expression of the structure and plastics of architectural forms. The projects of exterior architectural lighting should be the part of general urban design and lighting skylines of an evening city [1–4].

In terms of qualitative estimation of the implemented lighting solutions, there are the following challenges today:

• Formation of exterior of night cities without a developed lighting strategy in Russia causes appearing of separated objects;

• Urban hierarchy of the objects within the urban environment is not taken into account;

• The implemented objects do not comply with the requirements of standard regulations in terms of luminance level;

• There are no quality control mechanisms of the implemented objects;

Lack of attention to the said problems causes destruction of integrity of urban environment during evening time, irrational consumption of energy resources, negative impact on visual perception and psychoemotional state of a person [1–4].

Tula is a small city with area of 145.8 km^2 located at 200 km from Moscow. For small towns,

Fig.1. Mapped objects with architectural lighting

specialist design lighting of objects remotely, which also affects the quality of the implemented solutions.

Application of the methods of luminance distribution study within the field of view is a relevant challenge which allows qualitative objects to subsist in the urban structure and to plan modifications of the lighting design structure of the city. The analysis of luminance characteristics of existing lighting may be conducted as a preliminary phase before developing the lighting strategy, the lighting master plan of the city [5–7].

The goal of the study was to investigate the luminance distribution over the illuminated facades by optoelectronic instruments using the example of central streets of Tula. In the course of the study, the existing lighting environment was evaluated, which allowed the most common problems to define. The luminance distribution was estimated by means of a direct method in accordance with GOST 26824–2010 and GOST R55707–2013 using LMK Mobile Advanced luminance meter on the basis of a CCD matrix. Application of the specialised LMK LabSoft software for analysis of the acquired results allows process, analyse and display the values of luminance of the measured surfaces. The measurements were conducted in August 2017, prelim-

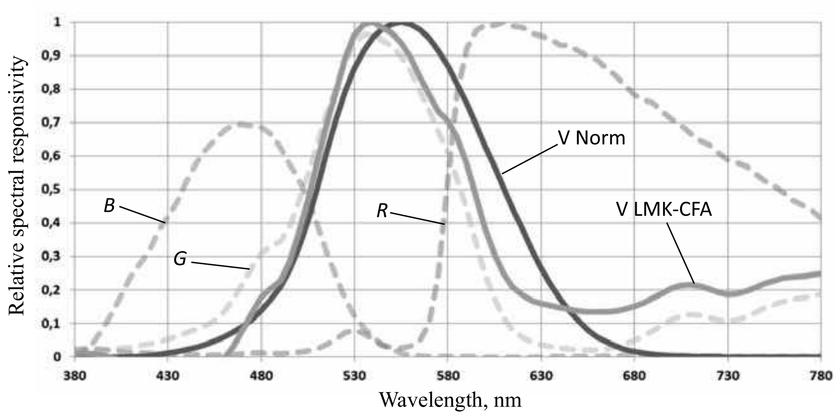

Fig.2. Relative spectral responsivity of the luminance meter (black curve)

2, Mosina st.			■ THE OBJECT ■ Buildings with AHL Arch. Dominants: ● Level 2 ● Level 3	The building of the Ryabikov Tula Machine-Building Plant is not a dominant. The architectural lighting fully complies with the status of the building, excellently uncovers its architecture and decorative elements of the facade.
1A, Sovetskaya st.	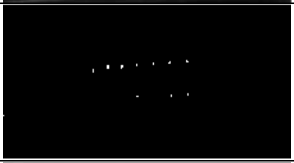		■ THE OBJECT ■ Buildings with AHL Arch. Dominants: ● Level 3	The building of the Tula Arms Plant is not a dominant. The architectural lighting fully complies with the status of the building, excellently uncovers its architecture and decorative elements of the facade.
2, Sovetskaya st.			■ THE OBJECT ■ Buildings with AHL Arch. Dominants: ● Level 2 ● Level 3	The building of the City Concert Hall is not an architectural dominant. The architectural lighting of the building uniformly lights the facade facing the Sovetskaya st. In the context of the surrounding lighting environment and town-planning value, the luminance of the main facade of the building is too high.
78, Sovetskaya st.			■ THE OBJECT ■ Buildings with AHL	The building at 78 Sovetskaya st. is not an architectural dominant. The architectural lighting of the building expresses the architectural distinctions, but due to different chromaticity of sources and high luminance, the building is visually torn out of the evening urban environment. The Lenin square where the closest major dominants are concentrated is located nearby. In the context of the surrounding lighting environment and town-planning value, the luminance of the main facade of the building is too high.
13, Turgenevskaya st.			■ THE OBJECT ■ Buildings with AHL	The luminance of the lighting of the building at 13, Turgenevskaya st. is too high, which is inappropriate due to the fact that the building is not a dominant. The used methods of architectural lighting express all architectural distinctions of the building, but due to high luminance, the building is visually torn out of the evening urban environment. The Lenin square where the closest major dominants are concentrated is located nearby.

Fig.3. Example of the objects database with the existing lighting

56A, Sovetskaya st.			66 cd/m^2, the most luminous part of the light spot is 140 cd/m^2, luminance of the advertising line is 220 cd/m^2	15 cd/m^2, 200 cd/m^2 (for advertising)	Luminance standard is exceeded by 4.4 times. Average luminance of the most intensive light spot is 9.3 times higher than the standard value, the luminance of the advertising lighting is 1.1 times higher. The relation between the maximum and the minimum value of illuminance within the illuminated surface exceeds 30:1, which causes high contrast, the building volume cannot be perceived.
4 Puteyskaya st.			46 cd/m^2, the most luminous part of the light spot is 98 cd/m^2	30 cd/m^2	Luminance of the facade complies with the standard. The building of the Moscow train station is the architectural dominant of the 3rd level, therefore exceeding of the luminance standard by 50% (up to 45 cd/m^2) is acceptable.
48k1, Krasnoarmeyskiy prospect.			73 cd/m^2, the most luminous part of the light spot is 167 cd/m^2	15 cd/m^2	Luminance standard is exceeded by 4.8 times. Average luminance of the most intensive light spot is 11 times higher than the standard value. The relation between the maximum and the minimum value of illuminance within the illuminated surface exceeds 30:1, which causes high contrast, the building volume cannot be perceived.
Tula tea-party. Sculpture			7 cd/m^2	10 cd/m^2	Luminance of the monument is slightly lower than the standard. The solution is acceptable since the surface of the monument is dark.
78, Oktyabrskaya st.			37 cd/m^2, the most luminous part of the light spot is 65 cd/m^2, luminance of the advertisment is 91 cd/m^2	30 cd/m^2	Luminance of the facade complies with the standard. The building of the Church of St. Sergius of Radonezh at the Moscow Pike is the architectural dominant of the 2nd level, therefore exceeding of the luminance standard by 50% (up to 45 cd/m^2) is acceptable. Advertising illumination of the pizza restaurant is 2.5 times more luminous that the illumination of the church facade, which interferes into visual perception of the dominating object.

Fig.4. General Database of the measurement objects

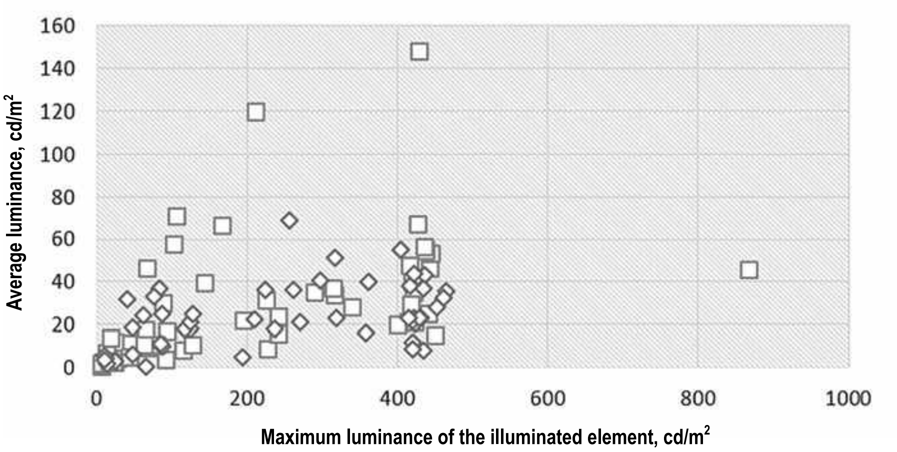

Fig.5. Average and maximum values of luminance of the analysed objects

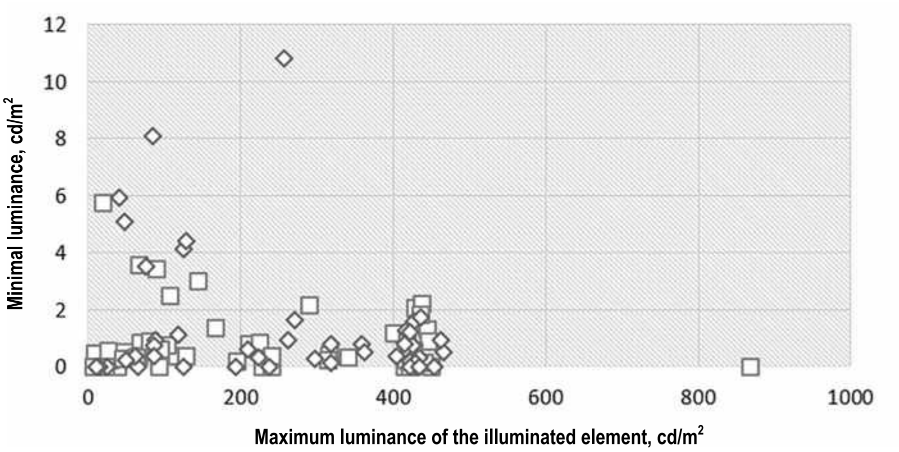

Fig.6. Minimum and maximum values of luminance of the analysed objects

inary preparation of lighting installations was not conducted [8, 9].

2. METHODOLOGY OF THE STUDY

The methodology of the study comprised town-planning analysis and subsequent photometric analysis of the existing lighting environment. The town-planning analysis comprised studying of the most important characteristics of the city, the structural analysis of the city, analysis of pedestrian routes, squares and important social centres, setting of areas of probable location of spectators and mapping of all the listed.

The objects with architectural lighting located in 11 central streets of Tula were considered during the study: Sovetskaya st., Metallistov st., Oktyabrskaya st., Lozhevaya st., Proletarskaya st., Pervomayskaya st., Friedrich Engels st., Krestovozdvizhenskaya st., Krasnoarmeysky prospect and Lenin prospect. 235 measurement files were processed, the hierarchy of the objects within the urban structure was formulated, luminance relations between the objects were analysed.

The town-planning analysis was conducted using GIS systems, the data regarding the illuminated objects was mapped layer by layer for subsequent analysis. The buildings with architectural lighting in the considered 11 streets are presented in Fig. 1.

The luminance distribution estimation was performed using the direct method by means of LMK Mobile Advanced luminance meter based on CCD matrix, matrix type: CMOS Canon APS-C, corrected for relative spectral responsivity of a standard observer, the instrument was calibrated for measurement of luminance at values of focal number ranging between F4 and F11, focus distance is 18 to 50 mm, ISO light sensitivity of 100 to 1600, resolution 5566×3706 (2748×1834 effective pixels), field angle: for focus distance of 17 mm: 65°×45°, for focus distance of 50 mm: 28°×19°, exposure

Fig.7. Evening photograph and luminance distribution over the facade, Staronikitskaya st. 1

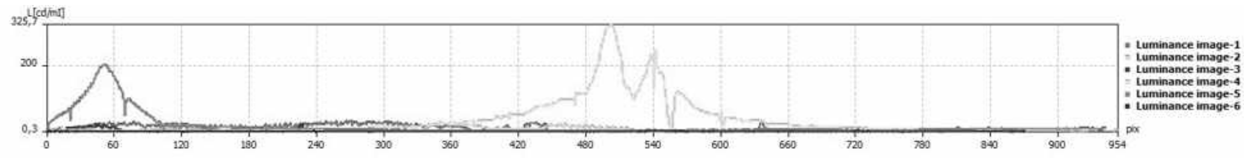

Fig.8. Relation between the values of luminance over the image, Staronikitskaya st. 1

Fig.9. Evening photograph and luminance distribution over the facade, Mendeleevskaya st.1

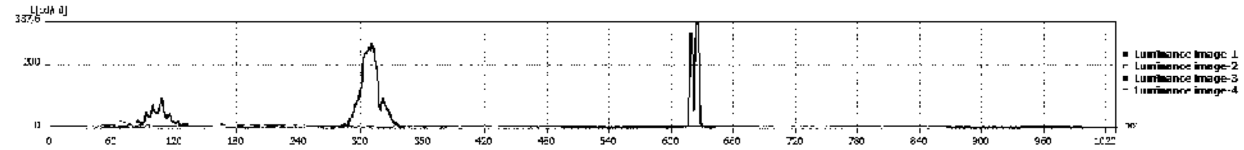

Fig.10. Relation between the values of luminance over the image, Mendeleevskaya st. 1

time 30–1/1000 s, thresholds of acceptable relative measurement error of luminance are ±5 %.

Conditions of measurements:

– The luminance meter lens is protected from entry of stray light;

– The shadow of the luminance meter or the person conducting the measurements does not fall on the measured surface;

– The luminance meter is located on the line coming from the centre of the survey area in direction of the object;

– The luminance meter is installed at height of 1.5 m from the surface of the road.

Before the measurements, preliminary preparation of the lighting installation (replacement of burned-out bulbs and cleaning of luminaires) was not performed.

Spectral responsivity of the measurement instrument is shown in Fig. 2.

The quantitative criterion of the phorometric evaluation was average luminance of the lighted element in accordance with SR 52.13330.2016 as well as the minimal and the maximum values of luminance and relation between them. In the course of the study, 56 objects were considered within the town-planning context with the existing architectural lighting, the stylistics of approaches was analysed, the data was registered in the general data base of objects [10].

3. RESULTS

The conducted study allowed us to define the most qualitatively implemented objects within the area of the city fragment limited by the 11 central streets, general trends of the existing lighting of Tula were found, put, and analysed for compliance with the major goals of lighting standardisation. The luminance characteristics of 12 out from 56 objects comply with the regulatory requirements; the average luminance level of a number of objects is more than 10 times higher than the standard one.

The data of photometric evaluation of luminance characteristics of the considered 56 objects were registered in the general data base of the objects the example of which is given in Fig. 3.

The data of measurement results was also registered in the general database of the objects and the example is given in Fig. 4.

The average values of luminance of the elements illuminated by light for 6 objects significantly exceed the values specified in regulatory requirements. For a number of objects, the average luminance value is close to the standard on, at the same time, the relation between the minimum and the maximum values significantly exceeds the values specified by SP 52.13330.2016 [10]. The values of average, minimum and maximum luminance of the illuminated elements of buildings with architectural lighting are shown in Figs. 5 and 6.

In accordance with the results of the measurements, in 82 % of cases, average luminance of the illuminated element for buildings with local lighting exceeds 10 cd/m^2. The value of 30 cd/m^2 which is the maximum acceptable value in accordance with SP 52.13330.2016 is exceeded for 54 % of objects, which leads to compositional destruction of urban fragments, irrational using of energy resources, negative affect on visual perception.

Minimal values of luminance of illuminated elements do not exceed 1 cd/m^2 in 85 % of cases. In accordance with SR 52.13330.2016, the relation between the minimum and maximum values of illuminance should not exceed 1:30. Due to the fact that the surfaces of facades may be considered diffusely-reflecting surfaces, it is possible to consider relations between minimal and maximum values of luminance instead of relations between values of illuminance. The data acquired in the course of experiments allow to make a conclusion that the acceptable level of the said relation is exceeded in 87 % of cases. This leads to compositional destruction of the facade and wrong vision of the architectural exterior of the city during night-time.

The examples of illumination methods negatively affecting visual perception of facades are given in Figs. 7–10.

4. CONCLUSION

The new generation of measurement instruments allow us to conduct comprehensive analysis of the lighting environment; therefore, increase of the quality of the conducted photometric studies is of great interest and is important for lighting quality development.

Significant non-compliance of actual values of facade luminance with the standard ones is largely owing to the fact that regulation and quality assessment of the introduced solutions are not always conducted at the moment of putting an object with architectural lighting into operation. Architectural lighting of objects is not always on the books of companies operating exterior lighting installations, and architectural lighting is not always regulated.

The results of the study confirm the importance of considering clarifications for the existing standard requirements, e.g. setting of maximum acceptable values of luminance of illuminated elements in order to maintain integrity of urban environment during evening time and rationalisation of energy resources consumption.

REFERENCES

1. Bustryantseva Natalia V. Development of the Theory of the Evening City Light Medium// Light & Engineering Journal, 2013, Vol.21, #2, pp. 21-24

2. Bystryantseva N.V., Aesthetics of Lighting Environment [Bystryantseva N.V. Estetika svetovoi sredy] // Science, Education and Experimental Design: Materials of the scientific conference of April 11–15: Theses of reports. Moscow: MARKhI, 2014, pp. 331–332.

3. Bystryantseva N.V., Formula of Light: the Study of the Lighting Environment of the Volhonka Area [Bystryantseva N.V., Formula sveta: issledovanie svetovoi sredy raiona Volkhonki] / N.V. Bystryantseva, R. Van der Heide // Territory of Culture. Volhonka Blocks: Monography

[Territoriia kultury. Kvartaly Volkhonki: Monografiia]. Moscow: Belyi Gorod Project, 2014, 115 p.

4. Shchepetkov, N.I. Lighting Design of a City: study guide [Shchepetkov, N.I. Svetovoi dizain goroda: uchebnoe posobie] / N.I. Shchepetkov. Moscow: Architecture-S, 2006, 320 p.

5. Luminance field of the façades: from aggressive to attractive lighting W. Malska, H. Wachta, Elements of Inferential Statistics in a Quantitative Assessment of Illuminations of Architectural Structures, Conference: IEEE Lighting Conference of the Visegrad Countries (Lumen V4) Location: Karpacz, POLAND Date: SEP 13–16, 2016.

6. J. Lopez-Besora, A. Isalgué, H.C. Roura, A digital image processing method for urban scenes brightness assessment, ACE: Architecture, City and Environment = Arquitectura, Ciudad y Entorno, 11 (32): 157–170, 2016. DOI: 10.5821/ace.11.32.4837. ISSN: 1886–4805.

7. T. Schielke, Tutorial: Rationale, Concepts, and Techniques for Lighting Vertical Surfaces, LEUKOS Volume: 9 Issue: 4 Pages: 223–243 Published: APR2013.

8. GOST R55707–2013 Road lighting. Methods of normative performance measurements.

9. GOST 26824–2010 Buildings and structures. Methods for measuring the luminance.

10. SR 52.13330.2016 Daylighting and artificial lighting (revised edition of SNiP 23–05–95).

Svetlana V. Kolgushkina,
Master of Engineering and Technology in Electronics and Nanoelectronics, Theoretical and Applied Lighting Engineering. She graduated from NIU MPEI in 2012. Postgraduate student of ITMO University (Saint Petersburg, Russia)

Nataliya V. Bystryantseva,
Ph.D. in Architectural Sciences, Associate Professor, head of the Light Design educational programme of the ITMO University

Viktor T. Prokopenko,
Prof., Dr. of Technical Sciences Honourable Science Worker of Russia, Professor of the Lighting Technology and Optoelectronics sub-department of the ITMO University. Graduated from the V.I. Ulyanov (Lenin) LETI State Electrotechnical University in 1963 with specialty in Dielectrics and Semi-Conductors

Light & Engineering
Vol. 27, No. 6, pp. 41–48, 2019
https://doi.org/10.33383/2018-031

THE EVALUATION OF AN OFFICE BUILDING ACCORDING TO LEED CERTIFICATE LIGHTING CRITERIA

İdil Bakir Küçükkaya[1] and Ebru Alakavuk[2]

[1]Izmir University of Economics, Izmir, Turkey
[2] Yasar University, Izmir, Turkey
E-mails: idilbakr@hotmail.com,
ebru.alakavuk@yasar.edu.tr

ABSTRACT

The progress in industrial and technological areas, which started with the Industrial Revolution, has deteriorated the ecological balance and depleted the natural resources. Sustainability, which initially seemed as a solution within this concept, became an important part of Interior Architecture as in disciplines related to design. The lighting systems of the offices that are the secondary living areas should be evaluated in terms of sustainability as well.

In this paper, the energy savings and loss of the artificial office lighting systems has been calculated according to the ASHRAE/IES standard 90.1–20078 [1] which are included in the Leadership in Energy and Environmental Design (LEED) certificate's lighting criteria [1]. The wattage of the artificial lighting systems has been calculated while the systems were in use. The results of these measurements have been compared with lighting wattage and thus the lighting energy savings and loss have been configured. The office has been comparatively analyzed according to LEED criteria.

Keywords: office, lighting, sustainability, energy efficiency, LEED criteria

1. INTRODUCTION

Natural Lighting is the lighting system designed to meet the visual comfort requirements of the daylight whose main source is the sun.

Some of the light sources produce light on their own. These are called natural light sources. Sun, stars, fireflies, lightning, streak and some species of fish living deep in the sea are natural light sources [2].

A principal characteristic of daylight is its variability. The colour of daylight changes with the time of day, the cleanliness of the atmosphere, and the inter reflection of surrounding objects. The intensity of the sun changes with the time of day, the time of year, and the latitude of the site. The luminance of the sky depends on whether the light is coming from an overcast sky, from a clear sky only, or from a clear sky and direct sunlight [3].

Direct sunlight is usually an impractical source for interiors unless it is shielded. Just as electric luminaires are designed to reduce glare, direct sunlight entering interior spaces requires careful control [3].

For centuries, daylight has played an important role regarding the design of the buildings. As a result of technological developments, the electric power started to be used for lighting and it became widespread. This situation enabled the architects to become free in their designs; however, the necessity of the careful consumption of the energy resources became a fact which has to be accepted

[1] At present time, there is a new version of this standard *ANSI/ASHRAE/IES* Standard 90.1–2016 (editor remark)

by everyone. That's why the effective use of sunlight and the creation of the solutions regarding the decrease in the consumption of electric power have become the most important topics of today's architecture [4].

Light emitting diodes (LED) is also an important solution for sustainability as an artificial lighting system. It is uses for energy efficiency at the spaces.

LEDs are light sources based on electro luminescence and are very similar to conventional semiconductor diodes. The light is generated in the depletion layer by the recombination of electrons and hole, the emitting spectra is depending on the composition of the semiconductor material. Beside the typical coloured LED also white LEDs are available since several years. The white radiation is not the direct result of the LED emission but is generated by fluorescence conversion in blue LEDs covered with a phosphor layer [5].

Sustainability has arrived in the field of interior architecture pretty late from the design-based disciplines. Lighting is one of the most important subjects designed within the framework of interior architecture. When the daylight usage is increased, used properly and supported by the least artificial lighting, the energy consumption and CO_2 emission can be decreased, the greenhouse gas emission related to energy can be prevented, and also light pollution can be decreased. In this paper, it can be seen that when the sustainable lighting criteria are applied properly, all the above-mentioned economic, social and environmental factors can be managed.

Sustainable design is an exciting area of architecture and building which has been moving into the mainstream. And there's a good reason that 'green' or sustainable buildings are also known as 'high performance buildings': they not only tend to save on running costs, there is also growing evidence that they can increase productivity and well-being for occupants through improved lighting and air quality. Where office buildings have been designed or refurbished to be more sustainable, productivity gains in terms of better quality of work and reduced absenteeism can often dwarf the reductions in energy bills [6].

In this paper, the evaluation of the artificial lighting usage of office buildings according to the LEED certificate lighting criteria is done. This is based on a DENGE Company Office, which is designed by MATT Architectural Company in Izmir. The energy savings and loss of the artificial office lighting systems are calculated and then are divided into office sections and types in accordance with the ASHRAE/IES standard 90.1–2007 which are included in the LEED certificate's lighting criteria.

1.1. LEED and Lighting

Due to the environmental problems arising from global warming, ways to decrease carbon dioxide emissions is become ever more important. According to various studies, buildings are responsible for approximately 40 % of overall CO_2 emissions in the world. Due to this fact, green building certification systems that aim to reduce the carbon emissions of the buildings and the negative impact of building construction on the environment are being developed worldwide [7].

LEED (Leadership in Energy and Environmental Design) is a product of the US Green Building Council, and is the most well-known rating system for commercial buildings. The LEED framework consists of several rating categories, applicable to different points in a building's lifecycle [8].

Within this system, in order to meet the requirements of the designed artificial environments, the building is classified according to its typologies, and 9 different options – new buildings, present buildings, commercial buildings, shell – core, schools, places for sales, health buildings, residences, urban development centres- were suggested for the planned certification. All the points needed for the certification of the building are different from each other within the framework of the each evaluation system created for each typology, and a certain value is present for each of the measurements [9].

In LEED version 4 [10] the lighting categories are:

- Light pollution reduction,
- Optimize energy performance,
- Advanced Energy Metering,
- Interior lighting.

1.1.1. Light pollution reduction

The lighting design must avoid light trespass from exterior luminaires onto neighbouring property. As well as preventing sky glow from both interior and exterior luminaires [11].

Fig.1. DENGE open office and cell office spaces (Idil Bakır Küçükkaya Photo Archive, 2015)

In LEED2009, the light trespass criteria included both a horizontal and vertical foot-candle maximum, which varied by Lighting Zone, without a lot of specificity in how the criteria should be documented. In addition, the horizontal foot candle requirement was <0.1 fc (1.08 lx), which meant that if you had a high-density design with lighting anywhere near the LEED boundary, this credit was nearly impossible to attain even if your exterior lighting was very sensible and dark-sky friendly. In LEED V4, there is only a vertical foot-candle requirement, with clear guidance on how the calculation grids should be built, or you can comply by using fixtures with an appropriate bug rating [12].

1.1.2. Optimize energy performance

This credit intends to achieve increasing levels of energy performance beyond the perquisite standard to reduce environmental and economic harms associated with excessive energy use [10].

In requirements there is an option for small to medium office building. This option is ASRAE50 % advanced energy design guide for small to medium office building.

This credit includes:

- Building envelope, opaque: roofs, walls, floors, slabs, doors, and continuous air barriers (1 point);
- Building envelope, glazing: vertical fenestration (1 point);
- Interior lighting, including daylight and interior finishes (1 point);
- Exterior lighting (1 point);
- Plug loads, including equipment and controls (1 point).

1.1.3. Interior lighting

This credit incorporates the former Controllability of Systems – Lighting credit (IEQ 6.1), with the further requirement spaces have bi-level switching [12].

1.1.4. Advanced energy metering

This credit intends to support energy management and identify opportunities for additional energy savings by tracking building-level and system-level energy use. The requirements are to install advanced energy metering for the following:

- All whole-building energy sources used by the building;
- Any individual energy end uses that represents 10 % or more of the total annual consumption of the building [10].

2. THE EVALUATION OF AN OFFICE BUILDING: DENGE OFFICE IN IZMIR

DENGE is a certified consultant company in Izmir. DENGE Office situated at thirteenth floor in Punta Residence. The settlement of the working areas is done according to 35 people's comfort and suitable working conditions.

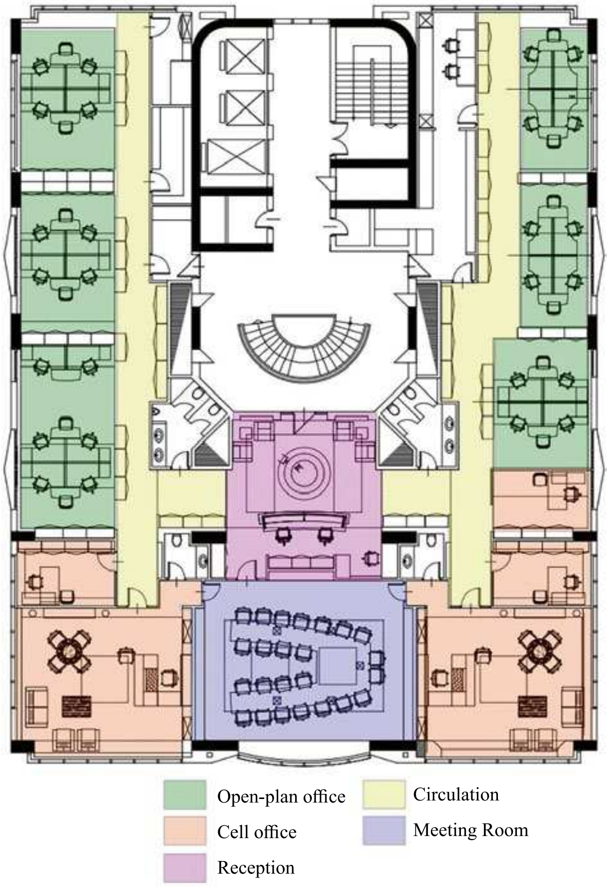

Fig.2. DENGE office layout

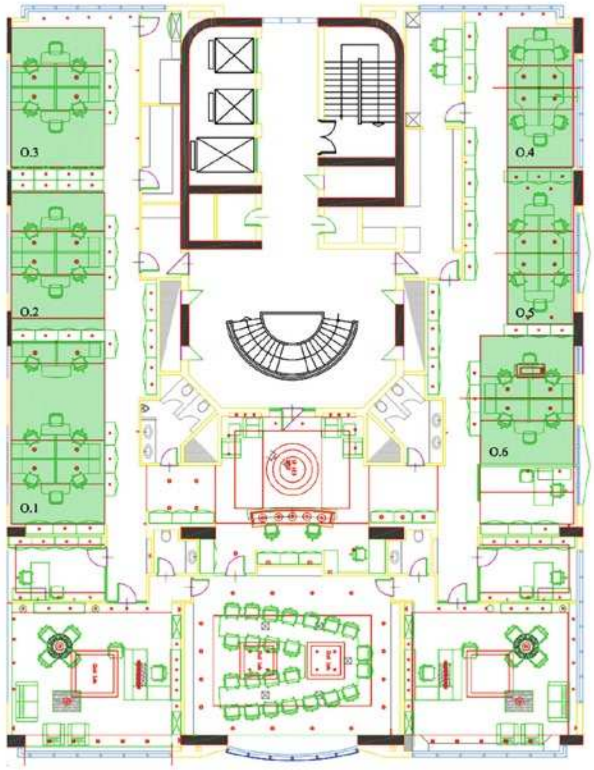

Fig.3. DENGE office lighting layout

This office includes both, cell and open-plan offices, a conference room, kitchen, bathrooms, reception, corridors, storage and a technical room. The lighting systems are designed according to this office models.

In the DENGE Office, the natural and artificial lightings are designed together. The location of the building is situated very convenient for fluent usage of daylight as seen in Fig.1. The spotlight systems are used to provide aesthetic view. The spotlights are chosen as LED lighting spots for reducing the energy demand for lighting. Above every worker spotlights are located providing working conditions very comfortable without glare. In the corridors, reception and the cell offices, wall fixtures are used to illuminate the paintings by creating an aesthetic view and also illuminating corridors [13].

The Layout diagram illustrates a typical space, identifying the specific locations where lighting and energy performance have been calculated, Fig.2.

The DENGE office lighting layout is shown in the Fig.3. At the top of each table in open office space there is a drop ceiling and the spotlights are fixed in them. Tiny LED spotlights are also located at the top of the closets. In cell offices, it has six types of lighting fixtures. There are round and square spotlights, wall (painting) fixtures, two types of ceiling lightings, and also LED band lightings. At the top of the working table spotlights and ceiling light is located. The drop ceiling has concealed lightings, which is LED band lighting. The other ceiling light is the top of the meeting table and visitor's coffee tables. In the meeting room, a lot of spotlights are used. It has drop ceilings which has concealed lightings. The lightings are located according to chairs and tables places. In the entrance of the DENGE office there is a drop ceiling with the 18 pieces power LED (1 watt) and concealed lighting. Top of the reception tables, there is ceiling fixtures and wall fixtures. At the side of the door, there are two niches with the spotlights. LED lighting was used through the corridors. And there is also wall lighting and drop ceiling with the concealed lighting. And top of the cabinets, there is spotlights, Table 1.

The calculations of the lighting power presented in Table 2 are added to the number showing the power of the lighting written on the "watt" section, and were divided with square meter. Presented in Table 2 lighting energy saving are as follows: open office 1–68 %, open office 2–31 %, open office

Table 1. DENGE Office Lighting Systems Analyses

	Luminaire	Nominal Size	Light Source	Power, W	Luminous flux, lm	Voltage	Rated life, h
Open Office Lighting Systems	NASSA LED Spotlight	Radius 19.5	LED	18	2000	85–265	50000
	NASSA LED Spotlight	Radius 15.5	LED	20	2000	86–265	50000
Cell Office Lighting Systems	NASSA LED Spotlight	13×13×8 cm	LED	20	2000	85–265	50000
	NASSA LED Spotlight	Radius 15.5	LED	20	2000	86–265	50000
	NASSA Jupiter Ceiling lighting	35×35×37 cm	Energy Smart Bulb	40	475	220–240	8000
	PHILIPS	206×117×5 cm	Fluorescent	28	2900	230	24000
	NASSA Wall Fixture	53×52×29 cm	4xE4	2×20	2000	230	24000
	NASSA Band LED Lighting	16 m	3x300 LED	14,4 (1 m)	475	12	24000
DENGE Meet-ing Room Lighting Systems	NASSA LED Spotlight	Radius 19.5	LED	18	2000	85–265	50000
	NASSA LED Spotlight	Radius 15.5	LED	20	2000	86–265	50000
	NASSA Band LED Lighting	16 m	3x300 LED	14,4 (1 m)	475	12	24000
DENGE Reception Lighting Systems	NASSA POWER LED	Radius 5	LED	1	130–150	3–4	10000
	NASSA LED SPOTLIGHT	Radius 15.5	LED	20	2000	86–265	50000
	NASSA Jupiter Ceiling lighting	35×35×37 cm	Energy Smart Bulb	40	475	220–240	8000
	NASSA Wall Lighting	10×10×18 cm	Halogen	20	320	12	2000
	NASSA Spotlight	6×6×8 cm	LED	20	2000	86–265	50000
	NASSA Band LED Lighting	16 m	3x300 LED	14,4 (1 m)	475	12	24000
DENGE Corridors Lighting Systems	NASSA Wall Fixture	53×52×29 cm	4xE4	2x20	2000	230	24000
	NASSA LED Spotlight	Radius 15.5	LED	20	2000	86–265	50000
	NASSA Wall Fixture	10×10×18 cm	Halogen	20	320	12	2000

3–41 %, open office 4–56 %, open office 5–12 %, open office 6–53 %. At the office's cabinets: 1 shows 59 % loss, 2 shows 59 % loss, office cabinet 3 shows 18 %, cabinet 4 shows 18 %, and office's cabinet 5 shows 18 % lighting power loss. According the results of meeting room 21 % loss of energy is obtained, 9 % energy loss in lighting power is obtained at the reception, and 100 % loss of lighting power at the corridors.

As shown in Table 3, appropriate watt according to ASHRAE and the current watt at the office are compared and then the amount of power savings are calculated. The lighting power saving of the DENGE office is 3 % in total, which is a low rate in comparison to the desired 10 % according to LEED certificate.

DENGE office building which is without a certificate is presented with lighting projects, analyzed regarding lighting in terms of sustainability, and measured in terms of their lighting power. According to the results seen in Table3 DENGE Office only shows 3 % energy saving. Even though DENGE Office is not sustainable, energy saving is provided only by using the efficient types of light.

According to the LEED certificate, in the criteria of optimize energy performance, the saving must be 10 % in general office buildings. DENGE Office can't provide this rate. DENGE Office consumes more than enough lighting power. According to the results, in the meeting rooms and corridors, DENGE Office consumes more than enough energy. Especially in the corridors section, the wall

Table 2. DENGE Open Office and Cell Office Lighting Energy Analyses

Lighting Space	Area, m^2	% of total	Standard 90.1 Allowance		Connected power, W	Savings, %
			W/m^2	Power, W		
Cell Office 1	49	6	12	588	933	–59
Cell Office 2	49	6	12	588	933	–59
Cell Office 3	12	2	12	144	170	–18
Cell Office 4	12	2	12	144	80	18
Cell Office 5	12	2	12	144	170	–18
Open Office 1	34	4	12	408	132	–68
Open Office 2	28	4	12	336	232	31
Open Office 3	30	4	12	360	212	41
Open Office 4	25	3	12	300	132	56
Open Office 5	20	3	12	240	212	12
Open Office 6	20	3	12	240	112	53

lightings and spotlights indicate a 100 % over-used lighting.

Table 4 shows the interior lighting criteria of LEED certificate's implementation and evaluation on the DENGE Office project. While the sustainable Office Buildings include all of the lighting criteria such as controllability of lighting systems, interior lighting quality, optimized energy performance, daylight and view, DENGE Office does not. In the DENGE office, the Artificial Lighting Systems aren't controlled. As a result, DENGE Office Building doesn't provide the LEED sustainable lighting criteria [13].

3. CONCLUSION

In this paper, the energy savings and loss of the office artificial lighting systems is calculated according to the ASHRAE/IES standard 90.1–2007 which is included in the LEED certificate's lighting criteria. The wattage of the artificial lighting systems of DENGE Office is calculated while the systems were in use.

As a result of this evaluation, for DENGE Office the lighting energy savings or loss for open offices is the 45 % savings, for cell offices – 0,3 % loss. Energy saving through individually controlled artificial lighting with sensor of daylight for meeting rooms that has been made by DENGE office, the percentage could decrease drastically about 21 % loss. For reception areas are 9 % of losses and for circulation areas are 100 % losses in lighting energy saving. This percentage is considerably high. These are significant losses both, economically and environmentally. The lighting energy saving is not sufficient regarding circulation areas. Luminaires choices were not selected adequately and further studies must be done about this subject.

DENGE Office only fulfils suitable fenestration and interior configuration criteria. The most important for lighting energy saving is suitable and efficient luminaire specification. Because of the unsuited luminaire choices; DENGE office has a large loss of lighting energy in circulation areas, meeting room and reception areas. The lighting systems should be controllable and supported by daylight-connected sensors. The lamps of the lighting systems should be changed into LED lights. In the circulation areas which consume the energy the most, the spotlights should be changed and the wall lightings should be replaced by lighting systems with led lights which consume less energy. In the reception areas fewer spotlights should be used, their lamps should be replaced by LED lights. In the cell

Table3. The Lighting Energy Savings or Loss Calculation of DENGE Office

Space	Area m^2	% of Total	Standard 90.1 Allowance		Connected, W	Savings (–)/loss, %
			W/m^2	W		
Open Offices	157	20	12	1884	1032	–45
Cell Offices	134	17	12	2278	2286	0.3
Meeting Room	65	8	11	715	872	21
Corridors	102	13	5	510	1025	100
Reception	45	6	14	630	691	9
Other	297	37	10	2970	2820	–5
Total	800	%100	–	8987	8726	–3

Table4. The Assessment of DENGE Office with the LEED Sustainable Lighting Criteria

Credit	Description	
SS Credit 8	Light Pollution Reduction	Not in Scope
EA Prerequisite 2	Minimum Energy Performance	Achieved 3 % reduction in lighting power
EA Credit 1	Optimize Energy Performance	Achieved 3 % reduction in lighting power
IEQ Credit 6.1	Controllability of Systems -Lighting	The Artificial Lighting Systems aren't controlled.
IEQ Credit 8.1	Daylight and Views – Daylight	Insufficient
IEQ Credit 8.2	Daylight and Views – Views	Insufficient
Pilot Credit 22	Interior Lighting – Quality	Insufficient

offices, fewer spotlights should be used and when it comes to individual lightings, less-energy using lightings should be preferred. By these ways the energy performance in the office can be optimized. The eye exhaustion and screen glare of the employees will disappear and the work efficiency will increase.

As mentioned in the LEED criteria, providing the requirements carries great importance for the lighting control. Controllable systems should be designed for the building and automatic lighting systems connected to a general system should be implemented. LED lights, which have great effect on energy savings in artificial lighting systems, should be used. Implementation of these criteria can increase the productivity of the employees.

The issues studied, analyzed and presented in this paper can serve as a guideline for a designer. The design of the lighting systems should be managed in order to provide visual comfort conditions in the office and also to reduce the energy consumption; and within this subject it should be improved by using technological methods.

Finally, all of the studies about sustainability aim to leave a sustainable world in which the future generations can live, the resources are efficient, and there is no light pollution. Lighting covers a great part of this cycle. In all of the studies that are being or will be done, the understanding of a sustainable design is required. All around the world including Turkey, interior architecture and the other disciplines related to design should accept the subject of sustainability as a priority, embrace the sustainable lighting criteria and feed it with modern methods. In the offices in which people spend most of their time, lighting systems that provide comfortable study areas without any glare effect on our eyes, efficient daylight angle support the artificial lighting and spend less energy in an appropriate way.

REFERENCES

1. ASHRAE/IES, 2007, Standard 90.1for Energy Standard for Buildings Except Low-Rise Residential Buildings, USA.

2. Kılıçaslan, U.G., 2011, Aydınlatma Tasarımı Kriterlerinin Hastane Mekanlarnda İrdelenmesi, Yüksek Lisans Tezi, MSÜ Güzel Sanatlar Fakültesi, İstanbul, 159p. (Published)

3. Gordon, G., 2003, Interior Lighting for Designers, ss. 292. John Wiley & Sons, Inc. New Jersey.

4. Yener, A.K., 2008, Binalarda Günışığından Yararlanma Yöntemleri, Çağdaş Teknikler VIII. Ulusal Tesisat Mühendisliği Kongresi 231 Sempozyum Bildirimi, 11p

5. Pohl, W. and Zimmermann, A., 2003, SynthLight Handbook Artificial Lighting, ss.66. Munich.

6. http://www.morganlovell.co.uk/knowledge/white-papers/sustainable-office-design-unlocking-performance-and-productivity.

7. Ilıcalı, E. and Somalı, B., 2009, LEED ve BREEAM Uluslararası Yeşil Bina Değerlendirme Sistemlerinin Değerlendirilmesi, ss.1081–1082. IX. Ulusal Tesisat Mühendisliği Kongresi, İzmir.

8. http://www.betterbricks.com/graphics/assets/documents/RatingSystem_Final.pdf.

9. Uyan, F. Binalarda Aydınlatma Sistemlerinin Sürdürülebilirliklerini değerlendirme ilkeleri, 2010, İstanbul.

10. LEED, 2013, Version 4 Reference Guide for Building Design and Construction.

11. Philips, 2012, Lighting for LEED Application Guide for Sustainable Offices, ss.19. New York.

12. http://www.maxpierson.me/2013/08/01/leed-v4-for-the-lighting-designer/.

13. Bakır, I. The Evaluation of the Office Buildings According To LEED Certificate Lighting Criteria. Yaşar University Graduate School of Natural and Applied Sciences Interior Architecture Master Thesis, Izmir, 2015.

İdil Bakir Küçükkaya

M. Sc., she studies on sustainable lighting systems and biophilia. Since September 2017, she has been studying Design Studies Ph.D. at İzmir University of Economics

Ebru Alakavuk,

Ph.D., Yasar University. She studies on sustainable buildings, advanced facade systems and advanced construction systems

Light & Engineering
Vol. 27, No. 6, pp. 49–57, 2019 *https://doi.org/10.33383/2017-101*

OPTICAL UTILIZATION FACTOR FOR ARCHITECTURAL LIGHTING

Cătălin Daniel Gălăţanu[1]*, Muhammad Ashraf[2], Dorin Dumitru Lucache[1], Dorin Beu[3], and Călin Ciugudeanu[3]

[1]*Technical University "Gh. Asachi", Iaşi, Romania*
[2]*Capital University of Science and Technology (CUST), Islamabad, Pakistan*
[3]*Technical University Cluj Napoca, Romania*
**E-mail: catalin.galatanu@tuiashi.ro*

ABSTRACT

Optical utilization factor (OUF) is applied to architectural lighting, searching to obtain low light pollution. It is demonstrated that OUF could not be used for the assessment of light pollution, because the inter-reflections could not be neglected. DIALUX simulations and MATLAB original functions are used. Onsite measurements for illuminance and luminance are performed. It is demonstrated that OUF could be greater than one for the facade. For the small scale inter-reflections, a luminance gain is demonstrated. Due to this, the floodlighting could be reduced. The understanding about the light pollution assessment is changed, which is a major achievement. It means that a greater OUF don't represent a lower light pollution, and also a facade could be more "visible" on lower level of floodlighting.

Keywords: luminance gain, concave inter-reflections, luminance measurements, mesh generation

1. INTRODUCTION

The traditional light pollution approach is based on visual comfort and saving energy. Light pollution is seen as an individual comfort criterion, and not at global scale as today, when one finds "studies for limiting the impact of light pollution on human health, environment and stellar visibility, the effects of light pollution on ecosystem and countermeasures or even focusing on society's disregard for the loss of a cultural asset that has been a part of art, science, and culture for as long as these things have existed" [1]. One direction of the researchers is to measure the global light pollution, observing the sky glow [2]. Other approach is focus on the sources of Light pollution. Obviously, the main source of light pollution is the street lighting, but the architectural lighting has also an important weight factor [3, 4]. Leaders in the fight of reducing the light pollution are astronomers, but with a wider approach [5]. Other interesting example is STARS4ALL network, a project funded by the European Union H2020 Program. This project is based on a comprehensive definition: "Light pollution is excessive, poorly directed or unnecessary artificial light at night" [6]. This definition is very clear with the terms excessive and poorly directed, but unnecessary could generate a special discussion, especially in context of facade lighting. The paradigm of this paper consists in the acceptance of hypothesis that the light is necessary for the beautification of the facade, with non-excessive level and perfectly directed, but the light pollution level could be different. This aspect could optimize through the Optical utilization factor (OUF). A supplementary example about the necessity of this study one find in [7], where light pollution is seen only like obtrusive lighting, sky glow, disability glare and trespass lighting are mentioned.

Optical Utilization Factor (OUF) demonstrates his relevance also in [8], where the real dimension of the problem can be found: "The dominant part of the light source luminous flux (70–80) % misses the building and is emitted towards the sky. This fact is much more important for determining light pollution than the fact when light reflected from even a too brightly illuminated facade" [8]. This estimation enhances the importance of OUF, more than traditional approach [9], where utilization factor (UF) was used as an indicator for energy efficiency of road lighting. From [10] one could take more similarity between facade lighting and road lighting, considering "the road lighting energy efficiency evaluation based on the normalized power density including the impacts of the applied lighting equipment, the reflection properties of the road surface (facade!), and the maintenance factor. The road lighting energy efficiency evaluation based on the installed power density permits including, in addition, any over sizing of lighting arising from too high (irrational) levels of road surface luminance compared to the required levels (or facade!)".

2. THE RELEVANCE OF OPTICAL UTILIZATION FACTOR (OUF)

OUF is a classical indicator in designing interior artificial lighting or street lighting. OUF is still used in recent papers [6].

OUF is the ratio of the lumens actually received by a particular surface to the total lumens emitted by a luminous source.

A specific definition, adapted to floodlighting is given below:

$$FUF = \frac{\varnothing_u}{\varnothing_t}, \quad (1)$$

where:

FUF – floodlighting utilization factor, similar to OUF,

$\varnothing_u$ – useful luminous flux

$\varnothing_t$ – rated luminous flux of the light source

The light output ratio (LOR) of luminaire is also very important parameter as the total loss of light energy including transmission through fittings is also taken into account.

The following expression (2) is used.

$$LOR = \frac{Output\ of\ Luminaire}{Output\ of\ luminous\ source}\ . \quad (2)$$

This convention could be accepted (FUF is equivalent to OUF), but the next affirmation, in equation (3) from [10], must be analyzed carefully:

$$FUF \le LOR \quad (3)$$

Any attempt to deny equation (3) seems to deny energy conservation law. Contrary this, one demonstrate that equation (3) is not true. The argument is based on inter-reflections (The illumination of an object by reflected light from other objects that are not light sources), which generates an effect of "multiplying" the luminous flux. After the demonstration of this, one uses the results to obtain the maximum visual effect with minimum luminous flux, equivalent with a reduction of light pollution.

A discussion is necessary, because ϕ_u (useful luminous flux) is not a theoretical parameter. Also in [10] it is determined using the luminance measurement of the facade, which includes, finally, the inter-reflections!

Following the same author, in [11] discovered details about how useful luminous flux is measured, based on field luminance measurements: "When the average level of luminance of the facade, its surface S and reflectance factor ρ of its materials are known, it is possible to calculate the useful luminous flux … (assuming that there are no inter-reflections)". But this last hypothesis was not studied at all in [10], and for a large number of facades (different from a flat surface) it is difficult to be accepted that the inter-reflections are absent.

3. THE FLUX AMPLIFICATION FACTOR OF CONCAVE INTER-REFLECTIONS

The idea of flux amplification factor is based on the well-known expression of illuminance in an integrating sphere [12]:

$$E_{fin} = E_1 \frac{\rho}{1-\rho}\ , \quad (4)$$

where

E_{fin} is the final (after inter-reflections) illumination in interior of the sphere,

E_1 is the initial (direct) illumination in interior of the sphere (lx),

ρ is the reflectance factor of the interior surface.

Obvious, affecting the equation (4) with the interior surface of the sphere (S), one obtains the expression of useful luminous flux:

$$\varnothing_u = \varnothing_t \frac{\rho}{1-\rho}, \quad (5)$$

Table1. Luminous Intensity for the Lighting Fixture Used In DIALUX Model

Angle	0°	1°	2°	3°	4°	5°	6°	7°	8°	9°
cd/1000 lm	8000	7900	7800	7700	7500	7200	6800	6300	5700	0

Table2. The Results Obtained from DIALUX Simulation (see Fig.1.)
(S_{facade} is the target surface, M_f is maintenance factor, and E_{med} is average illuminance)

	Entry				Results		
Symbol	$\varnothing_t$	S_{facade}	M_f	LOR	E_{med}	$\varnothing_u$	OUF
Units	lm	m^2	-	%	lx	lm	%
Values	2700	1.2x4	0.85	46.7	223	2696	99.8

Notice: the value for OUF is practically 100 % but its calculated value is 99.8. It is due to error as there is lack of sufficient decimals in DIALUX.

whence follows equation (6):

$$OUF = \frac{\varnothing_u}{\varnothing_t} \cdot 100\ \% = \frac{\rho}{1-\rho} \cdot 100\% > 100\%. \quad (6)$$

Off course, OUF is greater than one for an integrating sphere due to a maximum inter reflections phenomena. It can be concluded that for other facade configurations the OUF will be in different proportion. To observe this, one should start from simple hypothesis to more complexes one.

3.1. The Perfect Planar Facade

This is the most common situation, considered to represent a reference for the next configurations.

The DIALUX model is based on a vertical facade, dimensions 1.2 m x 4 m (surface area) implemented with a cuboid with 0.5 m thickness, positioned at (0, 4, 0) and rotation (0°, 0°, 180°). The dimensions give the possibility to replicate the model in DIALux. A floodlight is orientated from a distance of 0.3 m to the facade, respectively from the point in DIALux coordinates (0; 3.4; 0.1) and an angle of 165° from horizontal, respectively (0°; 165°; –90°). The floodlight has a source of 2700 lm, with LOR = 46.7 %. This extremely low value is calculated in LDT Editor Software (by DIAL), after the original file of the luminaire was modified, in order to eliminate the luminous intensity emitted over 9° from optical axis. The purpose of this constraint is to impose an OUF equal with 100 %, based on a total control of light. Considering a punctual rotational-symmetrical lighting fixture, the values imposed for this luminous intensity are presented in Fig.1. and Table 1.

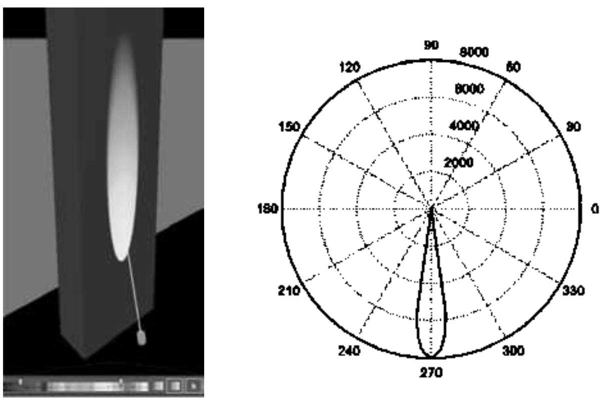

a) b)

Fig. 1. The DIALUX model for a planar facade (a), and the polar curves for luminous intensity *(cd/1000lm)* of the luminaire (b)

The results (Table 2) are predictable, but useful for the next considerations.

We anticipate that OUF equal with 100 % is not the ideal situation, in the sense that no spilling light is generated by the luminaire. A fast estima-

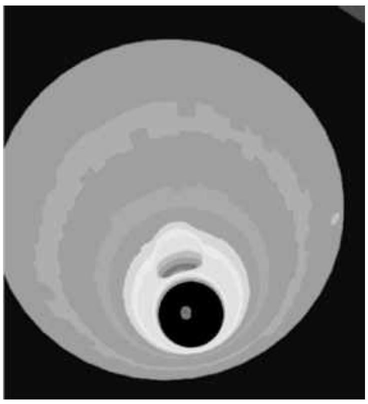

Fig. 2. The interreflections in an interior of a cylinder

Table 3. Optical Utilization Factor for the Cylinder Used in DIALUX Model

Wall reflectance	0.0	0.10	0.50	0.86
$\varnothing_u$ – useful luminous flux (lm)	2715	3110	23885	30340
$\varnothing_t$ – total luminous flux (lm)	2700	2700	2700	2700
OUF	1	1.152	8.846	11.237

The OUF for an integrating sphere.

Wall reflectance factor (ρ)	0.0	0.10	0.50	0.86
$OUF = \dfrac{\rho}{1-\rho} + 1$	1	1.11	2.0	7.14

tion can be done with (5), considering a white painting ($\rho = 0.86$) for that the flux amplification value results greater than six!

3.2. The Useful Flux Amplification from a Complete Cylinder

The inter-reflections on the usual facades are generated by cylindrical shape, in a small scale (window framing) or in a larger scale (on soffit or arches). In order to estimate the possible values, the limit of the useful flux amplification will be generated by a close cylinder by similarity with the integrating sphere as shown in Fig.2.

For a better understanding, Fig.2 was obtained by maintaining the lamp in the same position as in Fig.1.The wall is replaced by a cylinder with 0.3 m radius and positioned at (0, 3.4; 0.1). The height of the cylinder is the same 4 m, and the number of elementary surfaces used to approximate the cylinder was 44 (dimensions 42.84 mm x 4 m, equivalent to surface equal to 0.17136 m^2). For every individual surface in Fig.3, an average illuminance (lx) was calculated, giving the possibility to compare the direct illumination (available for reflection factor $\rho = 0.0$) with the other situation, where inter-reflections are presented with $\rho = 0.10$; $\rho = 0.50$ and $\rho = 0.86$. Result shows that $\rho = 0.10$ is very close to direct illumination and $\rho = 0.86$ gives maximum inter-reflections.

A technical observation is necessary: due to specific export of the results from DIALUX, all the data must be extracted individually, especially because in DIALUX the cylinder is solved like a collection of disconnected elements with particular values, not as a specific vector. Even with those difficulties, one obtains the balance between total flux of the lamp $\varnothing_t$ and useful luminous flux $\varnothing_u$ on the cylindrical wall:

Once again, OUF indicates that the total luminous flux will be amplified by the interreflections. Due to the specific method of computing of DIALux (photon method) and the difficulties in setting the calculus points for the cylindrical elements, a certain uncertainty over the results from Table 3 must be avoided. The main source of uncertainty is the comparison with the integrating sphere, where

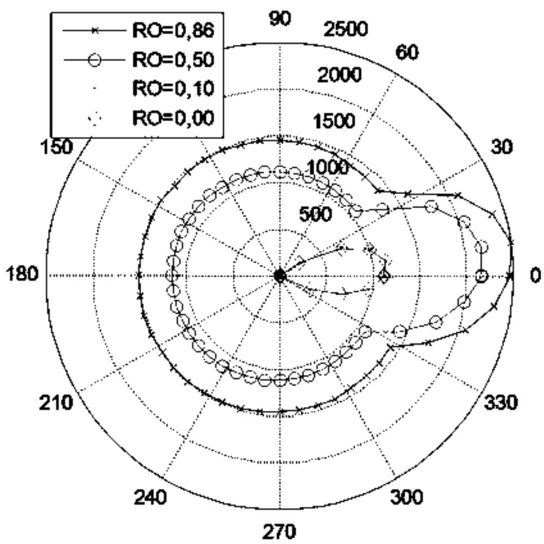

Fig. 3. The average illuminance (*lx*) in the interior of the cylinder, for different reflection factors RO(ρ)

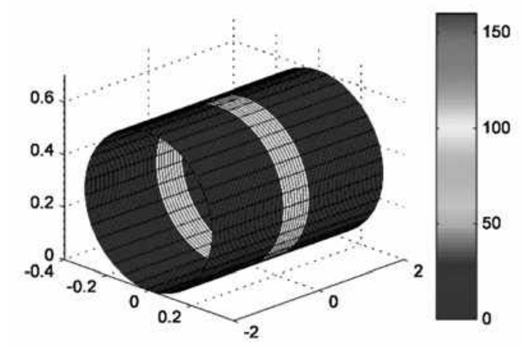

Fig. 4. The MATLAB model for interreflections in a close cylinder (initial illuminance,100 lx)

Table 5. The OUF Calculation After Every Reflection in the Cylindrical Concavity

No.. of reflection	1	2	3	4	5	6
Transmitted Flux (lm)	5679	1587	512	159	50.2	15.7
Attenuation	-	0.279	0.323	0.312	0.314	0.313
Total flux (lm)	5679	7267	7779	7939	7990	8005
OUF	1.000	1.279	1.370	1.398	1.407	1.409

the OUF has a well-known value, calculated starting from the constant of the sphere $\rho/(1-\rho)$ in addition with one (the direct illumination from the source), as in Table 4:

This correction is possible using the exact calculus of the interreflections, developed in MATLAB by the authors.

3.3. The MATLAB Calculation for OUF for a Complete Cylinder

The interior of a similar cylinder as in Fig. 2, with diameter of 0.6 m and length of 4 m was generated in MATLAB. A direct illumination was imposed for a central region, with a constant level of 100 lx. This hypothesis could simplify the analysis of the reflected flux, with contribution to the final value of OUF. The advantage of MATLAB calculation consists in successive evaluation of every reflected flux.

Mesh generation for this cylinder is presented below:

R=0.3m;% Radius of the cylinder used for interior inter-reflections

j=1–59, Number of elements on the generatrix of the cylinder

i=1–36, Number of elements on the directrix of the cylinder

*XCIL(j, i)=R*cos((i-1)*2*pi/35);% domain (–0.5 to 0.4) in Fig.4*

*YCIL(j, i)=2-(j-1)*4/58;% domain (–2 to 2) in Fig.4*

*ZCIL(j, i)=.30-R*sin((i-1)*2*pi/35);% domain (0 to o.6) in Fig.4*

end

end

After the imposing of the direct (initial) illumination level equal to 100 lx (light grey colour in Fig.4), the initial model for inter-reflections in MATLAB was obtained:

The inter-reflections in the deep interior of the cylinder ***follow the model of the integrating sphere*** as in Table 4. It is due the fact that the luminous flux spill through the extremity of the cylinder could be neglected (as it is 4 m long). In this way a fast confirmation of the precision of our calculation is obtained.

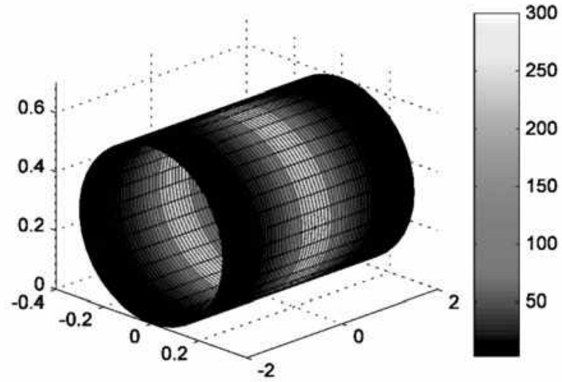

Fig. 5. The interior illuminance (lx) after six inter-reflections

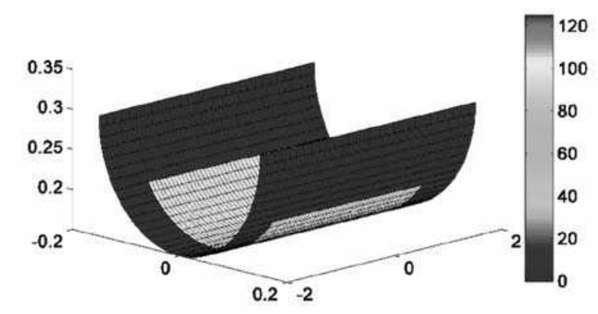

Fig. 6. The cylindrical concavity, with initial direct illuminance (lx)

A visual examination indicates that luminous flux, *after six Lambertian reflections*, is located in the central region of the cylinder also, as shown in Fig.5.

3.4. The OUF of a Cylindrical Concavity of a the Facade

After the previous validation of the MATLAB model, a general situation of a cylindrical concavity with a central illuminated zone could be evaluated. This hypothesis is based on the small or medium size concavity in facades, and the purpose is not the

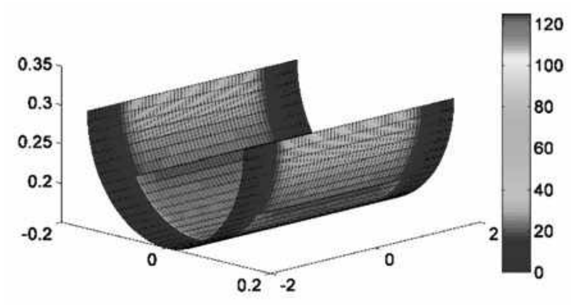

Fig. 7. The cylindrical concavity with final reflected illumination after six steps

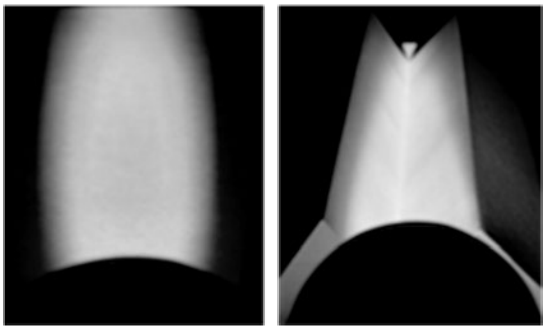

a) b)

Fig. 8. The image for luminance measurement for (a) the planar surface and (b) prismatic concavity

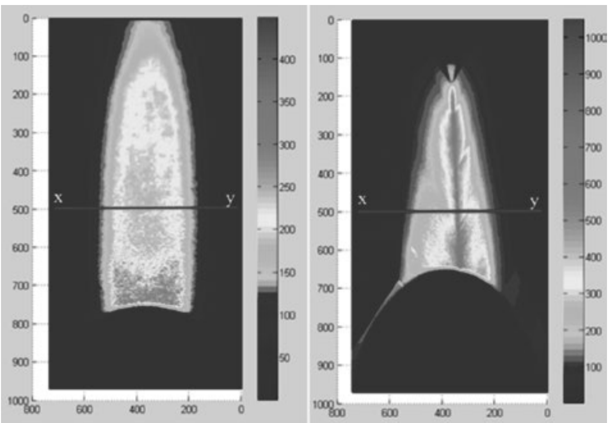

a) b)

Fig. 9 The luminance (cd/m^2) for the planar surface (a) and prismatic concavity (b)

calculation of the OUF, because it depends by random factors. OUF is greater than 100 %, just to illustrate that OUF is not a good indicator for light pollution.

In Fig. 6 the initial configuration is presented with 36 x 56 cylindrical elements, illuminated with 100 lx (from element 9 to 28 on the directrix and from element 9 to 49 on the generatix).

In Fig.7 the total reflected flux after six steps of cflculations can be visualized.

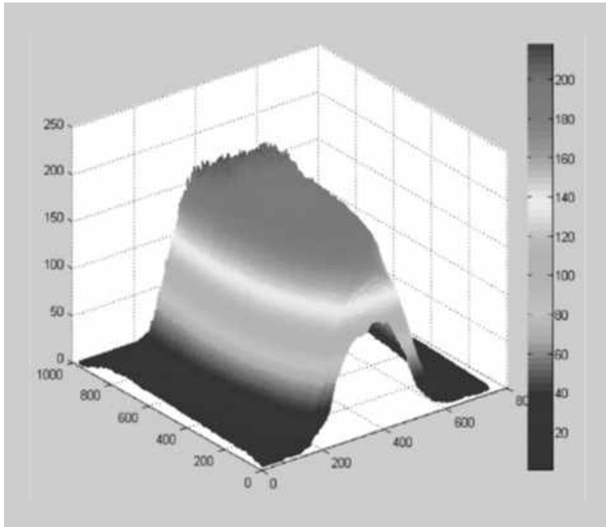

Fig. 10. The RGB values for the flat illuminated surface of the facade, as in Fig.9, a.

After qualitative assessment, a quantitative assessment is available in Table 5, where the reflected luminous flux is evaluated at every step.

A fast comment is very important, because after sixth inter-reflections, the luminous flux has decreased significantly and may be neglected. Even in this particular situation, value of OUF changes very fast and becomes bigger than 1 (or 100 %), indicating that OUF could not be used for as a quality light pollution indicator.

4. MEASURING THE OUF AUGMENTATION

A higher OUF represents a good objective for designing to obtain low light pollution, even if it will not be an objective criterion. Using inter-reflections, where the facade gives the possibility to increase the luminance of the facade, with the same luminous flux emitted by the luminaires. An experimental demonstration will bring the scale of benefit when inter-reflections on facade are involved. A simple test bench was used, consisting in a floodlight working tangential on a planar surface. This initial configuration serves like a referential for the situation when the planar surface is replaced by a decorative prismatic profile surface of 3cm at an angle of 80°. The field luminance was measured, using a photo camera with the same parameters of exposure and particular transformation from RGB to luminance [13, 14]. In Fig.8 the visual aspect of the bench and in Fig.9 the luminance (cd/m^2) are presented.

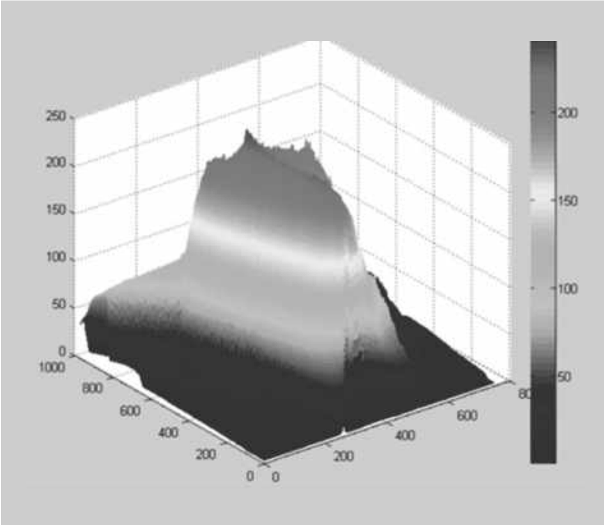

Fig. 11 The RGB values for the prismatic concavity illuminated in the same condition as in Fig. 10

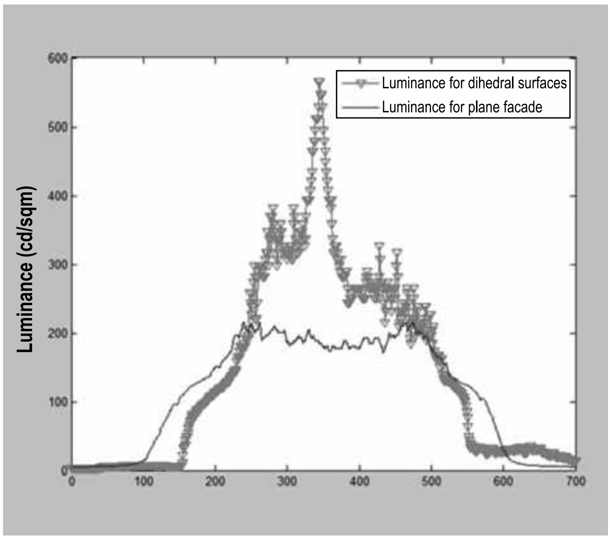

Fig. 12 Luminance comparison (cd/m2) for central field of the images from Fig.8, with specification x-y in Fig. 9

The initial results for Fig.9 (a) are presented in Fig.10, where it can be noticed that the luminance in the central illuminated region is cvasi constant, with RGB level close to the value of 180.

After the introduction in the luminous field of a small prismatic concavity (without any other change), the luminance field generates different results, as shown in Fig. 11.

In Fig. 11 it is illustrated that the data from Fig.9 (b), and the luminance in the central field has an obvious increase with maximum RGB values close to 230. The interior dihedral angle has a higher luminance, which is a positive effect considering the accent on the facade. It is worth mentioning that this effect is obtained with the same lighting configuration as in Fig.8.

Even after a qualitative conclusion obtained from Fig. 10 as compared with Fig.11, a quantitative assessment of the luminance is necessary, based on the fact that the CCD sensor (used for this work is NIKON D5300 photo camera) has not linear characteristics [13, Fig.1] and introduces a saturation effect for higher values of luminance. Using an experimental OECF (optoelectronic conversion function) obtained for our photo camera and considering the particular settings (exposure time 1/20s, diaphragm F8 and ISO100), luminance (cd/m^2) for those two different hypothesis is presented.

In Fig.11 the luminance field has different colour map as compared to Fig.10, but it can be noticed that the effective differences are very high. To obtain the increase in intensity, the luminance values from the direction x-y (the horizontal line in Fig. 9) are extracted and presented on the same plot and the same axis for a better comparison as in Fig. 12.

In absolute values, the amplification effect of the luminance is greater than double, and this is another interesting effect, giving the possibility to obtain the same visual effect with less luminous flux and less light pollution. A supplementary comment is necessary for the high level of the luminance in Fig. 12, which was chosen due to the small scale of the model.

5. LUMINANCE GAIN ON MULTI LONGITUDINAL PROFILES

For architectural details, the luminance gain generated by the longitudinal profiles could be useful to decrease the floodlighting level, due the increasing of luminance contrast on some window frames, for example. The decreasing of the general floodlighting represents the method to reduce the light pollution. To demonstrate how the luminance gain occurs, one study not a prismatic concavity as in Fig.8, but one compare the luminance obtained from a flat facade (Fig.13, a) with a facade with one longitudinal (triangular) profile (Fig.13, b), respectively three longitudinal profiles (Fig.13, c).

The transversal luminance, for the midle of the scene, will demonstrate the luminance gain, as in Fig.14.

Finally, introducing three longitudinal profiles, one can compare all three scenes.

The profiles dimensions are 25 mm at the base and 48 mm in height, and the material is bright

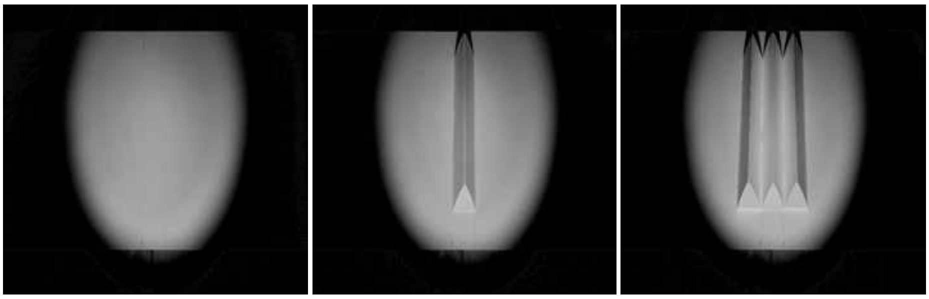

a) The flat facade b) Facade with one profile c) Facade with three profiles

Fig. 13 Luminance gain on longitudinal triangular profiles

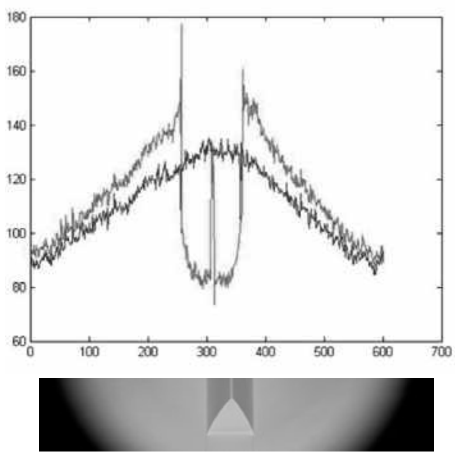

Fig. 14 Luminance gain (cd/m^2) from one longitudinal profile (upper curve) compared with the flat facade luminance (lower curve)

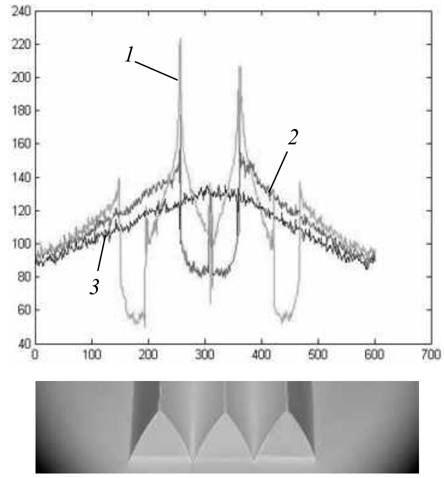

Fig. 15. Luminance gain (cd/m^2) from three longitudinal profiles (1) compared with the single profile luminance (2) and flat façade luminance (3) as reference

white paint. The geometry and the electrical parameters were constant for all the scenes.

A single profile don't produce a significant luminance gain (curve 2, Fig.15), but multiplying the profiles, the effect will be more intensive in the concavity, where the inter-reflections will be present (curve 1, Fig.15), producing 160 to maximum 200 cd/m^2 compared with 120 cd/m^2 as initial value, for flat facade. The luminance gain of 50 % is very important, especially for the close observer. This could encourage the lighting designer to reduce the general (average) illuminance level, knowing that some details on the facade will generate increased luminance levels.

6. CONCLUSIONS

OUF augmentation (calculated and measured) shows that a greater OUF don't represent a criterion for lower light pollution. The OUF is one important criterion, but only in the early steps of the designing process, giving some information about the direct light spill to the sky.

If the inter-reflections are considered, the situation is different. Using the small scale profiles existing on the facades, some important luminance gain could be obtained. Due this, the design process could decrease the general floodlighting, with an important effect for light pollution reduction. Starting from luminance gain of 50 %, this could be the reduction ratio for the floodlighting, a very interesting challenge.

Reducing the light pollution is possible maintaining the beautification of the facades. This is possible if the facade details could be involved in a creative way, changing the philosophy of the "wall of light" with one of "beauty of the details". The details will be more visible due the luminance contrast as in Fig.15, obtained not by using the shadows, but through luminance gain.

ACKNOWLEDGEMENTS

The work is supported by the UE grant COST Action ES1204, Loss of the Night Network and also by STARS4ALL.EU, an European project raising awareness about the negative effects of artificial

light on human wellbeing, biodiversity, visibility of stars, safety and energy waste.

REFERENCES

1. Muñoz Conte T., Ferrandis I.G., Ferrandis X.G., Light pollution in natural science textbooks in Spanish secondary Education, European Journal of Science and Mathematics Education, Vol. 4, No. 2, 2016, 129-139.
2. Haenel, A., Posch, T., Ribas, S. J. et al. Measuring night sky brightness: methods and challenges, Journal Of Quantitative Spectroscopy & Radiative Transfer, Volume 205, 2018, 278–290.
3. Falchi, F., et al. Limiting the impact of light pollution on human health, environment and stellar visibility. Journal of Environmental Management 2011, doi:10.1016/j.jenvman.2011.0 6.029.
4. Garner, C. Talking unwanted light: an international perspective. Light & Engineering 2012. Vol. 25 no. 1, pp.24–39.
5. Saraiji, R., Saju Oommen, M. Light Pollution Index (LPI): An Integrated Approach to Study Light Pollution with Street Lighting and Facade Lighting. Leukos 2012. 9:2, pp. 127–145.
6. http://stars4all.eu/index.php/lp/, cited on 15.05.2017.
7. *** – Colchester Borough Council, External Artificial Lighting Guidance 2012, http://www. colchester.gov.uk/CHttpHandler.ashx?id=17398&p=0, cited on 12.04.2017
8. Zagan W., Opinion: Obtrusive light and floodlighting, Lighting Res. Technol. 2015; Vol. 47: 640.
9. Pracki P, A proposal to classify road lighting energy efficiency, Lighting Res. Technol. 2011; 43: 271–280.
10. Skarżyński K, An attempt at controlling the utilization factor and light pollution within the context of floodlighting, Przegląd Elektro-techniczny, ISSN0033–2097, R. 92 NR9/2016.
11. Skarżyński K, Field Measurement of Floodlighting Utilization Factor, Proceedings of 2016 IEEE Lighting Conference Of The Visegrad Countries (LUMEN V4), IEEE, 345 E47TH ST, New York.
12. Gălățanu, C.D., Geometry Influence on the Precision of Light Flux Measurement with Ulbricht Integrating Sphere, 9th International Conference and Exposition on Electrical and Power Engineering (EPE), 2016, pp.604–608.
13. Wüller D., Gabele H, Digital Photography III, edited by Russel A. Martin, Jeffrey M. DiCarlo, Nitin Sampat, Proc. Of SPIE-IS&T Electronic Imaging, SPIE Vol. 6502, 65020U, © 2007 SPIE-IS&T · 0277–786X/07/$18.
14. Gutierrez JA, Ortiz de Lejarazu D, Real JA, Mansilla A and Vizmanos J, Dynamic measurement of traffic sign luminance as perceived by a driver, Lighting Res. Technol. 2012; 44: pp.350–363.

Cătălin Daniel Gălățanu,
Professor, Department of Building Services, Faculty of Civil Engineering, Technical University "Gh. Asachi" from Iaşi, Bd. Mangeron 67, Iaşi 700050, Romania (e-mail: catalin.galatanu@tuiasi.ro)

Muhammad Ashraf,
Assoc. Professor, Department of Electrical Engineering, Faculty of Engineering, Capital University of Science and Technology CUST, Kahota Road, Islamabad, Pakistan, Email: ashraf@cust.edu.pk

Dorin Dumitru Lucache,
Professor, Department of Electrical Engineering, Faculty of Electrical Engineering, Energetics and Applied Informatics, Technical University "Gh. Asachi" from Iaşi, Bd. Mangeron 21–23, Iași. 700050, Romania, E-mail: dorin.lucache@tuiasi.ro

Dorin Beu,
Assoc. Professor, Department of Electrical Engineering, Faculty of Building Services, Technical University Cluj Napoca, B-dul 21 Decembrie 1989, nr. 128–130, Cluj Napoca 400604, Romania E-mail: dorin.beu@rogbc.org

Călin Ciugudeanu,
Lecturer, Department of Electrical Engineering, Faculty of Building Services, Technical University Cluj Napoca, B-dul 21 Decembrie 1989, nr. 128–130, Cluj Napoca 400604, Romania E-mail: calin.ciugudeanu@rpe.ro

Light & Engineering
Vol. 27, No. 6, pp. 58–64, 2019
https://doi.org/10.33383/2018-076

COMPUTER MODELLING AND RECOMMENDATIONS FOR RESTORATION OF THE HISTORICAL TRANSLUCENT STRUCTURES OF THE PUSHKIN STATE MUSEUM OF FINE ARTS

Alexander V. Spiridonov and Nina P. Umnyakova

Research Institute of Structure Physics of Russian Academy of Architecture and Construction Sciences, Moscow
E-mail: spiridonov@aprok.org

ABSTRACT

On the basis of the previous examinations of the historical windows of the main building of the Pushkin State Museum of Fine Arts by the authors [1] using a certified software package, the multi--variant analysis of the methods of increasing efficiency of the existing translucent structures was conducted. The recommendations for restoration of the historical translucent structures which are the parts of this state-protected cultural heritage object were developed.

Keywords: restoration, historical translucent structure, frame, sash, impost, computer modelling, computer calculations, heat transfer resistance, air permeability, condensate, recommendations

1. INTRODUCTION

As a result of the surveys of historical translucent structures [1], it became obvious that they do not comply with the current requirements, neither in terms of heat transfer resistance nor in terms of air permeability. In case of preservation of metal window frames (according to the requirements of the law on protection of cultural heritage sites and the Customer's order [2]) the large-scale computer calculations should be performed to determine the best ways of window restoration.

Calculation of thermo-technical characteristics of the historical translucent structures proposed for restoration as well as temperature distribution on the inner surfaces of glazing and profiles of metal frames was performed using the certified *WINDOW* – TEST (version 2017) software package [3] with different boundary conditions for each of the compared variants of translucent structures.

The calculation method is based on modelling of a steady-state process of heat transfer through structures using PC software and thermal design of the fragments of building structures (including translucent ones), glazing systems and joints of window units and the walls.

This method allows the next performs:

– Comparative analysis of the variants of translucent structures of different designation on the basis of reduced total thermal resistance;

– Selection of optimal structural solutions on the basis of the conducted thermal designing;

– Determination of the dimensions of the areas of one-dimensional and two-dimensional temperature fields of the translucent structures for preparation to testing in a climatic chamber;

– Evaluation of the temperature mode of the joints of window units and the walls and selection of the most optimal structural solution of erection joints.

For calculation, the following 6 design variants of the translucent structures were selected:

1. The existing historical translucent structure in accordance with the detail measurements performed in the course of on-site investigations; the translucent filling is made of transparent M1 glass

with thickness of 6 mm in an inner and outer metal frames;

2. Similar to variant 1 but the translucent filling is sun-protecting glass with thickness of 6 mm in the outer metal frame and the glass with hard heat-reflective coating (K-glass) with thickness of 6 mm in the inner metal frame;

3. Similar to variant 1 but the translucent filling is sun-protecting glass with thickness of 6 mm in the outer metal frame and the 4–10Ar-4И double-glazed unit with internal heat-reflective glass in the inner metal frame;

4. Similar to variant 1 but the translucent filling is the 4СЗ-10Ar-4 double-glazed unit with external heat-reflective glass in the outer metal frame and the 4–10Ar-4И double-glazed unit with internal heat-reflective glass in the inner metal frame;

5. Similar to variant 1 but the translucent filling is the 4СЗ-10Ar-4И double-glazed unit with external sun-protecting glass and internal heat-reflective glass in the outer metal frame and heat-reflective high abrasive-resistant glass with soft low-emission coating with thickness of 6 mm in the inner metal frame;

6. The outer frame remains historical one and the inner metal frame is replaced by a contemporary fibreglass frame with similar dimensions; the translucent fillings are similar to variant 5.

The internal microclimate conditions for calculations were taken in accordance with the Pushkin State Fine Art Museum (hereinafter referred to as the Pushkin Museum) main building reconstruction project: temperature of 20±1 °C and relative humidity of 50±5 %.

In accordance with set of rules [4, Table 3.1], the ambient temperature of 28 °C was used for all variants calculation. But the evaluations of thermo-technical parameters of the building structures were performed with other values ambient temperature for the variant 1 and the best of the variants 2–5 (based on the results of preliminary calculations): – 30,– 20,– 15,– 10, 0, + 10 and + 21 °C for variant 1 and – 20,– 15,– 10 and 0 °C for variant 5.

In the course of calculation, the reduced total thermal resistance for all variants of translucent structures and possibility of condensation on the internal surfaces of glazing were evaluated.

The results of computer calculations are listed in the Table.

The Table shows that the translucent structures manufactured in accordance with variants 3 and 4

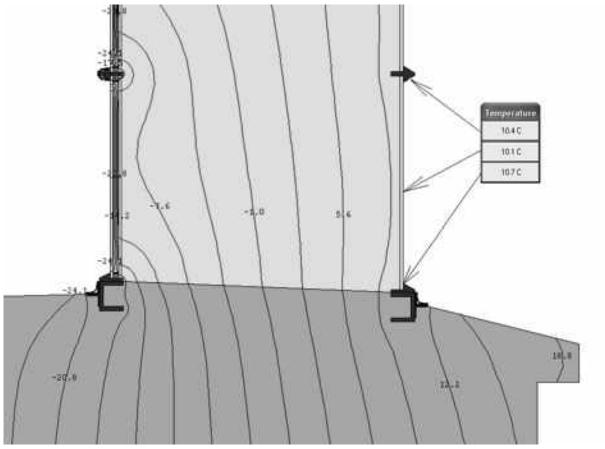

Fig. 1. Distribution of temperatures on the inner surface of the lower part of a translucent structure manufactured in accordance with variant 5 with ambient air temperature of minus 28 °C

(lines 10 and 11) comply with thermo-technical requirements of all applicable regulations and are the best in terms of glazing temperature. However, due to changing of the heat transfer mode in the space between glasses in case of installation of the double-glazed units in the inner metal frame, the possibility of condensation on the angular elements of the inner metal frame increases dramatically.

On the basis of the conducted survey of different variants of restoration of the historical translucent structures, the experts proposed to use the variant 5 (the corresponding temperature distribution is shown in Fig. 1).

On the basis of the numerous on-site investigations of the historical windows of the 1st floor of the main building of the Pushkin Museum, the following major conclusions were made:

– The historical translucent structures require immediate restoration;

– The characteristics of the translucent structures (reduced total thermal resistance, air-permeability) do not comply with the applicable standard regulations, and it is hard to comply with the requirements of the applicable standard regulations regarding reduced total thermal resistance [5] provided that the historical translucent structures are preserved but it is possible to significantly increase their thermal efficiency;

– The temperature on the inner surfaces of the existing historical translucent structures is lower than the dew point temperature almost at all negative values of ambient temperature, which causes significant condensation;

– The condensate generated on the inner surfaces of the translucent structures in cold periods causes negative impact on the pieces of art exhibited in the museum;

– It is necessary to provide special sun-protecting devices and curtains diffusing direct sunlight for the translucent structures of the East, South, and West facades of the main building of the Pushkin Museum.

Due to the fact that a clear and incontestable requirement of [2] is preservation of the historical translucent structures installed in 1912, the main goal of our recommendations was restoration and increasing of efficiency of the metal frames, elimination of condensate on the inner surfaces of the windows and protection of pieces of art from direct sunlight using the most contemporary construction technologies.

The developed recommendations based on the results of the on-site investigation and computer modelling of different variants of glazing in the historical translucent structures are divided into 6 sections related to modernisation of specific elements of the design.

2. RESTORATION OF METAL FRAMES OF THE HISTORICAL TRANSLUCENT STRUCTURES

The metal frames are largely corroded. Due to this fact, the following actions are required to be taken during the restoration (the word "reconstruction" probably fits more)[1]:

– Remove both inner and outer frames;

– Clean them from the traces of numerous paintings performed over the previous one hundred years;

– Disassemble the metal frames (including the main vertical impost consisting of a large number of elements);

– To clean absolutely ***all*** elements of the structures from corrosion and to treat them with contemporary corrosion preventive compounds;

– In case of possible replacement of the historical elements with newly-manufactured ones due to full impossibility of restoration of the former, it is necessary to prevent application of contemporary materials which may cause an electrochemical reaction when contacting the historical ones;

– The elements of the metal frames should be painted only ***after*** taking the above listed actions.

3. MODERNISATION OF JOINTS

Currently, the translucent structures are fixed to the wall directly, which increases the possibility of condensate penetration due to negative impact by the enclosure structure.

It is necessary to perform heat insulation of the historical window frames from the enclosure structures using contemporary materials.

For this purpose, after removal of the metal frames for restoration (see the first part of our recommendations), it is necessary to perform wall chasing in the areas of installation of the outer metal frames, to install a contemporary and efficient heat insulation material in the chases, e.g. penoplex, and to install the historical translucent structures into position only after that.

The recommended cross-section dimensions of the heat insulation materials are 200 (width) × 20 (depth) mm. In Fig. 2, one of the variants of the recommended heat insulation of the perimeter of the window opening in the course of restoration of the historical translucent structures.

4. MODERNISATION OF DRAFT-PROOFING OF THE HISTORICAL TRANSLUCENT STRUCTURES

In the course of installation of the restored historical translucent structures in the window openings, it is necessary to provide maximum draft-proofing of the inner metal frame to prevent penetration of internal moist air in the space between the glasses as far as possible to minimise the possibility of condensation on the inner surface of the outer metal frame.

For the same purpose, it is necessary to restore and to adjust the historical hardware of the window leaf (both in the outer and especially inner metal frame) and to open them only if strictly necessary. The ledges of the leaves should be equipped with

[1] The experts are afraid that some elements of the frames cannot be restored and will require to be replaced (in particular, it is definitely required to replace steel angle elements underneath the lower inner decorative plates of many frames which are mostly affected by the condensate as well as the lower inner parts of the main vertical impost).

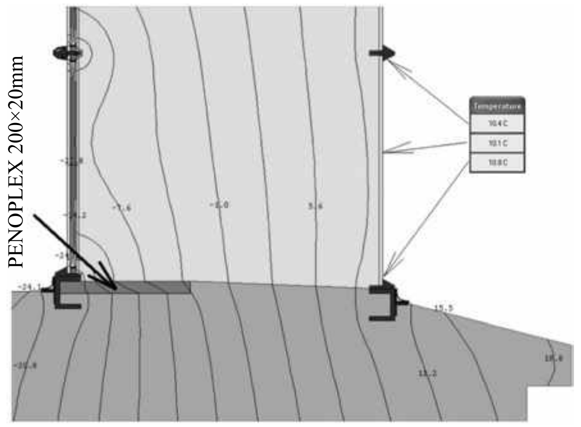

Fig. 2. Heat insulation of the perimeter of the outer metal frame

a contemporary sticky sponge material (there are lots of such sealants nowadays).

In the course of draft-proofing of the outer metal frame, it is necessary to provide air drains for natural ventilation of the space between the glasses and for access of relatively dry ambient air during the cold period for minimisation of condensation on the inner surface of the outer metal frame. The total length of the openings for natural ventilation of the space between the glasses should not exceed (1–3) % of the overall perimeter of the joint of a window and an enclosure structure.

5. MODERNISATION OF GLAZING OF THE HISTORICAL TRANSLUCENT STRUCTURES

In the course of the on-site [1] and computer investigations and based on the results of evaluation of the 6 variants of restoration of the historical translucent structures, the variant 6 (see above) was selected.

It is this variant which provides the best temperatures of the inner surfaces of glazing excepting condensation at the standardised air temperature in Moscow –28 °C.

The reduced total thermal resistance of such translucent structure will be equal to 0.58 $(m^2\cdot°C)/W$, which complies with the requirements of SP (set of rules: 0.54 $(m^2\cdot°C)/W$) for the Moscow climate conditions. But after introduction of the Amendment No. 1 to the above mentioned SP (which is expected soon), the standardised reduced total resistance of windows will be equal to at least 0.70 $(m^2\cdot°C)/W$.

It is recommended to use a "warm" *SWIGGLE STRIP* spacer bar in the double-glazed unit since it will change the exterior of the translucent structures minimally. It is possible to select black upper colour of the spacer (like that of the frame itself) and minimal available thickness of the spacer.

It is necessary to install standard plastic plates of minimal possible thickness between the double-glazed unit and the metal frame and the double-glazed unit shall be fixed by means of one of the sealants for structural glazing along its perimeter. The glass of the inner metal frame should be fixed too.

The width of the seat of the metal frame where the double-glazed unit will be installed is 21 mm, therefore it is impossible to use more efficient units with spacer bars of (12–16) mm in width. But even the proposed type of the double-glazed

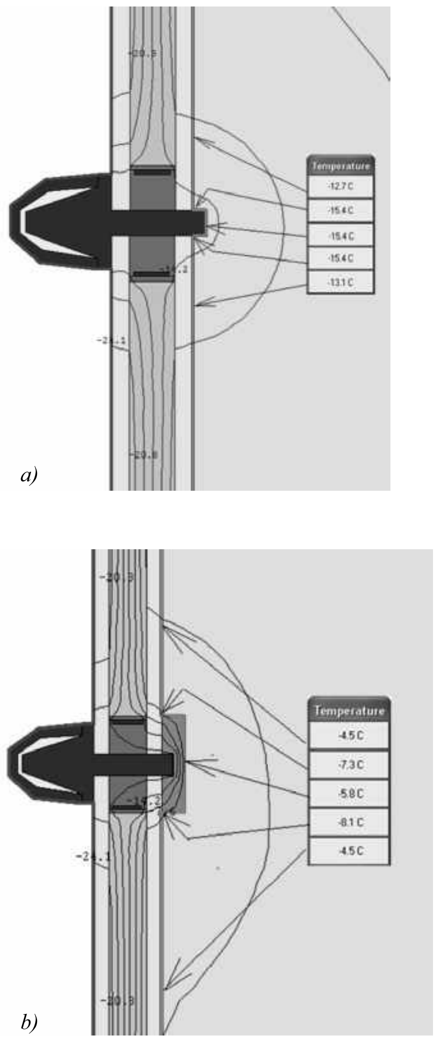

Fig. 3. Temperature fields in the area of the main vertical impost of the outer metal frame without (*a*) and with (*b*) installed water bar calculated in accordance with variant 5

Table. Generalised Results of Computer Calculation of Variants of Restoration of Historical Translucent Structures

($R^{пр}_{о}$ is reduced total thermal resistance, $t_{н}$ is ambient air temperature, $t_{ост}$ is the temperature in the middle of the inner glass, $t_{рам}$ is the temperature of the inner surface of the metal frame)

<table>
<tr><th>Variant of glazing</th><th>$R^{пр}_{о}$, (m²·°C)/W</th><th>$t_{н}$, °C</th><th>$t_{ост}$, °C</th><th>Condensate generation possibility</th><th>$t_{рам}$, °C</th><th>Condensate generation possibility</th></tr>
<tr><td rowspan="8">1</td><td></td><td>–681</td><td>–1.9</td><td rowspan="5">yes</td><td>–1.1</td><td rowspan="4">yes</td></tr>
<tr><td>0.34</td><td>–681</td><td>–1.0</td><td>–681</td></tr>
<tr><td></td><td>–20</td><td>3.2</td><td>3.5</td></tr>
<tr><td></td><td>–681</td><td>4.8</td><td>5.5</td></tr>
<tr><td></td><td>–681</td><td>6.8</td><td>7.7</td><td>yes*</td></tr>
<tr><td></td><td>0</td><td>11.2</td><td>yes**</td><td>11.5</td><td>yes**</td></tr>
<tr><td></td><td>10</td><td>15.6</td><td rowspan="2">no</td><td>15.8</td><td rowspan="2">no</td></tr>
<tr><td></td><td>21</td><td>20.4</td><td>20.4</td></tr>
<tr><td>2</td><td>0.38</td><td>–681</td><td>–681</td><td>yes</td><td>–681</td><td rowspan="3">yes</td></tr>
<tr><td>3</td><td>0.56</td><td>–681</td><td>13.0</td><td rowspan="2">no</td><td>–681</td></tr>
<tr><td>4</td><td>0.67</td><td>–681</td><td>14.6</td><td>–681</td></tr>
<tr><td rowspan="5">5</td><td>0.58</td><td>–681</td><td>11.4</td><td rowspan="2">yes**</td><td>10.4</td><td rowspan="2">yes**</td></tr>
<tr><td></td><td>–681</td><td>11.5</td><td>11.1</td></tr>
<tr><td></td><td>–681</td><td>12.6</td><td rowspan="3">no</td><td>12.0</td><td rowspan="4">no</td></tr>
<tr><td></td><td>–681</td><td>13.6</td><td>13.1</td></tr>
<tr><td></td><td>0</td><td>16.1</td><td>15.6</td></tr>
<tr><td>6</td><td>0.66</td><td>–681</td><td>5.8</td><td>yes</td><td>12.8</td></tr>
</table>

Notes:
* Only in one situation (air temperature: 19 °C, relative humidity of air: 45 %, dew point temperature: –6.81 °C), condensate generation is excepted;
** Only in one situation (air temperature: 21 °C, relative humidity of air: 55 %, dew point temperature: –11.62 °C), condensate generation is excepted.

unit (4СЗ-10Ar-4И) with thickness of 18 mm provides required temperature on the inner surface of glass.

Due to the fact that there are metal plates installed on the glass in the upper quarters of the historical translucent structure, double-sided porous adhesive tapes should be installed between the plates and the glass/double-glazed unit (there is a wide selection of such materials in the market).

If necessary, to increase safety, it is possible to apply a polymer film on the glass located in the inner metal frame like it is done currently.

6. PREVENTION OF CONDENSATION ON THE METAL SASHES

Among the most critical elements of the historical translucent structures in terms of condensation are the metal sashes, especially the main vertical metal impost.

On its inner surface, sub-zero temperatures were registered almost at all sub-zero temperatures of ambient air, which will obviously assist in condensation or even generation of frost on them.

For enhancement of temperature mode of this element of structure, it is proposed to install a special plate made of, for example, extruded foamed PVC and painted black (so that it cannot be seen against the background of the metal frame) on the invisible part of the element so that the temperature on the inner surface of the main vertical impost of the historical translucent structure will be significantly increased.

According to the variant 5 recommended for application in the course of the said restoration of the historical translucent structure, it is necessary to insulate the main vertical impost only of the outer metal frame inside the space between the glasses (Fig. 3).

At the most sub-zero ambient temperatures, condensation on the inner surfaces of the main sashes of the inner metal frame is possible.

We propose to place a special heating cable along the perimeter of these sashes in the space between the glasses hidden from view from the premises. It is recommended to use adjustable cables with maximum temperature of up to 38 °C made of composite materials (there are a lot of variants of such devices on the market).

It is necessary to provide uninterrupted convection of warm air from heating devices which are now hidden behind the decorative racks and windowsills. For this purpose, it is necessary to install special ventilating grids in the windowsills (there are lots of variants on the market).

One of possible solutions of the problem of temperature increasing of the inner glazing and metal frames surfaces is installation of convector heaters in the space between the glasses, but it is considered not the best solution for prevention of condensing on glazing.

7. INCREASING OF VISUAL COMFORT

A large amount of the translucent structures of the main building of the Pushkin Museum is oriented towards the solar rhumbs of the horizon.

Apart from the fact that excess direct and diffuse solar irradiation of the premises causes negative impact on efficiency of the air conditioning systems, direct sunlight may also negatively affect the pieces of art and interfere in perception of the same.

In that respect, the experts propose to install special electric-driven sun-protecting curtains in the space between the glasses. Such sun-protecting devices are manufactured by many companies.

Due to the fact that there are metal staples installed between the inner and the outer metal frames which, apart from the ladder function, also connect the frames, it is practically impossible to install integrated sun-protecting curtains and it will be necessary to divide them into two parts.

The authors hope that:

- The conducted surveys and the developed recommendations regarding restoration of very complicated historical translucent structures of one of the important federal cultural heritage objects will allow drawing attention of specialists to necessity of consideration of distinctions of the old-design windows in the course of restoration of old buildings and will show the main aspects of this work;
- After the comprehensive restoration, the facades of the main building of the Pushkin Museum will be included in the next summary of achievements of the *International Council on Monuments and Sites* [6] which also describe the translucent structures.

The authors are ready to participate in similar works regarding other historical buildings as they deserve all their elements to comply with the concept of architects from the one hand and to comply with the contemporary energy saving requirements from the other hand. Nowadays there are many opportunities to give a new lease of life for old translucent structures by means of contemporary window technologies.

ACKNOWLEDGEMENT

The authors express their deep gratitude to employees of OOO GK ROBITEX N. Rumyantsev and I. Istomina for their assistance in calculations and preparation of the recommendations for restoration of the historical translucent structures of the Pushkin Museum.

REFERENCES

1. Alexander V. Spiridonov and Nina P. Umnyakova "Inspection of the State (General and Instrumental) of Historical Translucent Structuresof the Pushkin State Museum of Fine Arts"// Light&Engineering Journal, 2019, V.27, #3, pp.26–31.
2. "Complex reconstruction, restoration and adaptation to modern museum technologies of the major building of the Pushkin State Museum of Fine Arts (Moscow, Volkhonka Str., 12)" [Documentation prepared by the

Federal State Unitary Enterprise Central Scientific and Restoration Design Workshops].

3. WINDOW TEST Software Including THERM and WINDOW User's Manual. Moscow, APROK-TEST, 2006, 140 p.

4. SP 131.13330.2012. Building climatology. The updated version of SNiP 23–01–99.

5. SP 50.13330.2012 Thermal performance of the buildings. The updated version of SNiP 23–02–2003.

6. International Charters for Conservation and Restoration. Chapter1. Monuments and Sites. ICOMOS, 2004, 184 p. URL: http://openarchive.icomos.org/431/1/Monuments_and_Sites_1_Charters.pdf (reference date 20.09.2018).

Alexander V. Spiridonov,
Ph.D. in Technical Sciences, graduated from the Moscow Power Institute (MPEI) in 1975, majoring in "Lighting and light sources". At present, he is the Chief Research Fellow of the NIISPh of RAACS, President of the Association of Manufacturers of Energy Efficient Windows (APROK), Laureate of the RF Government Prize in Science and Technology

Nina P. Umnyakova,
Ph.D. in Technical Sciences, Associate Professor. graduated from the Moscow Civil Engineering Institute. At present, she is Deputy Director of the NIISPh of the RAACS. Her research interests are thermal protection of buildings, energy saving, and evaluation of thermal protection qualities of cladding in the presence of reflective thermal insulation

Light & Engineering
Vol. 27, No. 6, pp. 65–72, 2019 *https://doi.org/10.33383/2018-101*

STUDIES OF APPLICATION OF LED-BASED LIGHTING DEVICES IN A CAR ASSEMBLY SHOP

Svetlana Yu. Minaeva and Vladimir P. Budak

NRU MPEI, Moscow
E-mail: budakvp@gmail.ru

ABSTRACT

The article describes the problem of replacement of active fluorescent lamp lighting installations of an assembly line of a car assembly plant with LED LDs including a comparison of the gained lighting and economic indicators. Therefore, several LED-based LDs by different manufacturers were selected. Based on LI computer modelling using *DIALux Evo*, an optimal option in terms of light engineering and economy was found. Lighting characteristics of the active LI and areas of the assembly line with the application of LED-based LDs were determined experimentally. The results of the study allow assessing relevant changing of visual performance of shop workers and to compare the pay-off periods of LED and fluorescent lamps-based lighting devices.

Keywords: industrial lighting, LED, lighting installation, lighting, assembly line, lighting quality

1. INTRODUCTION

Due to increasing application of LED-based lighting devices (LD), recently the number of publications related to LED-based LDs lighting of, in particular, industrial premises has been increasing (see, for instance, [1, 2]). In the meantime, it should be noted that:

• The main aspect of shop lighting design is consideration of not only quantitative but also qualitative characteristics of lighting installations (LI) such as visual discomfort indicators and flicker index;

• The transfer to LEDs requires correct solutions related to optics, *IP*, and luminous efficacy of a LED-based LD.

It is also known that:

• In many industries, there are assembly shops where intermediate or final assembly of products is performed; the working process in them is associated with both small parts (assembly of domestic appliances, soldering of electronic components, etc.) and large parts (assembly of car body elements, installation of large units of industrial machines/installations, etc.) operation, which, in return, require different approaches to design of lighting in such premises;

• The artificial lighting conditions in an industrial facility are extremely important since they largely affect the workers' health and quality of manufactured products [3]; differentiation of items against a particular background, light perception, and visual comfort of workers depend on characteristics of LI;

• Light is a natural condition of a human life and activities, which plays an important role in health preservation and high working capacity. Human visual performance is the main source of information about the world.

This study comprises LED-based LDs application capabilities analysis for the lighting of car assembly lines with consideration of enhancement importance of visual performance conditions and increase of labour productivity.

The studied object was an active car assembly line (located in the Russian Federation), and the subject of the study was local lighting along it.

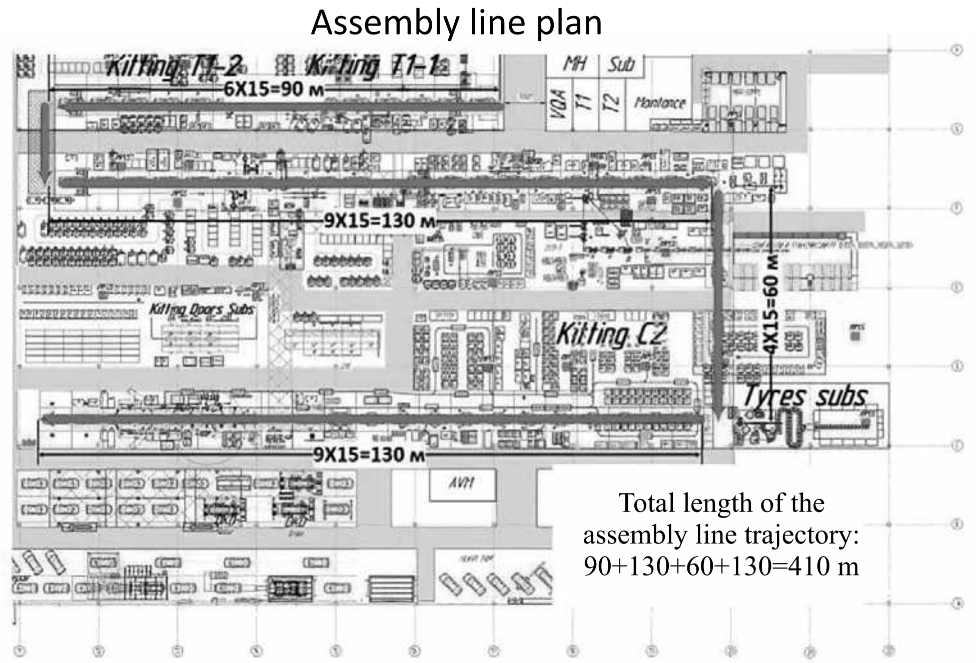

Fig. 1 Assembly line plan

Development of the optimal lighting (for this line) with the application of LED-based LDs instead of the active ones was considered the practical relevance of the study.

In addition, several variants of LI fitting for car production were studied; for the avoidance of mistakes, the distinctions of workplaces, the reflectance of the floor, the walls, and the ceiling, etc. were taken into account in the course of development of the computer model (see below).

2. LI COMPUTER MODELLING AND ECONOMIC CALCULATION

The study object is located on the first floor of the building. The height of the ceiling with the ambient illumination LDs (luminaires) installed on it is 10 m, the height between the floor and the girder is 8 m. The height of the local illumination LI is 3.5 m. The total area of the illuminated premises is 39,600 m^2 and the total length of the line is 420 m. The plan of the illuminated assembly shop and its photos are presented in Figs. 1 and 2. There are no windows in the premises, and it is used for permanent human presence. The finishing of the premises complies with its designation and the values of reflectance of the ceiling, the walls, and the floor are approximately the same: 0.49. At both sides of the line, at the height of 3.5 m, the LIs for local illumination are installed. The active variant uses *Lighting Technology ARS254*-type fluorescent lamps (FL) (Fig. 2).

For lighting engineering calculations, *DIALux Evo* software was used since it is one of the most popular lighting design tools, among its advantages are: free license; good quality of images after model calculation (similar to the images after ray tracing); completely new calculation algorithm, which takes the correlated colour temperature T_{cc} of LD into account [4].

Fig. 2. Active LI of the assembly line

Table 1. Characteristics of LDs (Luminaires)

Type of LD	Luminous intensity distribution curve	Efficiency (%)	*P*, W	IP	Dimensions, mm	Note
Glamox i50	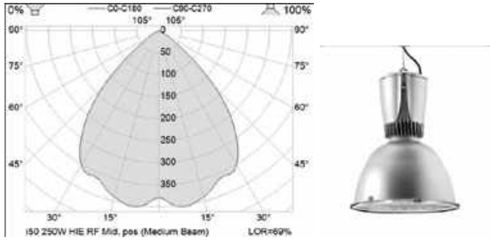	69	250	20	Diameter 222 Height 319 Weight 9 kg	Ambient illumination
Lighting Technologies ARS254	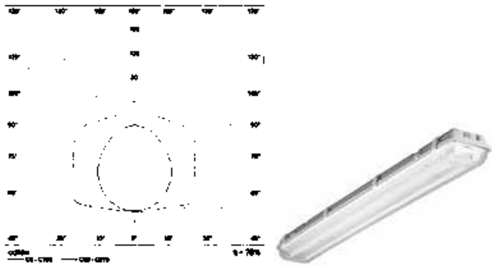	70	54	65	Width 100 Length 1280 Height 110 Weight 2.3 kg	Existing illumination of the line (Fl luminaires)
Osram Compact Monsun LED	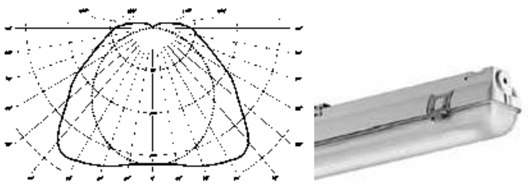	92.5	38.8	65	Width 84 Length 1577 Height 102 Weight 2.7 kg	Variant No. 1
Philips Coreline Waterproof	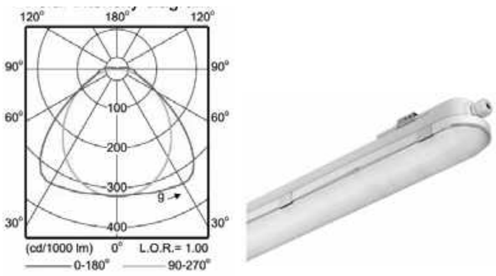	97	29	65	Width 87 Length 1530 Height 96 Weight 1.8 kg	Variant No. 2

Type of LD	Luminous intensity distribution curve	Efficiency (%)	*P*, W	IP	Dimensions, mm	Note
Lighting Technologies SLICK. PRS LED	 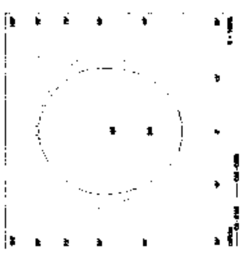	95	31	65	Width 96 Length 953 Height 86 Weight 2.6 kg	Variant No. 3
Philips GreenUp Waterproof	 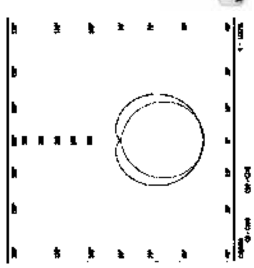	95	36	65	Width 90 Length 1400 Height 110 Weight 1.5 kg	Variant No. 4

In the course of LI modelling and illumination engineering analysis, the authors relied on the documents [5, 6].

Depending on the nature of production and location of workplaces, the local illumination may be established using two methods: 1) by means of individual LDs for each workplace; 2) for a group of closely located workplaces such as lines, streams, etc.

It is mandatory to consider ambient illumination for calculation of illuminance; otherwise, some indicators will become irrelevant. That is why the calculation of combined illumination of the assembly shop with existing ambient illumination LDs (LDs with 250W *Glamox i50* MHL) was conducted, and the LDs of local illumination LIs were varied. The ambient illumination was considered for the whole premises and combined illumination was used for the assembly line. There were 4 variants of LI with the following LED-based LDs selected for replacement of the existing LI with FL-based LDs: *Osram Compact Monsun LED*, *Philips Coreline Waterproof*, *Lighting Technologies SLICK. PRS LED*, and *Philips GreenUp Waterproof* (Table 1).

These variants were selected with consideration of economic efficiency, environmental conditions, and the customer's feedback.

In the course of modelling, the following parameters were estimated for all LI variants (the existing variant, the variant No. 1 (*Osram* LD), the variant No. 2 (*Philips* LD), the variant No. 3 (*Lighting Technologies* LD), and the variant No. 4 (*Philips* LD)):

- Horizontal and vertical illuminance (minimal, average, maximum) at the heights of 0.0 m and 1.8 m above the floor level;
- Unified glare rating *UGR* in the whole shop and at each point of the assembly line at the heights of 1.2 m and 1.7 m above the floor level;
- Illuminance uniformity U_o (in accordance with GOST [6]).

The results of these estimations are listed in Table 2, and the results of calculation of annual depreciation costs of the selected variants of LI/LD are listed in Table 3.

For the selection of the most efficient LI variant for the assembly line, the comparative analysis of annual expenditures for maintenance of all 5 variants of LI was performed. These expenditures are composed of the sum of annual depreciation costs of LI and annual cost of power consumed by the LI [7].

Table 2. Results

Parameters	Name of LD				
	Lighting Technologies **Existing variant**	***Osram Compact Monsun LED*** **Variant No. 1**	***Philips Green-Up Waterproof*** **Variant No. 2**	***Lighting Technologies SLICK.PRS LED*** **Variant No. 3**	***Philips Green-Up Waterproof*** **Variant No. 4**
E_m, lx (H-0.0)	503	504	508	508	503
E_m, lx (V-0.0)	352	343	347	336	310
E_m, lx (H-1.8)	510	519	514	510	508
E_m, lx (V-1.8)	355	366	335	341	336
U_o, on a horizontal plane (0.0 m)	0.93	0.93	0.92	0.90	0.89
U_o, on a vertical plane (0.0 m)	0.89	0.89	0.92	0.86	0.9
U_o, on a horizontal plane (1.8 m)	0.85	0.84	0.83	0.84	0.82
U_o, on a vertical plane (1.8 m)	0.72	0.88	0.62	0.87	0.65
UGR, the whole shop	21.7	22.1	21.7	21.0	22.3
UGR, on the assembly line (1.2 m)	More than 30	24.1	22.8	22.0	23.8
UGR, on the assembly line (1.7 m)	27.1	24.9	23.4	23.0	25.0
Number of LD in LI, pcs.	232	250	371	306	374

3. COMPARATIVE ANALYSIS OF LI WITH DIFFERENT TYPES OF LD

The values of the maintained average illuminance E_m and U_o of the existing variant of LI comply with the standard, and the *UGR* is significantly larger than the standardised one (Table 2). Apparently, ambient illumination is not used for this reason. In addition, Table 2 shows that:

• The values E_m and U_o of the variant with the LD *Osram Compact Monsun LED* (variant No. 1) comply with the standards, and the value of *UGR* complies neither in the shop nor on the line itself; however, these indicators are better than those of the existing variant of LI;

• The values E_m and U_o of the variant with the LD *Philips Coreline Waterproof* (variant No. 2) comply with the standards, and the value of *UGR* complies with the standard only in the shop; *UGR* does not comply with the standard on the assembly line, but its value is close to it at the height of 1.2 m;

• The values E_m and U_o of the variant with the LD *Lighting Technologies SLICK.PRS LED* (variant No. 3) comply with the standards, and the value of *UGR* complies with the standard just insignificantly exceeding it at the height of 1.7 m;

• The values E_m and U_o of the variant with the LD *Philips GreenUp Waterproof* (variant No. 4) comply with the standards, and the value of *UGR* does not. In the meantime, these values are better than those of the existing LI variant but worse than those of the other selected ones.

Table 2 and the above-mentioned analysis show that the optimal solution in terms of overall acquired characteristics is LI with *SLICK.PRS LED* LD by *Lighting Technologies* (variant No. 3).

Calculation of annual energy costs was also performed (Table 4). The duration of LI operation was accounted for in accordance with the number of working hours per year with 40-hours working week and one-shift operation. The summary economical calculation showed (Table 5) that existing illumination is the most expensive variant and the most efficient one may be provided using LI with *SLICK.PRS LED* LD by *Lighting Technologies* (variant No. 3).

Table 3. Calculation of Annual Depreciation Cost of the Artificial Lighting System

Illumination variant	Useful life, hours	Lifetime, years	Initial cost of LI, ₽	Annual depreciation costs, ₽
Lighting Technologies Existing variant	24,000	8	1,149,560	143,695
Osram Compact Monsun LED Variant No. 1	50,000	10	1,500,000	150,000
Philips Coreline Waterproof Variant No. 2	50,000	10	1,595,300	159,530
Lighting Technologies SLICK.PRS LED Variant No. 3	50,000	10	887,400	88,740
Philips GreenUp Waterproof Variant No. 4	40,000	10	1,047,200	104,720

Table 4. The Cost of Consumed Energy per Year

Illumination variant	Power consumption of one LD, W	Number of LDs, pcs.	Operation time of LI per year, hours	Electricity cost, ₽/kWh	The cost of consumed electricity per year, ₽
Lighting Technologies Existing variant	108	232	1973	5	247177
Osram Compact Monsun LED Variant No. 1	36	250	1973	5	88785
Philips Coreline Waterproof Variant No. 2	29	371	1973	5	106138
Lighting Technologies SLICK.PRS LED Variant No. 3	31	306	1973	5	93579
Philips GreenUp Waterproof Variant No. 4	36	374	1973	5	132822

4. MEASUREMENT OF LIGHTING ENGINEERING CHARACTERISTICS OF LI

The values of horizontal and vertical illuminance on workplaces created by the existing variant of LI were measured at the heights of 0.0 and 1.0 m from the floor level, and the values of LD luminance were measured at the distance of 10 m from the working area. By way of experiment, LDs of the four selected variants were installed in some areas of the line. *UGR* was calculated for all variants (Table 6). Wherein:

- In the course of experiment, the LDs were descended down to the height of 2.5 m;
- In the model of the local illumination, there is spacing between LDs of the LI, but actually they are located close to each other (due to application of excessive LDs), therefore, the "measured" (calculated on the basis of the measured data) value of *UGR* is less than the modelled one;
- Ambient illumination was not switched on in the course of measurements and luminance meter, spectrometer/illuminance meter, distance meter, and a photo camera were used.

The distance (10 m) between the studied LD and the luminance meter was measured by means of the distance meter. The luminance of the studied LD was measured by luminance meter. The required photos were made. Horizontal and vertical illumi-

Table 5. Total Annual Maintenance Cost of Lighting Installations

Illumination variant	Annual depreciation costs, ₽	The cost of consumed electricity per year, ₽	Annual maintenance cost of LI, ₽
Lighting Technologies Existing variant	143,695	247,177	390,872
Osram Compact Monsun LED Variant No. 1	150,000	88,785	238,785
Philips GreenUp Waterproof Variant No. 2	159,530	106,138	265,668
Lighting Technologies SLICK. PRS LED Variant No. 3	88,740	93,579	182,319
Philips GreenUp Waterproof Variant No. 4	104,720	132,822	237,542

Table 6. Measurement Results

LD	*Lighting Technologies* Existing variant	Philips GreenUp Waterproof	Philips GreenUp Waterproof	*Lighting Technologies SLICK.PRS*
E (H-0.0), lx	698	778	799	686
E(V-0.0), lx	267	341	311	392
E(H-1.0), lx	1140	1050	933	1300
E (V-1.0), lx	429	473	344	558
L, overall luminance of the luminous part of the i-th luminaire in the direction of observer's eyes, cd/m^2	772	1189	769	616
UGR	26.2	25.3	24.7	23.5

nance values were measured at the heights of 0.0 and 1.0 m above the floor level on the line itself. All instruments for measurement of lighting indicators had undergone calibration, and the acquired results are presented in Table 6.

As compared to the initial technical specification, the differences of suspension height and the number of LDs of the local illumination LI were discovered. Therefore, the LDs of the local illumination LI model were located at a height of 2.5 m and close to each other (after measurement).

The analysis of illumination in the new model of LI showed, in particular, that switching off the general lighting increases visual discomfort.

5. DISCUSSION AND RESULTS

This article describes the efficiency study of LED-based LDs application in the car assembly shop and determines the optimal replacement variant of the existing LI.

Using *DIALux Evo*, the model of LI was formed, the lighting analysis was performed, and qualitative and quantitative lighting indicators were considered. The aspects of operation on the assembly line were taken into account during modelling of LI: operation with separate units and their subsequent adjustment, movement of the working surface. Based on the models created by ourselves for selection of the optimal solution, several variants of illumination of the assembly line were analysed. The following indicators were taken into account during the analysis: average illuminance, U_o, and *UGR*. The economical calculation was performed additionally with comparative analysis of annual maintenance expenditures of each LI variant. The comparative analysis of the lighting and economical parameters showed that the *UGR* level (more than 30), operational, and maintenance costs of the existing variant are the worst.

The optimal solution within the scope of this study is LI with *SLICK.PRS LED* luminaires by

Table 7. "Measured" and Modelled Values of *UGR*

LD	*Lighting Technologies* Existing variant	*Philips GreenUp Waterproof*	*Philips Coreline Waterproof*	*Lighting Technologies SLICK.PRS LED*
UGR, "measured"	26.2	25.3	24.7	23.5
UGR, calculated using the *3D* model	27.3	25.1	23.8	23.1
Relative error,%	4.0	0.8	3.6	1.7

Lighting Technologies. The values of average illuminance and U_0 are within the acceptable ranges, and the *UGR* level is close to the standard value: at the height of 1.2 m above the floor it is equal to 22 (in compliance with GOST [6]), and at the height of 1.7 m above the floor, it is equal to 23 (insignificantly exceeding the standard value). Therefore, by compliance with the standard [6], this variant of LI provides the required level of workers' visual performance.

Comparison of the results of *UGR* calculation with the results of *3D*-modelling in *DIALux Evo* showed a relative error of (0.8–4) %. This confirms that the computer model is relevant to the object (Table 7).

Analysing all the presented conclusions, we can conclude that the values of *UGR* of the most of the reviewed cases (among the presented variants of LI) are higher than the standard ones, and it should be taken into account during further improving of LI for the assembly line.

REFERENCES

1. Prokofiev A. Reiting promyshlennykh svetodiodnykh svetilnikov [Rating of the Industrial LED Luminaries] // Sovremennaia svetotekhnika, 2012, Vol. 1, pp. 3–13.
2. Titkov S. Svetodiodnye svetilniki dlia tsekhov i ulits [LED Luminaires for Shops and Streets] // Sovremennaia svetotekhnika, 2014, Vol. 1, pp. 32–36.
3. Aizenberg Yu.B. Spravochnaia kniga po svetotekhnike [Reference book on lighting engineering. 3rd revised edition // Znak Publ., Moscow, 2006, 972 p.
4. Tatyana V. Meshkova and Vladimir P. Budak "DIALux 4.10 and DIALux EVO – Main Differences"// Light & Engineering Journal, 2013, Vol.21, #3, pp.58–63.
5. SP 52.13330.2016 Daylighting and artificial lighting.
6. GOST R55710–2013 Lighting of indoor work places. Norms and methods of measuring.
7. Rekomendacii po tekhniko-ekonomicheskoj ocenke osvesheniya proizvodstvennyh zdanij [Recommendations for technical and economical assessment of illumination of production facilities. NIISF of Gosstroy of the USSR] // Stroyizdat Publ., Moscow, 1983, pp. 10–14.

Svetlana Yu. Minaeva,
student of M. Sc. program of NRU MPEI (Lighting Engineering department)

Vladimir P. Budak,
Prof., Dr. of Tech. Science. In 1981, graduated from MPEI. Editor-in-Chief of Svetotekhnika / Light & Engineering journal, Professor of Light Engineering department of NRU MPEI. Corresponding member of the Academy of Electrotechnical Science of Russia

Light & Engineering
Vol. 27, No. 6, pp. 73–81, 2019 *https://doi.org/10.33383/2017-018*

DEVELOPMENT AND PERFORMANCE ANALYSIS OF A COST-EFFECTIVE INTEGRATED LIGHT CONTROLLER

Sangita Sahana and Biswanath Roy

Jadavpur University, Kolkata, India
E-mail: sahana.sangita@gmail.com

ABSTRACT

An integrated sensor based daylight responsive light controller has been designed and developed. The developed cost-effective light controller performs on logical decision derived from output of integrated sensor circuit comprising of daylight sensor and occupancy sensor. The performance analysis has also been carried out to understand the actual operating condition of the system using different sensors to control lamp circuits in small indoor lighting applications. The sensitivity levels of the photo sensor (i.e. a Light Dependent Resistor or LDR) and the occupancy sensor (i.e. a Passive Infrared Sensor or PIR) circuits can be adjusted through in-built tuning facility in developed circuit after experimental measurement of the response characteristics of the both sensors. By monitoring the indoor lighting system with the developed controller, it is possible to reduce the usage of electrical energy during the absence of occupant in any room. It is also possible to vary lamp output according to the seasonal variation in daylight level by selecting different reference voltage level and to use minimum electrical energy by utilizing the available daylight. It is a low cost solution due to the advantage of components and the sensors in the market at low cost.

Keywords: energy saving, LDR, light controller, PIR sensor

1. INTRODUCTION

Electrical energy is one of the most important resources in economic development for any country. To meet the increasing demand of electrical energy for rising population and rapid urbanization, optimal utilization of energy is very necessary. Previous research shows that energy used in lighting system is (20–40) % of total electrical energy consumption for commercial buildings [1] and 50 % in case of residential buildings [2]. Therefore saving in lighting systems can save a considerable amount of electrical energy. Saving in lighting energy can be done by the improvement in lighting energy management system with proper lighting control strategies. Lighting automation enables automatic control of electric lights based on occupancy, daylight levels, personal preferences of the user regarding the lighting environment and even peak demand [3, 9]. Proper use of daylight with the artificial lighting system can save a considerable amount of electrical energy. This can be achieved with a photosensitive light control system by adjusting the output of artificial lighting system based on the available daylight [4]. The photosensitive light control systems generally operates based on the detectors like occupancy sensor, photo sensor etc. [5–8, 10–16]. The lighting control systems that are commonly available are based on different technologies. The Philips ActiLume (1–10) V has been developed to achieve ambitious energy savings (up to 70 %) by combining presence detection and natural daylight [17] where the ActiLume Wireless (1–10) V system consists of the ActiLume (1–10) V sensor and the ActiLume Wireless (1–10) V Switch Box[18]. There are few systems also available based on DALI protocol [19, 20]. In this paper we have presented a light controller that can sense daylight level and occupancy and to control the light output of the artificial lights accordingly. Therefore, the developed controller can be used as On-Off controller and as well as dimming controller. Due the high price of the available lighting controller sometimes they are avoided. Therefore, the aim is to develop the cost effective controller to encourage the users towards minimal use of electrical energy.

2. OBJECTIVES

The specific objectives of the work are energy saving, automatic light control and low cost solution by developing a light controller which consists of occupancy sensor and photo sensor to make an occupancy based and daylight responsive lighting control system for maintaining the required illuminance value in presence of occupancy. At present, there are lots of technologies available for dimming control of lamps but in this paper a simple dimming controller for indoor applications has been developed utilizing the pulse width modulation (PWM) technique and using triac firing by generated pulse for different firing angles. A LDR, which is used as photosensor, is a very low cost solution and the PIR sensor is also easily available in market at low cost. The most commonly used lamps in indoor lighting i.e. fluorescent lamps (FTL), compact fluorescent lamps (CFL) are used for measurement purposes.

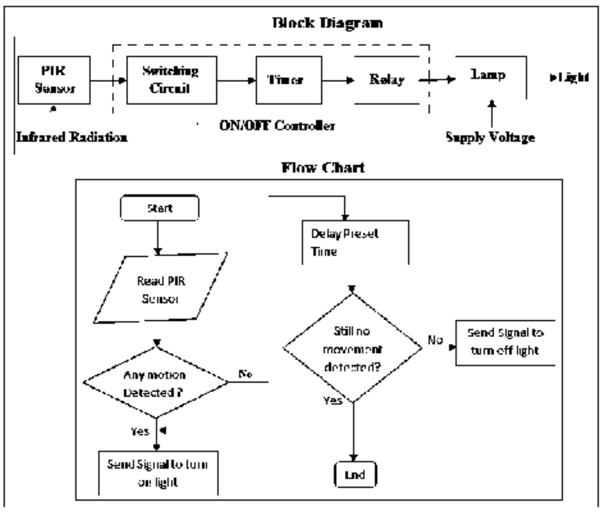

Fig.1. Representation of Scheme I

However, any LED modules with in-built driver can be controlled using this light controller. In this work performance of the developed controller is evaluated using some conventional lamps viz. FTLs and CFLs as test sample, by measuring electrical and photometric parameters. Therefore, the system can be used in rural areas as well as in different indoor lighting application areas to reduce the use of electrical energy in lighting system.

3. DESIGN AND DEVELOPMENT OF LIGHT CONTROLLER

Two different sensor circuits were designed and electronically integrated with the controller circuit through various schemes for continuous control of lamp circuit by using both PIR and LDR sensors.

3.1. Light Control Scheme I

In this scheme the lamp circuit is automatically switched on/off by monitoring the occupancy using LHI 968.

Passive Infrared (PIR) LHI 968 with typical responsivity of 3.8kV/W is used as the occupancy sensor in the circuit. It is a commercially available and very cheap occupancy sensor which perceives, measures and responds to the infrared radiation being emitted from an object in its field of view to detect presence or any motion of objects. This sensor is termed as passive because it does not emit any energy itself, but generates a signal based on the pattern of infrared radiation within its detection area. PIR sensors elements are usually designed in a symmetrical form and placed in discrete manner to separate thermally induced charges from the piezoelectrically induced charges and for better rejection of the in-phase signals. These discrete elements are called inter digitized electrodes. A Fresnel lens is used to focus the IR radiation from objects on its sensing element and also protects from outside hazards. The PIR sensor is most sensitive to the radiation of 10 μm which is the peak wavelength of radiation coming from a human body. However PIR sensors require an unobstructed view of the occurrence of motion and cannot easily discern between humans and small animals. They are susceptible to "dead spots" which are areas where motion cannot be detected within the field of view.

The lamp controller circuit was designed with proper electronic circuitry for automatically switching on/off by monitoring the occupancy of a room. The power voltage level has been converted to dc control voltage to operate the circuit. The block diagram and corresponding flow chart are shown in Fig.1. When any motion is detected, a higher voltage signal is applied to the base of the transistor and it switches on and triggers the relay to glow the lamp.

The necessary circuit consists of:

- Power Supply;
- Sensor Circuit;
- Control Circuit;
- Lamp Circuit.

3.2. Light Control Scheme II

In this scheme, LDR is used as daylight sensor. A Cadmium Sulfide (CdS) Light Dependent Resistor (LDR) has been used as the photosensor. It is a small, round and passive semiconductor device with variable resistance according to the amount of light falling on its surface. The value of the resistance decreases as the amount of incident light increases, and vice versa. In the absence of incident light, LDR exhibits maximum resistance in the order of mega-ohms which is termed as "Dark Resistance". The typical value is 100 MΩ in this case. The LDR sensor was covered with a white diffuser to collect the light from all the directions as well as to minimize cosine error.

The block diagram representation and the flow chart of this scheme are shown in Fig.2. The circuit works by incorporating a balancing bridge and one comparator IC741. The comparator compares LDR output voltage with the set reference voltage and accordingly operates the relay to switch ON/OFF lamp. One capacitor and diode were used to avoid relay-chattering and sparking of relay coil during operation.

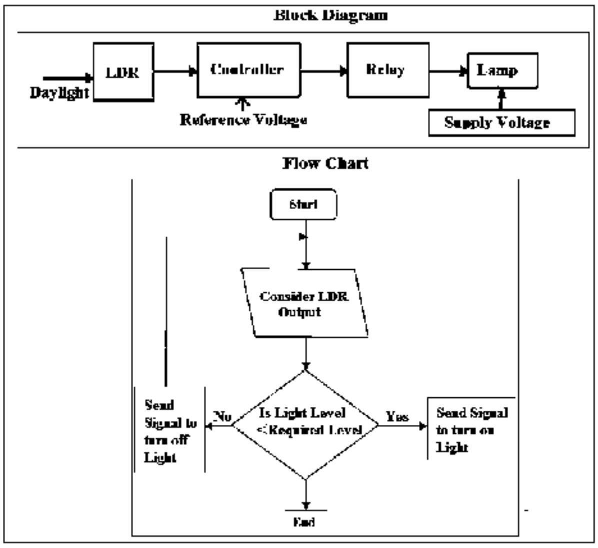

Fig.2. Representation of Scheme II

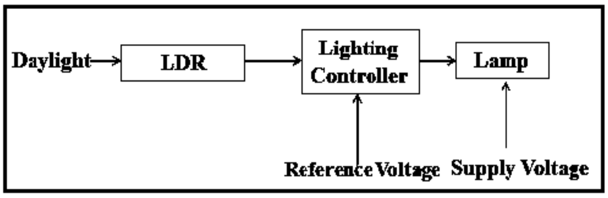

Fig.3. Block Diagram representation of Scheme III

The necessary circuit consists of:

- Power Supply;
- LDR Control Circuit;
- Lamp Circuit.

3.3. Light Control Scheme III

In this scheme, the controller has been developed for continuous dimming and also to meet the required illuminance level in response to the

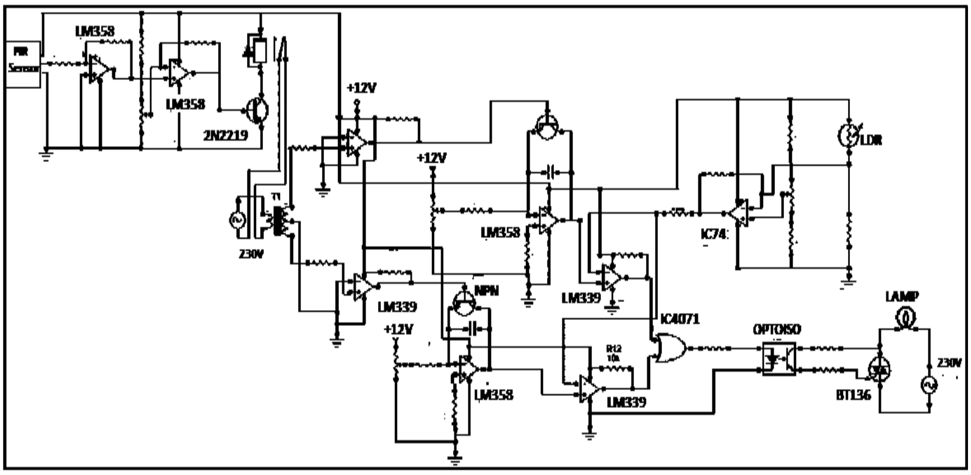

Fig.4. Circuit Diagram of the controller

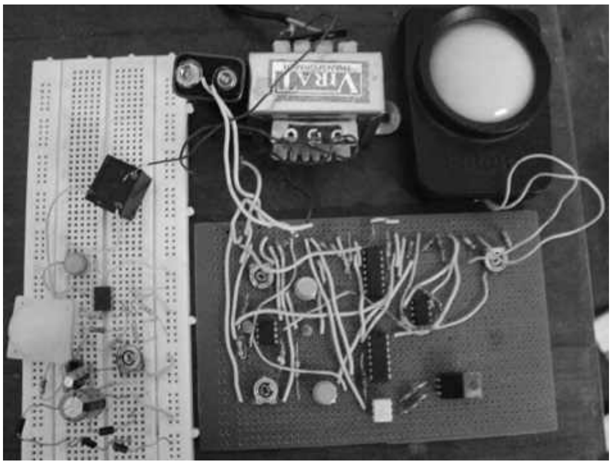

Fig. 5. Developed Light controller

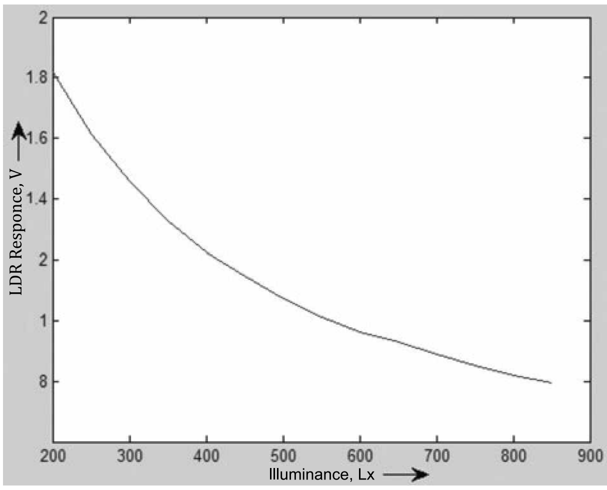

Fig.6. Response Characteristics of the LDR

amount of daylight falling on the LDR. Block diagram representation of the dimming controller is shown in Fig.3. The developed circuit consists of:

- LDR circuit;
- Dimming Controller Circuit;
- Firing Circuit;
- Lamp Circuit.

The DC voltage level corresponding to the required light level is set as controller reference voltage. The firing angle of the triac was controlled by generated PWM signal. One opto-isolator has been used to isolate the low voltage control side from the high voltage power side for safety purposes.

3.4. Light Control Scheme IV

The final circuit is designed for detecting both occupancy and daylight illuminance and also to control the light output of the lamp according to the variation in daylight illuminance. While using in practical cases, the sensors can be used as ceiling mounted applications with a direct line of sight. For some cases, it may happen that daylight illuminance is very low in that position. For those cases, the required illuminance level can be achieved by adjusting the set –point of the pot resistance. The developed circuit consists of three parts:

- PIR Circuit;
- LDR Circuit.
- Dimming Controller Circuit: both the sensor circuits were coupled electronically and integrated with the main controller circuit. The dimming controller circuit operates only when the PIR sensor circuit detects occupancy. The lamp output can be dimmed according to the required illuminance level by varying the firing angle of the triac as per the width of the PWM signal.

The photograph and final developed controller circuit of the controller is shown in Fig. 4 & Fig.5.

4. EXPERIMENTAL RESULTS & PERFORMANCE ANALYSIS

The developed dimming controller was experimented and analyzed through various stages. The

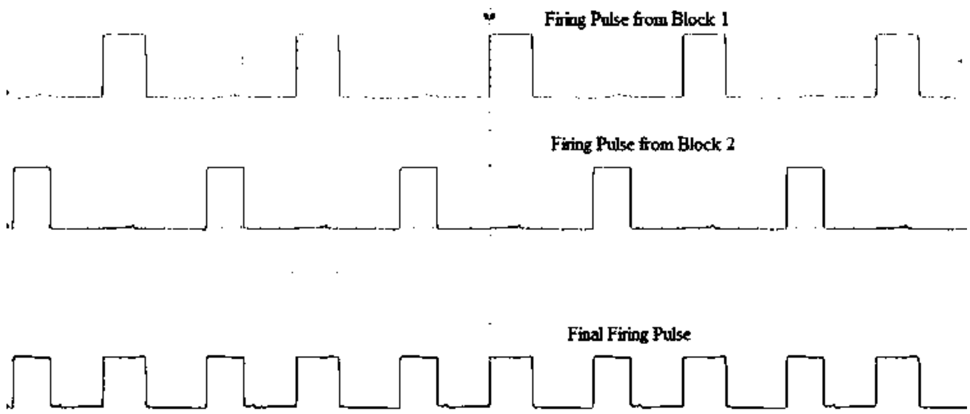

Fig.7. Final Control Pulse

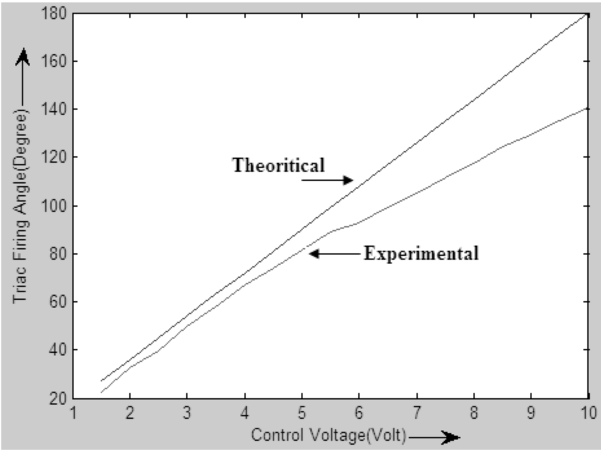

Fig.8. Variation of Triac Firing Angle with Control Voltage

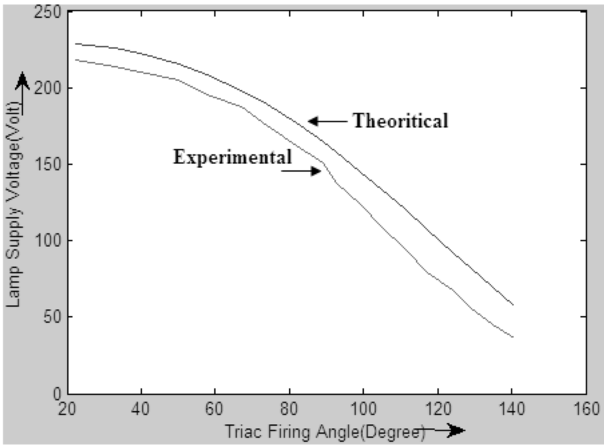

Fig.9. Variation in Lamp Supply Voltage with Firing Angle

dimming characteristics of the lamps for indoor applications were observed experimentally using the developed controller.

4.1. LDR Response

The spectral response of the LDR is close to the V(λ) curve i.e. human eye responsivity curve. In this study the LDR sensor was not provided any colour correction. The illuminance values were measured by using a Konica Minolta Chromameter, CL 200. The LDR response with variation in incident illuminance level is shown in Fig.6.

4.2. Lamp Voltage Control Signal

The generated waveforms from each block of the developed controller were observed and recorded through 4 channels Digital Phosphor Oscilloscope DPO 4034 of Tectronix. The generated control pulse (i.e. PWM signal) of the controller circuit is shown in Fig.7.

4.3. Experimental Setup & Analysis

The developed daylight responsive dimmer circuit can be used to dim the lamps generally used in indoor lighting for general purposes. A 60 W, 230V Incandescent lamp, 36 W fluorescent lamp with magnetic ballast and three non-retrofit compact fluorescent lamps (CFL) of 15 W and sample 1 of 23 W and sample 2 of 23 W lamps were dimmed using the developed circuit. Here all three 15 W CFLs are non retrofit type. But in case of 23 W CFLs, the sample 1 is non retrofit and cool white type and the sample 2 is retrofit and warm white type. According to the daylight variation, the width of the control pulse changes which results in firing of the triac for different firing angles. The variation of lamp supply voltage with different firing angle has been measured & compared with theoretical values using the expression:

$$U_i = U_r[\frac{1}{\pi}(\pi - \alpha + \frac{1}{2}\sin(2\alpha))]^{1/2},$$

where U_i is the lamp supply voltage (V), U_r is the RMS value of system voltage (V), and α is the firing angle of the triac (degree). Variation of 1 V of the control voltage is equivalent to corresponding change in the pulse width of 18 degrees of control signal. The experimental and theoretical values of triac firing angles and corresponding variation in lamp supply voltage (as shown in Fig. 8 & Fig. 9) are compared to validate the response of the controller. It is found that with the increase in the value of the control voltage i.e. with the increase in the pulse width, the triac triggering angle increases and vice versa. Again with the increase in the triac firing angle, the lamp supply voltage decreases, and as a result the lamp output also decreases. It is observed that there is a slight difference between the theoretical values and the experimental results of triac firing angle and lamp supply voltage.

The generated control voltage output from the controller and the corresponding lamp voltage output are shown in Fig.10, Fig.11 for two different types of lamps of different power as sample cases which are generally used in indoor applications.

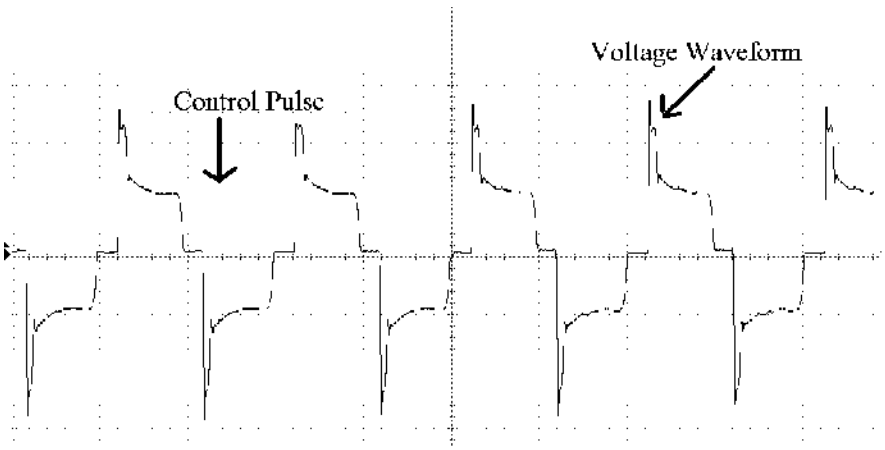

Fig.10. Control pulse & Lamp Voltage waveshape of FTL at 70 % dimming

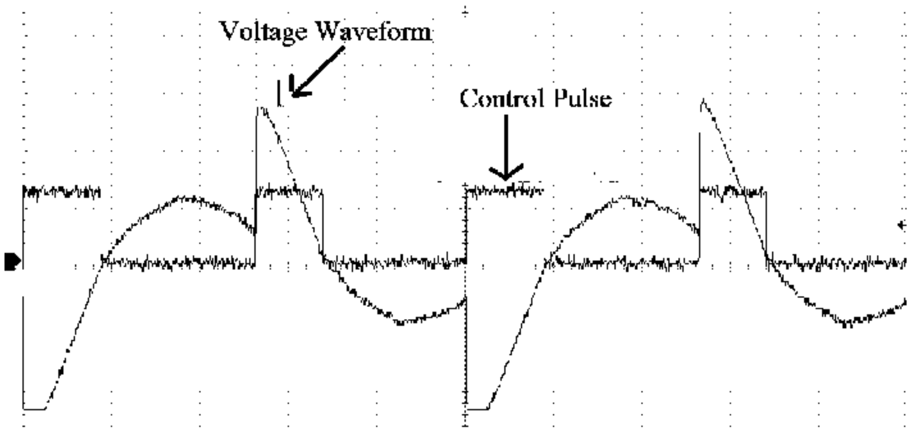

Fig.11. Control pulse & Lamp Voltage wave shape of 15W CFL at 70% dimming

4.4. Dimming of Lamps

The performance of developed controller was verified with few lamps. The luminous flux of lamps was measured using large integrating sphere of 2.5m diameter and luminous flux standard lamp. The dimming characteristics of the incandescent lamp (GLS), fluorescent lamp (FTL), and three retrofit compact fluorescent lamps (15W CFL, 23W CFL1, 23W CFL2) are shown in Fig.12.

From the above plots, it is clear that with the increase in control voltage, the lumen output of the lamp decreases. For the 15W CFL lamp the light output can be dimmed upto 36 %. But in case of 23W lamps, two different samples were used to verify the performance of the dimmer. The sample 1 was of lower luminous flux (i.e. 1300 lm) and lower power factor (i.e. 0.85) than the sample lamp 2 (i.e. 1350 lm and 0.89 pf). But the sample1 (non-retrofit) was cool white and the sample 2 (retrofit) was warm white. Now if the characteristics of these two lamps are observed then it is evident that sample 2 was dimmed upto only 10 % and the sample lamp 1 was dimmed upto 30 %. As we have used dimmable and non-retrofit CFLs with 4 pins, where ballast is not integrated, rather the ballast is to be connected externally. However, the retrofit CFLs are generally non-dimmable. This is due to the fact that at present, all the retrofit CFL lamps are so designed that they can prevent the variation in the light output due to voltage fluctuation. So it can be stated that the sample lamp 1 was designed properly to resist the variation in light output due to voltage fluctuation. But in case of sample lamp 2 more dimming is possible and the luminous flux reduces almost linearly.

5. EXPERIMENTAL RESULTS & PERFORMANCE ANALYSIS

In the developed light controller, the required control voltage to generate the firing pulse comes from the LDR unit. The value of daylight illuminance was transformed into corresponding control voltage level by the LDR circuitry.

5.1. Control Voltage from LDR Unit

The control voltage coming from the LDR unit was varied by varying the incident illuminance level

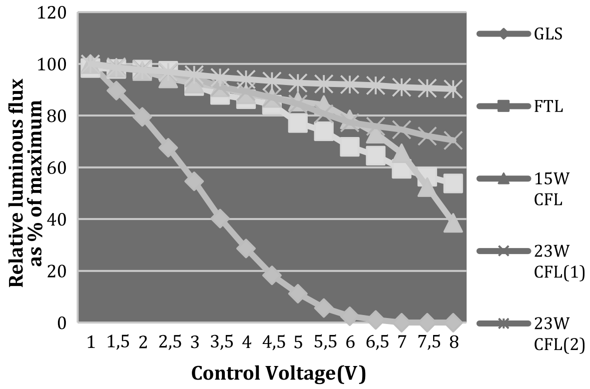

Fig.12. Dimming Characteristics of different Lamps using the developed controller

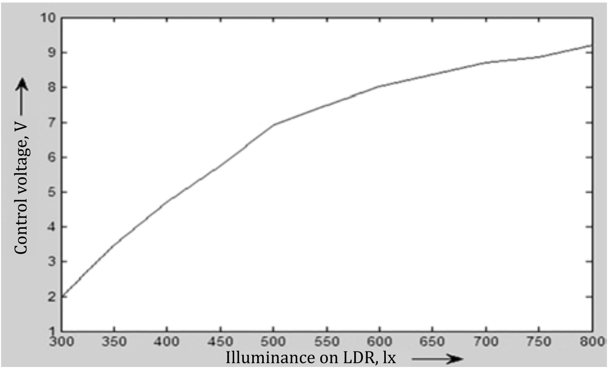

Fig.13. Variation in control voltage with daylight level on LDR

on the diffuser surface. For a fixed reference voltage, the control voltage output from the LDR unit increases with the increase in incident light level. The characteristic is shown in Fig.13.

5.2. Variation of Light Output for Different Reference Voltages

One experiment was carried out to find out the control voltage output from the LDR unit for different reference voltage level of 2V to 10V to dim a 36W FTL lamp. The control voltage was recorded for different reference voltage levels. The reference voltage can be varied by adjusting the pot resistance. The indirect illuminance from integrating sphere was measured by Chromameter while placing the lamp at the centre of integrating sphere. The nature of the variation of the control voltage with daylight level is shown in the Fig.14 for 3 different sets of control voltage. The variation in the light output of the FTL with the natural illuminance on LDR surface for different corresponding control voltage level is also shown in Fig.15.

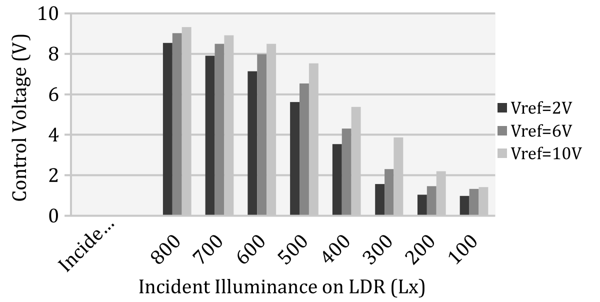

Fig.14. Variation in Control Voltage with Daylight

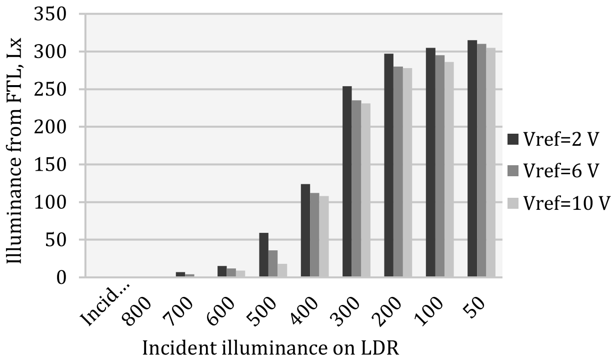

Fig.15. Variation in lamp output with daylight level for different reference voltages for FTL lamp

6. COST ANALYSIS

The components used to develop the circuits are easily available in market. The comparison of cost between different schemes is shown in Fig.16. As the cost of IR sensor is more than the cost of the LDR sensor, the cost for Scheme II is lower than the other types of schemes. The cost comparison is done on the basis of INR (i.e. Indian National Rupee).

7. OBSERVATIONS

It is observed that for the developed integrated sensor based daylight responsive light controller,

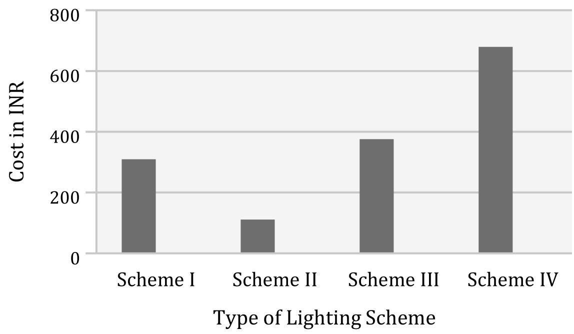

Fig.16. Comparison of light controller cost for different schemes

with the increase in the control voltage the lamp supply voltage decreases and as a result the lumen output of the lamps also decreases. The control voltage is supplied from the LDR unit. The control voltage output from the LDR unit is increased with the increase in daylight level. As a result, the lamp light output is decreased for the decrement of lamp supply voltage. On the other hand, when daylight level is low, the control voltage output is decreased. Therefore, the lamp light output is increased for the increment of the lamp supply voltage. If the reference voltage set for the LDR unit is varied, the control voltage can also be varied. For a higher reference voltage, higher control voltage is achieved for higher illuminance level. From Fig.14 it is evident that for same daylight illuminance, the control voltage values are more for the reference voltage of 10V than the lower reference voltage levels. For the same daylight illuminance, the control voltage values are lesser for the reference voltage of 2V than the higher reference voltage levels. As a result less light output will be available for higher reference voltage level. Therefore, when the availability of daylight is less i.e. during winter season or when the daylight availability is more i.e. in summer, the reference voltage is to be adjusted accordingly to achieve the required illuminance level. However, the control voltage has to be set manually by adjusting the pot resistance.

8. CONCLUSION

The objective of the work was to develop a cost effective integrated light controller and also to evaluate the performance of the developed controller in small indoor applications. In the present work, it is seen that the sensitivity levels of the photosensor and the occupancy sensors circuits can be adjusted through in-built tuning facility in the developed circuit. The artificial lamps can be switched off by using the simple developed controller to reduce the waste of electrical energy in the absence of any occupancy or in the presence of any occupant with sufficient daylight illuminance. The dimming controller can dim the light output of the lamps used in indoor lighting for general purposes, according to the daylight availability. It was also possible to vary light output according to the seasonal variation in daylight level by selecting different reference voltage level. The system will be more effective if we apply zoning control. Another detailed study is also required for understanding the lamp performance using the developed light controller. Commercially available LEDs can be controlled with few modifications in this circuit. The effectiveness of this system in controlling LED lamps is not shown in this paper. Only the results for FTLs & CFLs are shown as sample cases. However, the system can be installed in indoor application areas for detecting occupancy and reducing the use of electrical energy by utilizing the the daylight illumination.

9. ACKNOWLEDGMENT

This work is part of project of M.E. Illumination Engineering done by the first author. We are thankful to Ms. Debjani Ganguly, Associate Professor, Electrical Engineering Department, Indian Institute of Engineering Science and Technology, Shibpur and Dr. Biswendu Chatterjee, Assistant Professor, Electrical Engineering Department, Jadavpur University for their valuable suggestions in carrying out this work.

REFERENCES

1. Shashi R.V., Secretary, Government of India, Ministry of Power, Energy Markets And Technologies In India // Keynote Address in Global Energy Dialogue at Hanover (Germany), April 25, 2006.
2. Slater A.I., Lighting and Energy in Buildings. Presented at the 23rd Session of the CIE, New Delhi, Published by International Commission on Illumination, Vienna, 1995, Vol.1.
3. Rubinstein F., Siminovitch M. and Verderber R., Fifty Percent Energy Savings with Automatic Lighting Control // IEEE Transactions on Industry Applications, 1993, Vol.29, #. 4, pp. 768–773.
4. Fraden J., Handbook of Modern Sensors: Physics, Designs, and Applications. Fourth Edition, 2010.
5. Guo X., Tiller D.K., Henze G.P. and Water C.E., The performance of occupancy-based lighting control systems // Lighting Research and Technology, 2010, Vol. 42, pp.415.
6. Tiller D.K., Guo X., Henze G.P. and Waters C.E., Validating the application of occupancy sensor networks for lighting control // Lighting Research and Technology, 2010; Vol.42, pp.399–414.
7. Newsham G.R., Aries M.B.C. and Mancini S and Faye G, Individual control of electric lighting in a daylit space // Lighting Research and Technology, 2008, Vol.40, pp. 25–41.

8. Rubinstein F., Siminovitch M. and Verderber R., Fifty Percent Energy Savings with Automatic Lighting Control // IEEE Transactions on Industry Applications, 1993, Vol.29, no. 4, pp. 768–773.

9. Rea, M. (Ed.), Lighting Handbook Reference & Application, Illuminating Engineering Society of North America. Ninth Edition, 2000.

10. Kim S. and Mistrick R. "Recommended Daylight Conditions for Photosensor System Calibration in a Small Office // Journal of the Illuminating Engineering Society, 2001, pp. 176–188.

11. Mistrick R.G. and Sarkar, A., Daylight-Responsive Photosensor Control in Classrooms with Different Daylight Delivery Systems", presented at the IESNA Annual Conference in Tampa, Florida, July 2004.

12. Bierman A. and Conway K.M., "Characterizing Daylight Photosensor System Performance to Help Overcome Market Barrier // Journal of the Illuminating Engineering Society, 2000, pp. 101–115.

13. E Source Emerging Technology Series, Kinney L., Practical Control Strategies for Harvesting Daylight Savings, ER-00–13, July 2000.

14. Slater A.I., Lighting and Energy in Buildings, presented at the 23rd Session of the CIE, New Delhi, Published by International Commission on Illumination, Vienna, 1995, Vol.1.

15. Rubinstein F., Avery D., Jennings J. On the Calibration and Commissioning of Lighting Controls. Right Light Conference, Copenhagen, Denmark, 1997.

16. Kim S. and Mistrick R. Recommended Daylight Conditions for Photosensor System Calibration in a Small Office // Journal of the Illuminating Engineering Society, 2001, pp. 176–188.

17. Philips Actilume1–10V Application guide http://www.lighting.philips.com/pwc_li/main/products/controls/assets/actilume1–10V-applicationguide-v2fin2-new.pdf.

18. Philips 1–10V OEM application guide http://www.lighting.philips.com/pwc_li/main/products/controls/assets/actilume%20wireless1–10v-oem-application-guide-dec2012-new.pdf

19. Philips DALI Application guide http://www.lighting.philips.com/pwc_li/main/products/assets/pdf/Actilume_DALI_Gen2_ApplicationGuide-V4_Apr-2014.pdf

20. Philips ActiLume OEM Application guide] http://www.lighting.philips.com/pwc_li/main/products/assets/pdf/ActiLume_OEM_ApplicationGuide_V2Fin.pdf

Sangita Sahana,
is currently working as Assistant Professor, of the Electrical Engineering Department, Jadavpur University, India. She received her Master Degree in M.E. Illumination Engineering in 2012 & BE in Electrical Engg in 2010 from Jadavpur University

Dr. Biswanath Roy,
Professor of Illumination Engineering Section of the Electrical Engineering Department of Jadavpur University, India. He received a Ph.D. (Engg.) in Daylighting in 1999 from Jadavpur University after receiving an M. Sc. (Tech.) in optics and optoelectronics in 1993 and B. Sc. (Hons.) in physics in 1989 from the University of Calcutta. He is Life Fellow of the Indian Society of Lighting Engineers (ISLE), Life Member of the Institution of Engineers (India)

Light & Engineering
Vol. 27, No. 6, pp. 82–87, 2019 *https://doi.org/10.33383/2018-112*

ANALYSIS OF CHARACTERISTICS OF LED LAMPS WITH *T8* BULB BY VARIOUS MANUFACTURERS

Nina P. Nestyorkina, Olga Yu. Kovalenko, and Yulia A. Zhuravlyova*

N.P. Ogarev Mordovia State University, Saransk
**E-mail: ulypil@mail.ru*

ABSTRACT

The article analyses the operational characteristics of 10W LED lamps with *T8* bulb manufactured by *ASD* (Russia), *Smartbuy* (Taiwan), and *VOLPE* (PRC) and 18W FL with *T8* bulb manufactured by *PHILIPS* (Poland) including the dependence of these lamps on the supply voltage. The results of measurements show that: a) the period of stabilisation of electric parameters and luminous flux of LED lamps does not cause discomfort of illumination unlike the said FL, the luminous flux of which at the moment of switching on is 70 % of the nominal value, which is reached after 13 minutes; b) with nominal voltage of supply network, the value of luminous flux of *10W ASD LED-T8R-STD* LED lamp (Russia) is 6 % less than the declared one, and that of *Smartbuy SBL-T8–10–64K-A* (Taiwan) and *VOLPE LED-T8–10W/DW/G13/FR/FIX/N* (PRC) is even less; c) the general colour rendering index of all studied LED lamps is less than the declared one (72 instead of 80); d) the flicker index of all studied LED lamps does not exceed the declared value of 5 %; e) the characteristics of LED lamps almost do not depend on changes of the supply voltage within the range of ±10 %.

The recommendations regarding the application of the studied LED lamps are given.

Keywords: LED lamp, *T8* bulb, luminous flux, colour temperature, colour rendering index, luminous flux stabilisation, nominal voltage, luminous efficacy, flicker index

1. PROBLEMS OF INTRODUCTION OF LED-BASED LIGHTING DEVICES IN NATIONAL ECONOMY

The LED-based lighting devices have been increasingly introduced in different areas of life attracting the attention of scientists [1–3]. The apparent advantages of LEDs and LED lamps (efficiency, small size, environmental friendliness) are positively perceived by consumers of different branches of economy. However, experience has shown that, in the early 2010s, manufacturers attributed the high characteristics of LEDs obtained in the laboratory environment to their industrial samples reaching consumers in the form of LEDs and LED-based light sources with declared high characteristics. For instance, the values of the luminous flux of four types of LEDs of the *XLamp XP-E/XP-G/XM–L* series by *Cree* measured by the L.I.S.T. laboratory in 2011 were averagely almost 10 % lower than the declared ones [4].

Studying the efficiency of agricultural application of lighting and irradiating devices based on LEDs and LED lamps, we found that the samples of these devices manufactured for experiments did not always provide required values of luminous flux calculated according to the LED characteristics declared by manufacturers.

In general, our studies of agricultural plants and animals showed an increase of their productive indicators with illumination and irradiation by means of LEDs and LED lamps [5–8], which confirms good perspectives of widening of their application if

a) *b)* *c)*

Fig. 1. Exterior of LED lamps with *T8* bulb: a) *ASD LED-T8R-STD*10Вт 230В *G13*6500K 800lm 600mm (Russia); b) *Smartbuy SBL-T8–10–64K-A* (Taiwan); c) *VOLPE LED-T8–10W/DW/G13/FR/FIX/N* (PRC)

there is reliable information on parameters of such sources.

The articles [1–3] underline the problems related to lighting conditions affecting the visual performance indicators, and the article [9] shows non-compliance of the declared light parameters of LED-based luminaires with actual ones.

Concerning, the goal of the article is the analysis of the practical issue of compliance of the LED lamp parameters declared by manufacturers with the actual ones, which may be of interest to designers of illumination or irradiation and energy departments of consumer enterprises.

2. RESEARCH OF CHARACTERISTICS OF LED LAMPS WITH *T8* BULB

For experimental comparative studies, three LED lamps with *T8* bulb (*ASD LED-T8R-STD10W 230V G13 6500K 800lm 600mm* (Russia), *Smartbuy SBL-T8–10–64K-A* (Taiwan), and *VOLPE LED-T8–10W/DW/G13/FR/FIX/N* (PRC)) and one *PHILIPS TL-D18W/33–640* FL with *T8* bulb manufactured in Poland [10–13] (Fig. 1) were purchased in retail shops of Saransk.

The studies were conducted in the laboratory of the Centre of collective usage "Light Engineering Metrology" (in the Institute of Electronics and Light Engineering of N.P. Ogarev MSU). The electrical and light parameters were measured in normal conditions in accordance with the methodology of GOST [14]. The parameters of all said LED lamps were measured by means of photo colorimeter, *DPS1060* AC power unit, goniophotometer, TKA-PKM (08) flicker/illuminance meter, and TKA-VD/02 spectral colourimeter.

For determination of chromaticity coordinates, the spectral radiometry method was used. For evaluation of colour rendering, the multispectral method was used. In addition, the methods of measurement of correlated colour temperature T_{cc} and dominant wavelength according to GOST [14] were used.

The measurements of power and luminous flux changes of the lamps during the stabilisation period of electrical and light engineering characteristics at nominal U_n were performed using a *Gooch & Housego* photo colorimeter containing an *OL IS7600* Ulbricht sphere with the diameter of 2 m, multi-channel *OL 770 VIS/NIR* spectroradiometer, *770–7G-3.0* fibre-optic cable, *OL410–200 PRECISION LAMP SOURCE* precision DC power unit for power supply of auxiliary lamp *AUX LAMP A180*, and rebar for fixing of the lamps and PC.

The limits of acceptable relative error of luminous flux measurement are ± 9 %; the limits of acceptable absolute error of measurement of x and y chromaticity coordinates are ± 0.002; the limits of acceptable absolute error of measurement of T_{cc} are ± 25 K; relative error of the output current unit is ± 0.02 %.

The functional principle of the photo-colorimeter measuring setup (state register number of a measurement instrument is 66263–160) is based on measurement of absolute spectral distribution of radiant flux, its integrating, and determination of the radiant flux received by the photometric plate that is the end of the fibre-optic input linked with the spectrometer and CCD line. All calculations were made automatically. The setup software represents the information on the control computer screen and sets the measurement conditions [15].

First, the stabilisation period of electrical parameters and luminous flux was determined (Fig. 2 and 3)[1].

The results of all measurements were processed using built-in *GQ-Sof* software with the output of the results to PC and on paper.

The measurements were performed in stable electrical mode after 15 min of continuous lighting ac-

[1] The stabilisation period is the period required for reaching of stable heat conditions of operation of a LED lamp according to GOST [16]. The electrical and light parameters of a lamp are stabilised during this period

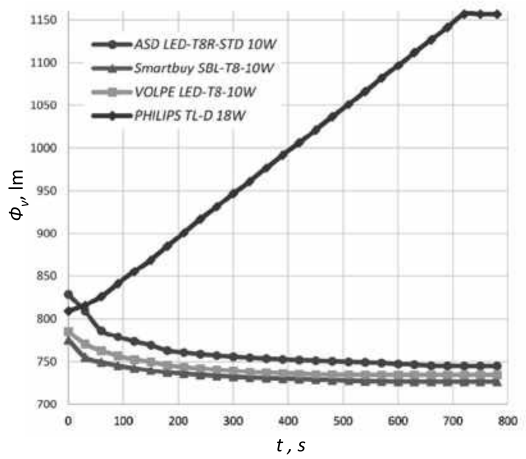

Fig. 2. Changing of luminous flux of the studied lamps Φ_v over the stabilisation period

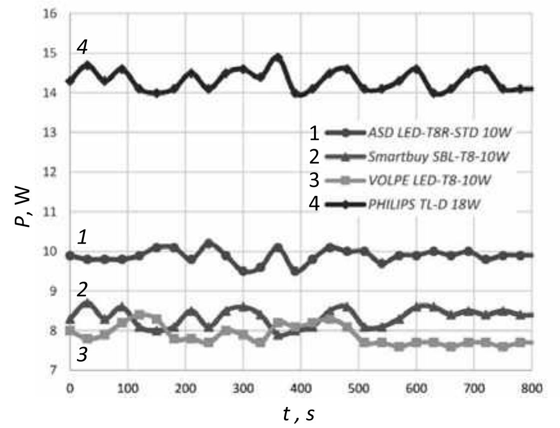

Fig. 3. Changing of power of the studied lamps P over the stabilisation period

cording to GOST [14] at an ambient temperature of 25±2 °C, relative humidity of 65±20 %, the atmospheric pressure of 101±4 kPa, U_n of 220±22 V, and current frequency of 50 Hz.

The results of all listed measurements at nominal voltage are presented in Table 1.

In addition, the dependencies of the lighting and electrical parameters of lamps on U_n (Fig. 4–6) were determined.

In accordance with the method of GOST [17], the dependence of the lamp flicker index k_f[2] on U_n with U_n changing within the range of ± 10 % was determined by means of the TKA-PKM (08) flicker/illuminance meter. The k_f measurements were performed during the night time with 45 minutes of luminous flux stabilisation and typical location of all reference points in the premises. In each reference point, the illuminance values were measured three times during 5 minutes period. The relevant results are shown in Figs. 7 and 8.

3. MEASUREMENTS RESULTS ANALYSIS OF CHARACTERISTICS OF LED LAMPS WITH *T8* BULB

The analysis of the results of measurements has shown that the stabilisation periods of electrical parameters and luminous flux of *ASD LED-T8R-STD*10*W*, *Smartbuy SBL-T8–10W*, and *VOLPE LED-T8–10W* LED lamps and *PHILIPS TL-D18W* FL were equal to 12, 10, 9, and 13 minutes respectively; the corresponding fluctuations of luminous flux of LED lamps were equal to 93 lm (11.2 %), 49 lm (6.3 %), and 51 lm (6.4 %). However, it does not cause discomfort of lighting unlike the *PHILIPS TL-D18W/33–640* FL with its luminous flux at the moment of switching on equal to 70 % (809 lm) of the nominal value, which is reached in 13 minutes.

The analysis of the measurements results of characteristics of lamps at nominal U_n allows us to conclude:

- The values of the luminous flux of all studied lamps are lower than the declared values: *ASD LED-T8R-STD*10*W*: 46 lm (5.7 %), *Smartbuy SBL-T8–10W*: 376 lm (34.1 %), *VOLPE LED-T8–10W*: 171 lm (18.9 %), and *PHILIPS TL-D18W*: 44 lm (3.6 %);
- The measured T_{cc} of *ASD LED-T8R-STD*10*W* LED lamp and *PHILIPS TL-D18W* FL are almost equal to the declared values, whereas those of

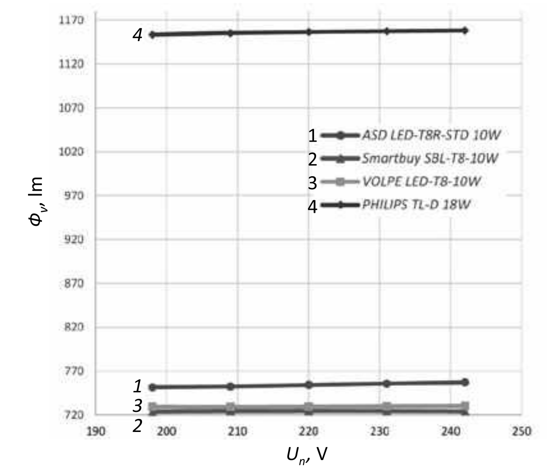

Fig. 4. Dependence of luminous flux of the studied lamps Φ_v on U_n

[2] k_f is the evaluation criterion of relative amplitude of illuminance fluctuation in a lighting installation as a result of time change of luminous flux of light sources with supply of alternating current [18]

Table 1. The Results of Measurements of Electrical and Light Engineering Characteristics of Lamp Samples with Nominal Supply Voltage

Lamp type		*ASD LED-T8R-STD10W*		*Smartbuy SBL-T8–10W*		*VOLPE LED-T8–10W*		*PHILIPS TL-D18W*	
Values		declared	measured	declared	measured	declared	measured	declared	measured
Luminous flux, lm		800	754.3	1100	724.3	900	729.5	1200	1156.6
T_{cc}, K		6500	6491	6400	6260	6500	6362	4000	4037
R_a		> 80	72	> 80	72	> 80	72	> 63	61
Colour purity			0.077		0.058		0.058		
Dominant wavelength, nm			493.6		497.2		494.9		
Chromaticity coordinates	x	0.313	0.3118	0.313	0.3160	0.313	0.3145	0.380	0.3818
	y	0.337	0.3364	0.337	0.3402	0.337	0.3351	0.380	0.3879
	u		0.1945		0.1960		0.1968		
	v		0.4721		0.4747		0.4718		
Power, W		10	9.5	10	7.9	10	8	18	14.72
Luminous efficacy, lm/W		80	79.4	110	91.6	90	91.1	67	76.7
k_f,%		< 5	0.8	< 5	0.4	< 5	0.6		8

Smartbuy SBL-T8–10W and *VOLPE LED-T8–10W* LED lamps are 140K (2.1 %) different from the declared ones;

• General colour rendering index R_a of all studied LED lamps is lower than the declared one (72 instead of 80) and is a little less than the declared value;

• k_f of all studied LED lamps is lower than the declared 5 % and is equal to (0.4–0.8) %.

The analysis of the measurements results of characteristics dependence of lamps on U_n has shown that:

• The value of luminous flux of *PHILIPS TL-D18W* FL is decreased by 3.3 lm (0.2 %) with U_n decreasing by 10 % and is increased by 1.6 lm (0.1 %) with U_n increasing by 10 %;

• The power of *PHILIPS TL-D18W* FL is decreased by 1.7 W (11.7 %) with U_n decreasing by

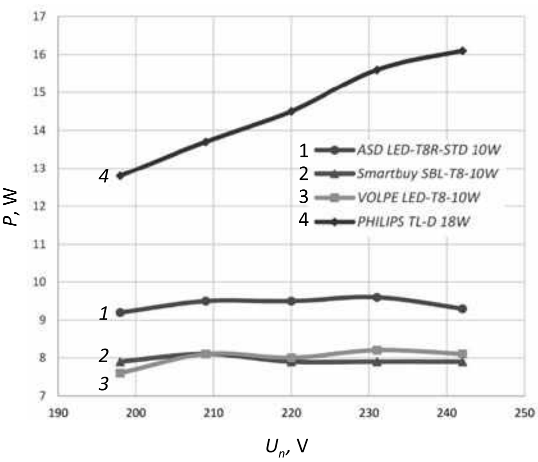

Fig. 5. Dependence of power of the studied lamps P on U_n

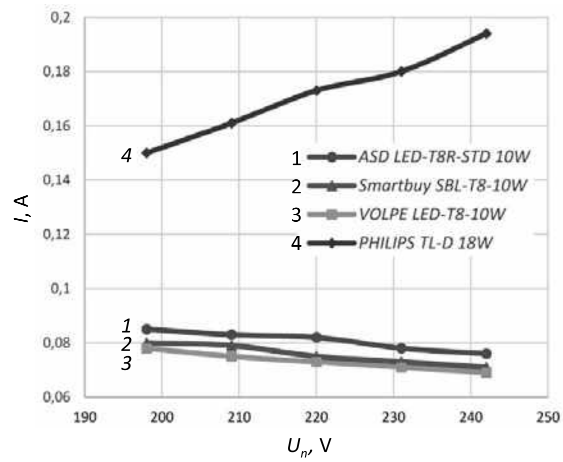

Fig. 6. Dependence of current of the studied lamps I on U_n

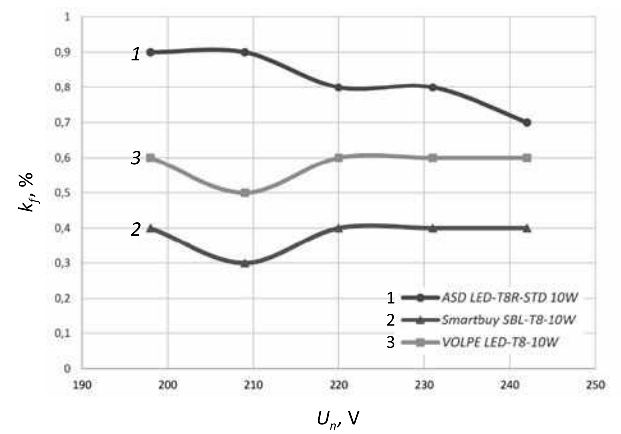

Fig. 7. Dependence of flicker index of the studied lamps k_f on U_n

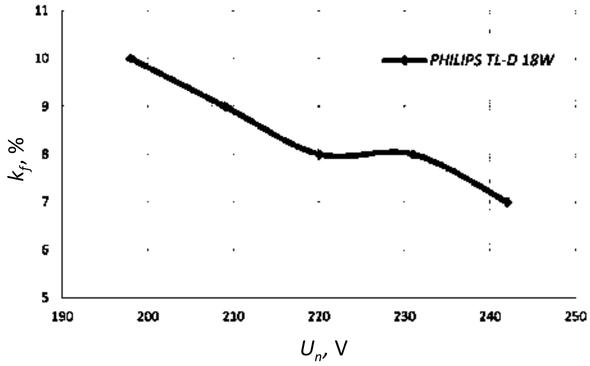

Fig. 8. Dependence of k_f of the *PHILIPS TL-D18W* FL on U_n

10 % and is increased by 1.6 W (11 %) with U_n increasing by 10 %;

- The value of current of *PHILIPS TL-D18W* FL is decreased by 0.023 A (13.2 %) with U_n decreasing by 10 % and is increased by 0.021 A (12.1 %) with U_n increasing by 10 %;
- With U_n changing within the range of ± 10 %, the values of luminous flux, power, and current of all LED lamps are changed within the range of ± 0.4 %.

Therefore, the characteristics of LED lamps nearly do not depend on changes of U_n within the range of ± 10 %.

The analysis of the results of measurements of k_f has shown that:

- With U_n changing within the range of ±10 %, k_f of *Smartbuy SBL-T8–10W* and *VOLPE LED-T8–10W* LED lamps practically does not change equalling 0.4 % and 0.6 % respectively;
- With U_n increasing by 10 %, k_f of *ASD LED-T8R-STD10W* LED lamp practically remains the same, and with U_n decreasing by 10 %, it slightly increases (from 0.8 % to 0.9 %);
- With U_n increasing by 10 %, k_f of *PHILIPS TL-D18W* FL decreases from 8 % to 7 %, and with U_n decreasing by 10 %, it increases from 8 % to 10 %.

Based on the conducted study, the following recommendations may be given:

- According to GOST [18], the *ASD LED-T8R-STD10W* 230*V G136500 K 800 lm 600 mm* (Russia), *Smartbuy SBL-T8–10–64K-A* (Taiwan), and *VOLPE LED-T8–10W/DW/G13/FR/FIX/N* (PRC) LED lamps cannot be recommended to be applied in luminaires for lighting of premises of administrative buildings, kindergartens, educational institutions since their R_a appeared to be 10 % less than 80;
- The *Smartbuy SBL-T8–10–64K-A* (Taiwan) and *VOLPE LED-T8–10W/DW/G13/FR/FIX/N* (PRC) LED lamps should undergo pre-installation inspection of luminous flux since its value of both lamps was significantly lower than the declared one.

The main conclusion of the conducted study is that the actual values of the luminous flux of some LED lamps do not comply with the declared values. For instance, the values of the luminous flux of *Smartbuy SBL-T8–10W* and *VOLPE LED-T8–10W* LED lamps appeared to be (20–30) % lower[3].

REFERENCES

1. Ashryatov A.A., Kokinov A.M., Mikaeva S.A. Issledovanie lineinykh svetodiodnykh lamp [Research of Linear LED Lamps] // Estestvennye i tekhnicheskie nauki, 2012, No. 6, pp. 338–353.

2. Baineva I.I., Bainev V.V. Opticheskie sistemy dlia svetodiodov [Optical Systems for LEDs] // Fotonika, 2016, Vol. 56. No. 2, pp. 84–92.

3. Svetlana A. Amelkina, Olga E. Zheleznikova, and Lyudmila V. Sinitsyna " On the Efficiency of Lighting by LEDs in Visual Work", Light & Engineering Journal, 2018, Vol.26, #3, pp.81–87.

4. Nikiforov S.G. Issledovaniia parametrov svetodiodov CREEXLampXP-E/XP-G/XM–L [Studies of Param-

[3] The lighting installations with such LED lamps will not provide required illumination, and with consideration of actual values of luminous flux of these lamps in the course of designing of installations, the number of luminaires in these installations should be increased by (20–30) %, which therefore correspondingly increases investment and operational costs, which decreases the required effect of introduction of LED equipment

eters of CREEXLampXP-E/XP-G/XM–L LED's] // Poluprovodnikovaia svetotekhnika, 2011, No. 2, pp. 12–18.

5. Kovalenko O. Yu., Ovchukova S.A., Belov V.V. Vliianie parametrov istochnika izlucheniia na bioobieekt [Impact of Parameters of a Light Source on a Biological Object] // Bulletin of the International Academy of Agricultural Education, 2016, Vol. 30, pp. 122–126.

6. Kovalenko O. Yu., Pilshchikova Yu.A. Povyshenie effektivnosti i kontrol parametrov istochnikov izlucheniia i obluchatelnykh ustanovok v selskom khoziaistve [Increase of Efficiency and Monitoring of Parameters of Light Sources and Irradiating Installations in Agriculture] // Photonics, 2017, Vol. 68, No. 8, pp. 68–73.

7. Kovalenko O. Yu., Pilshchikova Yu.A., Ashryatov A.A., Amelkina S.A., Kudashkina M.V. Bird irradiation facility // Patent of the Russian Federation for utility model No. 147826. 2014. Bul. No. 32.

8. Kovalenko O.Y., Pilshchikova Y.A. Enhancement of efficiency of irradiation facility for domestic bird husbandry // International Journal of Pharmacy and Technology, 2016, Vol. 8, No. 2, pp. 14473–14479.

9. Belykh N., Chuvatkina T., Syromyasov D. Energeticheskaia effektivnost svetodiodnoi svetotekhnicheskoi produktsii raschety i realnost [Energy Efficiency of LED Lighting Devices: Calculations and Reality] // Poluprovodnikovaia svetotekhnika], 2014, No. 2, pp. 18–19.

10. URL: http://www.philips.ru/ (reference date: 12.12.2018).

11. URL: http://asd-electro.ru/ (reference date: 12.12.2018).

12. URL: http://www.smartbuy-russia.ru/.(reference date: 12.12.2018).

13. URL: http://volpe.ru/ (reference date: 12.12.2018).

14. GOST R55702–2013 Electric light sources. Methods of measuring of electrical and luminous characteristics.

15. URL: http://fundmetrology.ru/10_tipy_si/11/view.aspx?num=qJbKqJpWgBeM/ (reference date: 12.12.2018).

16. GOST R54815–2011 Self-ballasted LED-lamps for general lighting services by voltage over 50 V.

17. GOST 33393–2015 Buildings and structures. Methods for measuring of illuminance pulsation factor.

18. GOST R55710–2013 Lighting of indoor work places. Norms and methods of measuring.

Nina P. Nestyorkina,
Engineer. In 1975, graduated from the N.P. Ogarev Mordovia State University, specialty Light Engineering and Light Sources. Head of the laboratory, senior lecturer of the Light Sources department of the Institute of Electronics and Light Engineering of N.P. Ogarev Mordovia State University. Scientific interests: modern energy saving discharge and LED light sources, lighting installations, circuit engineering

Olga Yu. Kovalenko,
Dr. of Tech. Science, Associate Professor. In 1983, she graduated from N.P. Ogarev Mordovia State University, specialty Light Engineering and Light Sources. At present, she is Professor of the Metrology, Standardisation, and Certification Department of the Institute of Electronics and Light Engineering of N.P. Ogarev Mordovia State University. Scientific interests: measurement and monitoring of parameters of lighting and irradiating systems

Yulia A. Zhuravlyova,
Ph.D. in Tech. Science. In 2010, graduated from N.P. Ogarev Mordovia State University, specialty Light Engineering and Light Sources. Associate Professor of the Light Sources Department of the Institute of Electronics and Light Engineering of N.P. Ogarev Mordovia State University. Scientific interests: energy saving lighting installations, parameters of modern compact fluorescent lamps and LED light sources, vacuum equipment

Light & Engineering
Vol. 27, No. 6, pp. 88–96, 2019 *https://doi.org/10.33383/2018-074*

DISTINCTIONS OF THE DESIGN OF UHP XENON LAMPS WITH SAPPHIRE ENVELOPE

Sergey V. Gavrish

Branch of AO Stella-K, Moscow
E-mail: svgavr@list.ru

ABSTRACT

This article describes the major development results of the first Russian sample of a UHP xenon discharge lamp with sapphire envelope. The article proposes a method of monitoring of thermal fields of semi-transparent materials and studies the thermal distribution of quartz and sapphire envelopes of UHP discharge lamps. Mechanical strength of sapphire tubes depending on the temperature is studied, the thickness of the discharge envelope wall is calculated, and distinctions of the design of a UHP xenon lamp with the sapphire envelope are considered.

Keywords: discharge lamp, UHP discharge, quartz and sapphire envelope, xenon, mechanical strength, thermal distribution, thermal field of a bulb

1. INTRODUCTION

Nowadays, despite the rapid development of the market of various light sources (MHL, fluorescent amalgam lamps, LEDs, etc.), ultra-high pressure xenon lamps in quartz ball bulbs are irreplaceable for spotlights for different applications [1]. Another distinction of these light sources (short-arc lamps) is that after publication of the first works by Kaptsov N.A., Gouhberg D.A., Rokhlin G.N., Rovinsky R.E., et al. [2–4] describing this class of lamps, which became classical ones; the design of these lamps almost has not changed (Fig. 1). UHP lamps still have a ball (elliptic) envelope made of quartz glass with various degree of transparency (doping), current inputs in the form of cylindrical or flat molybdenum foil, etc. Among the disadvantages of the described design are: large dimensions, which determine the size of the spotlight; low mechanical strength caused by strains in the joint of the ball bulb and the electrode unit; spectral range of radiation of the lamp of up to 4.2 μm determined by the transparent region of quartz; complex design and manufacturing technology caused by necessity of precise adjustment of cathode pin to the basic surface of the cap. Therefore, the search for new technical solutions allowing to prevent the said disadvantages is a relevant challenge.

2. BACKGROUND OF DEVELOPMENT OF DISCHARGE LAMPS WITH SAPPHIRE ENVELOPE

Mass production of high-pressure sodium lamps started in the 70-s and search of new materials for their efficiency increasing assisted in the development of the method of tubes directional crystallization made of mono-crystal aluminium oxide (sapphire, corundum) proposed by A.V. Stepanov [5]. This was justified since corundum has unique properties: high optical transparency (up to 96 %) in the spectral region of up to 6 μm, mechanical strength, chemical resistance to vapours of alkali metals, etc. In the beginning, application of sapphire tubes in the design of discharge lamps was economically unviable due to complexity of the crystal-growing process, the high power consumption of the process, low quality of sapphire processing (lapping, polishing), lack of high-purity raw materials and methods of their treatment. At the beginning of the 90-s, the listed problems were practically solved, the sapphire tubes were serially grown by means of group method, which made these products cheaper, and, at the same time, intensive development of discharge lamps with plasma supporting media based on alkali metals have begun [6]. Therefore, the established situation and obtained results of successful application of sapphire preconditioned necessity of development of UHP lamps in corundum envelope.

The material of envelope of any discharge lamp should meet the following requirements: optical transparency in a broad spectral range, resistance to operating temperatures and filling pressure, lack of gas releases, chemical resistance to components of the plasma supporting medium, mechanical strength, etc. [2, 4]. Such a wide range of limitation is caused by energy deposition on the envelope from both sides. From the plasma side, it comprises emitted radiation and the energy caused by thermal conductivity, charged particles, impact waves, from the outside, it comprises the returned radiation from the light-forming optical system or from other lamps (in case of multi-lamp systems), external factors (X-radiation, neutron radiation, etc.), chemical interaction with the environment, etc. In case of UHP discharge lamps, the bulb should additionally provide mechanical strength with the impact of internal filling pressure of up to 50 atm at operational temperatures of the lamp. Therefore, three relevant challenges arise for designing of the envelope of UHP DL with sapphire envelope:

1. Development of the method and measurement of thermal distribution of the quartz bulb (T_{en}) of the xenon lamp at various specific electrical loads for forecasting of the thermal fields of light sources with sapphire envelope;
2. Studying of the dependence of mechanical strength of sapphire tubes on structural perfection of crystals and temperature;
3. Evaluation of the size of the sapphire bulb and development of the UHP lamp with sapphire envelope manufacturing technology.

Fig. 1. Design of UHP xenon lamps with quartz ball envelope and cylindrical sapphire envelope

3. STUDIES OF LONGITUDINAL THERMAL DISTRIBUTION OF A QUARTZ BALL BULB OF AN UHP XENON DISCHARGE LAMP

3.1. Study Methodology

Due to simplicity and wide range of the measured temperatures in the course of studies of the thermal condition of discharge lamp bulbs, the thermocouple method has become the most widely used [4, 7]. However, in this case, the measurement of T_{en} has a number of significant aspects, which should be taken into account when selecting the design of a thermocouple and evaluating the measurement error of temperature. First, the surface temperatures of thin-wall envelopes are usually measured, with conductivity coefficient χ nearly a hundredfold lower than χ of the thermal electrodes material. Second, the envelopes on the surface of which the temperature is measured are transparent, and the thermocouple is affected by the radiant flux of the discharge.

The methods of pyrometry (thermography) [8] allow eliminating the said disadvantages. Due to volume nature of radiation of semi-transparent quartz and sapphire crystals, the standard thermography methods are not applicable to them. Therefore, for measurement of temperature, special partial radiation pyrometers operating beyond the bandwidth of a studied object are developed [8, 9]. With the growth of temperature from room values to operational ones, the non-transparency interval of the envelope material within the range of wavelength $\Delta\lambda$, which can be used for pyrometry, is being changed. For instance, with the heating of sapphire its $\Delta\lambda$ insignificantly shifts to the short-wave region of the spectrum of infrared bandwidth [9].

Short-wave absorption (UV region) of quartz or corundum where the value of absorption coefficient reaches (10^3–10^4) cm^{-1} is the result of the interaction of the electromagnetic wave with the electrons of the crystalline grid. The position of the long-wavelength side of this absorption is defined by impurities in the material structure [8, 9]. Therefore, the absorption coefficient may significantly vary in case of insufficient variation of flaw concentration and is not of interest for pyrometry due to this.

The most interesting is the short-wavelength border of the first vibrational absorption band of quartz

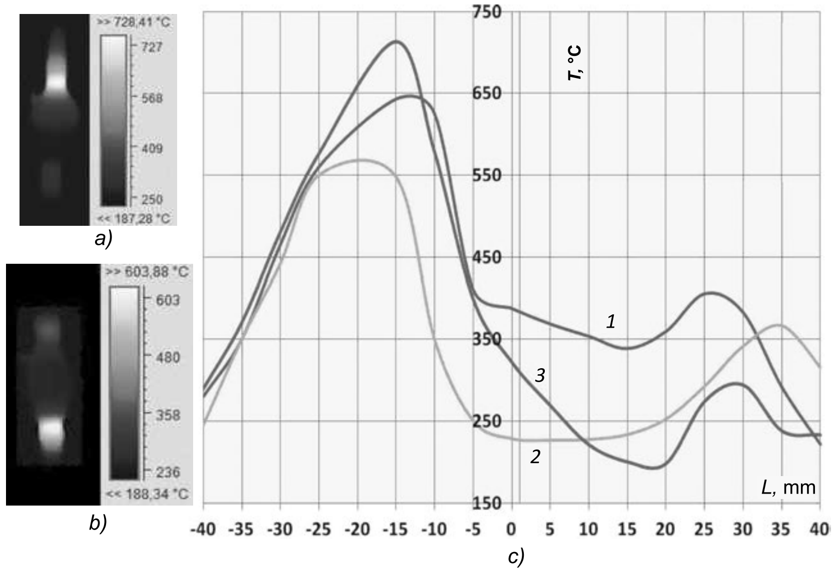

Fig. 2. Photos of thermal fields of the xenon lamp DKsSH-150 with vertical operating position of anode (a) and cathode (b) in the upper part and lateral thermal distribution (c) in the course of operation of the lamp in a horizontal (1) and vertical (2) positions with cathode (2) and anode (3) in the upper part

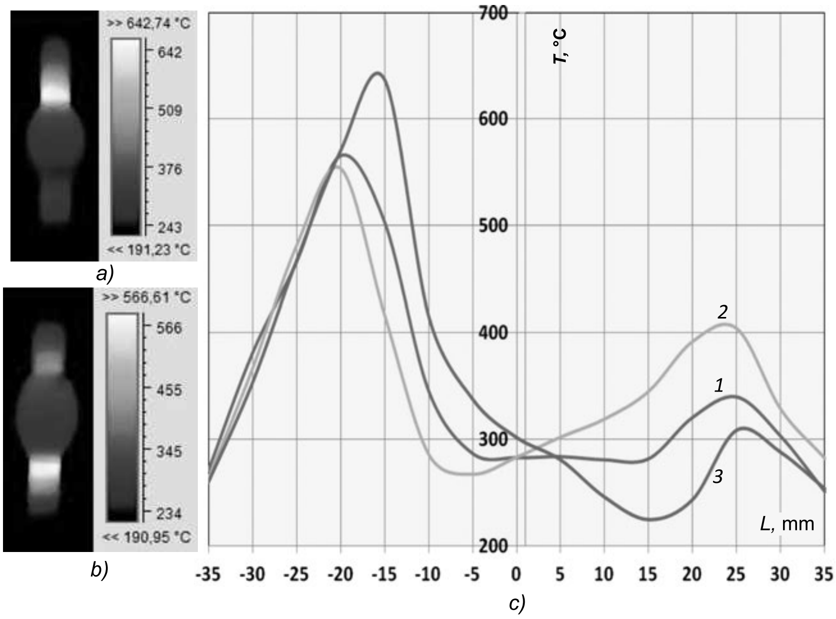

Fig. 3. Photos of thermal fields of the xenon lamp DKsSH-500 with vertical operating position of anode (a) and cathode (b) in the upper part and lateral thermal distribution (c) in the course of operation of the lamp in a horizontal (1) and vertical (2) positions with cathode (2) and anode (3) in the upper part

and corundum. In this region, k_λ of semi-transparent materials may reach k_λ = (10^2–10^3) cm^{-1}, and emissivity approximates one. For instance, according to [8] for corundum at temperature of 2000 K within the spectral region of (6–10) μm, 95 % of energy is radiated by the near-surface layer with thickness of just 0.65 mm, which allows to consider the surface temperature of the discharge tube given the conventional thicknesses of discharge lamp envelopes (1.5–3.5) mm. Due to the low value of reflectance $k_{r'}$ in this region, its effect on the measurement results is insignificant. Therefore, if the receiver receives radiation from this non-transparency region of sapphire, the signal of the receiver will be definitely related to the temperature of the surface of the envelope made of this material.

3.2. Experimental Study of Thermal Distribution of the Surface of UHP Discharge Lamp Ball Bulb

For our experiments in the determination of thermal fields of sapphire envelopes, we used the SDS HotFind-LXT thermal vision system based on multi-element radiation receivers, i.e. matrices, the number of elements of which allows forming a TV image with good spatial resolution. The operational spectral range of this pyrometer is (7.5–14) μm, which allows measuring temperature within the range from –20 °C to +1500 °C.

The studies of thermal fields of UHP xenon lamps with quartz ball bulb were conducted with design and electrical characteristics listed in Table 1.

Table 1. Design and Electrical Characteristics of the DKsSH-150 and DKsSH-500 Lamps

Lamp type	Design parameters				Electrical characteristics				
	d_1*, mm	d_2*, mm	$l_{b.e.}$, mm	p_{Xe}, MPa	P_l, W	U_l, W	I_l, A	$j_{an.}$, A/cm^2	$P_{sp.}$, W/cm^2
DKsSH-150	20	14	2.5	2.0	154	18.8	8.4	60.0	25.0
DKsSH-500	30	26	1.3	1.2	514	13.6	38	54.3	24.2

* – *d_1 and d_2 are outer and inner diameters of the ball bulb respectively*

The bulb temperature was measured in 10 minutes after reaching the nominal electric power of the lamp. As a result of such heating, thermal distribution along the envelope was stabilised and took the form shown in Figs. 2, 3. For clarity of the obtained thermal profiles of the quartz ball bulb, the photos from the thermal camera display are shown in the said figures. During measurements, for the curves shown in Fig. 2, 3, the location of the cathode spot was taken as a zero point for calculation of distance along the bulb.

The obtained data shows that the courses of thermal curves of the studied lamps are similar. There is a deviation of T_{en} of two lamps in a plane crossing the cathode spot perpendicularly to the lamp axis. This effect is related to differences in the distance between electrodes $l_{b.e.}$, which provides higher losses of discharge by radiation on the bulb in case of DKsSH-150. An important distinction of the obtained results is the availability of high lateral temperature gradients of the lamp caused by high losses of power by xenon thermal conductivity and effect of the heated anode radiation on the closely adjacent part of the ball bulb [2–4].

As it is seen from Table 1, the specific electric power per unit of the inner surface of the ball bulb is the same and the values of anode current density j_{an} are commensurable, therefore, the temperatures of the bulb surface in the anode area of both lamps are close to each other and do not exceed 700 °C. The minimal temperature of the ball envelope can be seen at distance of (15–20) mm from the cathode pin and is within the range of (180–350) °C depending on the type of lamp and its operating position. The said temperature range is related to convection of xenon after changing the lamp position.

Therefore, in the course of designing of a UHP xenon lamp with a sapphire bulb and with the power of up to 500W, it is necessary to take into account the lamp envelope should provide mechanical strength in conditions of a pressure of up to 50 atm at operational temperatures of up to 700 °C.

4. DEVELOPMENT OF XENON DISCHARGE LAMPS WITH SAPPHIRE ENVELOPE

Using of sapphire as an envelope of a discharge lamp is a new problem, therefore, for its solving, it is necessary to study the relation between strength properties of this material and structural perfection of a mono-crystal and operational conditions of an instrument, primarily, its operational temperature.

4.1. Studies of Mechanical Strength of Sapphire Tubes

Mechanical strength of tubes made of monocrystal colourless corundum grown using the Stepanov method depends on the structural perfection of a crystal [4, 9, 10]. Detailed analysis of the flaws of sapphire tubes is described in the article [10]. In this publication, the author proved that the

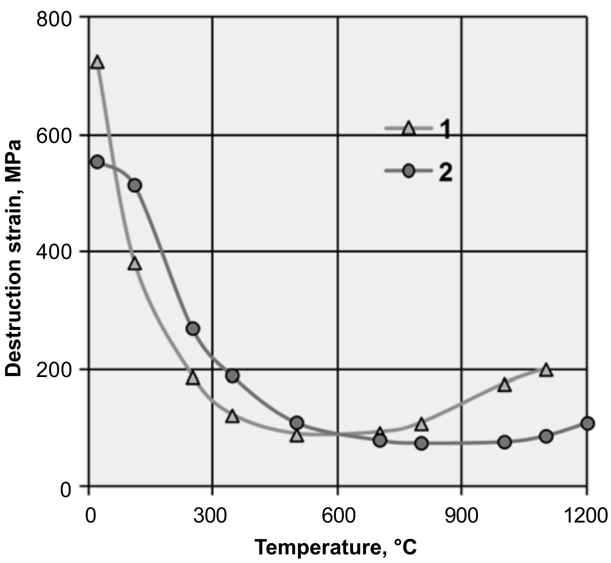

Fig. 4. Thermal dependence of ultimate strength of corundum tubes grown with crystallographic orientations: 1 – [0001]; 2 – [1012.]

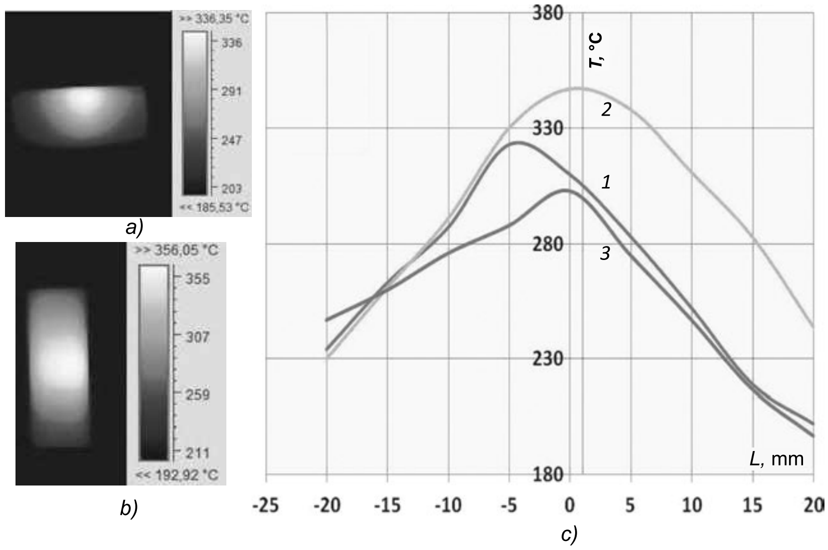

Fig. 5. Photos of thermal fields of the xenon lamp SPKs-500 with horizontal (a) and vertical (b) operating position of anode in the upper part and lateral thermal distribution (c) in the course of operation of the lamp in a horizontal (1) and vertical (2) positions with cathode (2) and anode (3) in the upper part

main factor determining mechanical strength is the availability of a large amount of disordered crystalline regions with macroscopic size (crystallites). The borders of crystallites are strains concentrators, and the values of these strains are determined by macro-region boundary angle and temperature condition of a crystal. Part of strains is removed by means of uniform annealing of the grown corundum. However, the high-temperature gradient in the wall of the lamp sapphire envelope will inevitably leads to increase of internal strains and destruction of a mono-crystal. It is clear that the more the number of crystallites is and the higher the temperature gradient is, the less is the mechanical strength of the sapphire tube [4, 10].

The corundum strength, like that of other brittle materials, depends on many factors: testing speed, temperature, quality of sample surface, environment, different orientation of a crystal in relation to the applied load. The operating principle of the instrument for the destruction of tube samples proposed in [10] is based on the application of a yielded composed medium allowing to reliably and simply seal a particular volume of a sample thus providing uniform and all-round loading of inner walls of the sapphire tube. Since the load is applied to the inner surface of the tube uniformly in the radial direction in the medium part of 1/3 of the sample length during testing of samples using this instrument, boundary disturbance is negligible. The butts of the tested tubes were sanded only for ensuring straightness.

The value of strength, i.e. tangential fracture strain of the walls of a tube sample σ_f, was calculated using the formula [10]:

$$\sigma_f = \frac{F}{\pi \times R_1^2} \times \frac{(R_2^2 + R_1^2)}{(R_2^2 - R_1^2)}, \quad (1)$$

where F is the force; R_1 is the inner diameter; R_2 is the outer diameter. Measurement accuracy provided by the method is about 5 kg/mm^2.

In Fig. 4, the experimentally obtained temperature dependence of mechanical strength of crystallite-less tubes with a wall thickness of 1.4 mm grown using the Stepanov method with the crystallographic orientation of [000$\bar{1}$] (curve 1) and [1012] (curve 2) within the temperature range from 200 to 1100 °C is shown. The temperature was increased with a step of 10 degrees per minute and controlled by a thermocouple. The samples were loaded for (5–10) seconds. After the destruction, critical strains were calculated using formula (1) and averaged.

Mismatch of the minimum values of strength on the curves is caused by the fact that destruction was conducted in different crystallographic planes. Despite some differences in mechanical strength values, the courses of the curves are identical. Fig. 4 shows that there is an obvious minimum of strength at the temperature range of (400–700) °C. Reduction of fracture strain caused by temperature is natural for many brittle materials and is caused by availability of overloaded sections in the latter characterised by the coefficient $n = \sigma_e / \sigma_{av}$, where $\sigma_{av} = P / S$ (P is the force, S is the cross-section of the sample) are local overstrains distributed over the volume, which depend on the microscopic structure of the sample.

The anomalous dependence of strength on temperature is explained by superposition of the processes of deformation and destruction. In the low-temperature region, the deformation processes are slowed down, the overstrain coefficient is high and almost constant. Increasing of temperature up to 800 °C accelerates deformation, local strains reduce during the test and after increasing of temperature, the coefficient n dramatically decreases, therefore, σ_f also increases after increasing of temperature. Therefore, the coefficient of local overstrains affects, primarily, the temperature-strength dependence of the sapphire tube in the first instance. The influence of disorientation of crystallites with an angle of up to 25° and strains of up to 16 kg/mm^2 are not discovered.

The above-listed results relate only to the mechanical strength of sapphire tubes. Meanwhile, a designer of high-intensive radiation discharge sources for different applications will take additional requirements obtained by the authors in [5, 9–12] into account. In terms of crystallographic properties, the geometrical axis of sapphire tubes should not deviate from the $[000\bar{1}]$ crystallographic orientation more than by 10 °, should not contain more than 5 crystallites in the wall volume cross-section with the disorder of adjacent crystallites exceeding 10 °. The transmittance of corundum tubes should be of at least 90 % within the spectral range from 0.3 to 5 μm, the tubes should not include second phase impurities, clouds, non-transparent flaws, blisters, and growth shifts and should sustain growth of temperature up to 1950 °C without losing optical transparency. In terms of dimensions for tubes with an inner diameter from 5 to 11 mm, deviation of ±0.3 mm is acceptable, maximum deflection is 0.2 mm with the length of 150 mm, surface waviness should be within the size tolerance. The concentration of blisters is standardised on the basis of categories and classes of optical materials.

5. DESIGN DISTINCTIONS OF UHP DISCHARGE LAMP

Some distinctions of operation of quartz xenon short-arc lamps [2, 3], which may significantly affect the operation of similar light sources with sapphire envelope, should be taken into account. The bulbs of high-intensity lamps should be designed so that the mechanical strains appearing inside the sapphire tube do not cause its destruction. The strains are caused by high pressure of filling gas and thermal strains due to temperature gradients in the walls of the envelope and in joints of sapphire and metal. Destruction of the sapphire bulb occurs in cases when the maximum tensile loads reach tensile strength rupture limit.

If the internal pressure is higher than the external pressure, the bulb will suffer breaking strains. Axial strain σ_a, which appears in the cylindrical bulb, in this case, is equal to [11]:

$$\sigma_a = \frac{pd}{2h}, \tag{2}$$

where d is the inner diameter of the discharge bulb, h is the sapphire tube wall thickness, p is the pressure of filling gas.

This expression is correct if the wall thickness h is a non-significant part of the inner diameter of the bulb d. The long experience of operation and tests of ultra-high pressure quartz lamps with natural cooling has shown that strength reserve of about 10 is sufficient for most of the lamps [11]. Therefore, it is necessary to calculate the wall thickness in the centre of the bulb for a case, when the maximum value of overall breaking strains does not exceed the acceptable value $\sigma_a/10$. According to Fig. 2c, the temperature of the bulb in the area of the anode is T_{en} = 700 °C. Given the higher thermal conductivity of sapphire, it is possible to expect T_{en} of up to 800 °C in this area. As it follows from the data shown in Fig. 4, the ultimate strength of a crystallite less sapphire tube at such temperature is 10^7 Pa. Then, according to formula (1) for UHP xenon lamp with the inner diameter of the bulb 115 mm and filling pressure of xenon of 1.5 MPa, the thickness of the wall of a sapphire tube should be equal to at least h = 1.65 mm.

It is necessary to note that the given calculated values are obtained for pressure of filling gas at room temperature. Increase of temperature of the filling gas will lead to increase of gas pressure by several times, but the foreseen strength reserve allows keeping the calculated values of the wall thickness in the course of design of UHP xenon lamps with sapphire envelope.

6. THERMAL PROFILE OF THE CYLINDRICAL SAPPHIRE BULB OF AN UHP XENON LAMP

The ball form is used for the quartz-glass bulb due to the necessity to provide uniform distance between the inner surface of the envelope and the high-temperature cathode spot. Given that ther-

Table 2. Design and Electrical Characteristics of the SPKs-500 Lamp

Design parameters				Electrical characteristics				
d_1*, mm	d_2*, mm	$l_{b.e.}$, mm	p_{Xe}, MPa	P_l, W	U_l, W	I_l, A	$j_{an.}$, A/cm²	$P_{sp.}$, W/cm²
20	15.5	1.3	1.2	514	13.6	38	30.4	26.5

* – *d_1 and d_2 are outer and inner diameters of the cylindrical sapphire bulb respectively*

mal distribution of the envelope depends not only on specific electric power but also on operation position of a lamp (Figs. 2, 3), it can be expected that replacement of the bulb form with sapphire cylinder will inevitably lead to the transformation of the thermal field of the lamp. This is related to the high thermal conductivity of sapphire and the difference between convection currents in the considered lamps. In its turn, due to anisotropic properties of the thermal expansion coefficient of corundum, appearing of high-temperature gradients in the wall of a sapphire tube may lead to the destruction of the envelope.

The thermal field studies based on the above-described method were conducted using a SPKs-500-type UHP lamp with a sapphire envelope, the design of which is given in Fig. 1 and the main technical specifications are listed in Table 2.

The results of the study of the lateral thermal distribution of the cylindrical sapphire envelope of an UHP xenon lamp with average electric power of 350 W are shown in Fig. 5. The highest temperature of the bulb is seen in the plane crossing the cathode spot perpendicularly to the lamp axis. It is related to heating of the sapphire envelope by radiation. Smooth temperature gradient to the area of cathode and anode equal to about 5°/mm is related to several design distinctions of the lamp:

1. There is a significant gap between the electrodes and the inner surface of the sapphire tube (3.5 mm for the anode and 6 mm for the cathode) along the whole length of the electrodes;
2. The electrodes are fixed to metal current inputs with high thermal conductivity, which provides reliable removal of heat from their operating surface (Fig. 6);
3. Thermal conductivity of sapphire is fifteen times higher than that of quartz (30 W/(m·°C) as compared to 1.7 W/(m·°C)) at a temperature of 100 °C and is three times higher at a temperature of 1000 °C [12].

It is worth noting that using of forced cooling through conical confusor by means of a directed airflow from the anode allows keeping thermal distribution along the surface of the bulb in the form similar to that shown in Fig. 5. The temperature gradient practically remains the same in case of increase of electric power of the designed lamp up to 500 W. Another position of the lamp, e.g. at an angle of 45° to the horizontal plane, insignificantly shifts the maximum temperature of the heated envelope surface to the electrode located above. In this case, the temperatures of the envelope surface are located between the curves 1 and 2 in Fig. 5.

An important distinction of the considered design is its high manufacturability. It is known that the cathode spot of a UHP discharge lamp should be located in the focus of the reflector of the spotlight system. It is reached by fixation of the cathode pin in relation to the base surface of the lamp cap. In the case of UHP xenon lamps with quartz ball bulbs, adjustment of the cathode is conducted during the final operation of the cap connection by means of complex devices and sealing compounds. In the proposed design (Fig. 6), installation of the electrode pin in relation to the butt (base) part of the cap is conducted during assembling of the cathode 2 with holder 3. Then the assembled electrode unit is hermetically connected to the sapphire en-

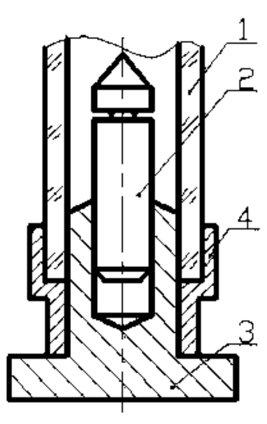

Fig. 6. Design of the cathode unit of the SPKs-500 lamp. 1 – discharge tube; 2 – cathode; 3 – holder (cap); 4 – cover cap

velope 1, which was soldered with kovar caps 4 in advance.

In the proposed design, for sealing of the connection of the cap 4 with the sapphire 1, the soldering technology with copper solder on the titanium coating applied by means of vacuum-arc method is used. For detail information of this technology, see [13].

The lifetime of the designed lamp was more than 200 hours. The quality criterion of the lamp was the decrease of luminous flux intensity by 30 %. During the whole testing period, the lamp provided stable operation, and reduction of its light parameters is related to electrode sputtering. Depositing of a film of the cathode material on the inner surface of the envelope insignificantly increases the bulb temperature in conditions of forced cooling of its surface.

7. CONCLUSION

This article describes the major results of the development of the first Russian sample of a UHP xenon discharge lamp with sapphire envelope. The article describes the method of designing of such class of discharge lamps including subsequent solving of the following problems:

1. Studying method development of thermal fields of semi-transparent materials and studying of the thermal profile of mass-manufactured UHP lamps in order to determine the requirements to sapphire envelope;
2. Studying of mechanical strength of sapphire tubes depending on temperature and calculation of the wall thickness of the discharge envelope;
3. Studying of the temperature condition of the sapphire bulb and development of the design of a UHP xenon lamp with a sapphire envelope.

The proposed methods of research aiming at designing of UHP discharge lamps with sapphire envelope will be useful for developers of discharge equipment with the use of new prospective materials, e.g. different types of transparent oxide ceramics [14]. After studying mechanical strength of ceramics depending on temperature, issues of optical transparency increasing, and obtainment of reliable connections with the metal current input, new materials of envelopes may be successfully used instead of sapphire in discharge lamps.

The author expresses gratitude to the colleagues Loginov V.V., Puchnina S.V., and Kondratiev A.N. for assistance provided in the course of the study, development of the design, and technology of manufacturing of a new class of Russian UHP discharge lamps.

REFERENCES

1. Basov Yu.G., Rakviashvili A.G., Sysun V.V. Spetsialnaia svetotekhnika [Special Light Engineering] // BSU, Minsk, 2008, 414 p.

2. Kaptsov N.A., Gouhberg D.A. Lampy sverkhvysokogo davleniia [Ultra-High Pressure Lamps] // UFN, 1951, Vol. 43, No. 4, pp. 620–664.

3. Gouhberg D.A., Rovinsky R.E. Gazorazriadnye ksenonovye lampy SVD postoiannogo toka moshchnostiu 1 i 3 kVt [UHP Xenon Alternate Current Discharge Lamps with Power of 1 and 3 kW] // Svetotekhnika, 1958, No. 10, pp. 1–4.

4. Gavrish S.V. Tekhnologiia vyrashchivaniia i kharakteristiki profilirovannykh sapfirovykh trub dlia obolochek razriadnykh lamp [Technology of Growing and Characteristics of Profiled Sapphire Tubes for Envelopes of Discharge Lamps] // Tekhnologiia mashinostroeniia, 2008, No. 6, pp. 56–61.

5. Gavrish S.V., Gradov V.M., Terentiev Yu.I. Osobennosti konstruktsii i raboty lamp s sapfirovymi obolochkami [Distinctions of the Design and Operation of Lamps with Sapphire Envelopes] // Svetotekhnika, 2008, No. 2, pp. 12–18.

6. Pchelin V.M., Rozovsky E.I., Rokhlin G.N. Osobennosti izmereniia temperatury kolb vysokointensivnykh istochnikov sveta termoparnym sposobom [Aspects of Temperature Measurement of High-Intensity Light Source Bulbs by Thermocouple Method] // Svetotekhnika, 1980, No. 11, pp. 11–14.

7. Lingart Yu.K., Petrov V.A. Izmerenie temperatury poverkhnosti nekotorykh poluprozrachnykh materialov [Measurement of Temperature of Surface of Some Semi-Transparent Materials] // TVT, 1980, Vol. 10, No. 1, pp. 174–180.

8. Loytty A. A new ark tube for HPS lamps // Lighing Design and application, 1976, pp. 14–17.

9. Gavrish S.V. The Effect of Structural Flaws on the Properties of the Sapphire Shell of a Discharge Radiation Source // Russian journal of nondestructive testing, 2010, Vol. 46, No. 8, pp. 603–610.

10. Brailovsky V.B., Gavrish S.V., Ryzhkov A.E. Defekty struktury i diagnostika kharakteristik trub iz profilirovannykh monokristallov korunda dlia obolochek impulsnykh razriadnykh lamp IK izlucheniia [Structural Flaws and Diagnostics of Characteristics of Profiled Co-

rundum Monocrystal Tubes for Envelopes of Pulsed Discharge IR Lamps] // Kontrol. Diagnostika, 2007, No. 2, pp. 49–59.

11. Rokhlin G.N. Razriadnye istochniki sveta [Discharge light sources] // Energoatomizdat, Moscow, 1991, 720 p.

12. Rubashev M.A., Berdov G.I., Gavrilov V.N. et al. Termostoikie dielektriki i ikh spai s metallom v novoi tekhnike [Thermal-Resistant Dielectrics and their Soldered Joints in New Equipment] // Atomizdat, Moscow, 1980, 246 p.

13. Gavrish S.V., Loguinov V.V., Puchnina S.V. Technology for producing permanent joints between sapphire and metals // Welding International, 2015, Vol. 29, No. 1, pp. 78–80.

14. Vydrik G.A., Solovyova T.V., Kharitonov F. Ya. Prozrachnaia keramika [Transparent Ceramics] // Energiya, Moscow, 1980, 96 p.

Sergey V. Gavrish,
Ph.D. in Tech. Science, graduated from the Moscow Institute of Electronic Technology (MIET) in 1985. Currently he is the head of the research and manufacturing facility of special radiation sources (NPK SII) of the branch of AO Stella-K. Research Interests: plasma physics, light engineering, material studies

Light & Engineering
Vol. 27, No. 6, pp. 97–105, 2019
https://doi.org/10.33383/2019-050

STUDY OF CHARACTERISTICS OF LEDS FOR PHYTOIRRADIATORS

Mikhail M. Erokhin[1,2], Pavel V. Kamshylov[1,3], Vladislav G. Terekhov[1,3], and Andrey N. Turkin[2,3]

[1] *S.I. Vavilov VNISI (Ltd), Moscow*
[2] *M.V. Lomonosov Moscow State University, Department of Physics, Moscow*
[3] *NIU MPEI, Moscow*
[4] *E-mail: andrey@turkin.su.*

ABSTRACT

The present study comprises comprehensive research of red, green and blue light emitting diodes (LED), which are widely used in phytoirradiators for plant growing in protected ground in the environment of a photo-culture including their spectrum measurements within the wide range of current values at room temperature. Shifts of spectral peaks of radiation of red and green LEDs after increase of operating current were discovered. On the basis of the conducted study, recommendations for selection of current operating mode of light sources used in phytoirradiators for plant growing in the environment of photo-culture were worked out, and a model of a phytoirradiator was proposed and studied in this work with red, green and blue LEDs, which have their spectrum covering all regions of photosynthetic active radiation (PAR).

Keywords: light emitting diode, LED, phytoirradiator, protected ground facility, greenhouse, plant, photo-culture

1. INTRODUCTION

Optical radiation has been increasingly used today in processing in industry and agriculture, becoming an inherent part of chemical plants, and playing an important role in kettle and poultry breeding, and greenhouse cropping [1–3].

The effects of visible spectrum radiation on plants were studied by many authors (see, for instance, [3, 4]). In [4], the effect of illuminance and chromaticity of the radiation on efficiency of photosynthesis and productivity of plants with special pigments such as chlorophyll-*a,* chlorophyll-*b*, carotenoids, and etc. responsible for light absorption, was studied. Chlorophylls absorb blue and red radiation spectral range whereas carotenoids absorb blue and green light. The radiant energy absorbed by different pigments is used for development of the root system, ripening of seeds, blossoming, etc. The other parts of the spectrum, except for the amber one, are almost not used by plants [3, 5, 6].

Greenhouses farms do not represent cutting-edge technologies; however, in conditions of constantly growing population of the Earth and pursuance of stable, highly-efficient and standardised production of food, they will become a norm in the future establishing a new large sector of agricultural industry. Rapid development of LED technologies has become one of the most important achievements defining the future of protected ground facilities and practicability of their construction [3]. Contemporary light emitting diodes (LED) allow developing of illumination and irradiation devices that have required chromaticity of radiation and are extremely resistant to harsh conditions of environment, and relatively small-sized as compared to other types of illumination and irradiation devices. Moreover, they have rather large service life, are distinctive

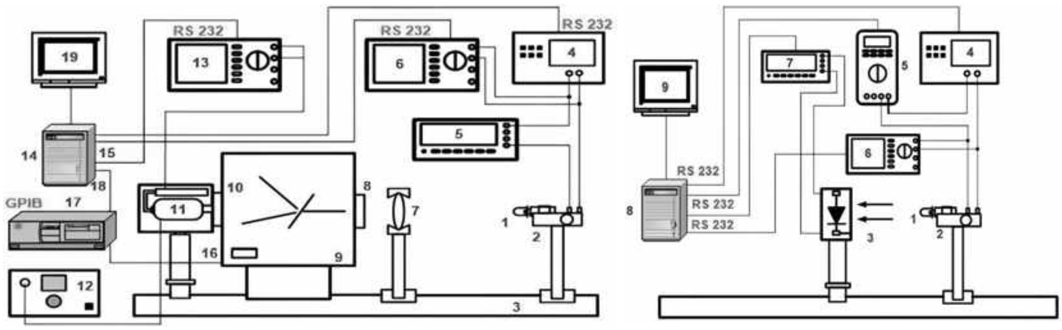

a) *b)*

Fig. 1. The scheme of the experimental installation:
a) LED radiation spectra measurement installation
1 – LED; 2 – adjustable LED holder; 3 – optical bench; 4 – power supply unit; 5 – ammeter; 6 – voltage meter; 7 – collimator lens; 8 – entrance slit; 9 – *SPM-2* prismatic monochromator; 10 – exit slit; 11 – PMT; 12 – PMT power supply unit; 13 – voltage meter; 14 – control unit; 15 – management port; 16 – stepper motor; 17 – computer; 18 – stepper motor management port, 19 – screen;
b) The installation for measurement of dependence between LED radiant intensity and current
1 – LED; 2 – adjustable LED holder; 3 – photoelectric detector; 4 – power supply unit; 5 – ammeter; 6 – voltage meter; 7 – control unit; 8 – computer; 9 – screen

with low operating voltage, and relatively low heat losses [7].

The purpose of this work is formation of the basis for selection of LEDs for application in phytoirradiators for growing plants in protected ground facilities in environment of photo-culture. In order to reach this goal, the task of studying spectral characteristics of red, green and blue light LEDs, explaining their spectral characteristics behaviour as well as modelling a phytoirradiator operating within the whole region of photosynthetic active radiation (PAR) and, not least importantly, with an adjustable radiation spectrum, was set.

These studies represent one of the directions currently taken which is based on application of coloured (monochromatic) LEDs for use in phytoirradiators. Selection of samples of three wavelength regions, blue, red and green, is based on it.

2. EXPERIMENT METHODOLOGY

The characteristics of red, blue and green LEDs were studied using an automatic experimental set based on a *SPM-2* spectrometer. This set, with its scheme shown in Fig. 1, allows us to measure LED radiation spectra within a wide range of current values as well as dependences between LED radiant flux and current. Red, green and blue LEDs with their crystals grown using the gaseous epitaxial method on the basis of organ metallic compounds were the study subjects. Approximate crystal dimensions in the studied LEDs are (0.350×0.350) mm. The crystals were mounted in a metal-base reflector with approximate area of 1.0 cm^2. Such base reduces heat-transfer resistance of LED and allows increasing of operating current. The structure of the base comprises metal pins for mounting and electrical connection of LED. The area of the reflector is filled with a polymer-based optical gel, which increases the radiation coupling-out ratio of a crystal. On top, the body of LED is closed by a polycarbonate lens which allows formation of a light distribution curve with angle of approximately 30°. Around the crystal, the optical gel creates an environment which does not cause large mechanical load on it and allows small deflections due to heat expansion. This is increasing the threshold value of current through the small-size crystal up to values exceeding 150 mA. The structure and production technology of the studied LEDs is rather typical for this type, which allows us to use the obtained results as a basis for approximation for other types of LED.

3. EXPERIMENTAL RESULTS

In the course of the work, the radiation intensity spectra of the studied LEDs at different values of current within the range of 5 mA up to 120 mA were measured in arbitrary units; typical examples of the spectra are given in Figs. 2–4.

In the case of red LED (Fig. 2), shift of the peak of relative spectral distribution of radiant flux to the long-wave region by approximately 20 nm can be observed after increasing current from the re-

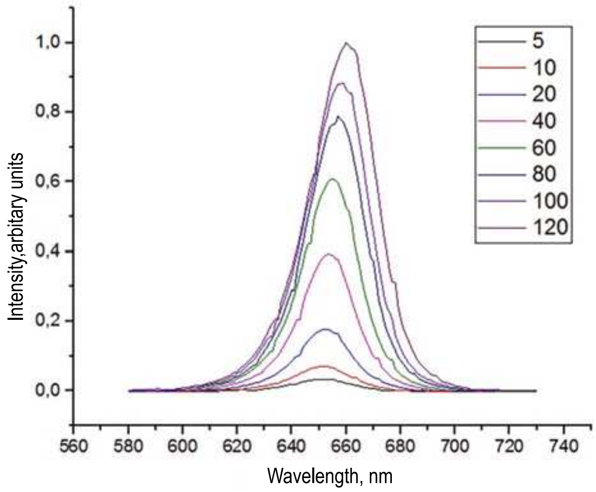

Fig. 2. Typical spectra of red LEDs at different values of current (the digits in the figure stand for values of current in mA)

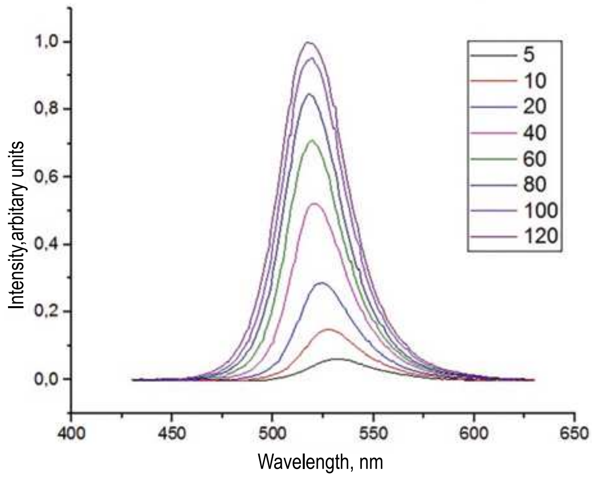

Fig. 3. Typical spectra of green LEDs at different values of current (the digits in the figure stand for values of current in mA)

gion approximately corresponding to wavelength of 650 nm to the region corresponding to wavelength of 670 nm. Such shift is typical for structures based on gallium phosphide and its solid solutions emitting red and yellow light [8].

In the case of green LED (Fig. 3), the shift of the peak can also be observed after increase of current. In this case, the peak shifts to the short-wave region approximately by 10nm from the wavelength region approximately corresponding to wavelength of 530 nm to the region corresponding to wavelength of 520 nm. Such a shift of the peak of radiation spectrum is rather typical for hetero-structures based on gallium nitride and its solid solutions emitting green light [9–12].

In the case of blue LED spectrum (Fig. 4), the shift of the peak with increase of current almost cannot be observed at all considered values of current, the peak wavelength of intensity spectral distribution is located in the region approximately corresponding to wavelength of 470 nm. Non-availability of the shift of peak wavelength of intensity spectral distribution after increase of current is also rather typical for crystals based on gallium nitride and its solid solutions emitting blue light [9–12].

Non-availability of the shift of peak wavelength of intensity spectral distribution in blue LEDs after current increase may be associated with more homogeneous structure of active region of blue LED crystals due to less indium content and, therefore, less dependence between recombination energy of media and temperature.

The graphs of dependence between LED intensity and current (Figs. 5–7) show that red LEDs intensity at values of current are less than (35–40) mA increases in linear fashion with increase of current. With further increase of current approximately up to 60 mA, intensity continues to increase; however, the speed of its increase is reducing. At currents less than (70–80) mA, the increase of radiant intensity with increase of current gradually ceases, and the dependences between intensity and current level are saturated at current of about 120 mA or higher.

The similar nature of the dependence between intensity and current is observed for green (Fig. 6) and blue (Fig. 7) LEDs. At values of current of less

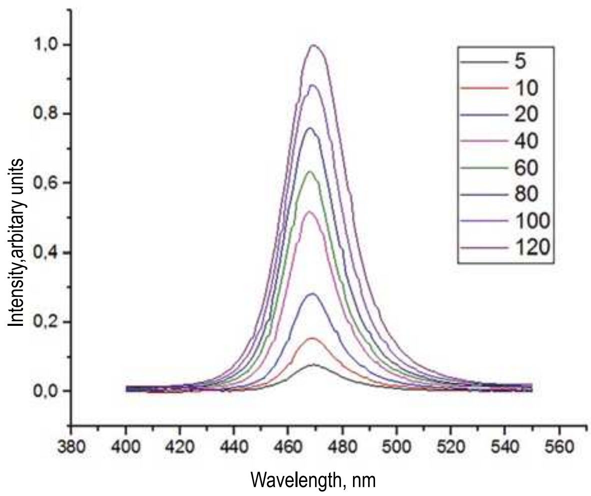

Fig. 4. Typical spectra of blue LEDs at different values of current (the digits in the figure stand for values of current in mA)

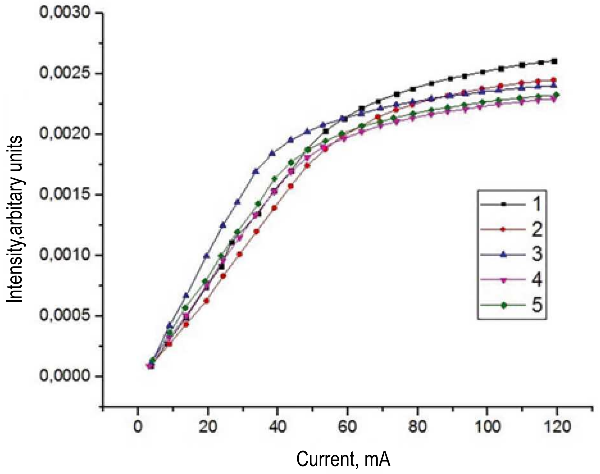

Fig. 5. Dependence between radiant intensity and current in red LEDs (the digits in the figure stand for sample numbers)

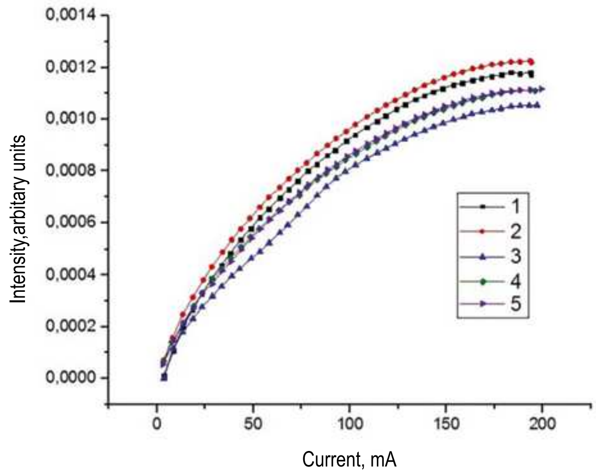

Fig. 6. Dependence between radiant intensity and current in green LEDs (the digits in the figure stand for sample numbers)

than approximately 35mA, the dependences between radiant intensity and current of green LEDs can also be roughly approximated by a linear function. The intensity increase is beginning to slow down with further increase of current. In the case of green LEDs, intensity levelling off is observed at higher values of current than those for red LEDs, at about (125–150) mA.

In the case of blue LEDs (Fig. 7), linear intensity and current dependence is observed at the current less than approximately (75–80) mA, whereas the increase of radiation intensity gradually starts slowing down with further increase of current, like in the case of green LEDs, and its levelling off for blue LEDs is observed at values of current equal to about (130–150) mA.

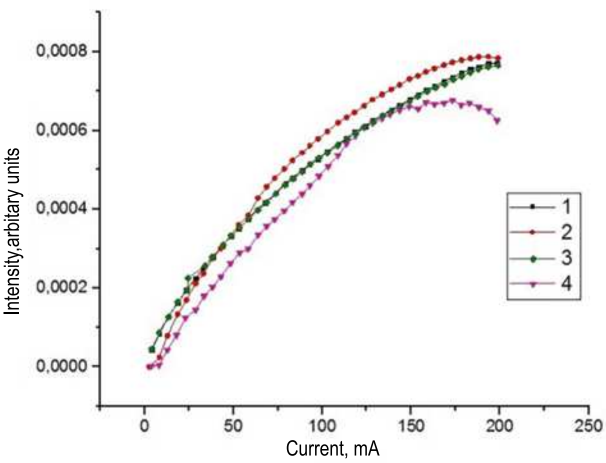

Fig. 7. Dependence between radiant intensity and current in blue LEDs (the digits in the figure stand for sample numbers)

4. DISCUSSION OF THE EXPERIMENTAL RESULTS

1. The above mentioned changes of slope in dependence of intensity from current in the region of current density about 130 A/cm^2 for red LEDs and exceeding 140 A/cm^2 for green and blue LEDs, may be explained by heating of active regions of LED crystals, which leads to changes of current passage mechanisms and mechanisms of media recombination in the active region.

2. For description of major peaks of radiation spectra, you can use the radiation spectrum approximation proposed in [14] which can be represented in the following form:

$$I(\hbar\omega) = A_0 \cdot \frac{1 + exp\left(-\frac{\hbar\omega_{max} - E_g}{E_0}\right)}{1 + exp\left(-\frac{\hbar\omega - E_g}{E_0}\right)} \times$$

$$\times \frac{1 + exp\left(\frac{\hbar\omega_{max} - \left(E_g + \Delta F\right)}{E_1}\right)}{1 + exp\left(\frac{\hbar\omega - \left(E_g + \Delta F\right)}{E_1}\right)}, \tag{1}$$

where $\hbar\omega_{max}$ is the spectrum peak energy, E_g is the energy gap of the crystal active region, ΔF are the shifts of energy bands (valence band and conduction band) in the crystal active region, E_0 and E_1 are the spectra approximation parameters in the long-wave and short-wave regions respectively.

Table 1. The Results of Approximation of Radiation Spectra of Red LEDs

J, A/cm^2	$\hbar\omega_{max}$, eV	E_g^*, eV	E_0, eV	E_1, eV
5.56	1.906	1.885	0.015	0.021
11.11	1.902	1.893	0.017	0.026
22.22	1.901	1.894	0.015	0.028
44.44	1.898	1.892	0.017	0.027
66.67	1.895	1.888	0.017	0.027
88.89	1.890	1.876	0.018	0.027
111.11	1.885	1.875	0.016	0.030
133.33	1.872	1.858	0.016	0.033

Table 2. The Results of Approximation of Radiation Spectra of Green LEDs

J, A/cm^2	$\hbar\omega_{max}$, eV	E_g^*, eV	E_0, eV	E_1, eV
5.56	2.332	2.282	0.048	0.029
11.11	2.350	2.341	0.055	0.030
22.22	2.365	2.361	0.056	0.030
44.44	2.379	2.391	0.058	0.033
66.67	2.387	2.408	0.058	0.035
88.89	2.391	2.401	0.057	0.039
111.11	2.390	2.386	0.057	0.041
133.33	2.390	2.377	0.056	0.046

Table 3. The Results of Approximation of Radiation Spectra of Blue LEDs

J, A/cm^2	$\hbar\omega_{max}$, eV	E_g^*, eV	E_0, eV	E_1, eV
5.56	2.644	2.634	0.045	0.027
11.11	2.644	2.634	0.043	0.028
22.22	2.644	2.634	0.038	0.029
44.44	2.649	2.640	0.040	0.030
66.67	2.649	2.640	0.041	0.033
88.89	2.649	2.649	0.044	0.034
111.11	2.644	2.649	0.045	0.039
133.33	2.640	2.640	0.048	0.041

The results of approximation for red, green and blue LEDs are shown in Tables 1, 2 and 3 respectively. The values of the parameters are given for several values of current density, which makes it possible to use them for comparison of LEDs with crystals of different area.

Table 1 shows that peak radiation $\hbar\omega_{max}$ of red LEDs shifts towards lower energies with increase of current density, which corresponds with the spectrum shift to the long-wave region observed during the experiment.

The results presented in Table 2 show that peak radiation of green LEDs shifts towards higher energies, which also corresponds with the experimentally observed shift of green LEDs spectra to the short-wave region of radiation with increase of density of current passing through the crystal. It also may be noted that the shift of peak diminishes with increase of current density and it is practically not observed with current density exceeding 100A/cm^2.

The results shown in Table 3 show that the shift of peak radiation is not observed in blue LEDs with increase of density of current passing through the crystal unlike red and green LEDs. Like in the cases of red and green LEDs, the presented cal-

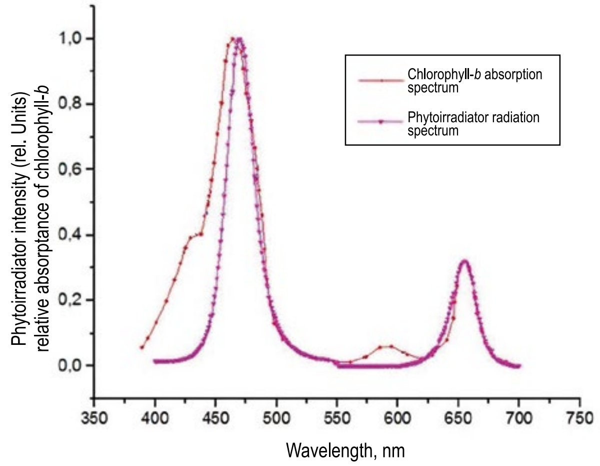

Fig. 8. Absorption spectrum of chlorophyll-*b* and modelled radiation spectrum of phytoirradiator

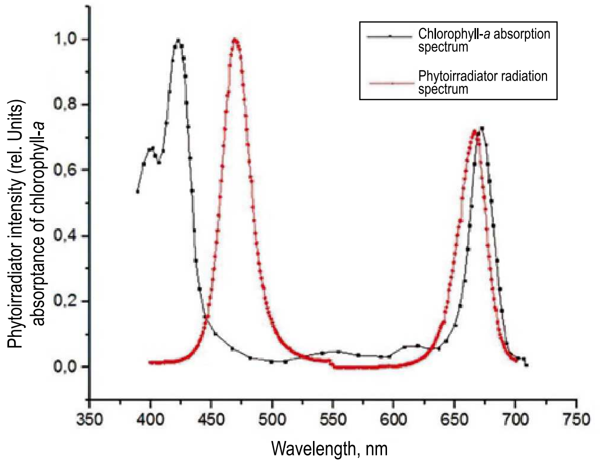

Fig. 9. Absorption spectrum of chlorophyll-*a* and modelled radiation spectrum of phytoirradiator

culation results correspond with the experimental data obtained for blue LEDs.

3. Heating of the structure may be assessed based on the approximation parameter E_1. It should be noted that for all studied LED it is possible to assume $E_1 \approx kT$ which is equal to about 26 meV at room temperature. Therefore, based on the results of approximation of radiation spectra at different values of current, it is possible to evaluate heating of the crystal active region at different values of current density.

The increase of peak width at half height visible in Figs. 2–4 with its average value of about 10 nm to 25 nm can also be explained by heating.

Such shift is especially visible in red LEDs the crystals of which are based on complex four-component solutions of aluminium, gallium, indium and phosphorus and in green LEDs with high indium content in the active region of their crystals. The indium content in the active region of blue LED crystals is lower and the shift is, therefore, not so visible.

4. For red, green and blue LEDs, the approximation parameter E_0 varies within the ranges of (15–20) eV, (45–60) eV and (50–62) eV respectively. It is seen that the values of this parameter in red LEDs are lower than kT, however, the difference is not very significant, whereas for green and blue LEDs, the value of the parameter E_0 is much higher than kT. This difference is especially significant in nitrides due to larger potential fluctuations.

5. Based on the obtained results, it is possible to formulate recommendations for development and manufacture of light sources and lighting devices based on red, green and blue LEDs. Since the shift of peak position is observed in the spectra of red and green LEDs with increase of current, the said shift shall be taken into account when selecting the operating mode of a lighting device by selecting both operating current range and heat mode. Correct selection of the operating current and the heat mode is also important due to the fact that increase of current density in the active region of a LED crystal leads to its overheating which may be critical for degrading of parameters of LEDs and light sources, and, so, phytoirradiators based on them. For selection of the heat mode, it is necessary to use efficient heat dissipation means, which include even forced cooling of a LED device in cases when it is critical.

5. PHYTOIRRADIATOR MODELLING

On the basis of the conducted studying of LED characteristics, a source of radiation with adjustable spectrum for use in phytoirradiators was modelled. The control parameters included current for changes of spectral peak positions in regions of active absorption of pigments and the number of operating single emitters for adjustment of the radiant flux ratio or photons in different ranges of PAR region [2, 3].

Such phytoirradiator would be capable to provide required radiation spectrum for different vegetation periods. In other words, it would be able to provide the required spectrum during the whole period of plant growing with minimum energy consumption. By changing the control parameters, it is possible to achieve high efficiency at each stage of plant growth. Another advantage of such phytoirradiator is that it uses a rather wide spectral range

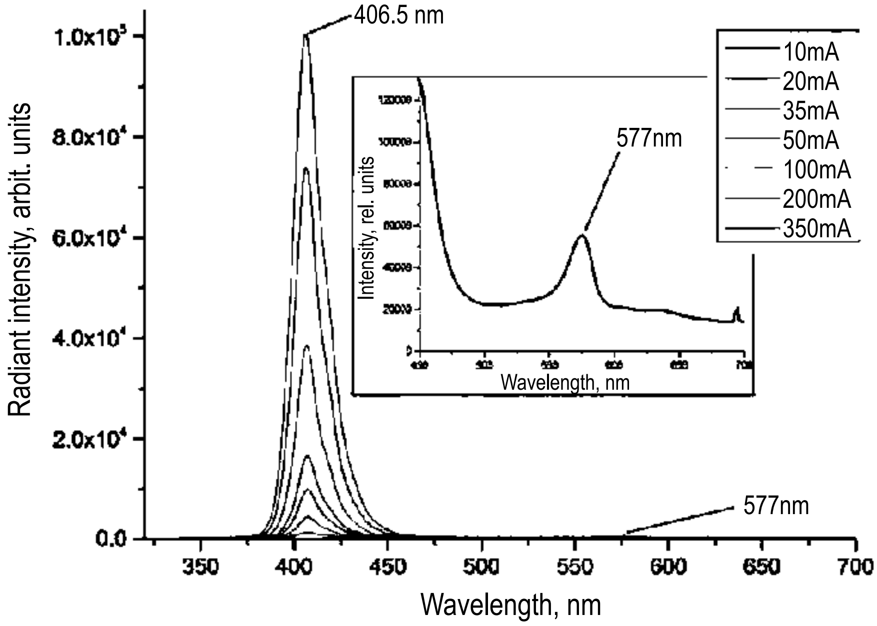

Fig. 10. Radiation spectrum of a violet LED at different values of current [13]

which includes all (red, green and blue) PAR regions. After modelling the radiation source with adjustable spectrum and conducting studies using it, it is possible to determine the optimal number of LEDs requiring for a specific plant and thus to develop an optimised phytoirradiator for each type of plants, which may be economically viable.

On the basis of the obtained results, phytoirradiator spectra were modelled. The modelling was conducted so that the radiation spectrum of the irradiator would be correlating well with the absorption spectrum of a given pigment of a plant. For instance, Fig. 8 shows the absorption spectrum of chlorophyll-*b* as well as the spectrum of the modelled phytoirradiator (the values of operating current of red, green and blue LEDs are equal to 60 mA, 0 mA and 80 mA respectively). Fig. 8 shows that the radiation spectrum of the modelled phytoirradiator correlates rather well with the absorption spectrum of chlorophyll-*b*, therefore, such emitter may provide relatively high energy efficiency.

It is worth noting that the studied LEDs do not cover a part of the chlorophyll-*b* absorption spectrum shown in Fig. 8 (the region of (600–620) nm). To use this spectrum region, it is necessary to use amber LEDs which had not been studied in this work.

Fig. 9 shows the absorption spectrum of chlorophyll-*a* as well as the spectrum of the relevant modelled phytoirradiator (the values of operating current of red, green, and blue LEDs are equal to 120 mA, 0 mA, and 100 mA respectively). This figure shows that using the studied LEDs it is possible to form a spectrum which relatively well correlates with the absorption spectrum of the pigment only at longer wavelengths.

For shorter wavelengths of the absorption spectrum of chlorophyll-*a* and other pigments it is necessary to use violet LEDs [13, 14]. Fig. 10 presents radiation spectra of such LEDs at different values of current [13, 14]. The figure shows that the radiation peak of such LEDs corresponds with the peak of absorption of chlorophyll-*a* in the violet region of the spectrum (Fig. 9), which indicates that with such LEDs a phytoirradiator may also efficiently operate with pigments at shorter wavelengths of the spectrum.

6. CONCLUSION

As a result of the conducted study of red, blue and green LEDs, the dependences of their spectra and radiation intensity (in arbitrary units) from current were obtained. By means of approximations, the mechanisms of current passage and recombination in the studied LEDs were explained and the correlation between the results of spectral measurements and measurements of the dependence of intensity from current was discovered for red, green and blue LEDs. On the basis of the obtained experimental results, the model of a phytoirradiator with adjustable radiation spectrum was proposed, formulated with consideration of experimentally discovered spectral features, e.g. the shift of peak of the radiation spectrum after increase of current towards long waves in red LEDs and towards short waves in green LEDs whereas no shift of the peak was observed in blue LEDs. The conducted modelling showed that these phytoirradiators allow us to adjust the radiation spectrum depending on the needs: different vegetation periods of plants require different radiation spectra since at different stages of a plant development the pigments with different absorption spectra are responsible for its growing.

A similar model of a multi-colour radiation source with adjustable spectrum was described in [15] with the authors proposing a multi--colour LED based light source with functionality of spectrum control by measuring the current passing through LEDs for use as a universal calibration source. The difference is that the authors of [15] also used white LEDs in their source apart from colour LEDs of different visible-light spectrum ranges. Given the results obtained in [15], fair to assume that white LEDs may be used in phytoluminaires, and research and modelling of their characteristics may be a subject for continuation of the study described above.

ACKNOWLEDGEMENT

The study was conducted with financial support of the Ministry of Science and Higher Education as part of the "Comprehensive Studies in the Area of Plant Photoculture and Design of Highly Efficient LED Phytoirradiators Providing Increase of Energy Efficiency of Industrial Greenhouses" project. Grant Provision Agreement No. 14.576.21.0099 dated on 26.09.2017. Agreement ID: 0000000007417PD20002. Unique ID of the work (project): RFMEFI57617X0099.

REFERENCES

1. Light Engineering Handbook [Spravochnaya kniga po svetotekhnike] / Edited by Ju.B. Aizenberg. 3rd Issue, revised and supplemented.Moscow: Znak, 2006, 972 p.

2. Prikupets L. B.Technological Lighting for Agro-Industrial Insolation in Russia // Light & Engineering Journal, 2018, Vol. 26, #1, pp.7-17.

3. Prikupets L.B., Boos G.V., Terekhov V.G., Tarakanov I.G. Research into Influence from Different Ranges of PAR Radiation on Efficiency and Biochimical Composition of Green Salad Foliage Biomass// Light & Engineering Journal, 2018, Vol.26, #4, pp. 38-47.

4. Protasova N.N. Photoculture as a Method to Identify Potential Capacity of Plants [Svetokultura kak sposob vyyavleniya potentsialnoy produktivnosti rasteniy] // Plant Physiology [Physiologiya rasteniy], 1987, Vol. 34, issue 4, pp. 812–822.

5. Bakharev I.A., Prokofiev A. Yu., Turkin A.N., Yakovlev A.A. Application of LED Luminaires for Greenhouse Illumination: Reality and Prospectives [Ispolzovaniye svetodiodnykh svetilnikov dlya osveshcheniya teplits: realnost i perspektivy] // STA, 2010, Vol. 2, pp. 76–82.

6. Prokofiev A. Yu., Turkin A.N., Yakovlev A.A. Prospectives of Application of LEDs in Cropping [Perspektivy primeneniya svetodiodov v rastenievodstve] // Poluprovodnikovaya Svetotekhnika, 2010, Vol. 5, pp. 60–63.

7. Blackey R. LED Illumination – the Future of Cropping [Svetodiodnoye osveshcheniye – budushcheye rastenievodstva] // Poluprovodnikovaya Svetotekhnika, 2018, Vol. 2, pp. 54–58.

8. Shubert F. Light-Emitting Diodes [Svetodiody]. Trans. from Eng. edited by A.E. Yunovich, 2nd ed, Moscow: FIZMATLIT, 2008, 496 p.

9. Zolina K.G., Kudryashov V.E., Turkin A.N., Yunovich A.E. Luminescence Spectra of Blue and Green LEDs Based on InGaN/AlGaN/GaN Multi-Layer Heterostructures with Quantum Wells [Spektry luminestsentsii golubykh i zelyonykh svetodiodov na osnove mnogosloinykh geterostruktur InGaN/AlGaN/GaN s kventovymi yamami] // FTP, 1997, Vol. 31, issue 9, pp. 1055–1061.

10. Kudryashov, V.E., Turkin, A.N., Yunovich, A.E., Zolina, K.G., Nakamura, S. Spectra of superbright blue and green InGaN/AlGaN/GaN light emitting diodes // Journal of the European Ceramic Society. Vol. 17, Issues 15–16, pp. 2033–2037.

11. Yunovich, A.E., Kovalev, A.N., Kudryashov, V.E., Turkin, A.N., Zolina, K.G., Kovalev, A.N., Manyachin, F.I. Mechanism of electroluminescence in InGaN/AlGaN/GaN heterojunctions with quantum wells // Proc.of the 2nd Symp. on III–V Nitride Materials and Processes. Electrochem. Soc., Pennington, NJ, 1998, Vol. 98–02, pp. 83–102.

12. Kudryashov V.E., Turkin A.N., Yunovich A.E., Kovalyov A.N., Manyakhin F.I. Lumenescent and Electric Properties of InGaN/AlGaN/GaN LEDs with Multiple Quantum Wells [Lyuminestsentnyye i elektricheskiye svoistva svetodiodov InGaN/AlGaN/GaN s mnozhestvennymi kvantovymi yamami] // FTP, 1999, Vol. 33, issue 4, pp. 445–450.

13. Avakyants L.P., Aslanyan A.E., Bokov P. Yu., Volkov V.V., Mateshev I.S., Turkin A.N., Chervyakov A.V., Yunovich A.E. Luminescent and Electric Properties of Ultra-Violet and Violet LEDs Based on Gallium Nitride Heterostructures [Luminestsentnyye i elektricheskiye svoistva ultrafioletovykh i fioletovykh svetodiodov iz geterostruktur na osnove nitrida galliya] // Transactions of the Department of Physics of M.V. Lomonosov Moscow State University [Uchyoniyye zapiski fizicheskogo fakulteta MGU im. M.V. Lomonosova], 2016, Vol. 3, 163401–1 – 163401–7.

14. Volkov V.V., Kogan L.M., Turkin A.N., Yunovich A.E. Luminescence Spectra of Gallium-Nitride-Based High-Output LEDs in Ultra-Violet and Violet Spectrum Regions [Spektry luminestsentsyiy moshchnykh svetodiodov na osnove nitrida galliya v ultrafioletovoy i fioletovoy oblastyakh spektra] // FTP, 2018, Vol. 52, issue 10, pp. 1172–1176.

15. Karli N., Sperling A., Bizyak G. Realisation of a Laboratory Sample of an Adjustable Multi-Colour Light Source [Realizatsyiya laboratornogo obraztsa nastraivaemogo mnogotsvetnogo istochnika sveta] // Svetotekhnika, 2019, #. 5, pp. 16–22.

Mikhail M. Erokhin graduated from Lomonosov Moscow State University in 2019. At present time, he is an engineer of the Testing Centre at VNISI named after S.I. Vavilov

Pavel V. Kamshilov graduated from Moscow State University of Geodesy and Mapping in 1998 with specialty in Optoelectronic Instruments and Systems. Chief Specialist of OOO VNISI, assistant of the Light Engineering sub-department of NIU MPEI

Vladislav G. Terekhov engineer. He graduated with honors from Moscow State University of Economics, Statistics and Informatics with a degree in Applied Informatics in Economics, and at present, he is a Head of the Department for the Promotion of LLC International Lighting Corporation BL GROUP and researcher in VNISI of S.I. Vavilov. He is a member of the Organizing Committee of the All-Russian Conference “Gallium, Indium and Aluminum Nitrides. Structures and devices” and an expert on energy saving technologies in the lighting of the Russian Union of Builders

Andrey N. Turkin, Ph.D. (Phys-Math). He graduated from M.V. Lomonosov Moscow State University in 1995. At present time he is Associate Professor of the Optics, Spectroscopy and Physics of Nanosystems Chair of the Department of Physics of Moscow State University and Associate Professor of the Lighting Engineering sub-department of NIU MPEI

Light & Engineering
Vol. 27, No. 6, pp. 106–111, 2019 *https://doi.org/10.33383/2019-065*

IRRADIATION SYSTEM FOR A CITY FARM AUTOMATED MULTI–LAYER PHYTOINSTALLATION

Vladislav G. Terekhov

IEC BL GROUP, Moscow
E-mail: terekhov@bl-g.ru

ABSTRACT

Contemporary light engineering is ready to make its contribution in the development of new, automated and (in the nearest future) fully computerised production facilities based on application of artificial irradiation for technological purposes.

It is referred to cultivation of plants using the photo-culture technology in multi-layer phytoinstallations with spectral characteristics and level of irradiation taking the species and tasks of cultivation into account. The major type of plants for these installations is lettuce cultures, consumption of which in Russia significantly lags behind the recommended values, especially during winter.

The article reviews major specifications of LED-based irradiation devices and lighting systems based on them, used for cultivation of lettuce in automated multi-layer phytoinstallations in photo-culture environment. An example of such phytonstallations is the automatic research installation developed in S.I. Vavilov VNISI, which has no parallel in Russia.

A principal distinction of the irradiation devices used in this installation is application of multi-component LED compositions based on white and colour elements allowing us to vary spectral characteristics in the PAR region within a wide range. Generally, the installation is notable for contemporary hardware and availability of computer control.

Keywords: multi-layer phytoinstallation, LED-based phytoemitter, irradiating installation, computer control, PAR, photo-culture, lettuce

1. INTRODUCTION

Appearing and dynamic development of LED-based equipment became a basis for creation of brand-new research and production facilities and installations of automated multi-layer plant cultivation which were called *City Farm*. As a matter of fact, this is about a new progressive technology of plant cultivation (mostly lettuce cultures), which solves an important problem of rational utilisation of protected ground areas which are becoming more expensive, provides high level of automation of technological process and reduces the fleet of required machinery and mechanisms as compared to a typical greenhouse technology. Application of multi-layer phytoinstallations (MPI) is possible in urban environment, which reduces transportation expenses. That is why MPIs are rather promising not only for Russian metropolises but also for a large number of small towns and settlements allowing to supply fresh and rich in vitamins vegetables for people, especially in winter[1].

MPIs for cultivation of plants using the photo-culture technology significantly differ from conventional protected ground structures (greenhouses) and deserve special consideration presented below not only for analysis of required light engineering solutions for production type MPIs but also for discussion (with consideration of the first results ob-

[1] It shall be noted that MPI had been under development in Russia in the $1980^{S} \div 1990^{S}$ [1] but these works were not completed mostly due to lack of emitters equal to contemporary LED light sources at that moment.

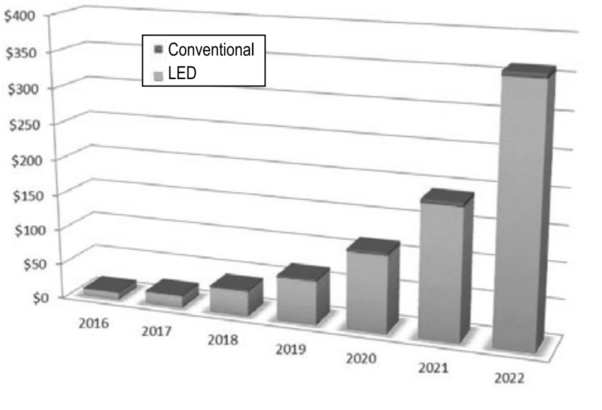

Fig.1. Development of the *City Farm* vertical multi-layer lighting systems with LED and conventional irradiation

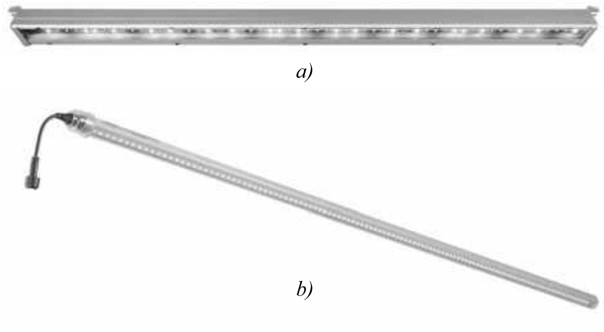

a)

b)

Fig.2. Examples of LED-based phytoemitters: *a*: *WAVE* series (18–105) W, *IGROX*; *b*: *L* series (14–35) W, *Valoya*

Fig. 3. Phytoemitters with GALAD Arcline Phyto LED series LEDs 30 W and 60 W designed for MPI

tained) of an opportunity to implement photobiological research programmes.

2. MULTI–LAYER PHYTOINSTALLATIONS HARDWARE

LED-based phytoemitters (LEDPE) for MPIs consisting of space-saving modules (layers) have no competition. Fluorescent mercury lamps cannot be used in phytoinstallations due to environmental reasons whereas HPSLs are not applicable due to high power concentration and high temperature of a bulb.

Opportunities to create any spectrum in the PAR region (400–700) nm with high level of radiation parameters, rather simple and efficient spectrum and irradiation level adjustment led to dynamic development of the photo-culture direction in research and production programmes of the leading LED manufacturers: *CREE* (USA), *OSRAM Semiconducters* (Germany), *Lumileds* (the Netherlands), etc. as well as light engineering companies, such as *Signify* (the Netherlands), *Valoya* (Finland), MSK BL GROUP (Russia), *Current-GE* (USA), *IGROX* (Italy), etc.

Characteristically that the specialists of *Strategies Unlimited* (USA) presume in their global forecast of development of protected ground LEDPE that the volume of LEDPE irradiation in *City Farm* will increase by about 7 times by 2022 (Fig. 1) [2]. These estimations are also shared in Russia: for instance, the matters of LEDPE irradiation in MPIs were reflected in new regulations in 2017 [3].

The specifications of LEDPE by different manufacturers are rather diverse; this is mainly caused by the fact that requirements to phytoirradiation spectra for specific species of plants are currently being formed; dimensions of MPI modules are also far from unification, and actual data on stability of irradiation characteristics of LEDPE during operation is not clear enough yet.

Nevertheless, the major parameters of LEDPE for MPI may be assumed as follows:

- Electric capacity: (30 ÷ 70) W;
- Radiation spectra: Binary (*RB*: red-blue with different portion of each component) or nearly white with different portions of the green component;
- Photosynthetic photon efficiency (*EPPF*): (2.0 ÷ 2.7) μmol/J (depending on the type of spectrum), maximum value is for the binary (*RB*) type of spectrum;
- Length: ~120cm (this is caused by the most common width of MPI modules);
- Specific electric capacity (per unit of length): (0.25 ÷ 0.75) W/cm (contains indirect information on temperature of a LED crystal and its possible operational life);
- Shell protection class: *IP*54, *IP*66.

There are two designs proposed for MPI LEDPE (Fig. 2):

– In the form of a long narrow emitter with aluminium body, polycarbonate diffuser, and passive cooling;

– In the form of a narrow pipe with the diameter of (26 ÷ 28) mm made of polycarbonate as a lamp for direct replacement (retrofit) of fluorescent lamps (FL).

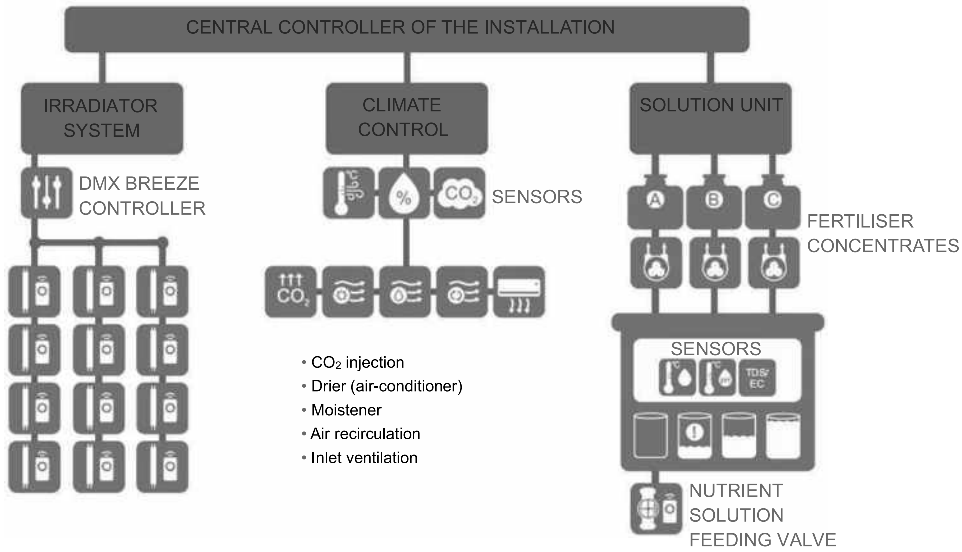

Fig.4. MPI block diagram

Recently, the second variant is getting widespread use.

In 2018, S.I. Vavilov VNISI together with KETZ developed a series of LEDPE GALAD Arcline Phyto LED30 W and 60 W (Fig. 3) with two spectral variants: with *EPPF* of 2.1µmol/J for the white radiation design (T_{cc}= 3700K) and of 2.5µmol/J for the *RB* spectrum design. Dimensions of LEDPE: (1201×115×67) mm, *IP65* class of protection.

It is worth noting that, unlike conventional lighting installations (LI) for greenhouses, LIs for MPI have a number of distinctions which are, in particular, related to the fact that the distance between PE and the planting plane does not exceed 60 cm and the distance between lettuce cultures may be equal to (10–20) cm in the end of the vegetation period. That is why it is very important that the PE surface temperature shall not exceed 80 °C and the heating component of the PE balance shall not cause overheating of the root area of the next (upper) layer of MPI. Light distribution of LEDPE shall provide uniform distribution of irradiance over the technological area.

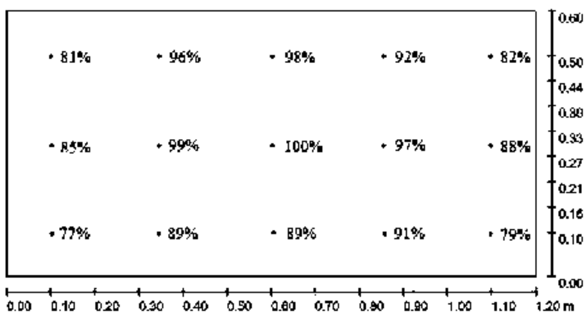

Fig.5. Level of technological area irradiation uniformity

The levels of irradiation and spectral characteristics of MPI are necessary to be selected on the basis of the results of photobiological studies (in our case, on the basis of [4, 5]). Sometimes, if the plants significantly differ from the studied ones, it is necessary to conduct additional experiments for elaboration of a "light engineering recipe" of efficient cultivation of specific plants[2].

Like in the case of greenhouses with a photoculture, the share of technological irradiation in the general energy consumption of MPI exceeds 90 %, therefore, the energy-saving factor of irradiation may be considered one of the most important ones.

Designing of a LEDPE starts with correct selection of parameters of the applied LEDs. In particular, this relates to the maximum possible luminous efficacy (lm/W) for quasi-monochromatic LEDs determining the level of *EPPFD* of LED.

As a universal indicator of energy efficiency of a LI for PI (including MPI), the ratio $EPPFD_{LI} = PPFD_{av} / P_1$ [µmol/J], where $PPFD_{av}$ is average *PPFD* on the studied surface, [µmol / (s·m^2)], P_1 is specific installed electric capacity of LI [W/m^2], may be assumed [6].

The matter of availability of the far-red (700–780) nm range in the PE spectrum, i.e. beyond the PAR region, is worth considering particularly. This radiation is not used for photosynthe-

[2] Wherein, the light engineering parameters of PE and LI shall be specified in photosynthetic photon units in accordance with GOST R57671–2017 "LED irradiators for greenhouses: General specifications".

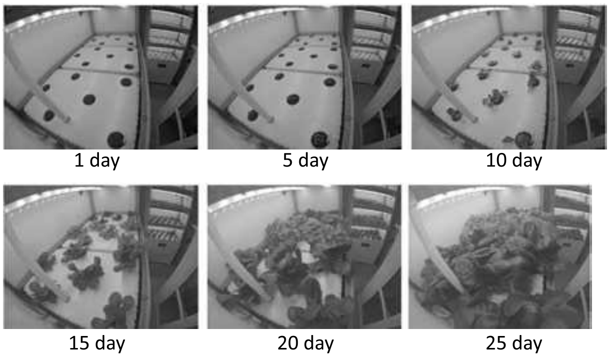

Fig.6. Vegetation stages of lettuce plants

Fig.7. Lettuce cultivation in the MPI in S.A. Vavilov VNISI

sis and does not cause energy impact on a plant; however, by actuating the active form of the phytochrome F_{730} plant pigment, it adjusts photo morphogenesis of a plant. The impact of this spectral rangeтon growth and development of plants is currently being studied, which makes it desirable that it would be available in the radiation spectrum of PEs for research programmes.

3. LI FOR A VERTICAL MPI IN VNISI

In S.A. Vavilov VNISI, the automated vertical MPI was designed, manufactured, and commissioned for conducting of photobiological studies with application of state-of-the-art LED emitters and methods of adjustment of plant irradiation modes. The research MPI is also designed for assistance in development of requirements to major light engineering parameters of PE and LI with a plant photo-culture.

Fig. 4 shows that the MPI contains three light-isolated units (modules) with four sections with area of 0.72 m^2 ((1.2⋅0.6) m) each[3] located above each other allowing us to cultivate up to 264 plants simultaneously. Two six-channel controlled PEs based on GALAD Arcline Phyto-72 which allow creating almost unlimited number of combinations of radiation spectra are installed in each section. The specifications of LED of each channel are presented in Table. Capacity of each PE may vary between 12.5 and 50.0 W. Maximum power of the whole LI is 1200 W and corresponding specific electric power of LI is 140 W/m^2. Maximum *PPFD* over the technological area of LI is up to 320 μmol/(s⋅m^2). High uniformity of irradiation was reached (Fig. 5).

[3] The total technological area of the MPI is 8.64 m^2.

Spectral characteristics of LI and irradiation level were measured using the devices by *Li-COR* (USA) and *UPRtek* (Taiwan).

Before each vegetation LI is adjusted by regulating spectral and irradiating characteristics of PE via *DMX512* protocol using a special control scheme consisting of a personal computer with a *USB – DMX 512 RDM* adapter and *RDM Controller 2.0* software. Based on the results of the spectrum selection procedure, the table of channel level values is input in the BRIZ-*DMX* controller operating in conjunction with the real-time timer BRIZ-RV.

Opportunities to set different spectral combinations are practically not limited in the MPI. The methodology and procedure of their selection were evaluated by us during studies of different PAR ranges on different installations in a phytotron [5].

MPI is fully automated with permanent control of parameters of the key cultivation systems: climatic installation, solution unit and LI. The remote monitoring and control system allow us to monitor the process of vegetation and to adjust parameters and cultivation modes, if necessary, using any device (PC, smart-phone or tablet) via a *web* interface in real time.

By means of special compact video cameras *HIKVISION DS-2CD1031* and *GoPro Session5* installed in the modules, the state and development of the plants were constantly remotely monitored. It is possible to conduct phenological monitoring of plants at different stages of vegetation (Fig. 6); their results may be further taken into account for adjustment of the LI radiation spectrum in the course of ontogenesis.

Table

Nominal Parameters of LEDs Used in the MPI in S.I. Vavilov VNISI*

Channel number	LED type (manufactured by *CREE*)	Dominant wavelength, nm	Current, mA	Voltage, V	Radiation parameters		Spectrum
1	XPE BGR-L1-0000-00F01	620–630	350	2.2	*PPF*, μmol/s	1.1	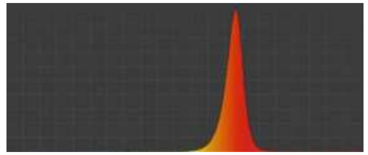
2	XPE BRD-L1-0000-00801	650–670	350	2.2		1.92	
3	XPEEPR-L1-0000-00C01	720–740	350	2.2		2.34	
4	XPEBBL-L1-0000-00Z01	465–485	350	3.2	Φ_v, lm	35.2	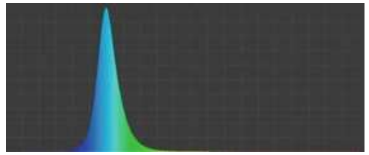
5	XPG DWT-U1-0000-00FE5	400–700 (4,000K)	350	3.2		120	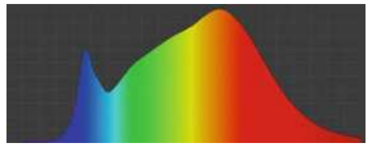
6	XPGDWT-B1-0000-00LE3	400–700 (5,000K)	350	3.2		150	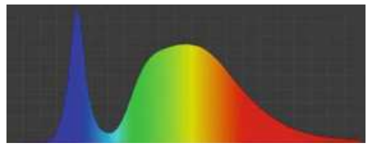

*According to the manufacturer's data presented on www.cree.com.

To sum up, we would like to note that the created automated installation for cultivation of plants in controlled environment provides brand new opportunities for conducting of photobiological studies: it reduces the experiment periods, expenditures for their conducting and minimises the routine maintenance part directly involving people.

CONCLUSION

Since April, 2019, the MPI in the S.I. Vavilov VNISI has been operating in the testing mode with variation of spectral characteristics and irradiation level. Currently, several vegetations of different varieties of lettuce and greengrocers have passed. The obtained crop capacity results are (30–40)% higher than those in lettuce lines of industrial greenhouses with the photo-culture technology, which directly confirms high efficiency of the light engineering decisions and other microclimate parameters taken in the MPI (Fig. 7).

ACKNOWLEDGMENT

Research was funded by the Ministry of Science and Higher Education of the Russian Federation (project “Comprehensive studies in the plant photo-culture and creation of high-effective LED phytoirradiators for increase of energy efficiency of industrial greenhouses”). Contract on granting subsidy #14.576.21.0099 dated 9/26/2017. Contract ID0000000007417PD20002. Project ID RFMEFI57617X0099.

REFERENCES

1. Tikhomirov A.A., Sharupich V.P., Lisovsky G.M. Plant Photoculture: Biophysical and Biotechnological Basics [Svetokultura rasteniy: biofizicheskiye i biotekhnologicheskiye osnovy], Novosibirsk: Siberian department of RAS, 2000, 213 p.

2. Philip Smallwood. Tracking the Horticultural SSL Market and Technology // Horticultural Lighting Conference, USA, 2017, Denver, Colorado.

3. Boos G.V., Prikupets L.B., Rozovsky E.I., Stolyarevskaya R.I. Standardisation of Light Engineering Devices and Installations for Greenhouses [Standartizatsyya svetotekhnicheskikh priborov i ustanovok dlya teplits] // Svetotekhnika, 2017, # 6, pp. 69–74. // Light & Engineering Journal, 2018, Vol. 26. #1, pp.18–24.

4. Prikupets L.B., Boos G.V., Terekhov V.G., Tarakanov I.G. Studying of the Affects of Radiation in Different Ranges of PAR Region on Capacity and Biochemical Composition of Biomass of Lettuce and Leaf Vegetables [Issledovaniye vliyaniya izlucheniya v razlichnykh diapazonah oblasti FAR na produktivnost i biokhimicheskiy sostav salatno-zelennykh kultur] // Svetotekhnika, 2018, № . 5, pp. 6–12 // Light & Engineering, 2018, Vol. 26, # 4, pp.38–47.

5. Prikupets L.B., Boos G.V., Terekhov V.G., Tarakanov I.G. Optimisation of Light Engineering Parameters of Lettuce and Leaf Vegetables Photo-culture Using LED Emitters [Optimizatsiya svetotekhnicheskikh parametrov pri svetokulture salatno-zelennykh rasteniy s ispolzovaniyem svetodiodnykh izluchateley] // Svetotekhnika, 2019, № . 4, pp. 6–13//Light & Engineering, 2019, Vol. 27, #5, pp.43–54.

6. Prikupets L.B. Process Illumination in the Russian Agriculture [Tekhnologicheskoye Osveshcheniye v agropromyshlennom komplekse Rossii] // Svetotekhnika, 2017, # 6, pp. 6–14. Prikupets L.B. Technological Lighting for Agro-Industrial Installation in Russia // Light & Engineering, 2018, Vol. 26, No. 4, pp. 7–17.

Vladislav G. Terekhov,
engineer. He graduated with honors from Moscow State University of Economics, Statistics and Informatics with a degree in Applied Informatics in Economics, and at present, he is a Head of the Department for the Promotion of LLC International Lighting Corporation BL GROUP and researcher in VNISI of S.I. Vavilov.
He is a member of the Organizing Committee of the All-Russian Conference “Gallium, Indium and Aluminum Nitrides. Structures and devices” and an expert on energysaving technologies in the lighting of the Russian Union of Builders

Light & Engineering
Vol. 27, No. 6, pp. 112–122, 2019
https://doi.org/10.33383/2019-025

TESTING AND ANALYSIS OF CHARACTERISTICS OF LOW-PRESSURE MERCURY AND AMALGAM BACTERICIDAL UV LAMPS BY VARIOUS MANUFACTURERS

Michael E. Allash[1], Leonid M. Vasilyak[2], Nikolay P. Eliseev[3], Oleg A. Popov[3], and *Dmitry V. Sokolov[4]

[1] Lighttech Kft, Budapest, Hungary
[2] OIVT RAS, Moscow
[3] NRU MPEI, Moscow
[4] NPO LIT, Moscow
**E-mail: sokoloff@npo.lit.ru*

ABSTRACT

The samples testing of bactericidal high-pressure UV lamps presented on the Russian Market showed their insufficient quality. These lamps were designed and manufactured based on the technical assignment of specific manufacturers or are copies of UV lamps by well-known brands but manufactured using own technology. Moreover, these devices do not comply with special aspects of UV irradiating equipment for water sterilisation such lamps may be used with by consumers.

Keywords: bactericidal lamps, low-pressure mercury lamps, amalgam lamps, UV radiation, water sterilising installations

1. INTRODUCTION

UV radiation (UVR) is widely applied in various areas, one of which is sterilising of water, air, and surfaces. Within the previous 15–20-years period, UVR sterilising has undergone rapid development and has allowed changing approaches to sterilising of media dramatically, but it has developed as a method of sterilising of potable and wastewater most significantly. UVR is also widely applied as a method of air and surfaces sterilising in medical institutions, in public areas, transport, and other application areas such as food, pharmacological and electronic industry, medicine, recycling water supply, fish farming, greenhouse facilities, etc. [1].

In most applications, low-pressure mercury and amalgam tube UV lamps as well as medium (high)-pressure mercury lamps are used as sources of UVR for sterilising [2]. In Russia, medium (high)-pressure lamps for water sterilising equipment have not been widely used due to their low radiant efficiency in the bactericidal UVR range [1], low lifetime [3], and high tube temperature, although they have been used, for instance, in pool facilities, ballast water sterilising installations and installations with Advanced Oxidation Processes (*AOPs*) [1, 4] for destruction of chemical trace contaminants in water.

Currently, the world's leading manufacturers such as *Philips* (the Netherlands), *Lighttech/LSI* (Hungary/USA), *Heraeus Noblelight* (Germany), and NPO LIT (Russia/Germany) offer low-pressure mercury and amalgam lamps with power ranging between 15 and 1000 W with radiant efficiency from 30 to 40 % at wavelength $\lambda = 254$ nm and lifetime from 8,000 to 16,000 hours. In Russia, mercury and amalgam UV lamps are manufactured by NPO LIT (Moscow) and OOO Lodygin A.N. NIIIS (Saransk). Based on these lamps, UV-irradiating (UVI) equipment for sterilising of water, air, and surfaces in different conditions with various performance is manufactured. The world's largest manufacturers of water UVI equipment include: *Tro-*

jan (Canada), NPO LIT (Russia/Germany), *Wedeco Xylem* (Germany/USA), *Halma group* (*Hanovia*, *Aquionics*, *Berson*) (UK/USA/the Netherlands), *Calgon Carbon* (USA), and *NewLand* (PRC). Apart from NPO LIT, Russian manufacturers of mercury or amalgam lamps-based water sterilising installations also include NPO ENT (Saint Petersburg), UFTECH (Sergiev Posad), Industrial UV Systems (Saint Petersburg), and some other companies.

Nowadays, the market of manufacturers and consumers of low-pressure bactericidal UV lamps has been formed in Russia. It includes both the above-mentioned manufacturers of UVI equipment and their customers: water network operators, food industry enterprises, manufacturers and buyers of pools and water parks, medical institutions as well as individual users of water and air sterilising equipment, the amount of which has been increasing every year.

Naturally, the so-called "relamping" market has been rapidly developing too, and suppliers of non-original accessories including UV lamps of unknown origin often work in it. A large amount of lighting equipment of unknown origin is installed in UVI equipment without taking its distinctions and maintenance regulations into account. Statistic data obtained from consumers shows large increase in the number of emergency situations and even accidents related to the application of UV lamps taken for specific equipment incorrectly. Sometimes there are funny situations when a purchased lamp has other dimensions or other electric inputs and just cannot be used in specific equipment, and sometimes there are tragic situations when the application of such lamps causes accidents: e.g. malfunctioning of supply and control systems and sometimes even inflammation of equipment, to say nothing of changing of the sterilising process mode.

Another complication of this problem is caused by the fact that certifying of such lighting equipment as UV lamps is voluntary in the Customs Union member states. The CU technical regulation conformity certificate has a declarative nature and informs a consumer on the safety of a product. At the same time, any other technical information such as electrical characteristics, UV radiant flux, results of lifetime tests, etc. remains on the conscience of a seller of UV lamps. Some companies frankly copy the technical specifications of the leaders of this market: *Lighttech*, *Osram*, LIT, etc. Radiometric measurement of UV lamps parameters is a rather complex problem that requires knowledge of UVR measurement methodology of long lamps, availability of special equipment, and skilled personnel. Bad-faith companies use it actively given that it is hard to confirm or to disprove the characteristics claimed by them in datasheets or technical specifications.

Recently, the specialists in such UVR sources are regularly being addressed by consumers aiming at conduct of expertise of UV lamps for compliance with the declared characteristics and often asking just to assess working capacity of such lamps. For example, the authors of this article were addressed by several customers of such water sterilising products with such requests: engineering companies, water network operators, service companies, and owners of several private pools.

The goal of this study was to test low-pressure amalgam and mercury UV lamps supplied to the Russian market under different brands and to analyse the fitness of the tested samples for different applications. In the course of testing, we paid the major attention to capabilities of operation of lamps in water sterilising UVI equipment. During our study, we took only the logo labelled on each specific lamp into account and we do not claim that any lamp was manufactured exactly by declared manufacturers. We would also like to note that both the testing and this article are not aiming at disparaging or dignifying of products of any specific company.

In lighting engineering laboratories of *Lighttech* (Budapest) and *LIT UV Elektro* (Erfurt, Germany), the samples of lamps with labels *Jelosil*, *JUV*, Eltos, *LightBest*, *UV Product*, and *Sean* were tested. For testing, a small number of lamps with each logo were used. The authors understand that a selection of one or two samples of lamps may provide a rather high margin of error but they think that all lamps for such vital systems as water sterilising installations should be of high quality.

2. FEATURES OF USE OF UV LAMPS IN STERILISING INSTALLATIONS

A lamp does not work in isolation in UVI equipment; it is an integral part of a UVR sterilising system. Designers of UVI equipment take such aspects into account as temperature modes of specific elements of a lamp, operational modes of amalgam, required current and pre-heating time for each type of electrodes, the required value of lighting voltage impulse, the durability and location of a lamp cap, etc. For the purpose of provision of all required operational modes of a lamp and an opportunity to provide guarantees of lifetime, decreasing of UVR flux, "unlimited" number of switching on/off, etc. to a customer, a designer of UVI equipment develops a *datasheet* for a lamp and manufactures it or cooperates with a reliable manufacturer of such lamps.

It is possible to provide a lot of examples when an installation with lamps by one manufacturer provides required UV dose and, hence, microbiological characteristics of water whereas an installation with lamps by another manufacturer with the same declared characteristics does not. It is caused by the fact that manufacturers of lamps specify their characteristics for some specific conditions. Most commonly, maximum characteristics (e.g. UVR flux or radiant efficiency) obtained during measurements in laboratory conditions at air temperature from 20 to 25 °C are specified. These maximum characteristics are provided in a technical specification or a datasheet. However, if a lamp is intended to be used for water sterilising, it should efficiently operate in a specific piece of UVI equipment, and it absolutely does not matter for a customer what UVR level the lamp showed during its testing on an air stand in the laboratory. A developer and a consumer require the maximum or quite close value of UVR flux specified in a technical specification to be obtained in the most operating modes of the lamp in an installation. It is possible to provide a lot of evidence of UVR flux decrease by several times with incorrectly selected amalgam. It occurs, for example, in the case of overcooling or overheating of a lamp. In case of decreasing of bactericidal UVR with $\lambda = 254$ nm, the UV dose of an installation also decreases, which leads to a reduction of sterilising efficiency. Changing of lamp temperature modes during water sterilising is related to the fact that a lamp of a UVI installation is placed in a quartz casing required for the provision of a specific temperature mode of amalgam operation and prevention of contact of electric circuits of a lamp with water. The gap between the lamp and the casing or, in case of the so-called pellet technology the amalgam location point, fully determines the operational mode of the whole lamp [5]. Hence, the lamps with other dimensions or other electric power will operate in another temperature mode the UVR flux depends on. One more parameter influencing operation of lamps is water temperature that may vary within the range between 1 and 40 °C. In this case, a lamp should contain a special amalgam maintaining a constant pressure of mercury vapours with a lamp wall temperature changing by approximately 30 to 40 °C. Manufacturers shall not specify this technical characteristic, that is why decreasing of UVR flux of a lamp in an installation is possible in case of replacing of specially selected or specially manufactured lamps with other ones with the same UVR flux specified in a datasheet but a smaller operating range of wall temperature change.

Another "classic" case of incorrect selection of lamps is ignorance or ignoring of parameters of electronic starter device a lamp will operate with. For instance, the power sources of high-output amalgam UV lamps significantly differ from the same for small bactericidal mercury lamps with power from 5 to 50 W. To perform a reliable start of a lamp with a power from 300 to 1000 W and to provide a sufficient number of switch-on, it is necessary to use special electronic starter devices, which sometimes have complex two-inverter designs. Manufacturers of high-output amalgam UV lamps know it well that 20 to 30 switch-on are enough for a complete failure of a lamp due to fast wearing of emission coating of an electrode unit in case of incorrect electronic starter device using. In this case, damaging the electronic starter device itself is possible too if its emergency protection does not operate timely. Understanding this problem, responsible manufacturers of lamps specify the type and manufacturer of electronic starter device they recommend to use specific lamps with. Other manufacturers of amalgam lamps do not specify such important parameter as the number of switch-on/off of a lamp since they cannot know which type of electronic starter device their product will be used with and in which operating conditions it will be used.

In flow-through air sterilising systems, a lamp usually operates without a quartz protective casing and operating temperature of its body will be less than during laboratory tests in the still air environment, especially in cold airflows of air-conditioning systems. Some manufacturers specify that a lamp may efficiently operate in the airflow but the UVR flux value may become significantly lower than the one specified in a datasheet after replacement with a lamp by another manufacturer.

We would like to underline it once more: UV lamp is a part of a UVI system just like an electronic

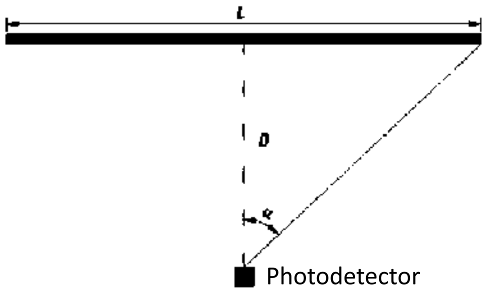

Fig. 1 Keitz method measurement scheme

Fig. 2. Labels of the *Jelosil* and *JUV* lamp samples

starter device and its other parts. The above-mentioned leaders of the markets of UVI equipment and UV lamps pay great attention to collaborative cooperation in the course of the design of their products. For instance, for the purpose of cooperative promotion of products in the Western European markets, *LIT UV Elektro GmbH* (Germany) and *Lighttech Kft* (Hungary) have developed a product range of water UVI equipment and the relevant range of UV lamps for it. Of course, the selection and replacement of a lamp or an electronic starter device in UVI installations by a customer is a common and normal practice in conditions of a competitive market. However, we think that such selection and replacement of accessories should be performed taking distinctions of specific equipment into account and on the basis of recommendations of specialists.

3. METHODOLOGY OF MEASUREMENT OF LOW-PRESSURE UV TUBE LAMPS AND TESTING INSTALLATION

Low-pressure quartz mercury lamps, low-pressure mercury lamps made of uviol glass (the so-called *soft glass lamps*) and low-pressure amalgam lamps with bactericidal UVR may be considered as sources of monochromatic radiation at λ = 254 nm. Generation of UVR at 254 nm line in low-pressure mercury plasma is well-known studied experimentally [1, 3, 59]. For the Lambert surface source like a low-pressure mercury or amalgam tube lamp (in respect of the said UVR), Keitz-method measurement scheme [10, 11] (Fig. 1) is the simplest and the most correct one for measurement of UVR flux with specific assumptions.

In accordance with it, the lamp is installed in a room without UVR-reflecting surfaces (“dark room”). The photo detector is located opposite to the centre of the lamp (Fig. 1). To obtain the value of UVR flux (Φ_e) of the lamp with the length of irradiating part L, it is necessary to measure the value of irradiance (E_e) on the entry window of the photo detector located at distance D from the axis of the lamp:

$$\Phi_e = \left(2\pi^2 DLE_e\right)/\left(2\alpha + \sin 2\alpha\right),$$

where α is the one-half angular size of the radiating part of the lamp in relation to the centre of the entry window of the photo detector sensor (Fig. 1).

For the study, two dark rooms with dimensions (7×3×3) m and (6×3.5×3) m (L×W×H) were used. Measurements of E_e were conducted by means of *SED240* sensor of *IL1700* radiometer (*International Light Technologies*) with a special cosine cap. It should be emphasized that *IL1700* with *SED240* or its analogues (*GigaHerz optik*, *Dr. Groebel*, etc.) are generally accepted for measurement of irradiance from low-pressure lamps. The error of *SED240* itself does not exceed 6.5 %.

A universal *EVG2001000W/3,510APHplus R3* electronic starter device, which allows setting the required current and duration of pre-heating and lamp current, was used for the lamps (with lamp power and maximum current of 1 kW and 10 A respectively). For monitoring of parameters, *YOKOGAWA PZ400* and *ZES LMG640* power digital analysers were used. After switching the lamp on, the maximum value of E_e (if any) is registered as well as the so-called “shelf” steady-condition mode. Then Φ_e is calculated using the acquired data.

For some samples of lamps, lifetime tests in conditions of operation in water sterilising installations were performed. For this purpose, the lamps in quartz casing were installed in UDV300/900TESTMST test-stand (manufactured by LIT) with recycling water, the temperature of which was artificially maintained by means of the *FT31180*

Table 1. Parameters of the *Jelosil* and *JUV*-labelled Lamps

Sample	U**, V	I, A	P**, W	Φ_e**, W	cap t, °C	Φ_v, W, after 12,000 hours
JUV	153.1	1.81	272	110.0	138	
Jelosil	121.6	1.81	218	57.5	73	
TU*	***	1.85 ± 0.05	235 ± 10	87 ±3	70	at least 74

* We consider it correct to compare the presented samples with the original LIT lamps since the *Jelosil* and *JUV* lamps were applied with the equipment manufactured by NPO LIT. The original LIT lamps are manufactured in accordance with TU3467003581832292002. The technical and operational characteristics of the lamps of other manufacturers also should comply with the standards of this TU for correct operation in NPO LIT sterilising installations.
** Maximum values were measured.
*** Not standardised.

thermostat. Electric parameters, UVR flux, and exterior of the lamps were inspected at the beginning of testing, then in 100 hours of continuous operation and then each regular time interval (usually each 1000 hours). Using the obtained data, it was possible to identify decreasing of UVR flux and changing of exterior of the lamps.

4. LAMP TESTING RESULTS

4.1. DB300 Lamps with *Jelosil* and *JUV* Labels

Two samples of DB300 lamps were tested: the one with the *Jelosil* (*JL19235*) label and the second one with *JUV* (DB300) label (Fig. 2). At the moment of testing, the latter was new and the *JL19235* lamp had been in operation for approximately 3000 hours. Since the electrodes of these lamps are significantly "deepened" in the cap, additional measurements of temperature in the middle point of cap length (by means of *ATT2000* thermometer with the *K*-type thermo-couple) were taken after 15 minutes of continuous operation of the lamps. The results of the measurements are listed in Table 1.

Despite the fact that the samples of products were generally functional (as a separate source of UVR), there are the following comments based on the results of visual examination and measurement of their characteristics.

JUV-labelled DB300 lamp:

The power consumption of the *JUV* lamp significantly exceeds the allowable value, which may lead to a shutdown of the electronic starter device supplying the lamp (activation of emergency protection after exceeding the threshold voltage by the lamp) and even to its breakdown.

The technical specification of LIT-manufactured water sterilising installations (TU4859021302158382014) specifies that the lamp cap temperature should not exceed 70 °C. The cap temperature of this sample was out-of-tolerance (140 °C), as a result, melting and destruction of elements sealing and fixing the lamp in the quartz casing is highly likely, which will lead to fouling of the lamp and the casing and breakdown of the sterilising installation.

Therefore, operation of such lamps in LIT water sterilising installations is not admissible and even dangerous since it may lead to overheating and breakdown of electronic starter device, destruction of sealing elements and even inflammation of equipment. The lifetime tests of this sample were not conducted due to the above-mentioned safety precautions.

Jelosil-labelled lamp (JL19235):

According to NPO LIT, for efficient operation in a water sterilising installation, the value of the UVR flux of the DB300-type lamp at λ = 254 nm shall be at least 74 W by the end of the lifetime, but it was already equal to 58 W after 3000 hours of continuous operation, which is unacceptably low. (Using lamps with low UVR flux provides an insufficient degree of water sterilisation.)

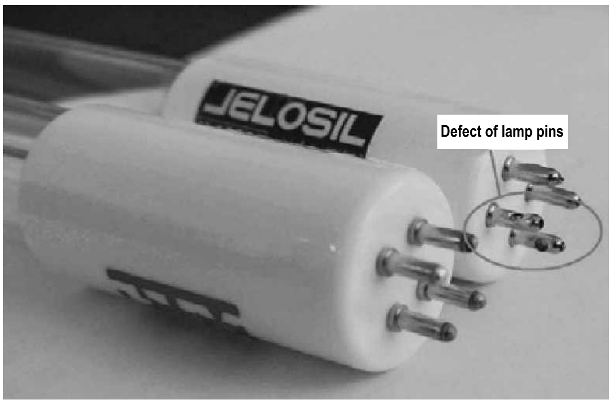

Fig. 3. Crimping of the *Jelosil*-labelled (*JL19235*) lamp sample

Table 2. The Parameters of the *ELTOS*-labelled DB350V Lamp Samples

Sample	*I*, A	Shelf			Maximum		
		U, V	*P*, W	Φ_e, W	*U*, V	*P*, W	Φ_e, W
1	3.2	100.7	322.4	129.6	109.2	349.4	132.7
2	3.2	101.9	326.0	134.5	111.5	357.3	134.1
TU	3.2 ± 0.1	*	*	*	*	325 ± 10	125 ± 5

* Not standardised.

Moreover, the method of connection of a wire with the lamp cap contacts by means of a crimp (Fig. 3) gives rise to doubts. Such connection method is rather well applied for mercury lamps with current from 0.4 to 0.8 A but is not applied for high-output amalgam lamps since, with such type of connection, it is complicated to provide sufficient reliability and mechanical strength of connection, which may lead to lack of electric contact in the lamp pins (and switching-off the lamp) and their breakdown in connection plugs of a sterilising installation. Careless application of cap cement may be also called a disadvantage (Fig. 3).

As a result of testing of the lamp in the UDV300900TESTMST water sterilising installation with a quartz casing (with an inner diameter of 25 mm), it was discovered that drips of melted amalgam had been generated on the inner surface of the tube, which is non-acceptable. Especially if the lamp is positioned vertically, the melted amalgam may reach the hot electrode area, which causes a release of a large number of mercury vapours in the discharge with the subsequent critical decreasing of the UVR flux at λ = 254 nm. The lifetime tests of this sample were not conducted since its flux value was already lower than the low threshold value according to TU3467003581832292002.

Conclusion of clause 4.1

The presented samples of lamps are presumably manufactured in one of the Asian countries. The *JUV*-labelled sample is manufactured more qualitatively than the *Jelosil*-labelled sample in general, but these lamps (both types) may not be applied in LIT installations and similar ones due to non-compliant parameters and non-qualitative design of the cap and contact pins.

4.2. DB350V Lamp with the ELTOS Label

Inspection of the two new samples of DB350V lamps with ELTOS label showed that they are manufactured with rather high quality and have the original constriction of the tube near the electrode. Their measured characteristics are shown in Table 2.

The samples have a high radiant efficiency at λ = 254 nm (37.54 %) and shelf-mode characteristics close to those specified in TU34670035818 32292002, but the maximum power consumption of the lamps was approximately 8 % higher. After 500 hours of the lifetime testing, it was discovered that the isolation of the wires was actively destructing, due to which the inner surface of both quartz casings was covered with a non-washable film. It is obvious that the manufacturer used some other type of wires instead of *PTFE*-isolated ones. Further testing was continued without the quartz casing on an air test stand in order to determine the decreasing of UVR in laboratory conditions. One of the samples stopped working in 200 hours due to breakdown of the electrode, and the other one stopped working after cumulative time of 4000 hours and spending of the emission layer of the electrodes. Fig. 4 shows the exterior of the samples after 2000 hours of operation. It can be seen that the isolation of their wires was destructed by UVR, which made operation of these products dangerous. Decreasing of UVR flux of both samples of the lamp was about 22 % after 2000 hours of operation.

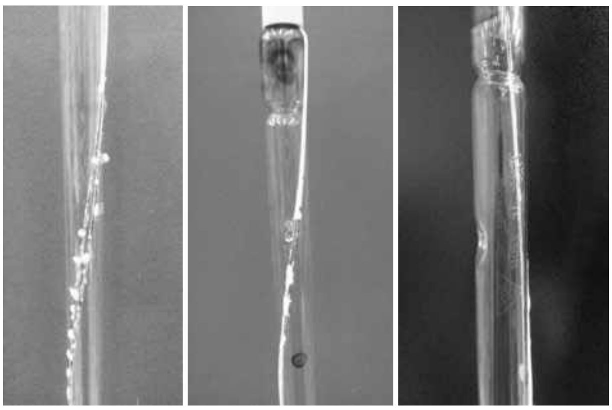

Fig. 4. The exterior of the ELTOS-labelled DB350V lamp sample after 2000 hours of operation

Table 3. The Parameters of the *Lightbest*-labelled Samples of the GPH436T5L/4 Lamp

Sample	*I*, A	Maximum		
		U, V	*P*, W	Φ_e, W
1	0.43	47.0	20.2	8.8
2	0.43	46.8	19.9	8.8
According to the *Lighttech* datasheet	0.425	*	21	7.3

* Not standardised.

Conclusion of clause 4.2

The characteristics of the new ELTOS-labelled lamps are close to those specified in TU34670035818322922002, their radiant efficiency at λ = 254 nm is high, and the exterior is rather good. Nevertheless, decreasing of the UVR flux of both samples was equal to 22 % after 2000 hours of lifetime with the maximum allowable decreasing of UVR of 20 % for lamps of this type after 12,000 hours of operation. The error-free running time was much lower than the required value of lifetime. Such lamps cannot be used in UVI installations for water sterilisation due to low lifetime, unacceptably fast decreasing of the UVR flux, danger of fouling of casings with the melted isolation and danger of short-circuit of wires after destruction of the isolation.

4.3. The Lamp with the *LightBest* Label

The authors of the article were requested to test two new samples of the *GPH436T5L/4* mercury lamp with the *LightBest* label (Figs. 5 and 6). For comparison, the specification of the original *GPH436T5L/4* lamp by *Lighttech* was used. The tested lamps are manufactured with the lacking quality, the caps are fixed unevenly, the electrodes are crimped tightly, but the dimensions are compliant with those of the original lamp. The measured parameters of both samples with the *EF23701 FL Golden Way* electronic starter device, which provides the lamp current from 0.40 to 0.45 A, and power of up to 70 W, are listed in Table 3. The UVR flux value of the tested samples of the lamp at λ = 254 nm is a little higher than the nominal value for the similar lamp by *Lighttech*. The decreasing charts of the said UVR flux of the samples during the lifetime on the UDV121NBSC water sterilising installation are shown in Fig. 7.

Fig. 5. The exterior of the *Lightbest* label of the *GPH436T5L/4* lamp sample

Fig. 6. The exterior of the electrode and the cap

Conclusion of clause 4.3

The initial value of the UVR flux of the *GPH436T5L/4* lamp at λ = 254 nm was a little higher than the nominal value of the original lamp manufactured by *Lighttech*, but the time decreasing of their UVR flux was too high. The normal decreasing for the original lamp of this type is (15–20) % after a standard lifetime of 8000 hours. As it can be seen in Fig. 7, the tested lamps reached

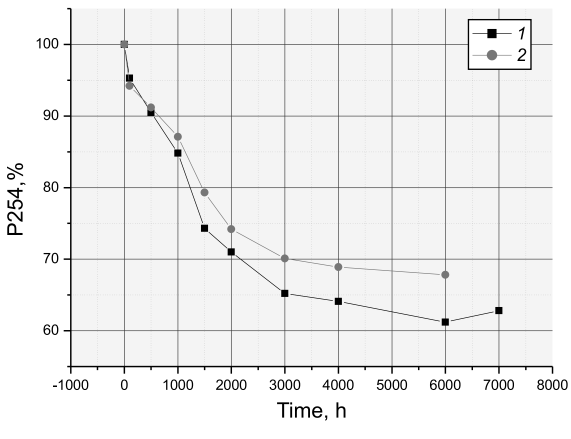

Fig. 7. The UV radiation flux decreasing curves of both samples of the *GPH436T5L/4* lamp with the *Lightbest* label

Table 4. The Parameters of the *UV Product*-labelled Samples of DB300 and DB800V Lamps

Type	*I*, A	Shelf			Maximum		
		U, V	*P*, W	Φ_e, W	*U*, V	*P*, W	Φ_e, W
DB300	1.80	143.9	259.6	98.6	151.8	272.3	102.9
TU	1.85 ± 0.05	*	*	*	*	235±10	87±3
DB800V	4.91	170.1	835.2	242.4	172.5	847.3	251.1
TU	5.0 ± 0.1	*	*	*	*	710 ± 15	240 ± 10

* Not standardised.

15 % in the water sterilising installation already after 1000 hours of operation, (25–30) % after 2000 hours, and (30–35) % after 3000 hours of operation. The lifetime testing of these lamps was stopped after 8000 hours of operation. Such increment of decreasing means that the installation with the tested lamps will not provide the required degree of sterilisation in 1000 hours of operation.

4.4. DB300 and DB800V Lamps with the *UV Product* Label

The exterior of the two tested lamps DB300 and DB800V is good, the dimensions comply with TU3467003581832292002, the electrodes have a sufficient weight increment (assessed visually), the amalgam is fixed correctly, and there is a laser label on the quartz glass (Fig. 8). The results of measurements of both lamps are listed in Table 4, the results of lifetime tests are shown in Fig. 9.

The UVR flux and the electric parameters of both lamps do not comply with TU3467003581832292002. Both *UV Product*-labelled lamps have a higher value of the UVR flux than that specified in TU but, unfortunately, a higher value of power too. It is worth noting that an increasing of the UV dose is not mandatory in case of the replacement of lamps in the existing equipment: UVI installations are designed with the technological reserve of the UVR bactericidal dose; however, the increased power consumption of lamps may lead to their additional heating in an installation as compared to the designed one, and the increased power consumption means additional financial costs. For instance, the tested DB800V amalgam lamp with the *UV Product* label consumes approximately 130 W more than the original lamp. With the price of electricity of 4 roubles per kWh, additional financial costs for a year of continuous operation of 100 such lamps (in WDI 100 type installations) will be equal to 455 thousand roubles.

The electronic starter devices in sterilising installations with such lamps are designed for a power load not exceeding 800 W. Its exceeding may lead to overheating and, therefore, to reduction of lifetime of the electronic starter device and even to the activation of protection and shutdown of this device.

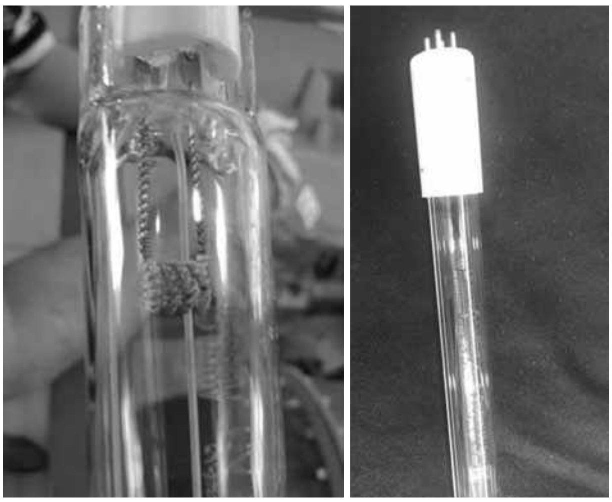

Fig. 8. *UV Product*-labelled samples of the *DB800V* and *DB300* lamps

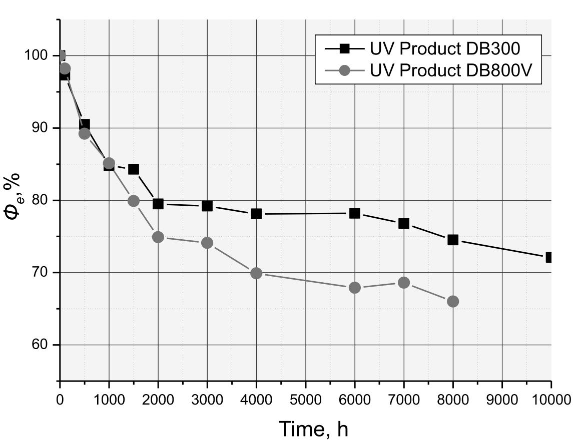

Fig. 9. Lifetime dependence of the UV radiation flux of *DB800V* and *DB300* lamp samples with the *UV Product* label

Table 5. The Parameters of the Samples of the *SeaN*-labelled DB350 Lamp

Sample	*I*, A	Shelf			Maximum		
		U, V	*P*, W	Φ_e, W	*U*, V	*P*, W	Φ_e, W
1	3.13	97.7	304.1	118.6	97.7	304.1	118.6
2		98.6	307.0	120.5	98.6	307.0	120.5
TU	3.2 ± 0.1	*	*	*	*	325 ± 10	125 ± 5

* Not standardised.

Conclusion of clause 4.4

The *UV Product*-labelled lamps have rather high quality of structure, the value of their UVR flux is higher than that of the original lamps by LIT (according to TU3467003581832292002), but their application in the installations manufactured by LIT will lead to an increase of power consumption by (15–18) % of the specified values. The lifetime tests show that the UVR decreasing of such sources reaches from 25 to 35 % after 8000 hours of operation, which is significantly higher that the recommended value of (15–20) %. Therefore, despite the higher UVR flux in the beginning of the lifetime, it may be significantly lower than the parameters specified in TU3467003581832292002 in the end of the lifetime. Higher power will cause overheating of the electronic starter device and its possible shutdown.

4.5. The Lamp with the *SeaN* Label (NTC SeaN)

Two samples of the DB350 lamp with the *SeaN* label (NTC SeaN) (Fig. 10), which were sent by a customer operating the potable water sterilising equipment manufactured by LIT, were tested. The samples have rather high quality of structure and their dimensions comply with TU3467003581832292002, but connection of the pins with the lamp wire by means of stamping, like in the case of the *Jelosil*-labelled lamps, is not acceptable for amalgam lamps of such power due to the low reliability. The measured characteristics of these samples are listed in Table 5.

It was discovered that the *SeaN* samples are underheated at an air temperature of 25 °C, therefore, their characteristics were lower than the maximum possible ones witnessing that the manufacturer selected the amalgam incorrectly. For checking of capability to apply such type of lamps in water sterilising installations, these samples were installed in the LIT-manufactured UDV300900TESTMST installation, and the values of the UVR flux with water temperature changing over a wide range were measured (Fig. 11). Fig. 11 shows that the maximum (optimal) value of the UVR flux is reached only after the water temperature reaches approximately 30 °C. Therefore, the *SeaN* lamp may be efficiently operated in LIT installations with a rather high water temperature of at least 30 °C. Probably, the tested samples of the lamp are designed for operation in another type of UVI equipment (e.g. with another diameter of the quartz casing), we would also like to note that the value of electric power of the lamp *P* significantly increases and in such conditions it becomes higher than the one specified in TU3467003581832292002. When using these

Fig. 10. The sample of the *SeaN*-labelled DB350 lamp

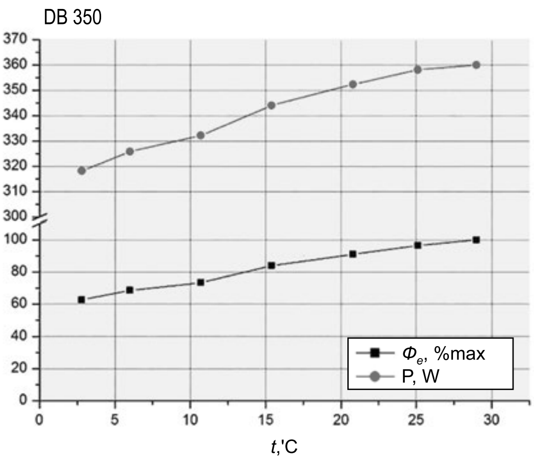

Fig. 11. Water temperature dependence of the UV radiation flux of the DB350 lamp sample

lamps for sterilisation of potable water at indicative values of temperature of 1 to 10 °C, the value of UVR flux of the lamps significantly decreases by 40 % of the maximum one. The lifetime test of these samples of the lamps in a water sterilising installation was not conducted since interpretation of the results of such tests would have been complicated by complexity of correct comparison of the obtained results.

Conclusion of clause 4.5

The *SeaN*-labelled lamp was probably designed for another manufacturer of UVI equipment and was probably supplied from one of the Asian countries. It cannot operate efficiently at water temperatures less than (10–15) °C significantly decreasing its UVR flux value.

5. CONCLUSION

The quality of the tested samples of low-pressure bactericidal lamps introduced in the Russian market under *Jelosil*, *JUV*, ELTOS, *LightBest*, *UV Product*", and *SeaN* (NTC SeaN) labels is low. Some manufacturers use stamping or crimping for connection the lamp wire with the cap pins. Such method of connection is used for mercury bactericidal lamps and FLs with the discharge current from 0.4 to 0.8 A, but does not fit for high-output amalgam lamps due to its low reliability. Instead of the *PTFE*-isolated wire, other type of wires had been used for the ELTOS-labelled DB350V lamps, which led to destruction of the isolation. Operating such samples is dangerous: the electronic starter devices and casings may breakdown and even inflammation of equipment may be caused. The value of the UVR flux at $\lambda = 254$ nm of all new tested samples of lamps complied with the declared nominal values, but its decreasing appeared to be too high and could reach (25–30) % after 2000 hours of operation, which is significantly higher than the recommended value of (15–20) % after 8000 hours of operation. Such decreasing means that the installation will not provide the required degree of sterilisation after 2000 hours of operation. The power consumption of all tested samples of lamps was higher than the one specified in the TU for the original similar lamps, which witnesses their lower value of the radiant efficiency at $\lambda = 254$ nm. Too high power of a lamp leads to its overheating and, therefore, to the decrease of the electronic starter device lifetime. Overconsumption causes additional financial costs compensating economy from purchasing cheaper lamps by an unknown manufacturer. The presented lamps were designed and manufactured based on design specifications of specific manufacturers or are copies of UV lamps by well-known brands, but manufactured using own technology. At the same time, the quality of their protective layer (apparently very low) accelerates the temporary decline of UVR; and the features of ultraviolet irradiation equipment for water disinfection were not taken into account. This may lead to numerous problems in the course of operation of the UVI equipment and negatively affect the reputation of the UVR sterilisation method. In the conditions of the competitive market, the consumers have the right to select and to replace the lamps or electronic starter devices in UVI installations by themselves. However, these actions should be taken only with the consideration of operation distinctions of a specific type of equipment and based on the recommendations of specialists.

REFERENCES

1. Karmazinov F.V., Kostyuchenko S.V., Kudryavtsev N.N., Khramenkov S.V. Ultrafioletovye tekhnologii v sovremennom mire: Kollektivnaia monografiia [Ultra-violet technologies in the modern world: Collective monography] // Intellect Publishing House, Dolgoprudny, 2012, 392 p.

2. Vasilyev A.I., Kostyuchenko S.V., Kudryavtsev N.N., Sobur N.N., Sokolov D.V. Tekhnologii UF obezzarazhivaniia dlia obrabotki vody, vozdukha i poverkhnosti [UV sterilisation technologies for treatment of water, air and surface] // Svetotekhnika, 2017, No. 5, pp. 6–11 // Light & Engineering, 2018, Vol.26, #1, pp. 25-31.

3. Veselnitski I.M., Rokhlin G.N. Rtutnye lampy vysokogo davleniia [High-pressure mercury lamps] // Energiya, Moscow, 1971, 328 p.

4. Parson S. Advanced Oxidation Processes for Water and Wastewater Treatment // IWA Publishing, 2004, ISBN: 1843390175.

5. Pirovich A.L. Germicidal low pressure mercury vapor discharge lamp with amalgam location permitting high output // Patent US2004/0195954, 07.10.2004.

6. Rokhlin G.N. Razryadnye istochniki sveta [Discharge light sources] // Energoatomizdat, Moscow, 1991, pp. 60–80.

7. Levchenko V.A., Vasilyev A.I., Vasilyak L.M., Kostyuchenko S.V., Kudryavtsev N.N. Uvelichenie fizicheskogo sroka sluzhby moshchnykh gazorazriadnykh lamp

nizkogo davleniia [Increasing of service life of high-output low-pressure discharge lamps] // Prikladnaia fizika, 2015, No. 5, pp. 90–94.

8. Levchenko V.A., Vasilyak L.M., Kostyuchenko S.V., Kudryavtsev N.N., Svitnev S.A., Sharanov E.P. VUF izluchenie rtutnogo razriada pri davlenii bufernogo gaza menee 1 Torr [UV radiation of mercury discharge at buffer gas pressure of less than 1 torr] // Uspekhi prikladnoi fiziki, 2016, No. 3, pp. 256–264.

9. Svitnev S.A., Popov O.A. Raschet funktsii raspredeleniia elektronov po energiiam v statsionarnom razriade nizkogo davleniia [Calculation of electron energy distribution function of a low-pressure stationary discharge] // MEI Bulletin, 2012, No. 3, pp. 100–105.

10. Keitz H.A.E. Light Calculation and Measurements // Macmillan and Co Ltd, London, 1971.

11. Vasilyak L.M., Drozdov L.A., Kostyuchenko S.V., Kudryavtsev N.N., Sobur D.A., Sokolov D.V., Shunkov Yu.E. Metodika izmereniia potoka UF izlucheniia trubchatykh bakteritsidnykh lamp ND [Methodology of measurement of UV radiation flux of low-pressure tube bactericidal lamps] // Svetotekhnika, 2011, No. 1, pp. 29–32 // Light & Engineering, 2011, Vol. 19. #1, pp. 81-86.

Michael E. Allash,
employee of Lighttech Kft

Leonid M. Vasilyak,
Dr. of Phys. and Math. Science, Professor.
Chief Researcher of the United Institute of High Temperatures (OIVT) of the Russian Academy of Science

Nikolay P. Eliseev,
Ph.D. in Tech. Science.
Associate Professor of the Lighting Engineering department of NRU MPEI

Oleg A. Popov,
Dr. of Tech. Science.
Professor of the Lighting Engineering department of NRU MPEI

Dmitry V. Sokolov,
Ph.D. in Tech. Science.
Head of the Lighting Engineering Department of NPO LIT

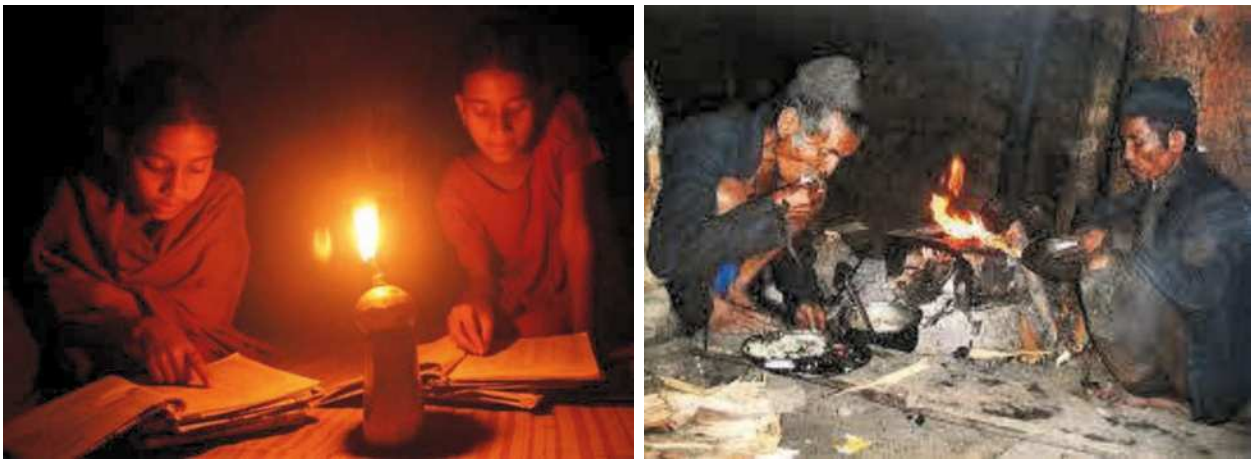

a) *b)*

Fig.1. People using fuel-based lighting for study, cooking and other activities [5,6]

Fig. 5. Lighting system used in heritage sites of Nepal

Fig.7. Evening photograph and luminance distribution over the facade, Staronikitskaya st. 1

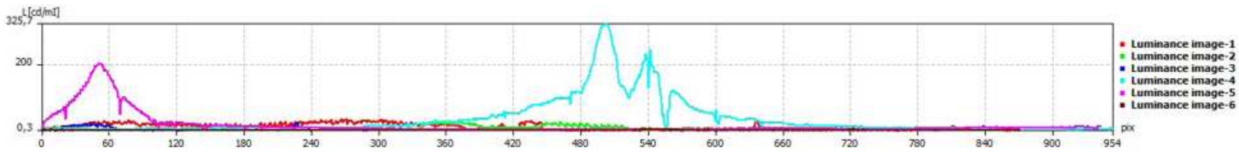

Fig.8. Relation between the values of luminance over the image, Staronikitskaya st. 1

Fig.9. Evening photograph and luminance distribution over the facade, Mendeleevskaya st.1

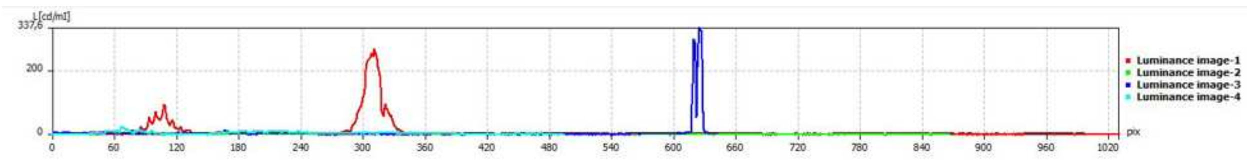

Fig.10. Relation between the values of luminance over the image, Mendeleevskaya st. 1

Fig. 2. Active LI of the assembly line

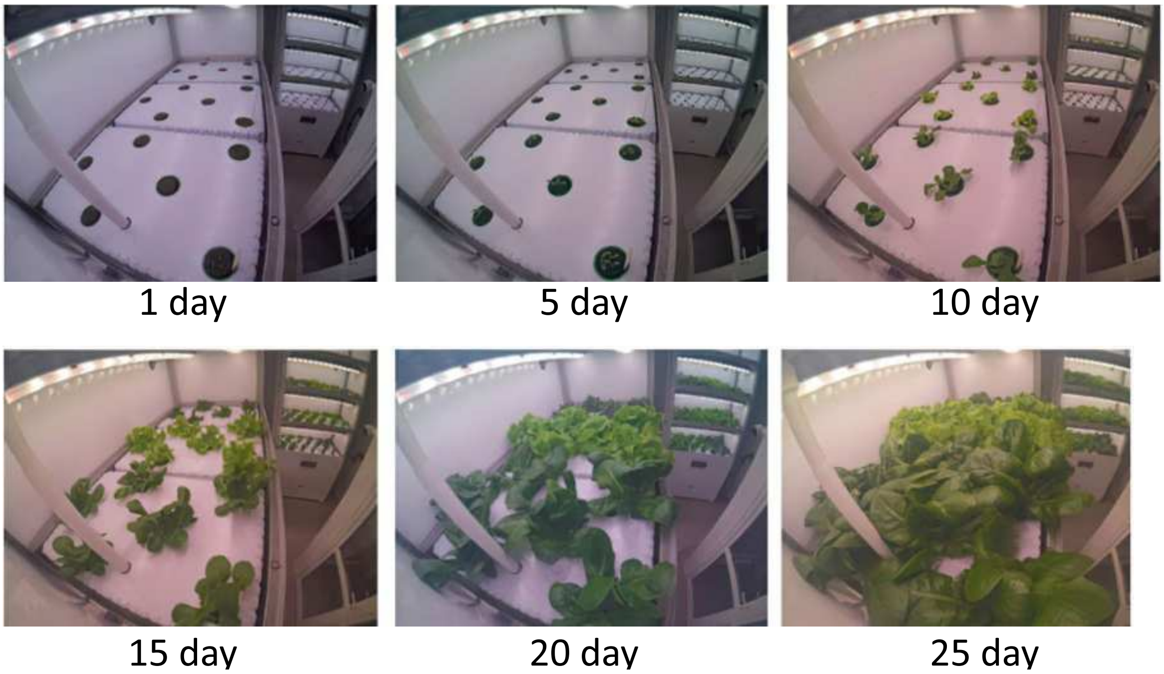

Fig.6. Vegetation stages of lettuce plants

Fig.7. Lettuce cultivation in the MPI in S.A. Vavilov VNISI

Light & Engineering
Vol. 27, No. 6, pp. 149–154, 2019
https://doi.org/10.33383/2018=058

IRRADIATING SET WITH UV DIODES AND MICROPROCESSOR SYSTEM OF AUTOMATIC DOSE CONTROL

Roman G. Bolshin[1], Nadezhga P. Kondratieva[2*], and Maria G. Krasnolutskaya[1]

[1] *NOU DPO UNIC Omega*
[2] *IzhGSKhA, Izhevsk*
* *E-mail: aep_isha@mail.ru*

ABSTRACT

The article describes the development and testing of an irradiating set with UV diodes for pre-sowing treatment of conifer seeds equipped with an original microprocessor system of automatic dose adjustment for maintenance of the required dose of UV irradiation.

Keywords: microprocessor system, automatic dose adjustment, UV irradiation of seeds, conifers, UV diodes, UV irradiation dose

1. INTRODUCTION

Human impact on the environment is not always positive and it has become necessary to develop and to take special measures for the preservation of the Earth biological resources including conifers. At the end of 1993, the Convention on Biological Diversity came into force. The main provisions of the Convention are reflected in the Russian programmes "Biological Diversity of Russian Forests" (1995) and "The Forests of Russia" (1997). For implementation of these programmes, the Forest Code was adopted in 2006 which states that only certified seeds should be used for forest regeneration [1–3].

Among all methods of activation of seed growth processes, we selected pre-sowing treatment since this method is based on natural mechanisms and therefore does not cause harm to human health and is relatively cheap. Besides, the analysis of literature has shown that treatment of seeds of agricultural plants with UV irradiation (UVI) produces positive results, consisting of increase of germinability and decrease of seeds consumption as well as even sprouts [4–7].

The most widely used sources of radiation for UVI are environmentally-dangerous low and high-pressure mercury lamps and capabilities of UVI using contemporary UV diodes (UVD), including using programming logical controllers, for maintenance of required dose of UVI has been insufficiently studied. This mainly relates to UVI of conifer seeds[1], especially Picea fennica.

It is known that the mechanism of UV radiation interaction with seeds provides significant acceleration of synthesis of functional substances by activating phenolic metabolism in plant cells [10]. Therefore, the studies of forest land capacity increase thanks to increasing of germinability of seeds by means of pre-sowing UVI of tree and bush seeds have large scientific and practical perspective. In the meantime, specific doses of UVI have regional nature to some extent since the changes occurring inside plant cells under UV radiation depend on the type of tissue, stage of development of biological entities, its genotype, breeding stock as well as duration of irradiation. Only low doses of UVI accelerate synthesis of ferments causing free-radical reactions [11].

[1] Conifers collect dust 30 times better than aspen and 12 times better than birch and extract 2 times more phytoncides than hardwoods. Therefore, it is more appropriate to use conifers for urban greening since they are evergreen, undemanding, more long-life than hardwoods and keep their decorative properties throughout the year [8–10].

Table 1. Technical Specifications of UV Diode

Technical parameters	Parameter value
Wavelength range, nm	395–400
Lens type	spherical
Body type	SMD3528
Radiant flux, mW	10
Diode voltage, V	3.0–3.4
Diode current, mA, less	15
Dimensions, mm	3.5 × 2.8 × 1.9

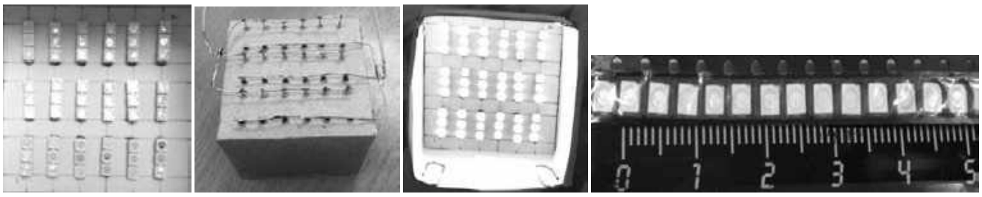

a) *b)* *c)* *d)*

Fig 1. Location (a), fixing and soldering (b), switched on state (c) and dimensions (d) of UV diodes of the irradiating set

The effect of UV radiation on seeds of Picea fennica is studied insufficiently. Therefore, development of environmentally-friendly (mercury-free) UV irradiating set based on UVD with microprocessor system of automatic control (MSAC) of UVI dose for pre-sowing treatment of seeds of this conifer is a relevant objective. Consequently, the goal of this work was the development of such irradiating set allowing to define the most efficient dose of UVI in terms of Picea seed germinability.

For this purpose, the following tasks were formulated: 1) to develop an UVD-based UV irradiating set with UVI dose MSAC; 2) to test this set to determine its efficiency for pre-sowing treatment of seeds of Picea fennica.

2. THE MAIN PART

In the studies by prof. D.A. Korepanov and his post-graduates regarding increase of germinability of the seeds of decorative crops, the *LH26-FS/BLB/E27* UV CFL manufactured by *Camelion* with broad radiation spectrum in the UV-*A* region (315–400 nm) was used [12–19]. For our experiments, we used *3528 UV SMD LED* UVD (radiation band of (395–400) nm) manufactured by *Hyelesiontek* (Table 1) and studied the impact of the right section of this region on germinability of the seeds of Picea fennica.

For this purpose, a relevant UV irradiating set for seed treatment was developed [19–21]. The dimensions of the UV irradiator of the set (Fig.1 and Fig.2) were (50×40×40) mm and its overall capacity was equal to about 1.6 W. For rather intensive and uniform irradiation, a module of 54 said low-output UVDs was used in it.

For measurement of irradiance on the working surface, the combined device TKA–PKM (Fig. 2) was used. With the suspension height of the irradiator of 2 cm (operating), it was equal to 1.6 W/m^2.

Then, provided that it is necessary to maintain the most efficient dose of UVI in the course of irradiation of seeds of different cultures, for instance, using programmable logical controllers, we have designed the UVI dose MSAC based on the *Arduino Uno* platform. The *ATmega328* microcontroller is installed on a board; its advantages are convenience of compiling a software algorithm and convenience of uploading the software in the microcontroller. The *Firmata* protocol is uploaded

Fig 2. UV irradiator and TKA–PKM

Table 2. Studied Doses of UV Irradiation

Exposure time	Dose of UV irradiation	Exposure time	Dose of UV irradiation
min	kJ/m²	min	kJ/m²
Seeds of **Picea fennica**, quality class 2		Seeds of **Pínus sylvéstris**, quality class 3	
18	11.9	18	11.9
22	14.5	25	16.5
26	17.2	30	19.8

Table 3. Experiment Results

Number of variant	Irradiation time, min	Germinability, %	Mould, %	Did not braird, %	Increase of germinability, %
	Seeds of **Picea fennica**, quality class 2				
Control	0	62	4	38	–
2	18	86	0	14	+24
3	22	74	6	20	+12
4	26	80	4	16	+18

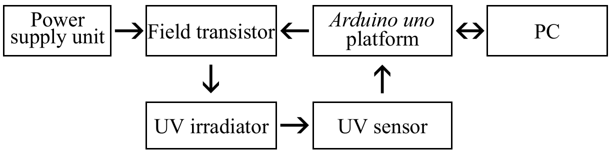

Fig 3. Structural diagram of the microprocessor system of automatic control (MSAC) of UV irradiation dose

to the latter for communication between the microcontroller and software installed on PC which (by means of *USB* interface) exchanges data with the *Arduino Uno* platform. All input data is stored in the program compiled on PC in the *Processing* programming environment. The PC (by means of *USB* interface) exchanges data with the *Arduino Uno* platform and controls the microcontroller [19–24].

For maintenance of the required dose of UVI, it is necessary to correct UVD operating time, by using an appropriate radiation sensor operating in the said spectral region, and by this sensor MSAC is tracking changes of irradiance (Fig. 3).

For signal amplification, field transistors are used (*STP16NF06*). Depending on the task transmitted by the microcontroller, the transistor controls the passing current thus activating the UV irradiator [25–27]. As a result, the seeds were irradiated by such compact UV set (Fig. 4).

3. RESULTS AND DISCUSSION

The tests of the energy-efficient compact and environment-friendly irradiating set with UV diodes were conducted in January 2017, in Udmurtia, using the seeds of Picea fennica and Pínus sylvéstris. The quantitative indicators of germination readiness and germinability of seeds were determined in accordance with GOST 13056.6–97 "Seeds of Trees and Bushes". The results are shown in Tables 2 and 3. The test has shown that UV radiation at wavelength of (395–400) nm positively affects the seeds of Picea fennica increasing its quality degree from the 2nd to the 1st, and the developed UV irradiat-

a) *b)* *c)*

Fig 4. UV irradiating set: a – the seeds are ready for irradiation; b – UV diodes are switched on, in a moment the tray will be placed into the set; c – the seeds are being irradiated ing set is energy-efficient and environment-friendly (mercury-free).

4. CONCLUSION

The energy-efficient environment-friendly UV irradiating set with UVI dose MSAC for pre-sowing treatment of seeds is developed.

The most efficient dose of UVI irradiation that increases the quality degree of seeds is found.

REFERENCES

1. Krasnolutskaya M.G., Kondratieva N.P., Romanov V. Yu., Chefranova M.N., Nureeva T.V., Korepanov D.A. Bolshin R.G. Prospects of Use of Electric Technologies for Increase of Sowing Qualities of Seeds with UV Irradiation [Krasnolutskaya M.G., Kondratieva N.P., Romanov V. Yu., Chefranova M.N., Nureeva T.V., Korepanov D.A. Bolshin R.G. Perspektivy ispolzovaniia elektrotekhnologii dlia povysheniia posevnykh kachestv semian UF-izlucheniem] // Bulletin of the International Academy of Agricultural Education, 2015, Vol. 1, # 24, pp. 10–13.

2. Kondratieva N.P., Dukhtanova N.V., Krasnolutskaya M.G., Litvinova V.M., Bolshin R.G. Compact LED Ultra-Violet Irradiating Set for Pre-Sowing Treatment of Seeds of Conifers [Kondratieva N.P., Dukhtanova N.V., Krasnolutskaya M.G., Litvinova V.M., Bolshin R.G. Kompaktnaia svetodiodnaia ultrafioletovaia obluchatelnaia ustanovka dlia predposevnoi obrabotki semian khvoinykh rastenii] // Bulletin of VIESKh, 2017. – Vol. 2 (27), pp. 62–69.

3. Krasnolutskaya M.G. Kondratieva N.P., Belov V.V., Bolshin R.G. Electric Technologies and Equipment for Optimal Content of Photosynthesis-Active Radiation for Plants of Protected Ground [Krasnolutskaya M.G. Kondratieva N.P., Belov V.V., Bolshin R.G. Elektrotekhnologii i elektrooborudovanie obespechivaiushchie optimalnyi sostav fotosinteticheski aktivnoi radiatsii dlia rastenii zashchishchennogo grunta] // Bulletin of the International Academy of Agricultural Education, 2015, Vol. 1, # 25, pp. 111–114.

4. Krasnolutskaya M.G., Kondratieva N.P., Bolshin R.G. Energy-Efficient LED Irradiating Sets [Krasnolutskaya M.G., Kondratieva N.P., Bolshin R.G. Energoeffektivnye energosberegaiushchie svetodiodnye obluchatelnye ustanovki] // Bulletin of VIESKh, 2016, Vol. 3 (24), pp. 48–53.

5. Krasnolutskaya M.G. Kondratieva N.P., Kolomiets A.P., Bolshin R.G. Increase of Efficiency of LED-Based Phytosets in Protected Ground [Krasnolutskaya M.G. Kondratieva N.P., Kolomiets A.P., Bolshin R.G. Povyshenie effektivnosti svetodiodnyi fitoustanovok (LED-fitoustanovok) v zashchishchennom grunte] // Bulletin of Izhevsk State Agricultural Academy, 2016, Vol. 4 (49), pp. 59–69.

6. Sterkhova T.N., Kondratieva N.P., Kornaukhov P.D., Kondratieva M.G. Grain Separator with UV Irradiator [Sterkhova T.N., Kondratieva N.P., Kornaukhov P.D., Kondratieva M.G. Trier s UF izluchatelem] // Patent # 2589781 Russia. 2016. Bul. 10.

7. Vasenev E.A., Romanov V. Yu., Korepanov D.A., Kondratieva M.G., Nigmatullin S.I. Lifting Mechanism of the Radiation Source of the Seed Pre-Sowing Treatment Device [Vasenev E.A., Romanov V. Yu., Korepanov D.A., Kondratieva M.G., Nigmatullin S.I. Mekhanizm podieema (opuskaniia) istochnika izlucheniia ustroistva dlia predposevnoi obrabotki semian] // Patent for Utility Model # 150044 Russia. 2015. Bul. 3.

8. Kondratieva N.P., Korepanov D.A., Krasnolutskaya M.G., Bolshin R.G. Pre-Sowing Treatment of Seeds of Decorative Conifers with Ultraviolet Radiation [Kondratieva N.P., Korepanov D.A., Krasnolutskaya M.G., Bolshin R.G. Predposevnaia obrabotka semian dekorativnykh rastenii khvoinykh porod ultrafioletovym izlucheniem]// Innovations in Agriculture [Innovatsii v selskom khoziaistve], 2017, Vol. 2 (23), pp. 45–54.

9. Kondratieva N.P., Krasnolutskaya M.G., Zembekov Yu.S., Bolshin R.G. [LED UV Set for Seed Irradiation [Kondratieva N.P., Krasnolutskaya M.G., Zembekov Yu.S., Bolshin R.G Svetodiodnaia UF ustanovka dlia oblucheniia semian] // Issues of Modernisation of Production and Processing Technologies in Agriculture [Aktualnye voprosy sovershenstvovaniia tekhnologii proizvodstva i pererabotki produktsii selskogo khoziaistva], 2017, Vol. 19, pp. 269–272.

10. Dubrov A.P. Effect of Ultraviolet Radiation on Plants [Dubrov A.P. Deistvie ultrafioletovoi radiatsii na rasteniia.] – Moscow: Academy of Sciences of USSR, 1963, 124 p.

11. Rogozhin V.V. Physiological and Biochemical Mechanisms of Formation of Hypobiotic Conditions of Higher Plants [11. Rogozhin V.V. Fiziologo-biokhimicheskie mekhanizmy formirovaniia gipobioticheskikh sostoianii vysshikh rastenii / Avtoref. dis. … d-ra biol. nauk]/ / Author's abstract of Doctor of Biological Sciences thesis. – Irkutsk, 2000, P. 59

12. Korepanov D.A., Romanov V. Yu., Loshchenov P. Yu., Bogatyryov M.D. Effect of Long-Wave UV Irradiation on Increasing of PINUS SILVESTRIS L Seeds Sowing Qualities [Korepanov D.A., Romanov V. Yu.,

Loshchenov P. Yu., Bogatyryov M.D. Vliianie dlinnovolnovogo UF oblucheniia na prevyshenie posevnykh kachestv semian PINUS SILVESTRIS L] // Forest Engineering Journal [Lesotekhnicheskii zhurnal], 2014. –Vol. 4, # 1(13), pp. 27–30.

13. Korepanov D.A., Romanov V. Yu., Vasenev E.A., Nigmatullin S.I. The Set for Increase of Seeds Sowing Qualities by Long-Length UV Irradiation [Korepanov D.A., Romanov V. Yu., Vasenev E.A., Nigmatullin S.I. Ustanovka dlia povysheniia posevnykh kachestv semian dlinnovolnovym UF oblucheniem // Bulletin of the Povolzhsky State Technological University. Series: Forest. Ecology. Environmental Management, 2014, Vol. 1 (21), pp. 62–68.

14. Pigalin D.I., Korepanov D.A., Goncharov E.A. Enhancement of Morphophysiological Indicators of Thúja Occidentális under UV Irradiation [Pigalin D.I., Korepanov D.A., Goncharov E.A. Uluchshenie morfofiziologicheskikh pokazatelei tui zapadnoi pod vliianiem UF oblucheniia] // The International Youth Scientific Natural and Technical Sciences Conference Young Creativity for Scientific Progress: Materials and Reports: in 3 parts, Povolzhsky State Technological Univerisity (Yoshkar-Ola), 2013.

15. Korepanov D.A., Chirkova N.M., Byvaltsev A.V., Ukraintsev V.S.] Increase of Germinability of the Seeds of Decorative Crops by UV Irradiation [Korepanov D.A., Chirkova N.M., Byvaltsev A.V., Ukraintsev V.S. Povyshenie gruntovoi vskhozhesti semian dekorativnykh rastenii UF-oblucheniem // Bulletin of the Izhevsk State Agricultural Academy, 2012, Vol. 3 (32), pp. 76–78.

16. Kondratieva N.P., Korepanov D.A., Byvaltsev A.V., Perevozchikov E.A. Ultraviolet Irradiation of the Seeds of Decorative Thúja Occidentális and Pīcea Pūngens [Kondratieva N.P., Korepanov D.A., Byvaltsev A.V., Perevozchikov E.A. Ultrafioletovoe obluchenie semian dekorativnykh rastenii tui zapadnoi i eli koliuchei] // Bulletin of the International Academy of Agricultural Education, 2011, Vol. 12. pp. 13–15.

17. Ukraintsev V.S., Korepanov D.A., Kondratieva N.P., Byvaltsev A.V. Effect of UV Irradiation on Increase of Sowing Qualities of Seeds of Conifers [Ukraintsev V.S., Korepanov D.A., Kondratieva N.P., Byvaltsev A.V. Vliianie UF oblucheniia na povyshenie posevnykh kachestv semian khvoinykh porod] // Bulletin of the Udmurtia University. Series: Biology. Earth Sciences, 2011, Vol. 1, pp. 132–137.

18. Korepanov D.A., Byvaltsev A.V., Ukraintsev V.S., Karavaev E.S. Increase of Sowing Qualities of Seeds of Conifers by Ultraviolet Irradiation [Korepanov D.A., Byvaltsev A.V., Ukraintsev V.S., Karavaev E.S. Povysheniem posevnykh kachestv semian khvoinykh porod ultrafioletovym oblucheniem] // Bulletin of the Izhevsk State Agricultural Academy, 2010, Vol. 4 (25), pp. 34–38.

19. Kondratieva N.P., Bolshin R.G., Krasnolutskaya M.G., Zembegov Yu.S. Energy-Efficient Set for UV Irradiation of Seeds before Sowing [Kondratieva N.P., Bolshin R.G., Krasnolutskaya M.G., Zembegov Yu.S. Energosberegaiushchaia ustanovka dlia UF oblucheniia semian pered posevom] / Materials of the XIII All-Russian Scientific and Technical Conference with International Participation "Problems and Prospectives of Development of Russian Light Engineering, Electric Engineering and Energy" as Part of the IV All-Russian Light Engineering Forum with International Participation // Resp. Editor O.E. Zheleznikova. – N.P. Ogaryov National State Research University of Mordovia, 2017, pp. 40–45.

20. Kondratieva N.P., Krasnolutskaya M.G., Zembekov Yu.S., Bolshin R.G. LED UV Set for Seed Irradiation [Kondratieva N.P., Krasnolutskaya M.G., Zembekov Yu.S., Bolshin R.G. Svetodiodnaia UF ustanovka dlia oblucheniia semian] // Issues of Modernisation of Production and Processing Technologies in Agriculture [Aktualnye voprosy sovershenstvovaniia tekhnologii proizvodstva i pererabotki produktsii selskogo khoziaistva]: Mosolov Readings: materials of the international scientific and practical conference, Mari State University (Yoshkar-Ola), 2017, pp. 269–271.

21. Kondratieva N.P., Bolshin R.G., Krasnolutskaya M.G., Ilyasov I.R., Zembekov Yu.S., Litvinova V.M. Development of Design Scheme and Algorithm of Operation of an Ultraviolet LED Irradiating Set [Kondratieva N.P., Bolshin R.G., Krasnolutskaya M.G., Ilyasov I.R., Zembekov Yu.S., Litvi-nova V.M Razrabotka strukturnoi skhemy i algoritma raboty ultrafioletovoi svetodiodnoi obluchatelnoi ustanovki] // Agricultural Equipment and Power Supply [Agrotekhnika i energoobespechenie], 2017, Vol. 3 (16), pp. 50–57.

22. Bolshin R.G., Ilyasov I.R., Kondratyeva N.P., Korepanov R.I., Krasnolutskaya M.G., Litvinova V.M., Filatova O.M. Development of the Microprocessor System of Dosing of Photosynthesis-Active Radiation [Bolshin R.G., Ilyasov I.R., Kondratyeva N.P., Korepanov R.I., Krasnolutskaya M.G., Litvi-nova V.M., Filatova O.M. Razrabotka mikroprotsessornoi sistemy dozirovaniia fotosinteticheski aktivnoi radiatsii] // Bulletin of NGIEI, 2017, Vol. 9 (76), pp. 46–56.

23. Krasnolutskaya M.G. Software for the System of Automatic Adjustment of Parameters of Microclimate in Premises [Krasnolutskaya M.G. Programma dlia sistemy avtomaticheskogo regulirovaniia parametrov mikroklima-

ta v pomeshcheniiakh] / Certificate of state registration of software 2016617931 Russia, 2016.

24. Kondratieva N.P., Bolshin R.G., Krasnolutskaya M.G., Korepanov R.I., Ilyasov I.R., Litvinova V.M., Somova E.N. The Results of Experiments in Dosing of Photosynthesis-Active Radiation by means of a Microprocessor System Controlling Operation of a LED Phytoset [Kondratieva N.P., Bolshin R.G., Krasnolutskaya M.G., Korepanov R.I., Ilyasov I.R., Litvinova V.M., Somova E.N. Rezultaty opytov po dozirovaniiu fotosinteticheski aktivnoi radiatsii mikroprotsessornoi sistemoi upravliaiushchei rabotoi LED fitoustanovkami] // Bulletin of VIESKh, 2017, Vol. 3 (28), pp. 56–64.

25. Kondratieva N.P., Bolshin R.G., Krasnolutskaya M.G., Korepanov R.I., Ilyasov I.R., Baturin A.I., Litvinova V.M., Filatova O.M. Development of Microprocessor Systems of Automatic Controlling of Operation of LED Irradiating Sets [Kondratieva N.P., Bolshin R.G., Krasnolutskaya M.G., Korepanov R.I., Ilyasov I.R., Baturin A.I., Litvinova V.M., Filatova O.M. Razrabotka mikroprotsessornykh sistem avtomaticheskogo upravleniiam rabotoi svetodiodnykh obluchatelnykh ustanovok] // Bulletin of the Izhevsk State Agricultural Academy, 2017, Vol. 4 (53), pp. 72–80.

26. Kondratieva N.P., Korepanov R.I., Ilyasov I.R., Bolshin R.G., Krasnolutskaya M.G., Somova E.N., Markova M.G. Efficiency of Microprocessing System of Automatic Control of Operation of LED Irradiating Sets [Kondratieva N.P., Korepanov R.I., Ilyasov I.R., Bolshin R.G., Krasnolutskaya M.G., Somova E.N., Markova M.G. Effektivnost mikroprotsessornoi sistemy avtomaticheskogo upravleniia rabotoi svetodiodnykh obluchatelnykh ustanovok] // Agricultural Machines and Technologies [Selskokhoziaistvennye mashiny i tekhnologii]. 2018. Vol. 12. # 3. pp. 32–37.

27. Kondratieva N.P., Vladykin I.R., Baranova I.A., Yuran S.I., Baturin A.I., Bolshin R.G., Krasnolutskaya M.G. Development of the System of Automatic Control of Electric Equipment for Implementation of Energy-Efficient Technologies [Kondratieva N.P., Vladykin I.R., Baranova I.A., Yuran S.I., Baturin A.I., Bolshin R.G., Krasnolutskaya M.G. Razrabotka sistemy avtomaticheskogo upravleniia elektrooborudovaniem dlia realizatsii energosberegaiushchikh elektrotekhnologii]/ Bulletin of NGIEI. 2018. Vol. 6 (85). pp. 36–49.

Roman G. Bolshin,
Ph.D. in Technical Sciences, graduated from the Izhevsk State Agricultural Academy in 2004. Lecturer of the Non-State Educational Institution of Additional Professional Education Omega Educational and Scientific Innovative Centre (NOU DPO UNIC Omega). His research interests are agricultural lighting engineering, microprocessor control systems, information systems, electric safety

Nadezhda P. Kondratieva,
Doctor of Technical Sciences, Professor. In 1978, she graduated from Chelyabinsk Institute of Mechanisation and Electrification of Agriculture. At present, she is a head of the Automated Electric Drive Subdepartment of the Izhevsk State Agricultural Academy (IzhGSKhA); the founder of own scientific school in the field of agricultural light engineering and involved in the development of energy-efficient lighting technologies for agricultural enterprises, honourable worker of higher professional education of the Russian Federation

Maria G. Krasnolutskaya,
Ph.D. In 2013, she graduated from IzhGSKhA. She is a lecturer of NOU DPO UNIC Omega. Her research interests are agricultural lighting engineering, energy-efficiency in lighting engineering

Light & Engineering
Vol. 27, No. 6, pp. 155–158, 2019
https://doi.org/10.33383/2018-064

ELECTRODE-LESS UV LAMP ON THE BASIS OF LOW-PRESSURE MERCURY DISCHARGE IN A CLOSED NON-FERRITE TUBE

Pavel V. Starshinov[1], Oleg A. Popov[1], Igor V. Irkhin[2], Vladimir A. Levchenko[3], and Viktoriya N. Vasina[1]

[1] *NRU MPEI*
[2] *FGUP VEI*
[3] *NPO LIT, Moscow*
E-mail: popovoleg445@yahoo.com

ABSTRACT

Experimental study of characteristics of a non-ferrite electrode-less UV lamp with a length of 500 mm and width of 130 mm in the form of a closed quartz discharge tube with an inner diameter of 25 mm was conducted. The induction discharge was excited at a frequency of 1.7 MHz within the discharge lamp power P_{pl} ranging between 52 and 112 W in a mixture of mercury (~10^{-2} mm Hg) and argon (1.0 mm Hg) vapours by means of a 3-coil inductance located along the inner perimeter of the closed tube. With P_{pl} increasing: a) loss power in the inductance wire first decreased from 37 down to 22 W (P_{pl} = 84 W) and then increased up to 44 W; 2) the UV radiant flux of the lamp in a mercury light-band of 54 nm increased from 28 to 72 W; 3) radiant efficiency of the lamp at the light-band of 254 nm first increased from 31 to 48.5 % (P_{pl} = 84 W) and then slightly decreased down to 46 %; 4) radiant efficiency of the discharge plasma at the wavelength of 254 nm increased from 53 % to 65 %.

Keywords: UV radiation, induction discharge, closed tube, mercury lamp, low-pressure discharge plasma, inductance

1. INTRODUCTION

The low-pressure electrode-less mercury lamps are promising sources of UV radiation [1–4]. Due to lack of internal electrodes, they can operate at relatively low pressures of inert gas (0.05–0.5) mm Hg providing maximum radiant efficiency of the discharge plasma (η_{pl}) in mercury resonant lines of 185 and 254 nm [3, 4]. This provides a possibility to develop efficient resonance UV radiation sources within a wide range of power for water, air treatment, etc.

Of the special interest there is non-ferrite electrode-less lamps, in which high-frequency mercury plasma is excited in closed tubes by means of inductance located along the internal or external perimeter of the tube [5]. Such design allows going without ring-type ferromagnetic magnets decreasing reliability of the lamp's operation and increasing its cost. There are studies of the characteristics of non-ferrite electrode-less fluorescent lamps with closed glass discharge tubes with a relatively large diameter of (35–70) mm [5–7]. But the authors did

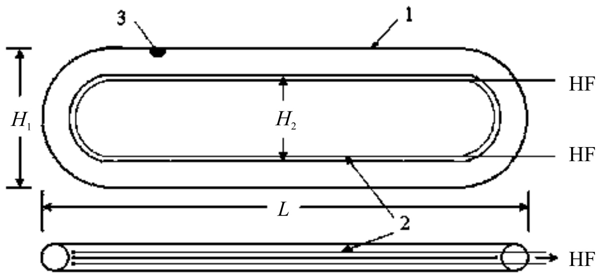

Fig.1. Scheme of the electrode-less non-ferrite lamp with closed discharge tube: *1* – discharge tube; *2* – inductance; *3* – amalgam; HF – high-frequency voltage

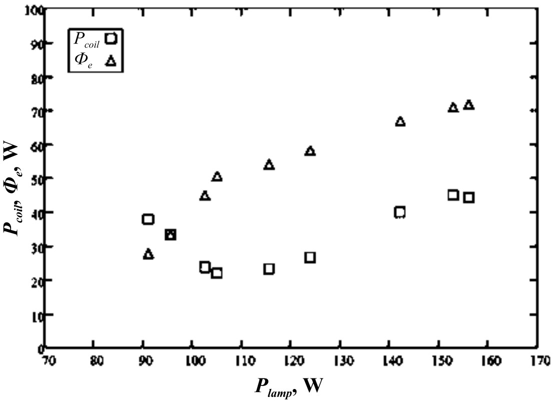

Fig. 2. Experimental dependencies of loss power in the inductance wire P_{coil} and lamp radiant flux at the 254 nm wavelength Φ_e on lamp power P_{lamp}

not manage to find publications on non-ferrite low-pressure electrode-less mercury lamps with closed quartz tubes used as UV radiation sources.

Below are the results of our experimental study of characteristics of a non-ferrite electrode-less mercury UV lamp with a closed quartz discharge lamp (bulb) with inner diameter of 25 mm, in which the plasma is excited by means of inductance located along the internal perimeter of the lamp.

2. EXPERIMENTAL INSTALLATION AND MEASUREMENT METHODS

The induction discharge was excited at frequency f equal to 1.7 MHz in a closed quartz tube with a wall thickness of 1.5 m and an inner diameter of 25 mm. The lamp had a form of a stretched ring with length L of 500 mm and width H_1 of 130 mm and distance between the long parallel sections of the discharge tube H_2 of 75 mm and the length of closed centre-line Λ_{pl} of 1060 mm (Fig. 1). HF inductor consisted of a 3-coil inductance made of copper wire with a diameter of 2.5 mm and specific resistance per length unit of 8×10^{-4} Ohm/cm located along the internal perimeter of the lamp. The mercury vapours pressure in the discharge tube was maintained optimal (with maximum radiant flux of the lamp Φ_e at the wavelength 254 nm) by means of temperature of mercury-indium amalgam located on the tube wall. *Ar* buffer gas pressure was equal to 1.0 mm Hg.

Φ_e was measured by means of an *IL1700* radiometer and *SED240/W* photometric head with cosine angular response [2]. The measurements were performed with package power P_k equal to (102–165) W and comprising: *a*) loss power of HF generator P_g; *b*) lamp power P_{lamp} comprising loss power of inductance wire P_{coil} and power of discharge plasma P_{pl}. The lamp was positioned in a black grounded box with a black screen in a plane normal to the lamp plane. There was a gap with a width Δ of 30 mm in the box for the lamp plane. The distance between the radiation detector (RD) and the gap d = 150 cm and the distance between the gap and the lamp ℓ = 10 cm, which allowed to consider the lamp section "cut out" by the gap as a point source of radiation [3]. Φ_e was calculated in accordance with [2, 3]:

$$\Phi_e = \pi^2 \cdot h \cdot d \cdot i \cdot L / (\Delta \cdot S), \qquad (1)$$

where $h = \ell + d$ is the distance between the lamp and RD, i is photocurrent of RD, S is total sensitivity of RD.

The value of the power generator efficiency η_g determined as $\eta_g = 1 - (P_g/P_k)$ was equal to 0.9 at frequency f of 1.7 MHz, and the value of P_{coil} was found using a substitution method without the discharge inside the lamp [5, 8].

3. MEASUREMENT RESULTS AND DISCUSSION

As it can be seen from the experimental dependencies of P_{coil} and Φ_e on P_{lamp} (Fig. 2), with increase of P_{lamp}: *a*) P_{coil} decreases from 39 W (P_{lamp} = 92 W) down to its minimum value of 22 W ($P_{lamp,\,min}$ = 105 W), then increases up to 44 W (P_{lamp} = 156 W); *b*) Φ_e "rapidly" increases from 28 W (P_{lamp} = 92 W, P_{pl} = 53 W) up to 45 W ($P_{lamp,\,min}$ = 105 W, $P_{pl,\,min}$ = 84 W), and then "slowly" up to 72 W (P_{lamp} = 156 W). Both dependencies are well correlated with each other.

As it can be seen from 3 other experimental dependencies (Fig. 3), with increase of P_{pl}: *a*) radiant efficiency of the lamp at wavelength 254 nm η_{lamp} ($\eta_{lamp} = \Phi_e/P_{lamp}$) increases from 32 % ($P_{pl}$ = 53 W) up to 46 % (P_{pl} = 84 W), and then insignificantly decreases down to 44 % (P_{pl} = 112 W); *b*) η_{pl} ($\eta_{pl} \approx \Phi_e/P_{pl}$) practically linearly increases from 52 to 66 %; *c*) Efficiency of the inductance η_{coil} ($\eta_{coil} = 1 - P_{coil}/P_{lamp}$) increases from 59 % ($P_{pl}$ = 53 W) up to 81 % (P_{pl} = 84 W) and then decreases down to 71 % (P_{pl} = 112 W). Also, we note that $\eta_{lamp} = \eta_{coil}\times\eta_{pl}$.

Increasing of P_{coil} with increasing of P_{pl} and corresponding decreasing of η_{coil} and η_{lamp} are related to skin effect in the HF induction discharge (with rather high density) at frequencies of hundreds of kHz and higher [9]. The skin effect is characterised by "pushing-put" of the HF electric field from the dense plasma area (near the centre-line of the tube) and its "pressing" to the walls of the discharge tube where the inductance wire is located and HF electric field density is maximum [10]. As a result, average density of HF electric field over the cross-section area $\bar{E}_{pl}$ of the discharge tube increases, HF voltage on the plasma coil U_{pl} rises ($U_{pl} = \bar{E}_{pl} \times \Lambda_{pl}$) and, therefore, in accordance with the transformer model of induction discharge, HF voltage and current of the inductance I_{coil} increase, therefore, P_{coil} ($P_{coil} = (I_{coil})^2 \times R_w$) where R_w is resistance of the inductance.

But the skin effect does not significantly affect the UV radiation generation which is witnessed by approximate linearity of the dependence $\eta_{pl}(P_{pl})$ within the whole studied range of P_{pl} (52–112) W.

It is worth noting that, screening of UV radiation by the coils of the inductance covering (3–5)% of the surface area of the discharge tube was not taken into account during calculation of η_{lamp}. As a result, part of UV radiation is absorbed by the inductance therefore the actual UV radiant flux of the lamp is less than the measured flux Φ_e in accordance with the formula (1). Subsequently, the clarified $\eta_{lamp} = \eta_{coil} \times \eta_w \times \eta_{pl}$, where $\eta_w \approx 1 - (d_w/\pi d_{tr})$ is the factor of screening of the discharge lamp by the inductance, d_w is the inductance wire diameter, d_{tr} is the external diameter of the discharge tube.

4. CONCLUSION

– High values of η_{pl} (60–65)% of the electrode-less non-ferrite lamp with a closed discharge tube with diameter of 25 mm operating at a frequency of 1.7 MHz and specific power of plasma (SPP) of (0.8–1.0) W/cm were acquired. These values exceed those of electrode-less non-ferrite linear UV lamps operating at a frequency of (1–4) MHz with SPP of about 1 W/cm [4] and transformer-type UV lamps operating at SPP of 1 W/cm with frequency of 265 kHz [2, 3].

– P_{coil} is relatively high, (20–50) W and η_{coil} is relatively low, (70–80)%. But thanks to high values of η_{pl}, the values of η_{lamp} are equal to (45–46)% with SPP of (0.8–1.0) W/cm, which is higher than those of non-ferrite linear electrode-less UV lamps [4, 11] and electrode tube UV lamps operating at frequencies of (20–80) kGz (low) [12].

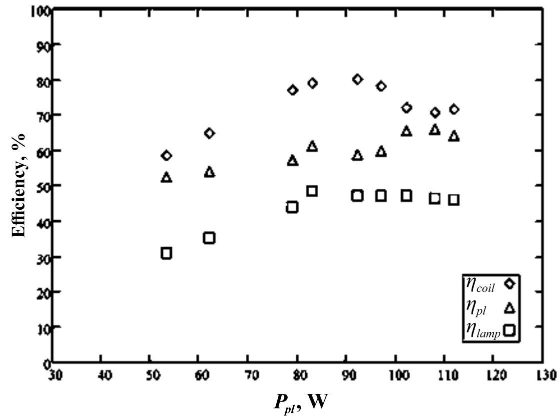

Fig. 3. Dependencies of the inductance efficiency η_{coil} and radiant efficiency of the lamp (η_{lamp}) and discharge plasma (η_{pl}) at the 254 nm wavelength on plasma power P_{pl}.

– η_{pl} may be increased by lowering the pressure of inert gas (*Ar*) down to (0.2–0.3) mm Hg. At such pressure, maximum efficiency of UV radiation generation by mercury plasma in a transformer-type lamp with a closed discharge tube and inner diameter of 16.6 mm was witnessed [3].

– η_{lamp} may be increased by increasing η_{coil} by decreasing P_{coil}. For this purpose the following actions may be taken: *a)* use a wire with low specific resistance per length unit for manufacturing of the inductance, < 3×10^{-4} Ohm/cm (litzendraht) [5, 6]; *b*) lower I_{coil} by increasing the number of coils up to 5–6 [13]; *c*) increase *of* up to (6–9) MHz [13].

REFERENCES

1. Isupov M.V., Krotov S.V., Litvintsev A. Yu., Ulanov I.M. Electrodeless UV Lamp [Isupov M.V., Krotov S.V., Litvintsev A. Yu., Ulanov I.M. Induktsionnaia ultrafioletovaia lampa] // Svetotekhnika, 2007, Vol. 5, pp. 37–40.

2. Vladimir A. Levchenko, Oleg A. Popov, Sergei A. Svitnev, and Pavel V. Starshinov Experimental Research into the Electrical and Optical Characteristics of Electrodeless UV Lamps of the Transformer Type// Light & Engineering Journal, 2015, Vol.23, #1, pp.60–64.

3. Vladimir A. Levchenko, Oleg A. Popov, Sergei A. Svitnev, and Pavel V. Starshinov Electric and Radiation Characteristics of a Transformer Type Lamp with a Discharge Tube of 16.6 mm Diameter// Light & Engineering Journal, 2016, Vol. 24, pp.77–81.

4. Svitnev S.A., Popov O.A., Levchenko V.A., Starshinov P.V. Characteristics of Low-Pressure Non-Ferrite Induction Discharge. Part 2. Radiation Characteristics of Plasma [Svitnev S.A., Popov O.A., Levchenko V.A., Star-

shinov P.V. KHarakteristiki besferritnogo induktsionnogo razriada nizkogo davleniia. Chast 2. Izluchatelnye kharakteristiki plazmy] // Successes of Applied Physics [Uspekhi prikladnoi fiziki]. 2016, Vol. 4, pp. 372–384.

5. Popov O.A., Chandler R.T. Ferrite-free High Power Electrodeless Fluorescent Lamp Operated at a Frequency of 160–1000 kHz // Plasma Sources Science and Technology, 2002, Vol. 11, pp. 218–227.

6. Popov O.A., Nikiforova V.A. Electrodeless Non-Ferrite Light Source with Power of 300–400 W at Frequency of 200–400 kHz [Popov O.A., Nikiforova V.A. Induktsionnyi besferritnyi istochnik sveta moshchnostiu 300–400 Vt na chastote 200–400 kGts] // Bulletin of MEI [Vestnik MEI], 2010, Vol. 2, pp. 159–164.

7. Popov O.A., Starshinov P.V., Vasina V.N. Electrodeless Non-Ferrite Fluorescent Mercury Lamp with a Closed Discharge Tube [Popov O.A., Starshinov P.V., Vasina V.N. Bezelektrodnaia besferritnaia induktsionnaia liuminestsentnaia rtutnaia lampa s zamknutoi razriadnoi trubkoi] // Svetotekhnika, 2018, Vol. 2, pp. 75–77.

7. Oleg A. Popov, Pavel V. Starshinov, and Victoriya N. Vasina Electrode-Less Ferrite-Free Closed-Loop Inductively-Coupled Fluorescent Lamp// Light & Engineering Journal, 2018, Vol.26, #3, pp.140–142.

8. Piejak R.B., Godyak V.A., Alexandrovich B.M. A Simple Analyses of an Inductive RF Discharge // Plasma Sources Sci.Technol, 1992, # 1, pp. 179–185.

9. Reiser Yu.P. Physics of Gas Discharge [Reiser Yu.P. Fizika gazovogo razriada]. – Moscow: Nauka, 1987, P. 591.

10. Nikiforova V.A., Popov O.A. Spatial Distribution of Plasma Parameters in Closed Non-Ferrite Discharge [Nikiforova V.A., Popov O.A. Prostranstvennoe raspredelenie parametrov plazmy v besferritnom razriade zamknutogo tipa] // Bulletin of MEI [Vestnik MEI], 2010, Vol. 5, pp. 114–119.

11. Svitnev S.A., Popov O.A., Levchenko V.A. Characteristics of High-Frequency 13.56 MHz Non-Ferrite Electrodeless UV Lamp [Svitnev S.A., Popov O.A., Levchenko V.A. KHarakteristiki vysokochastotnoi 13,56 MGts besferritnoi induktsionnoi ultrafioletovoi lampy] // Applied Physics [Prikladnaia fizika], 2015, Vol. 6, pp. 92–96.

12. Ultra-violet technologies in the modern world: Collective monography [Ultrafioletovye tekhnologii v sovremennom mire: Kollektivnaia monografiia] / Edited by Karmazinov F.V., Kostyuchenko S.V., Kudryavtsev N.N., Khramenkov S.V. – Dolgoprudny: Intellect Publishing House [Izdatelskii Dom “Intellekt”], 2012, P. 391.

13. Svitnev S.A., Popov O.A., Levchenko V.A., Starshinov P.V. Characteristics of Low-Pressure Non-Ferrite Induction Discharge. Part 1. Electrical Characteristics of HF Inductor [Svitnev S.A., Popov O.A., Levchenko V.A., Starshinov P.V. Kharakteristiki besferritnogo induktsionnogo razriada nizkogo davleniia. Chast 1. Elektricheskie kharakteristiki VCH induktora] // Successes of Applied Physics [Uspekhi prikladnoi fiziki], 2016, Vol. 2, pp. 139–149.

Oleg A. Popov,
Dr. of Technical Science. Graduated from the Moscow Power Engineering Institute in 1965, Professor of the Chair “Light and Engineering” of the “MPEI” National Research University

Pavel V. Starshinov,
Master Degree of engineering, graduated from the Light and Engineering Chair of the National Research University “MPEI” in 2015

Igor V. Irkhin, Ph.D. in Technical Sciences, Senior Engineer of FGUP VEI

Vladimir A. Levchenko,
Ph.D. in Physical and Mathematical Sciences, graduated from MIPT, Deputy Head of the Laboratory of NPO LIT

Victoriya N. Vasina,
student of the chair “Light and Engineering” NRU MPEI

Light & Engineering
Vol. 27, No. 6, pp. 127–141, 2019 *https://doi.org/10.33383/2019-042*

COLOUR PREFERENCE DEPENDS ON COLOUR TEMPERATURE, ILLUMINANCE LEVEL AND OBJECT SATURATION – A NEW METRIC

Quang Trinh Vinh,[1], Peter Bodrogi[1], Tran Quoc Khanh[1], and Tean Thuy Anh [2]

[1]*Laboratory of Lighting Technology, Technische Universität Darmstadt, Darmstadt, Germany*
[2]*University of Social Sciences and Humanities (USSH), Vietnam National University, Han Vietnam*
E-mail: bodrogi@lichttechnik.tu-darmstadt.de

ABSTRACT

A new metric ($R_{p,2019}$) is defined as a light source to predict the subjective colour preference impression of an interior scene containing coloured objects illuminated by this light source. The metric is based on the CIE2017 Colour Fidelity Index and the TM-30–15 Colour Vector Graphic. In addition to its dependence on object saturation level, the metric also includes the dependence on correlated colour temperature and on the characteristic illuminance level at the plane on which the coloured objects are arranged. The scale of the metric is labeled with criterion values corresponding to "good" or "very good" colour preference. The aim is to help lighting designers and engineers to determine the illuminance level, colour temperature and object saturation necessary to achieve "good" or "very good" colour preference.

Keywords: colour quality, colour preference, colour preference metric, colour fidelity, colour gamut, colour saturation, correlated colour temperature, illuminance level

1. INTRODUCTION

The concept of *colour quality of a light source* can be defined as the quality of the subjective impressions on the colour appearance of the coloured objects in an interior scene lit by that light source. Although colour quality is just one aspect of lighting quality, it plays an important role in interior lighting to achieve general user acceptance. Other aspects of lighting quality include brightness, visual clarity (the clear visibility of object surface structures), the avoidance of glare and the visibility of object shadows. Colour quality has several sub-aspects [1, 2] including:

– Colour naturalness [2–5]: the similarity of object colour appearance under a given light source to the colour appearance under daylight;

– Colour preference [2–7] (defined below);

– Colour vividness [2–4, 8]: the extent of how saturated the impression of a coloured object is;

– The similarity of object colours related to long-term memory colours [9]: the colour appearance of objects often seen in the past are stored in human colour memory, for example, banana, grass or skin;

– Colour discrimination ability [10–12]: the ability of the human visual system to distinguish between colours of a similar shade, for example, two versions of a greenish shade with slightly more or less blue;

– Colour harmony: the impression of colour harmony is related to the aesthetic appearance of colour combinations; for example red and orange or green and blue and yellow next to each other; the literature on colour harmony is abundant.

Among the sub-aspects, *colour preference* is possibly the most relevant one for lighting engineering according to its straightforward and generally understandable definition. This definition can be formulated as the "subjective extent of how an observer *likes* the colour appearance of the coloured objects in the room *under the current light source* taking all coloured objects into consideration" [1, 2, 13]. An important issue is that the observers' colour preference between different light sources depends on the viewing context or application field of lighting including restaurant, office, home or supermarket lighting [14].

The following parameters of the lighting system are known to influence the colour preference impression of the observers in an artificially lit interior scene:

1. Chroma shifts and hue shifts of the object colours (or test colour samples) between the test light source and its reference illuminant, see the TM-30–15 Colour Vector Graphic [2–5, 7, 13, 15], the Colour Vector Graphic represents how the colour appearance of different, selected object colours (test colour samples) changes if instead of the actual (test) light source a reference illuminant (a daylight spectrum or a blackbody radiator spectrum) is used;

2. The value of the colour fidelity index [2–5, 13,16]; the colour fidelity index expresses numerically how close the colour appearance of the test colour samples under a test light source is to the colour appearance of a reference illuminant at the same correlated colour temperature;

3. The size of the colour gamut [17, 18] which is equivalent to the *saturation level* of the illuminated coloured objects depending on the spectrum of the illuminant, the colour gamut of a light source spectrum expresses how many different shades of object colours including saturated colour shades can be observed under a given light source spectrum. *Object saturation level* is a property of the light source spectrum: it expresses, in average, how saturated the same coloured objects appear under different light source spectra;

4. The shape of the colour gamut (especially the amount of *red saturation* [13, 19–21]), the shape of the colour gamut can be elucidated as follows: in case of a certain light source spectrum, e.g. reddish object colours appear more saturated than in case of another spectrum. In this case, the colour gamut is more extended in the region of e.g. reddish hues;

5. The correlated colour temperature (CCT) of the white tone of the light source [2, 5, 21, 22], the correlated colour temperature means the shade of the white tone: CCT=2700 K is a yellowish warm white while CCT=7000 K is a slightly bluish cool white;

6. Distance of the white tone of the light source from the blackbody or daylight loci on a chromaticity diagram (expressed by the quantity *Duv* or $\Delta u'v'$) [21, 23–26]. If this distance is large then the colour of the light source spectrum will not be white, it will contain (perceptually) for example a disturbing shade of green;

7. The characteristic *illuminance level* (in lx) [27–29] on a "working plane" in the room on which the coloured objects are arranged.

It is interesting to describe some experimental findings in more detail at this point about the effect of three parameters, CCT, object saturation and illuminance level, on colour preference. This issue will be further elucidated in Section 2. Colour preference was found to be influenced by the CCT of the white tone (warm white, neutral white, cool white) illuminating the coloured objects [2]: a *higher* subjective colour preference was experienced under a *higher* CCT (4000 K) than under a *lower* CCT (2500 K) at the same object saturation level of the light source. In another study [5], colour preference was maximal at about CCT=5000 K (cool white) and not at CCT=3100 K (warm white). Previous studies [10, 30, 31] stated that another, related aspect of lighting quality, *scene preference* (the general subjective judgement about the lighting quality of a lit interior) *increases* with illuminance level (these studies did not change colour fidelity indices and object saturation levels and did not deal with colour preference specifically). In another study, subjective colour preference turned out to be a monotonically increasing function of illuminance level [32].

The problem is that today's colour preference metrics (either 1) ignores the CCT dependence and/or the illuminance level dependence and/or the colour *gamut shape* dependence (for example red saturation level dependence) of colour preference; and/or 2 do not use those new colorimetric descriptor quantities that result from the recent development of colour science including a new colour fidelity index, a new chromatic adaptation transform or a new colour space [15]. Accordingly, Table 1 summarizes the properties of a set of selected (more recent) colour preference metrics. Other colour rendition metrics including colour preference metrics were described and analysed in previous articles in detail [33, 34].

As can be seen from Table 1, in several cases, the illuminance dependence, the CCT dependence or the *colour gamut shape* dependence of colour

Table1. Properties of Selected (More Recent) Colour Preference Metrics
(The Concept of "Saturation", the Saturation Level of the Coloured Objects Caused by the Current Light Source, is Equivalent to the Size of the Colour Gamut)

Colour preference metric	Parameter Included	Parameter not included	Colourimetric Description	Test colour samples (TCS)
CQS Q_p [35]	saturation, CCT	illuminance, gamut shape	CIELAB	15 TCS [35]
CP [29]	illuminance, saturation, CCT	gamut shape	CIELAB	15 TCS [35]
LIKE [13]	saturation, gamut shape	CCT, illuminance	TM-30–15 [15, 36]	TM-30–15 [15, 36]
MCRI [9]	saturation, gamut shape (via memory colours)	CCT, illuminance	IPT colour space [37]	10 TCS [9]

preference is not included. The LIKE metric [13] includes the dependence on colour gamut shape. This is based on experiments at a fixed CCT (3500 K) and a fixed illuminance level (646 lx). The memory colour rendition index (MCRI) [9] is based on experiments at 5600 K (fixed) and 1150 lx (fixed). According to the above mentioned experimental evidence suggesting the significant effect of CCT *and* illuminance level (besides object saturation level) on colour preference, one previous metric (CP) was found to be able to model this dependence, see Eq. (1) [29].

$$\begin{gathered} CP = (14.089 \cdot \ln(E_{v,\,eq}) - 25.397) \times \\ \times [-0.003 \cdot \Delta C^{*2} + 0.0252 \cdot \Delta C^{*} + \\ +1.0192] + [-518.554((S/V)^{0{,}24})^2 + \\ + 864.872\,(S/V)^{0{,}24} - 356.578]. \end{gathered} \qquad (1)$$

Equation (1) [29] shows a dependence of this so-called CP (colour preference) metric on the so-called equivalent illuminance $E_{v,eq} = E_v \times \left(\frac{S}{V}\right)^{0.24}$ [38]. The quantity $(\frac{S}{V})$ represents the relative S-cone (short-wavelength sensitive human cone photoreceptor) signal which can be used as a proxy of correlated colour temperature [29]: the quantity $(S/V)^{0.24}$ was predicted [29] in case of a set of multi-LED spectra from CCT (in K) by Equation (2) with r^2=0.99. This prediction can be applied in practice if the value of $(S/V)^{0.24}$ is not readily available.

$$\begin{gathered} (S/V)^{0.24} = -0.0138 \cdot (CCT/1000)^2 + \\ + 0.1759 \cdot (CCT/1000) + 0.2859. \end{gathered} \qquad (2)$$

This means that, for example, a neutral white light source (at a higher *CCT* with higher S-cone signal values) exhibits a higher colour preference than a warm white light source at the same illuminance. There is a quadratic dependence on *object saturation level* in Eq. (1) peaking at a moderate object saturation level (ΔC^*=4.2). Object saturation level is expressed here by the quantity ΔC^* i.e. the mean CIELAB chroma shift of the 15 CQS test colour samples [35].

The quadratic term in Eq. (1) computed from the value of $\left(\frac{S}{V}\right)^{0.24}$ is intended to account for the following effect: warm white (3000 K) spectra at higher saturation levels result in less colour preference. As can be seen from the 4th column of Table 1, the CP metric [29] incorporates *CCT* and illuminance level dependence but it does not support more recent methods like the TM-30–15 concept [15, 36] or the new colour fidelity index [16].

According to the above considerations, the present article aims to define a new colour preference metric (so-called $R_{p,2019}$) by re-analysing and modelling two subjective (psychophysically obtained) colour preference assessment datasets resulting from previous experiments [3, 32]. The new colour preference index $R_{p,2019}$ shall exhibit the following features:

1. $R_{p,2019}$ shall include a dependence on illuminance level, CCT and object saturation level. According to the limitations of the underlying experimental datasets, we do *not* include *gamut shape* dependence and *Duv* dependence (*Duv* is the distance of the white tone of the light source from the blackbody locus or the daylight locus on a chro-

maticity diagram) in the present version of the new metric;

2. $R_{p,2019}$ shall be based on the following internationally well-known, recent and readily applicable quantities:

– A descriptor of object saturation level (caused by the light source spectrum) derived from the TM-30–15 Colour Vector Graphic,

– The value of R_f [16],

– CCT (K),

– E_v (lx);

3. $R_{p,2019}$ shall have a psychophysically relevant scale fitted to the subjective colour preference scale of the observers in the underlying experimental colour preference datasets [3, 32].

This scale [39] was labelled by rating categories including "very good", "good", "moderate". Therefore, a criterion value of the new index $R_{p,2019}$ can be readily determined for the "good" colour preference (as a minimum acceptance criterion of lighting design) if the spectrum of the light source and the illuminance level are known.

2. SUBJECTIVE COLOUR PREFERENCE DATASETS USED TO OBTAIN THE NEW COLOUR PREFERENCE METRIC ($R_{P,2019}$)

The colour preference metric $R_{p,2019}$ is based on a new mathematical analysis of two previously published subjective colour preference datasets resulting from two previous studies [3, 32]. In this Section, the experimental method and the findings of these studies [3, 32] are summarized. Both studies were laboratory tests in a dedicated experimental room with white walls and white cloths on the tables with different multi-coloured arrangements of coloured objects including artificial flowers, paintings, books, a multi-coloured textile object and Macbeth ColourChecker® charts, see Fig. 1. These arrangements represent a general indoor viewing environment with coloured objects to assess colour preference independent of a specific lighting application [14].

In the first study [3], a multi-LED engine with red, green, blue and warm white LEDs illuminated two still life arrangements with coloured objects (in Fig. 1 only the first one is depicted as an example) with a set of 36 white spectra at a fixed, single illuminance level of 750 lx at four CCTs (3100 K, 4100 K, 5000 K and 5600 K). Nine different multi-LED spectra were used at each CCT. Each one of these nine spectra represented nine different degrees of object saturation. This means that the multi-LED spectra used rendered the coloured objects more or less saturated. Observers assessed their colour preference impression of all coloured objects at the same time. "Colour preference" was defined for the subject as the "subjective extent of how the observer likes the colour appearance of the coloured objects under the current light source taking all coloured objects into consideration".

Subjects assessed their colour preference on an interval rating scale labelled by rating categories, see Fig. 2. The non-uniform spacing of the category labels along this rating scale is based on a previous study [39]. Observers in previous studies [3, 32] could use this interval rating scale labelled with categories successfully. The categories represented decision criteria and helped subjects put their rating

Fig. 1. Experimental room with multi-coloured arrangements of coloured objects in the two previous studies (left: first study [3] with Exp-1's arrangement; right: second study [32]) that constitute the basis of the present new colour preference metric ($R_{p,2019}$)
(Reproduced with permission from Lighting Research and Technology, both photos (left and right) contain copies of the MacBeth ColourChecker® Chart)

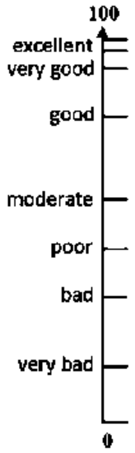

Fig. 2. Colour preference interval rating scale [39] labelled with the category ‘excellent’ at the value of 97.9; ‘very good’ at 91.6; ‘good’ at 79.6; ‘moderate’ at 52.9; ‘poor’ at 41.2; ‘bad’ at 26.5; and ‘very bad’ at 12.8 (*Reproduced with permission from Lighting Research and Technology [3]*)

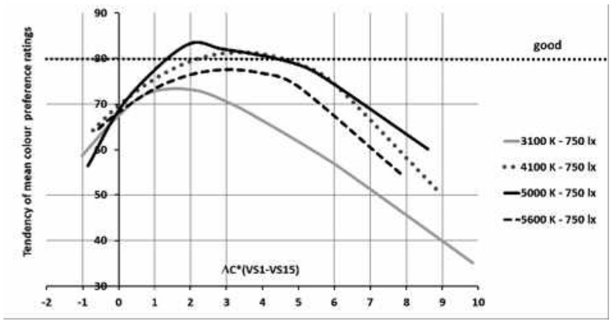

Fig.3. Tendencies of the observers’ mean colour preference ratings as a function of object saturation level (ΔC*) and CCT at the fix illuminance level of 750 lx in the first study [3]

cross on the scale [39]. Observers were instructed to put their rating cross at any place on the interval scale, not only at the categories (and they did so consciously). The category “good” with a value of 79.6 plays an important role in lighting design as a general acceptance criterion of the lighting system [29] from the point of view of colour preference.

The de-saturation or over-saturation of the coloured objects caused by the current light source was characterized by the mean *chroma difference* value (denoted by ΔC*) of the CQS test colour samples VS1-VS15 [35] (a set of fifteen different homogeneous colour samples) when their chroma under the current light source was compared with their chroma under the reference illuminant. Depicting the observers’ mean colour preference ratings as a function of ΔC*, the following tendencies were obtained [3]. Neutral white (4100 K) and cool white (5000 K and 5600 K) resulted in higher subjective colour preference ratings than warm white (3100 K), see Fig. 3.

It can also be seen from Fig. 3 that colour preference ratings exhibited a maximum at a moderate object saturation level. The location of this maximal colour preference (in terms of ΔC*) depended on CCT, higher CCTs requiring more object saturation. At 3100 K, the observers’ mean colour preference ratings were always less than “good” (see Fig. 3) because the illuminance level of 750 lx was too low for the observers at this CCT so that their colour preference judgements were always worse than “good”.

In the second study [32], subjects assessed the colour preference of a tabletop arrangement of coloured objects (see Fig. 1, right) illuminated by 36 different light sources with all 36 possible combinations of three object saturation levels (low with ΔC* between –0.1 and 1.0; medium with ΔC* between 1.7 and 4.4; and high with ΔC* between 10.7 and 12.2), three CCTs (3000 K, 4100 K and 5600 K) and four illuminance levels (200 lx, 500 lx, 1000 lx and 1800 lx). Subjects assessed their colour preference impression by the use of the same rating scale (Fig.2). Mean colour preference ratings in this second study increased with increasing illuminance level monotonically and a logarithmic function was fitted to describe the illuminance dependence of colour preference [29], see the first multiplicative term of Eq. (1) and Fig. 4.

As can be seen from Fig. 4, mean subjective colour preference ratings increased with increasing CCT. Colour preference maxima generally occurred at the level of ΔC*=4.2 (a medium saturation level) at every CCT and every illuminance level.

3. DEFINITION OF THE NEW COLOUR PREFERENCE METRIC ($R_{P,2019}$), ITS VALIDITY RANGE, COMPARISON WITH THE CP METRIC, AND VALIDATION

In this Section, the defining equations of the new colour preference metric ($R_{p,2019}$) are described. Equation (3) shows the main defining formula of the new colour preference metric.

$$R_{p,2019} = 0.70 \cdot R_f + p_1 \times \times \Delta C_t^2 + p_2 \cdot \Delta C_t + p_3. \quad (3)$$

In Eq. (3), R_f is the CIE2017 Colour Fidelity Index [16]. The symbol ΔC_t is the so-called total chroma difference defined by Eq. (4) while $p_1 - p_3$ are model parameters that depend on CCT and illuminance level, see Eq. (5).

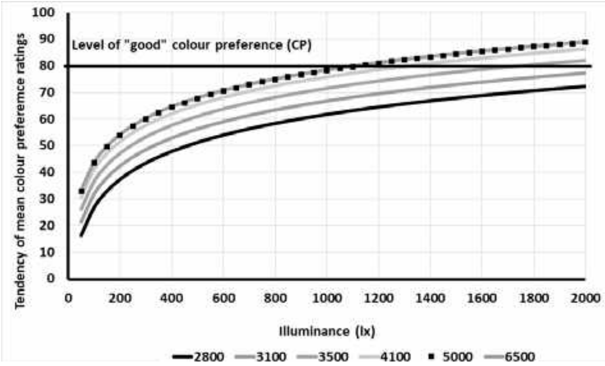

Fig. 4. Tendencies of the observers' mean colour preference ratings as a function of illuminance level (lx) and CCT in the second study [32] at the fixed object saturation level of ΔC^*=4.2 the level of maximum colour preference *(Reproduced with permission from Lighting Research and Technology [32])*

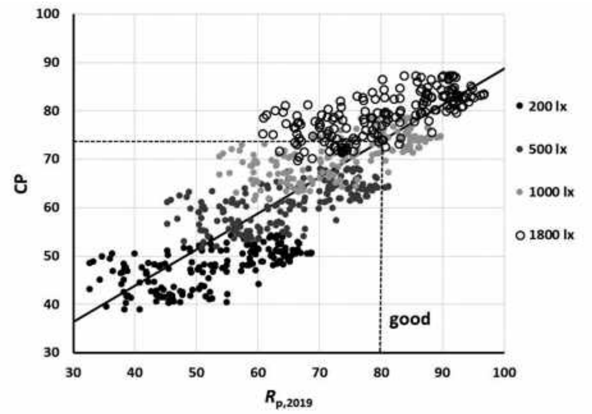

Fig. 5. Comparison of the values of $R_{p,2019}$ with the values of a previous metric (*CP*, Eq. 1) in case of a sample set of 180 light source spectra (see text) at four illuminance levels, 200 lx, 500 lx, 1000 lx and 1800 lx *(Best fit: $CP = 0.7476 \cdot R_{p,2019} + 13.965$ (r^2 = 0.71). The "good" colour preference level of $R_{p,2019}$ (79.6) is taken from the subjective scale of Fig. 2)*

$$\Delta C_t = \sum_{i=1}^{16} \frac{R_{cs,hi}}{100}. \quad (4)$$

In Eq. (4), the $R_{cs,\ hi}$ values (expressed in %; *i*=1–16) correspond to the "purely radial difference between vectors for the test and reference condition in each of the 16 hue bins" [20] in the TM-30–15 Colour Vector Graphic. The concept of *hue bins* can be defined as collections of test colour samples (with homogeneous coloured surfaces) of *similar* hues. There are 16 hue bins (*i*=1–16) evenly distributed along the hue circle: 1. red, 2. reddish-orange, 3. orange, 4. yellow, 5. greenish-yellow, 6. yellowish-green, 7. green, 8. bluish-green, 9. cyan-green, 10. cyan; 11. bluish-cyan, 12. blue, 13. bluish-violet, 14. violet, 15. purplish-violet, 16. purple. For example, the red hue bin (*i*=1) contains test colour samples of slightly different red tones. Colour Vector Graphic calculations are available in the TM-30 Calculation Tools. The sum of the $R_{cs,\ hi}$ values (ΔC_t) in Eq. (4) characterizes the overall saturating or de-saturating effect of the light source on the different coloured objects in the scene.

Equation (5) shows the dependence of the model parameters p_i (*i*=1–3) of Eq. (3) on CCT and illuminance level.

$$p_1 = a_1 \cdot CCT^2 + b_1 \cdot CCT + \\ + c_1 \cdot \ln\left(E_v + d_i\right) + e_i. \quad (5)$$

The optimum values of the parameters $a_i - e_i$ (i=1–3) of Eq. (5) (listed in Table 2) were obtained in the following way:

1. Only the light sources with ΔC_t values between –0.4 and 1.2 were considered from the set of the 36+36=72 light sources in the two studies described in Section 2 [3, 32], the reason is that the light sources of this set with ΔC^*>6.1 obtained only "moderate" or worse visual colour preference ratings, and this should not be the aim of interior lighting design, but therefore, we decided *not* to include these light sources in the fitting procedure; correspondingly, two light sources were excluded from the first study [3] and twelve light sources were excluded from the second study [32];

2. The values of R_f and ($R_{cs,\ hi}$ / 100) were computed for the remaining 58 light sources (their illuminance levels and CCT values were known);

3. Equations (4) and (5) were substituted into Eq. (3);

4. The sum of the squared differences between the 58 mean subjective colour preference ratings [3, 32] and $R_{p,2019}$ was minimized.

According to the above 4th condition, the numeric scale of the new colour preference metric $R_{p,2019}$ is equivalent to the visual scale labelled by the categories in Fig. 2. The value of $R_{p,2019}$ ≥79.6 shall be ensured during the lighting design procedure in order to achieve at least the criterion of "good colour preference" in the illuminated scene, see the caption of Fig. 2 in which the criterion val-

Table2. Optimum Parameter Values $A_i - E_i$ (I=1–3) in Eq. (5) Obtained by Fitting Eq. (3) to the Mean Subjective Colour Preference Ratings for 58 Light Sources of the Two Studies Described in Section 2 [3, 32]

i	a_i	b_i	c_i	d_i	e_i
1	$-1.074 \cdot 10^{-6}$	0.008406	-0.01883	0.000	-31.68
2	$-4.603 \cdot 10^{-6}$	0.04249	-0.4564	$1.02 \cdot 10^{4}$	-63.92
3	$-3.726 \cdot 10^{-6}$	0.03519	11.37	-51.6	-143.5

ues of the different colour preference categories are listed.

Concerning the fitting accuracy of the parameter values in Table 2, the mean absolute value of the difference between the value of $R_{p,2019}$ and the mean colour preference ratings of the observers in case of the 58 light sources equalled 2.0 (SD=1.9; min.=0.1; max. =7.2). This mean fitting accuracy (2.0 points on the rating scale of Fig. 2) is small compared to the distance of the adjacent rating categories on the rating scale (26.7 between "moderate" and "good" and 12.0 between "good" and "very good"). Pearson's correlation coefficient between the 58 mean colour preference ratings and the corresponding $R_{p,2019}$ values equalled r=0.97. During the development of the new metric, we also considered mathematically less complex versions but it turned out that we would need this level of complexity to achieve this fitting accuracy. In comparison, Pearson's correlation coefficient between the 58 mean colour preference ratings and the corresponding CP values (Eq. (1)) equalled r=0.75. The difference between the two correlation coefficients (r=0.97 and r=0.75) was statistically significant (p<0.001).

Concerning the validity range of the parameters in Table 2 according to the underlying experimental dataset, these parameters are valid for correlated colour temperatures between 3000 K and 5600 K, illuminance levels between 200 lx and 1800 lx and ΔC_t values between 0.4 and 1.2. The white points of the underlying experimental dataset were located in a range with $\Delta u'v' < 0.003$ above and below the blackbody locus (for CCT < 5000 K) or the daylight locus (for CCT ≥ 5000 K). According to this limitation and also because white points further away from the blackbody locus or daylight locus might contain visually disturbing tints (for example a greenish shade) [24, 40], $R_{p,2019}$ should not be applied to light source spectra with $\Delta u'v' \geq 0.003$.

The numerical predictions of $R_{p,2019}$ were compared with those of CP (see Eq. 1). Fig. 5 shows this comparison in the case of a set of 180 selected light source spectra. Latter set is a subset of 459 spectra including the 58 spectra used to derive the optimum parameter values in Table 2 [3, 32] plus the SPD library with 401 spectra of the R_f calculation tool made available in connection with the CIE publication [16]. The subset with 180 spectra was selected from the set of these 459 spectra in the following way:

1. Spectra with R_f < 70 were excluded (they are not relevant for interior lighting design);

2. Only the spectra in the validity range of $R_{p,2019}$ were used. This means that we considered only those spectra that exhibited CCTs between 3000 K and 5600 K and ΔC_t values between –0.4 and 1.2, the $R_{p,2019}$ and CP values were calculated at four illuminance levels, 200 lx, 500 lx, 1000 lx and 1800 lx, see Fig. 5.

As can be seen from Fig. 5, the relationship between the present $R_{p,2019}$ metric, see Eq. (3), and the previous *CP* metric [32], see Eq. (1), can be approximated by a linear function (R^2=0.71, see the caption of Fig. 5). As the underlying subjective colour preference datasets of both metrics were obtained using the same subjective rating scale (see Fig. 2), the absolute magnitudes of the two metrics can be compared. In tendency, the CP metric predicts about six units (see Fig. 2) lower colour preference values for the same light source spectrum at the same illuminance level. When the present $R_{p,2019}$ metric predicts "*good*" colour preference (79.6, see the caption of Fig. 2) in case of the sample illumination conditions of Fig. 5 then CP's prediction equals only 73.5 which can be considered as a "*good-moderate*" colour preference prediction.

The reasons for this absolute magnitude difference and also for the scatter of the data points are:

1. The CP metric is based just on the second dataset [32] while $R_{p,2019}$ also additionally incorporates the data of the first study [3] (see Section 2);

2. The two metrics are based on different colourimetric descriptor quantities and test colour sam-

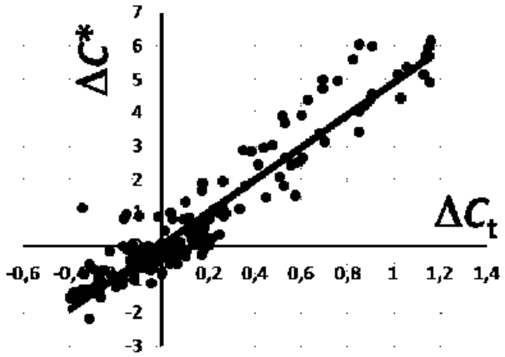

Fig.6. Comparison of two quantities used to describe the object saturating effect of the light source, ΔC_t (in case of $R_{p,2019}$, Eq. (3)) and ΔC^* (in case of CP, Eq. (1))
(Fit line: $\Delta C^* = 4.8645 \cdot \Delta C_t + 0.0434$ *(R^2=0.893))*

ples (CIELAB and 15 CQS test colour samples for the CP-metric vs. CAM02-UCS and the 16 hue bins of TM-30–15 for $R_{p,2019}$), which are applied to a broad range of different types of light source spectra in Fig. 5. To further elucidate this, it is interesting to compare the two quantities used to describe the object saturating effect of the light source, ΔC_t (in case of $R_{p,2019}$, Eq. (3)) and ΔC^* (in case of CP, Eq. (1)), see Fig. 6.

As can be seen from Fig. 6, differences in maximum about 0.7 ΔC_t units (even fluctuations between "*desaturating*" and "*saturating*") appear along the abscissa at the same value of ΔC^* at the ordinate. This might cause large differences in the predictions of colour preference if the two metrics are applied to an arbitrary light source. This finding corroborates the importance of the use of the TM-30–15 method and the CIE2017 colour fidelity index R_f [16] in lighting design.

For validation, the numerical predictions of $R_{p,2019}$ were compared with the mean subjective colour preference ratings resulting from selected previous studies satisfying the following criteria:

1. Using the same rating scale as in the present article (see Fig. 2);

2. Using multi-coloured arrangements of miscellaneous coloured objects (similar to Fig.1) and not only objects in a specific hue range (e.g. red);

3. Using light sources in the validity range of $R_{p,2019}$.

According to these criteria, we selected two previous studies [2,4]. In the first study (so-called "Part 1") [2], five light sources (phosphor-converted LED, compact fluorescent lamps and tungsten halogen lamps) were used at 470 lx (fixed) and CCTs between 2300 K and 4100 K. In the second study (so-called "Part 2") [4], seven multi-LED light sources were used at 3220 K (fixed) and 550 lx (fixed). Two light sources of the second study [4] that were out of the validity range of $R_{p,2019}$ (because of $\Delta u'v' \geq 0.003$) were excluded from this analysis. Fig.7 shows the result of this comparison.

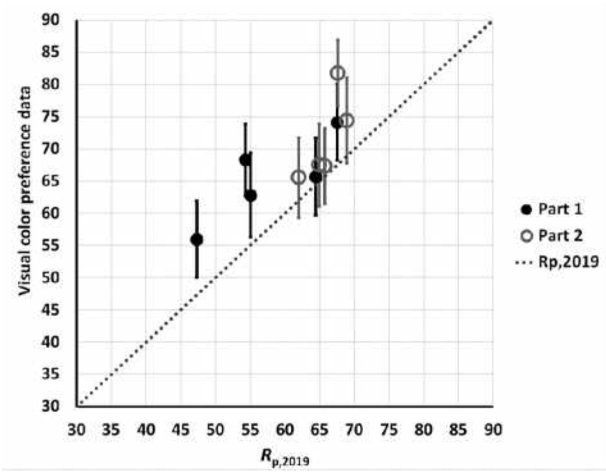

Fig.7. Comparison of the values of $R_{p,2019}$ with the mean subjective colour preference ratings (with 95 % confidence intervals representing inter-observer variability) resulting from two previous studies, "Part 1" [2] and "Part 2" [4]
(Two light sources were excluded from "Part 2" [4] because of $\Delta u'v' \geq 0.003$*)*

As can be seen from Fig. 7, $R_{p,2019}$ was able to predict the tendency of the mean subjective colour preference ratings. Pearson's correlation coefficient between $R_{p,2019}$ and these ten mean subjective colour preference ratings equalled r=0.78. The mean difference between the mean subjective colour preference ratings and the value of $R_{p,2019}$ equalled 7 units (STD: 4) on the rating scale of Fig. 2. This difference was significant in the case of five light sources, see those confidence intervals of the mean subjective ratings that do not overlap with the grey dot line of the $R_{p,2019}$ values in Fig.7. These differences did not cause a transition between two adjacent categories on the rating scale, e.g. "good" to "moderate", see Table 3.

It should be noted that the prediction of such subjective colour preference rating values that are *anchored* with categories (according to Fig.2) in the present article represents a different approach from other studies (e.g. [13, 33, 34]) that are based on the analysis of the *correlation* between a metric and a subjective rating value on an *arbitrary* scale. In the present article, we also analyse absolute differences on these anchored scales, and not only the

Table 3. Validation of the Numerical Predictions of $R_{p,2019}$ Based on the Mean Subjective Colour Preference Ratings from Two Previous Studies [2,4], *(See Also Fig. 7)*

	Interval scale (see Fig. 2)			Category (see Fig. 2)	
Study	**Subj. rating**	$R_{p,2019}$	**Difference**	**Subj. rating**	$R_{p,2019}$
“Part 1” [2]	68	54	14	good-moderate	moderate
“Part 1” [2]	63	55	8	moderate-good	moderate
“Part 1” [2]	66	64	1	moderate-good	moderate-good
“Part 1” [2]	74	68	7	good-moderate	good-moderate
“Part 1” [2]	56	47	9	moderate	moderate-poor
“Part 2” [4]	66	62	4	good-moderate	moderate-good
“Part 2” [4]	67	66	2	good-moderate	good-moderate
“Part 2” [4]	67	65	3	good-moderate	good-moderate
“Part 2” [4]	82	68	14	good	good-moderate
“Part 2” [4]	74	69	5	good-moderate	good-moderate

correlation, see Table 3. Possible reasons for these absolute differences include different observer panels, weather conditions, time of the day, time of the year. Another reason is viewing condition differences in “Part 2” [4] (in a viewing booth instead of a room) as well as the limited range of illuminance levels (470–550) lx without comparing them with higher illuminance levels in these two studies [2,4]. Therefore, further validating studies are necessary varying all three independent variables (illuminance, CCT, object saturation) systematically and with more data points in a real room.

4. APPLICATION OF $R_{P,2019}$ TO LIGHTING DESIGN

If the spectrum of a test light source to be applied in a lighting installation is known then the values of CCT, R_f, ΔC_t (Eq. (4)) can be computed. We can assume different illuminance levels at a “*working plane*” (for example a horizontal table surface in a room) on which coloured objects can be arranged. These coloured objects can be illuminated by the luminaire that contains the test light source. Fig. 8 shows the dependence of the value of $R_{p,2019}$ (Eqs. (3)-(5)) on illuminance level (E_v in lx) in case of four sample light sources of different type. Their spectra are shown in Fig. 9 while their CCT, R_f and ΔC_t values are listed in Table 4. Fig. 8 and Table 4 contain *criterion illuminance values* at which the value of $R_{p,2019}$ reaches the “*very good*” and “*good*” colour preference levels in case of the four different types of light source. Although the “*moderate*” level is rather irrelevant for lighting design, this level is also included in Fig. 8 for better understanding.

As can be seen from Fig. 8 and Table 4, it is not possible to reach neither the “*good*” nor the “*very good*” colour preference level by the aid of the 2nd spectrum (RGB LED) within the validity range of $R_{p,2019}$ (200–1800) lx. The reason is that this spectrum de-saturates the object colours (ΔC_t<0) and it has a lower R_f value (R_f =77). Just the opposite is true for the 1st spectrum (RGBW LED with R_f=90 and moderate object colour oversaturation,

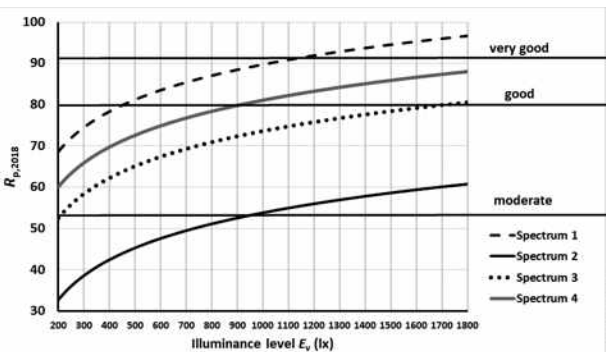

Fig. 8. Application of $R_{p,2019}$ to *interior lighting* design: dependence of $R_{p,2019}$ on illuminance (E_v in lx) for four sample light sources (see Fig. 9 and Table 4), where Table 4 contains the criterion illuminance values at which the value of $R_{p,2019}$ reaches the “*very good*”, “*good*” and “*moderate*” colour preference levels

Table 4. Application of $R_{p,2019}$ to Interior Lighting Design

*(Criterion illuminance values at which the value of $R_{p,2019}$ reaches the "very good" and "good" colour preference levels in case of the four different light source spectra (examples) shown in Fig. 8. *: it is not possible to reach the "good" category within the validity range of $R_{p,2019}$ (200–1800) lx)*

Spectrum					Criterion illuminance (lx) for the category	
No.	**Type**	R_f	CCT **(K)**	ΔC_t	**good** $R_{p,2019}$**=79.6**	**very good** $R_{p,2019}$**=91.6**
1	RGBW-LED	90	3993	0.61	440	1170
2	RGB-LED	77	3243	-0.34	*	*
3	RGBW-LED	88	4840	-0.17	1650	*
4	Fluorescent lamps	89	5091	0.05	890	*

ΔC_t=0.61): the "*good*" colour preference level can be reached at 440 lx while the "*very good*" level can be reached at 1170 lx if this light source is used to illuminate the coloured objects. Using the 3rd spectrum or the 4th spectrum, only the "*good*" level can be achieved at 1650 lx and 890 lx, respectively, according to their colorimetric properties.

Fig. 8 supports the procedure of ensuring high colour preference in lighting design. The luminaires containing a particular light source shall be designed (and later installed) in the room to provide at least the "*good*" criterion illuminance level at a working plane on which the coloured objects to be illuminated are arranged. After the design of the lighting installation, the electric power necessary to achieve this criterion illuminance level ($P_{el,\ crit}$) will be known and a measure of *electric efficiency for colour preference*, $\eta_{p,2019} = \frac{R_{p,2019,crit.}}{P_{el.,crit.}} = \frac{79.6}{P_{el.crit.}}$ (in W^{-1} units). These values can be calculated for every possible installation with different light sources. Thus, different theoretical lighting installations can be compared and the most efficient installation can be selected. A new metric of electric energy efficiency was published [41] recently but the latter metric was intended to characterize *light sources* and not lighting installations and it was not intended to predict colour preference.

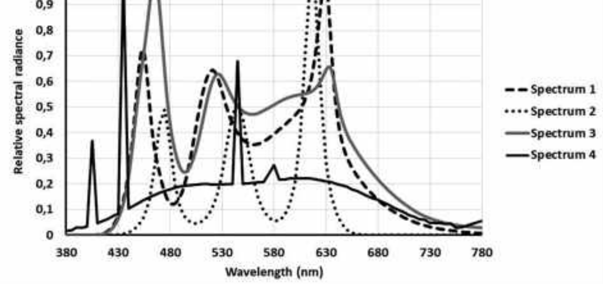

Fig. 9. Relative spectral radiance of the four samples of light sources in Fig. 8
1: RGBW-LED; 2: RGB-LED; 3: RGBW-LED; 4: Fluorescent lamp

Table 5 compares the colour preference levels to be obtained according to the $R_{p,2019}$ index at 500 lx and 1200 lx, respectively, in case of the four light source spectra in Fig. 9. As can be seen from Table 5, the colour preference level (predicted by $R_{p,2019}$) increases 10–11 points on the colour preference scale (Fig.2) if the illuminance level is increased from 500 lx to 1200 lx. This increment corresponds to a change between two categories in case of the 1st (good→very good) and 2nd (poor→moderate) light sources. For the 3rd and 4th light sources, such a full categorical shift does not occur.

It is also interesting to depict the dependence of the value of $R_{p,2019}$ on correlated colour temperature. Fig. 10 shows a computational example using Eqs. (3) and (5), independent of any specific light source spectrum, in case of R_f=84 and E_v=500 lx with different CCTs in the validity range (3000–5600) K and with different ΔC_t values as parameters. The following values were used: ΔC_t=1.2, 0.9435 (that maximizes the value of $R_{p,2019}$ in case of R_f=84 and E_v=500 lx), 0.8, 0.4, 0.0 and –0.4 (a de-saturating ΔC_t level).

As can be seen from Fig.10, according to the prediction of $R_{p,2019}$, the best colour preference takes place between 4500 K and 4800 K (neutral white – cool white) according to the tendencies of the un-

Table 5. Colour Preference Levels to be Obtained at 500 lx and 1200 lx in Case of the Four Light Source Spectra in Fig. 8 According to the $R_{p,2019}$ Index

Spectrum				E_v=500 lx	E_v=500 lx	E_v=1200 lx	E_v=1200 lx	500 lx →1200 lx
No.	R_f	CCT (K)	ΔC_t	$R_{p,2019}$	$R_{p,2019}$ Category	$R_{p,2019}$	$R_{p,2019}$ Category	$R_{p,2019}$
1	90	3993	0.61	81	good	92	very good	11
2	77	3243	-0.34	45	poor	56	moderate	11
3	88	4840	-0.17	65	moderate-good	76	good	11
4	89	5091	0.05	73	good-moderate	83	good	10

derlying experimental colour preference dataset. The magnitude of the absolute maxima of the $R_{p,2019}$(CCT) curves depends on the saturation level (ΔC_t). As $R_{p,2019}$ was constructed on the basis of artificial installations of coloured objects in an experimental room with white walls and white cloths (see Section 2), the CCT tendencies in Fig. 10 are expected to be valid to predict colour preference for different types of formal or official situations or working environments including offices, schools, exhibitions, conferences, lecture rooms, breakfast rooms in hotels or public vehicle interiors. For applications that require a more relaxing atmosphere (for example romantic evening events, dinners, creative mental activities), lighting installations with a lower CCT and a lower illuminance level might be more appropriate. In the latter case, colour preference should not be the (primary) aim of lighting design.

5. DISCUSSION

The new colour preference metric ($R_{p,2019}$) models the experimental finding that colour preference depends on CCT, object saturation and illuminance level. The metric has a built-in semantic interpretation of its numeric scale in terms of intuitive rating categories ("very good", "good", "moderate", see Fig.2). Criterion illuminance values can be derived to establish a "good" or "very good" colour preference level in case of a given lighting installation (see Fig. 8) except for spectra with poor colour rendition properties (for example the spectrum No. 2 in Fig. 9) that cannot reach the "good" colour preference level.

Besides the above advantageous properties, the new metric has the following limitations. The validity range of its input parameters is limited: the metric cannot be used for warm white spectra with CCTs less than 3000 K and for cool white light sources with CCT>5600 K. Its illuminance level dependence is also limited to the range of 200 lx to 1800 lx. This range covers, however, typical illuminance levels of today's general interior lighting practice.

Concerning saturation levels, light sources with ΔC_t >1.2 tend to over-saturate coloured objects and they generally obtain "moderate" or worse visual colour preference ratings. This should not be the aim of lighting design. In case of such higher saturation levels (ΔC_t >1.2), the value of the metric decreases rapidly. Accordingly, such light sources should not be applied in general interior lighting al-

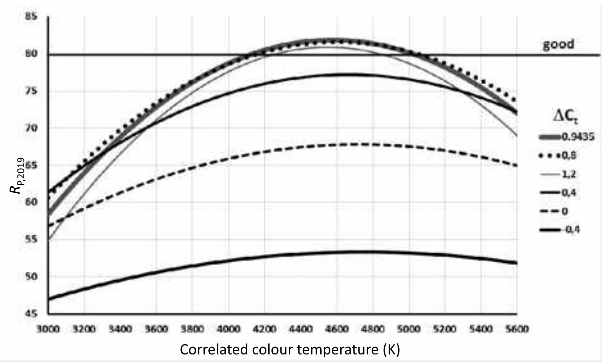

Fig.10. Dependence of the value of $R_{p,2019}$ on correlated colour temperature (CCT) in case of the fixed values R_f=84 and E_v=500 lx

(Computational example when Eqs. (3) and (5) with different ΔC_t values as parameters (see the legend) are using, and the absolute maximum of $R_{p,2019}$ occurs in case of ΔC_t = 0.9435, if R_f=84 and E_v=500 lx are fixed)

though they might have a special application including the lighting of theatre scenes for a strong emotional effect. A further limitation is the dependence of subjective colour preference ratings on lighting application [14], as already mentioned at the end of Section 4.

Experimental evidence suggests that the shape of the colour gamut (especially the red saturation component) influences the subjects' colour preference assessments [13, 19, 20] significantly. This red saturation factor was not included in the present $R_{p,2019}$ metric due to the limitations of the underlying subjective colour preference datasets [3, 32]: in their experimental method, the effect of CCT and illuminance was not combined with the change of *red* saturation level. This should be the task of a subsequent study. The red saturation effect is especially significant if dedicated spectra saturating red object colours are used (see the Colour Vector Graphic in Fig. 2 of [13]). The LIKE model (see Table 1) was developed to describe this effect. The LIKE model uses the parameters IES R_f [15], $R_{cs,\,h16}$ (as a proxy for red saturation; this quantity is also used in Eq. (4) of the present article as a component of the sum of all 16 $R_{cs,\,hi}$ values) and the parameter ψ (that represents the best-fit ellipse's rotation angle; this ellipse approximates the shape of the IES TM-30–15 Colour Vector Graphic).

Illuminating a scene of coloured objects, the *white tone* of the light source is usually also visible on white or neutral grey surfaces (walls, table cloths, window sills, curtains, furniture) and this white tone perception interacts with the impression of colour preference of the coloured objects. The CCT dependence of white tone perception (warm white, neutral white, cool white) and its interaction with colour preference is included in the CQS [35], CP (Eq. (1)) and $R_{p,2019}$ (Eqs. (3)-(5)) metrics. However, it was reported [25, 42, 43] that the distance of the white tone's chromaticity from the blackbody locus (expressed in terms of *Duv* or $\Delta u'v'$) also influenced colour preference. Chromaticities below the blackbody locus were generally preferred. The cause of this effect was identified by simulation [26]: "illuminants with chromaticity below the blackbody locus (that is, negative *Duv*) are more likely to have higher scores for relative gamut than illuminants on or above the blackbody locus while maintaining high scores for fidelity" [26]. This effect is not included in the new colour preference metric ($R_{p,2019}$) of the present article.

6. CONCLUSIONS AND OUTLOOK

Applying the scheme of Fig. 8 during the design of the lighting for an interior space, the colour preference vs. illuminance curves of different light source types (or different settings of a multi-LED light source) can be compared and the most energy efficient light source providing the "good" colour preference level can be selected. If only one light source is given then the *criterion illuminance value* can be computed for "good" colour preference depending on the number of luminaires (containing this light source) to be installed in the room and the height of the luminaires above the table on which the coloured objects shall be illuminated.

According to the viewing conditions of the experimental datasets underlying the new colour preference metric (a neutral environment with white walls, white tablecloths and miscellaneous coloured objects), the metric should be valid for different types of official, formal situations or working environments. For other applications including the lighting of living rooms or dining rooms in the evening and special collections of coloured objects (e.g. red makeup, blue jeans or important memory colours like banana or skin tone), a different colour preference metric should be applied.

According to Table 5, the typical interior illuminance level of 500 lx (the most common horizontal illuminance level required by the standard for general workplace illumination [44]) is often not enough to reach the "good" colour preference level. To do so, the illuminance level shall be increased either by allowing for daylight in the room or by increasing the electric energy consumption of the luminaires (if possible) in case of a demanding application (the related economic considerations are out of the scope of the present article).

A validation study using the same semantically labelled colour preference scale (see Fig. 2) is currently underway in a spacious experimental room with a multi-LED illumination system allowing for the variation of lighting parameters in a broader range than in the previous studies. The effect of all relevant variables, illuminance level, correlated colour temperature (from 2800 K up to 6500 K), and the white tone's chromaticity distance from the blackbody locus, object saturation level and red saturation are being varied. The aim is to validate and extend the framework of Eqs. (3)-(5) and re-optimize the model parameters of Table 2. The current value of the weighting factor 0.70 of the colour fidelity component (R_f) will also be fine-tuned.

REFERENCES

1. P. Bodrogi, S. Brückner, T.Q. Khanh, H. Winkler, Visual Assessment of Light Source Colour Quality// Colour Research and Application, 2013, Vol .38, pp. 4–13.

2. T.Q. Khanh, P. Bodrogi, Q.T. Vinh, D. Stojanovic, Colour preference, naturalness, vividness and colour quality metrics – Part 1: Experiments in a real room// Lighting Research and Technology, 2016, Vol .49, pp. 697–713.

3. T.Q. Khanh, P. Bodrogi, Q.T. Vinh, X. Guo, T.T. Anh, "Colour preference, naturalness, vividness and colour quality metrics, Part 4: Experiments with still life arrangements at different correlated colour temperatures// Lighting Research and Technology, 2017, Vol .50, pp. 862–879.

4. T.Q. Khanh, P. Bodrogi, Q.T. Vinh, D. Stojanovic, Colour preference, naturalness, vividness and colour quality metrics, Part 2: Experiments in a viewing booth and analysis of the combined dataset // Lighting Research and Technology, 2017, Vol .49, pp. 714–726.

5. T.Q. Khanh, P. Bodrogi, X. Guo, Q.T. Vinh, S. Fischer, Colour preference, naturalness, vividness and colour quality metrics, Part 5: A colour preference experiment at 2000 lx in a real room // Lighting Research and Technology; first published online 20 October; DOI 10.1177/1477153517737133, 2017.

6. S. Jost-Boissard, P. Avouac, P. Fontoynont, Assessing the colour quality of LED sources: Naturalness, attractiveness, colourfulness and colour difference // Lighting Res. Technol, 2015, Vol .47, pp. 769–794.

7. D. Durmus, W. Davis, Object colour naturalness and attractiveness with spectrally optimized illumination // Optics Express, 2017, Vol .25, pp. 12839–12850.

8. Y. Lin, J. He, A. Tsukitani, H. Noguchi, Colour quality evaluation of natural objects based on the Feeling of Contrast Index // Lighting Research and Technology, 2016, Vol .48, pp. 323–339.

9. K. A.G. Smet, P. Hanselaer, Memory and preferred colours and the colour rendition of white light sources // Lighting Research and Technology, 2016, Vol .48, pp.393–411.

10. P.R. Boyce, C. Cuttle, Effect of correlated colour temperature on the perception of interiors and colour discrimination performance // Lighting Research and Technology, 1990, Vol .22, pp. 19–36.

11. L. Xu, M.R. Luo, M. Pointer, The development of a colour discrimination index // Lighting Research and Technology, 2018, Vol .50, pp. 681–700.

12. T. Esposito, K. Houser, A new measure of colour discrimination for LEDs and other light sources // Lighting Research and Technology, 2019, Vol .51, pp. 5–23.

13. T. Esposito, K. Houser, Models of colour quality over a wide range of spectral power distributions // Lighting Research and Technology; first published online on April 13; DOI 10.1177/1477153518765953, 2018.

14. Y. Lin, M. Wei, K. A. G Smet, A. Tsukitani, P. Bodrogi, T.Q. Khanh, Colour preference varies with lighting application," Lighting Research and Technology, 2015, Vol .49, pp. 316–332.

15. IES (Illuminating Engineering Society), IES method for evaluating light source colour rendition // IES TM-30–15, 2015.

16. CIE (Commission Internationale de l'Éclairage), CIE2017 Colour Fidelity Index for accurate scientific use // CIE Publication 224:2017, 2017.

17. M.S. Islam, R. Dangol, M. Hyvärinen, P. Bhusal, M. Puolakka, L. Halonen, User preferences for LED lighting in terms of light spectrum // Lighting Research and Technology, 2013, Vol .45, pp. 641–665.

18. R. Dangol, M.S. Islam, M. Hyvärinen, P. Bhushal, M. Puolakka, L. Halonen, User acceptance studies for LED office lighting: Preference, naturalness and colourfulness // Lighting Research and Technology, 2015, Vol .47, pp. 36–53.

19. M. Wei, K.W. Houser, A. David, M.R. Krames, Colour gamut size and shape influence colour preference// Lighting Research and Technology, 2017, Vol .49, pp. 992–1014.

20. M.P. Royer, A. Wilkerson, M. Wei, K. Houser, R. Davis, Human perceptions of colour rendition vary with average fidelity, average gamut, and gamut shape // Lighting Research and Technology, 2017, Vol .49, pp. 966–991.

21. M.P. Royer, A. Wilkerson, M. Wei, Human perceptions of colour rendition at different chromaticities // Lighting Research and Technology, 2018, Vol .50, pp. 965–994.

22. Z. Huang, Q. Liu, S. Westland, M.R. Pointer, M.R. Luo, K. Xiao, Light dominates colour preference when correlated colour temperature differs // Lighting Research and Technology, 2018, Vol .50, pp. 995–1012.

23. H. Li, M.R. Luo, X.Y. Liu, B.Y. Wang, H.Y. Liu, Evaluation of colour appearance in a real lit room // Lighting Research and Technology, 2016, Vol .48, pp. 412–432.

24. P. Bodrogi, X. Guo, D. Stojanovic, S. Fischer, T.Q. Khanh, Observer preference for perceived illumi-

nation chromaticity // Colour Research and Application, Early View, 2018.

25. Y. Wang, M. Wei, Preference among light sources with different Duv but similar colour rendition: A pilot study // Lighting Research and Technology, 2018, Vol .50, pp. 1013–1023.

26. M. Wei, K.W. Houser, What Is the Cause of Apparent Preference for Sources with Chromaticity below the Blackbody Locus? // LEUKOS, 2016, Vol .12, pp. 95–99.

27. M. Wei, W. Bao, H.P. Huang, Consideration of Light Level in Specifying Light Source Colour Rendition // LEUKOS, published online on 11 May; DOI 10.1080/15502724.2018.1448992, 2018.

28. M. Wei, Maintaining Colour Preference under Different Light Levels, // presented at the 15th China International Forum on Solid State Lighting, Shenzhen, China, 23–25 Oct. 2018.

29. T.Q. Khanh, P. Bodrogi, X. Guo, P.Q. Anh PhD, Towards a user preference model for interior lighting Part 2: Experimental results and modelling // Lighting Research and Technology; published online on December 13; DOI 10.1177/1477153518816474, 2018.

30. H.W. Bodmann, G. Sollner, E. Voit, Evaluation of lighting level with various kinds of light // in: Proceedings of the CIE19th Session (CIE, 1963).

31. H.W. Bodmann, Quality of interior lighting based on luminance // Transactions of the Illuminating Engineering Society, 1967, Vol .32, pp. 22–40.

32. T.Q. Khanh, P. Bodrogi, X. Guo, P.Q. Anh PhD, Towards a user preference model for interior lighting Part 1: Concept of the user preference model and experimental method," Lighting Research and Technology; published online on December 13; DOI 10.1177/1477153518816469 (2018).

33. K. Smet, W.R. Ryckaert, M.R. Pointer, G. Deconinck, P. Hanselaer, Correlation between colour quality metric predictions and visual appreciation of light sources // Optics Express, 2011, Vol .19, pp. 8151–8166.

34. K.W. Houser, M. Wei, A. David, M.R. Krames, X.S. Shen, Review of measures for light-source colour rendition and considerations for a two-measure system for characterizing colour rendition // Optics Express, 2013, Vol .21, pp. 10393–10411.

35. W. Davis, Y. Ohno, Colour quality scale // Optical Engineering, 2010, Vol .49, pp. 033602.

36. A. David, P.T. Fini, K.W. Houser, L. Whitehead, Development of the IES method for evaluating the colour rendition of light sources // Optics Express, 2015, Vol .23, pp. 15888–15906.

37. F. Ebner, M.D. Fairchild, Development and testing of a colour space (IPT) with improved hue uniformity // in: Proceedings of the IS&T 6th Colour Imaging Conference, 1998.

38. S.A. Fotios, G.J. Levermore, Chromatic effect on apparent brightness in interior spaces, II: SWS lumens model // Lighting Research and Technology, 1998, Vol .30, pp.103–106.

39. P. Bodrogi, S. Brückner, N. Krause, T.Q. Khanh, Semantic interpretation of colour differences and colour-rendering indices // Colour Research and Application, 2014, Vol .39, pp. 252–262.

40. M.S. Rea, J.P. Freyssinier, White lighting // Colour Research and Application, 2013, Vol .38, pp. 82–92.

41. Q.T. Vinh, P. Bodrogi, T.Q. Khanh, Preliminary measure for the characterization of the usefulness of light sources // Optics Express, 2018, Vol .26, pp. 14538–14551.

42. E.E. Dikel, G.J. Burns, J.A. Veitch, S. Mancini, G.R. Newsham, Preferred chromaticity of colour-tunable LED lighting // LEUKOS, 2014, Vol .10, pp. 101–115.

43. Y. Ohno, M. Fein, Vision experiment on acceptable and preferred white light chromaticity for lighting // in: Proceedings of CIE2014 Lighting Quality and Energy Efficiency, CIE, 2014.

44. DIN (German Industry Standard), DIN EN12464–1, Lighting of work places – Part 1: Indoor work places, DIN, 2011.

Quang Trinh Vinh,
Ph.D. He deals with lighting engineering issues of solid-state lighting and automation processing. He obtained his M. Sc. degree at the Hanoi University of Mining and Geology. He received his Ph.D. degree on LED modelling, LED optimization, LED colour mixing and LED phosphor mixing as well as hybrid LEDs at the Technische Universität Darmstadt in Darmstadt, Germany. Currently, he is a research fellow at the Technische Universität Darmstadt

Tran Quoc Khanh,
Prof., Ph.D. He studied from 1980 to 1985 machine engineering and technical optics before he finished his Ph.D. thesis on the spectroscopy of UV–VIS radiation sources in 1989. Between 1990–1997 and 1997–1999, he was laboratory leader and project manager for photometry, radiometry and colorimetry at PRC Krochmann and Gigahertz Optik. Between 2000 and 2006, he was technical manager for optical imaging systems at ARRI, developed a digital CMOS camera, a film scanner and a laser recorder and optimized colour image processing for cinematography and TV signal processing. In 2005, he completed his Lecture Qualified Thesis (habilitation) on colour appearance and visual performance and started his current work as a Professor for lighting technology and solid-state lighting at the Technische Universität Darmstadt. He is conducting research and development projects on LED lighting technology. He is also the Chairman of the International Symposium for Automotive Lighting (ISAL). He is the author of several books and scientific articles and inventor of patents on lighting technology and related subjects. He is currently Dean of the Department of Electrical Engineering and Information Technology at the Technische Universität Darmstadt

Tran Thuy Anh,
Ph.D. Currently, she is an Associate Professor at the Vietnam National University in Hanoi. She obtained her Ph.D. from Vietnam National Institute of Culture and Arts Studies. She is an expert in conducting empirical research, textual analysis, as well as content analysis. Her research interests consist of various culture-related issues, including techno-culture and consumption behaviour

Peter Bodrogi,
Ph.D., studied physics at the Lorand Eotvos University in Budapest, Hungary. He obtained his Ph.D. degree from the University of Pannonia in Veszprém, Hungary and his lecture qualification thesis (habilitation) from the Technische Universität Darmstadt in Darmstadt, Germany. He is a research fellow at the Technische Universität Darmstadt. His research interests concern lighting engineering, mesopic (twilight) lighting, colorimetry, colour science, visual optimisation of displays and LED lighting systems

Light & Engineering
Vol. 27, No. 6, pp. 142–148, 2019 https://doi.org/10.33383/2019–059

NAVIGATION SYSTEM BASED ON VLC TECHNOLOGY FOR STAFF OF HERMITAGE MUSEUM

Emil Z. Gareev, Yuri B. Sorokin, Igor M. Antropov, Anton E. Kurako, Antonina A. Puchkovskaya, and Vladislav E. Bougrov

ITMO University, Saint Petersburg
E-mail: gareev.e@itmo.ru

ABSTRACT

We developed a navigation system based on wireless visible light data transmission channel and an algorithm for the decoding on smart-phones. The work aims to create an interactive navigation system inside the Hermitage Museum for museum staff. The system was designed for using a modern smart-phone device as a receiver, a conventional LED illuminator as transmitter and a RGB diode as a navigation point in each room of the museum. We developed a modulator for data transmission, an algorithm for receiving and processing information using a stock camera of an iOS-based smart-phone, organized a point-to-point network between the LED illuminators and the server with a full back-end and front-end communication. The system allows transmitting data with rates up to 2 kbps on distance up to 1 meter.

Keywords: navigation system, visible light transmission channels, VLC, RGB diodes, LED illuminator, luminous flux modulation

1. INTRODUCTION

In recent years, technologies that allow us to combine advanced functionality in conventional things have started emerging [1]. This trend has not bypassed the LED systems, an important task of which became the wireless communication through modulation luminous flux. Thus, VLC technology arose, using LED as an optical signal transmitter and a photo detector as a receiver [1]. The main signal transmission principle by such a system is based on the light emission modulation with a frequency of the order of several kHz and higher. The human eye is not able to perceive the frequency of flicker above 100 Hz, which allows you to make a data transfer using VLC technology imperceptible to a user. A conventional modulation of LED illumination On-Off Keying is based on changes of luminous flux intensity. Using a mobile device as a receiver in such data transmission systems allows you to make any information accessible to a large number of users, due to the absence of the need to have a special separate client module acting as a receiver, however, a mobile camera module shooting frame rate is often limited to (120–240) Hz, due to the lack of a camera matrix possession ability, which makes it necessary to apply special processing methods of shots. The target of this work was to develop the navigation system based on the LED illumination and VLC technology, and also create an algorithm allows using the maximum of channel capacity by special methods of working with camera frames.

2. SYSTEM DESCRIPTION

To demonstrate the work, a system was created consisting of an *Arduino* microcontroller with two LED modules: white phosphors LEDs and RGB LED. Whole work assumes that the Hermitage museum will have hundreds of similar *IoT* devices that are navigation gateways, so the server side should be capable of communicating with all the devices with low latency. This system has two main tasks:

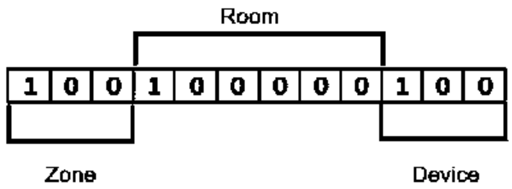

Fig.1. System number example

• Continuously send a message about its number using white diodes to smart-hone camera;

• Change the colour of the RGB diode to represent the path for user.

The system contains hundreds of devices with high frequency requests; it is possible to communicate with all the devices via one hub. Architecture consists of one hub and a number of gateways, where the hub operates the state of the navigation system and sends commands to gateways, which change their status for LED modules according to the proper path. In order to achieve maximum transmission capacity of the system, it needs secured local Wi-Fi connection, so all the devices will be located in one local network, at least, major part of the devices, and this can be achieved by using Wi-Fi boost adapters. Second, we should use optimized connection so that we could minimize overhead of transportation. We used UDP protocol as a transport layer for communication between the gateways and the hub, and compact byte data format. Each device of the system has its own number (Fig. 1). The number consists of three parts. 3 bits – zone number, 6 bits – room number, 3 bits – device number in the room.

System topology assumes that chances for package lost for most of the devices that are in local network are minimal and for the devices outside the local network in case of package drop we implement our own protocol handshake mechanism. Each gateway responses to a hub message, so in case of package drop, the hub that controls the state of the system makes additional attempts to contact with lost gateway. In case the gateway is dead, user who gets the directions is notified of a dead gateway in specific room on his path. All the mentioned above mechanisms make the system robust. In case of bigger scale, it is easy to make special services that read response messages from Kafka and synchronize the state of the navigation through Redis, in such case system can be scalable as any other micro-service architecture system and reliable even in high workloads with bigger scale.

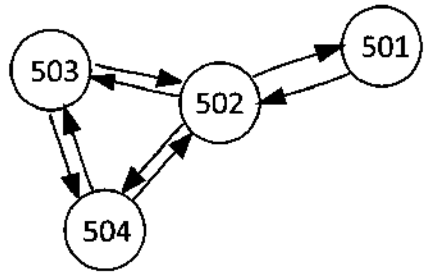

Fig.2. Example of maps of four connected rooms as a direct graph

The system always controls the whole state where each user path is mapped by colour so such structure will allow multiple search algorithm optimizations.

The system uses simple http protocol for communicating with smart-phone. Such approach allows a better and faster integration of system in third party clients and systems due to low entry threshold for http technology. In future hub will be rewritten in reactive stack for much more performance.

The whole map of the rooms are represented as direct graphs, so searching in such a data structure is not as simple as just in a simple graph (shown in Fig. 2).

The complete high-level navigation pipeline consists of several steps:

1. User scans nearby the gateway with its smartphone camera;
2. User prompts the destination room;
3. Hub receives data from user;
4. Hub calculates optimum and free route;
5. Hub notifies those gateways that are on the route and remembers their association with specific user;
6. Hub waits for responses from the gateways;
7. Hub retries N times for gateways that didn't respond in time.

Hub software was developed using Java language and can be used on multiple platforms not only x86 and ARM64, but also embedded devices with or without AOT compilation. Library has minimum third party dependencies and implements most of the functional using standard JDK library and API.

A smart-phone with a camera is an essential part for the system. It's a powerful and easy-to-use tool that connects sensors and the server and able to provide visual interface for user. The smart-phone has its own working algorithm that consists of following steps:

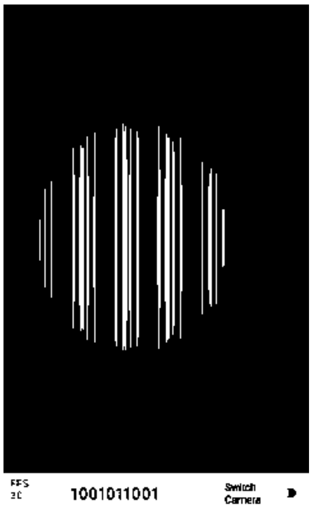

Fig. 3. Stripes

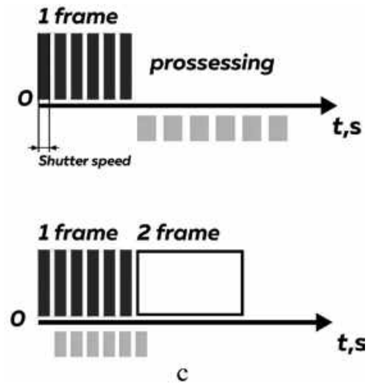

Fig.4. Classical sequential (top diagram) and developed parallel (bottom diagram) algorithm with the rolling shutter effect implementation, where black lines are the group of camera module matrix rows that were exposed sequentially, according to the rolling shutter effect, and grey lines depict the time periods needed to process each of the matrix rows group

1. Setup the camera;
2. Read the signal, represented in bytes;
3. Decode the bytes sequence and convert it to the location;
4. Make server request with decoded location;
5. Display the path and additional information that comes from the server.

All the steps except the first one are made by software and can be implements on any phone. The first step, though, requires the smart-phone to work on the operation system that provides an interface to work with camera settings: exposure and ISO. Two most popular mobile platforms iOS and Android both satisfy the requirement. Due to efficiency and simplicity of the camera interface we have chosen iOS platform. All devices with iOS version are older than 4.0 have an ability to configure camera and capture visual frames with certain resolution.

As it was already mentioned, the first step is to setup the camera configuration in a way that allows us to see the black-white strips on the frames (Fig. 3). iOS platform allows us to change the exposure value between 1/2 and 1/1000000 and change ISO value between 29 and 464. After some experiments the ideal values occurred to be max possible ISO value and 1/6000 exposure value. With this configuration everything is ready to start capturing the frames. Every visual frame is a two-dimensional matrix with pixels as elements. The size of the matrix depends on the camera resolution of the certain device. The average size is around 1920x1080 pixels. Every pixel can be represented in different ways. For our purposes the image shouldn't be coloured, because bytes data can be represented as only white and black stripes. So, we have chosen *YCbCr* format in which every pixel consists of three components: luma component(*Y*) and two chroma components (*Cb* and *Cr*). The *Y* image is essentially a gray scale image of the main image.

We created an algorithm that uses the "rolling shutter" effect. This effect is described in detail by N. Rajagopal et al. in [2]. The developed algorithm allowed us to process data at speeds up to 2 kbps with 5frames/sec shooting. The algorithm makes possible to minimize the loss of transmitted information. The Fig. 4 illustrated the main principal of rolling shutter effect and the implementation of this effect into developed algorithm.

When the session of the camera is started, the sequence of frames with the frequency of current exposure asynchronously comes for analysis. Each frame has three buffers, one for each component. First buffer contains *Y* image, so iterating through it gives the values for further decoding.

Even though only luma image is used, a lot of interference can cause the problems for results. Sensors emit consistent signal, which should be identical for the whole column of the frame. Finding the average luma value for each column reduces the amount of interference.

Luma value for each pixel is 1 byte that means that it can be any number between 0 and 255, so as 0 is black (dark) and 255 is white (bright). After averaging the column values, the array of the reliable values is got and it's saved to the FIFO buffer with arbitrary size. Bigger size of the buffer gives more accuracy but increases the amount of decoding time. When the buffer gets full, the analyzing

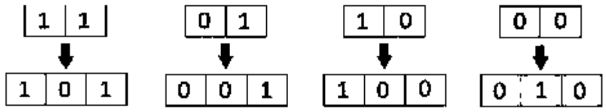

Fig. 5. Example of encoding

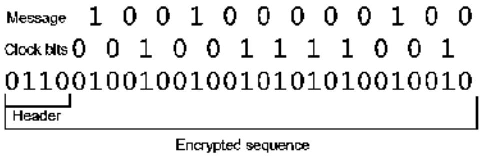

Fig.6. Full encoding example

is proceeded for every element. If all the elements transform into the same result it's sent to the server, otherwise the buffer cleans up, and cycles repeat. This sequence is another measure of correctness of the result.

3. RESULTS & DISCUSSION

Decoding at the smart-phone part is located at the sensor of camera. In order to get this value, the array of bytes goes through several steps:

1. Calculate border between 0 and 1;
2. Calculate min width of 0 and 1;
3. Iterate through sequence of widths, comparing current width with min width;
4. Decode location.

Even though the interference is reduced multiple times, the luma values are not perfect yet. Depending on the light, the range of the luma values is not always [0, 255], it can be shorter. To execute further calculations correctly, at first, the max and min value of current luma range is found, and the average value of these two is set as 0 and 1 border. It is used in next calculations for determining whether current luma value stands for 0 or 1.

The sensor emits a sequence of bits, which represents his location. This sequence can contain long sub-sequences of 0 or 1. The longer these sub-sequences are the higher change of false decoding is. In order to calculate the number of same bits in sub-sequence, firstly, the min width is calculated. Iterating through the array and comparing the current value with border value the array of widths is calculated. After that the min width values for both 1 and 0 are got. In some edge case, there is a chance that there is no single 0 or 1 in the sequence. For these reasons sensors always emit key sequence 0101, which always helps to determine single 0 and 1 width. After all the necessary values are got – the array of widths and min widths, it is easy to calculate the final bit sequence, just comparing current width with the min width at the same number (0 or 1).

The last step of the decoding process is to calculate the location. Location is represented by ids of the sensor and consists of different parts as shown above. Each part determines the zone, the room and the device (door where sensor is set). After converting the result sequence of 0 and 1 into decimal numbers the decoding process is complete.

At the device part a zero is encoded as 10 if preceded by a zero, and 00 if preceded by a one; a one is always encoded as 01 (Fig. 5). This allows we can avoid the case of two 1 bits following each other. We decided to use a header 0110, to uniquely identify the beginning of the message. Also this can help to count the width of columns.

Final encoded message is shown in Fig. 6. For correct representation of the path, the system contacts the server using the UDP protocol. When receiving the new path command from the server, system adds it to the list. The colour change of the RGB LED occurs according to the list of paths and colours. When receiving the finish command, the system removes the path from the list.

The whole logic of path between rooms is performed by the server. In order to provide it necessary data (which is start and destination point) the network request is performed. Using ordinary http request with data in body parameters the data is provided to the server. As soon as the server responds with the path it is displayed on the screen. The path is represented by sequence of rooms and the colour, which is unique and only assigned to this path.

Search algorithm at the server part plays important role in such a system because it essentially is the most complex computation activity that is presented over the whole application. The more efficient this part can be, the more responsive whole pipeline can be.

Core algorithm for path search we are using is Dijkstra algorithm. This is one of the classical algorithms for finding the shortest route in graphs. As our system uses direct graph for map, such algorithm is also working with this data structure. As our search algorithm should not just find the shortest path, but also a free path (where one LED colour is not occupied by other route), each node in directed graph also contains a set of occupied colours.

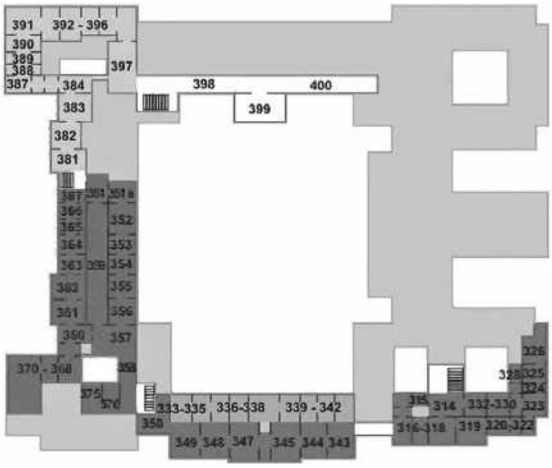

Fig.7. Visualized map split into four sectors

Fundamental principle of such an algorithm is that it literally searches through all possible routes to find the shortest one. This is not quite acceptable in our situation due to performance issues. We managed to optimize such an algorithm and visualization of such a map with an assumption that our map consists of rooms. We can split it in sectors, where each sector is minimized by its enter sectors (rooms that correlate with rooms from another sector), it means that rule to split map in sectors is that each sector should have minimum rooms that collide with other sectors and the size of the sector is reusable by other potential sectors. Such work is processed by humans as for now, but could be delegated by introducing special algorithm for dynamic sector mapping.

Such an approach with sectors allows us to remember shortest paths from boarder rooms from one sector to another, so in future we can just jump through sectors as after first full Dijkstra algorithm scan we remember the shortest jump routes from one sector to another. This mechanism can be applied on bigger scale for different map sizes that are direct graphs. Such algorithm allows us gain significant performance boost and make Hub even reliable and responsive as a part of such architecture.

Visualization represents four sectors with a number of Hermitage museum rooms, where each sector is grouped by its geographic location (Fig. 7). With such sectored map, it will be possible to easily jump through red sector when the route is from any of the rooms from purple sector to yellow sector. This can be done after first full calculation of all routes using standard Dijkstra's algorithm, after that algorithm will remember jump paths through red sector and next calculation will take a lot less time.

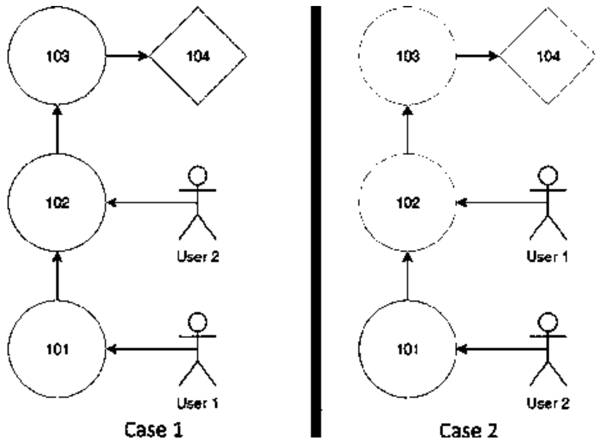

Fig.8. Route optimization strategies

Implemented search algorithm also allows optimization for already initiated routes. Two strategies can be applied for route optimization (Fig. 8). In first case, if User 1 calculates route and such route is assigned to blue colour. Then every other user that is building route from every room on such route will be assigned to same blue colour. So technically route will be shared for all users who have same destination and their start room is presented on such route.

In second case, User 1 calculates a route and gets orange colour assigned. Then User 2 wants to calculate route from room 101 but his destination room is the same as User's 1. In this case, first route can be expanded backwards up to room 101 and then assigned to User 2. However, in some cases User 2 can be assigned with another colour and when he reaches room 102, it's notified that his path colour has been switched up to yellow colour.

Such a mechanism allows reusing routes and expanding them if necessary. Also in some cases when there are many users it is essential to minimize colours so gateways will have as few colours as possible and their switch timeframe will be minimal. For those purposes, users can have multiple colours on their route to ensure that switch timeframes will be minimal and maximum amount of routes will be reused and linked together for different type of users. However, there should be a threshold for such a case, so there should be maximum 3–4 colour switches during the route in order to have an appropriate user experience, but it also depends on what scale system is operating.

As it was already mentioned, UDP is used for protocol for communication between hub and gateway. First reason for UDP protocol as mentioned above is the ability to minimize protocol mecha-

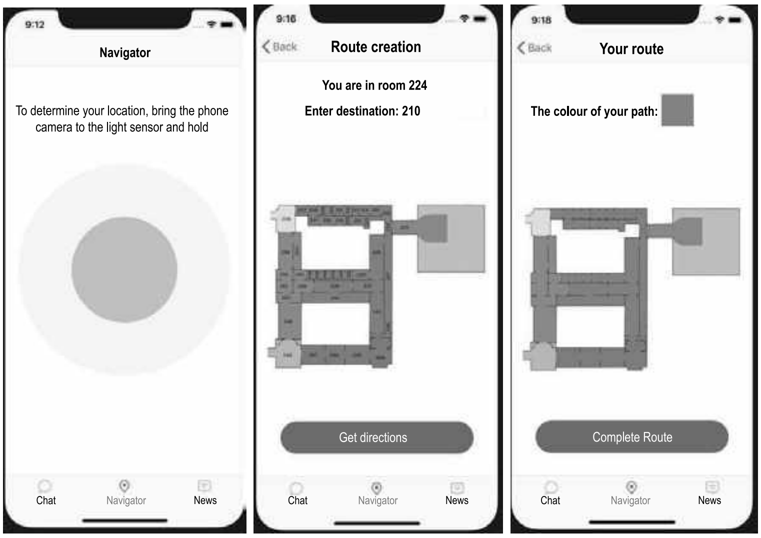

Fig. 9. iOS application

nisms for handshake or another communication between clients during package sending. UDP allows making simple things as package sends without any guarantees of receiving from protocol but with minimal package size and transfer speed. System protocol utilizes UDP broadcast technology that allows broadcasting package through whole network for better and faster data propagation. All those criteria are essential for *IoT* devices and whole system responsiveness itself.

Custom implementation for receiving handshake mechanism allows us to perform a more precise control over the way how gateway and hub communicate with each other and to ensure that workflow of the whole navigation process can be controlled from hub by developers. Also implementing custom handshake mechanism allowed us to minimize latency in comparison with TCP protocol.

UDP protocol allows us to utilize wireless connection at its maximum by just sending only valuable payload with minimum latency. In addition, other protocols such as TCP require much more resources, what may be unacceptable for *IoT* devices. Such protocol implementation allows us to use cheap hardware and perform most of calculation and business logic on the hub side.

Package that contains commands for the gateway is compact as it can be; it contains only route id and colour for that route. All those communication mechanisms and optimization on protocol levels as a package compression allows minimizing costs for implementing and supporting such system, which is crucial for business on initial phrase when the question of considering technology integration is opened.

4. CONCLUSION

In this work we demonstrated the data transmission via LEDs and mobile device camera and developed the processing algorithm for camera capable to decode signals with modulation frequency up to 2 kHz with the MFM algorithm with modifications OOK. Also we developed iOS application: screenshots shown in Fig 9.

This system can be used at the Hermitage museum for staff navigation. The colour of RGB diode will give intuitive path for each museum worker (smart-phone user). An exemplary view of the indoor system is shown in Fig. 10.

The future plan is the increasing of data transmission speed due to the introduction of special correction factors in the data processing algorithm, which makes camera solve long sequences better. Also the system has multiple extension points as well as optimization ones. The first system topology can be restructured using ZigBee protocol. Such

Fig.10. Application indoor example

a protocol could ensure that system stability will not depend on single point of failure as a local network with Wi-Fi router. ZigBee also introduces such a concept as coordinator but the whole topology is a communication between each other without using single channel such as Wi-Fi. In addition, the technology has far less energy consumption, which is also critical for IoT devices. So, there is no need of infrastructure setup for such a system, only the gateways should be installed. However, modules with such a technology cost more than any other hardware, so the system's price will be quite higher. This is an option and it depends on business requirements over all.

Reactive stack for http hub communication is for better performance. In addition, architecture can be expanded with facade services that reroute http requests to hub and play role of balancers to ensure hub stability and expect system failures in case of DDoS attacks.

ACKNOWLEDGEMENTS

This work was supported by the Ministry of Science and Higher Education of the Russian Federation in the framework of the Federal Target Program "Research and development on priority directions of scientific-technological complex of Russia for 2014–2020", the code 2017–14–582–0001, agreement № 14.581.21.0029 of October 23, 2017, unique ID RFMEFI58117X0029.

REFERENCES

1. Haas H, Yin L, Wang Y, and Chen C2016 What is Li-Fi? *J. of Lightw. Tech.* 34, 1544.
2. Rajagopal N, Lazik P and Rowe A 2014 *Visual Light Landmarks for Mobile Devices* (IPSN-14 Proceedings of the 13th International Symposium on Information Processing in Sensor Networks).

Emil Z. Gareev, graduated from the ITMO University magistracy in 2016. At present, he is post graduate student of the Laser Photonics and Optoelectronics Faculty, ITMO University

Anton E. Kurako graduated from the bachelor program of the Computer Engineering Department of ITMO University In 2018 and up to now he is continuing his studies in the magistracy, ITMO University

Igor M. Antropov graduated from the bachelor program of the Mathematics and Mechanics Faculty of the Saint Petersburg State University in 2018. At present, he is the Master student at ITMO University

Yuri B. Sorokin graduated from the Faculty of Software Engineering and Computer Engineering of ITMO University in 2018. At present, he continues his studies in the ITMO University magistracy

Antonina A. Puchkovskaya, Ph.D. in Cultural Science, she was a post graduate student at the Institute of Philosophy of Saint Petersburg State University in 2012. At present, she is a Head of the International Laboratory for Digital Humanities Research at ITMO University

Vladislav E. Bougrov, Associate Professor, Doctor of Phys.-Math. Sciences. In 1996, he graduated from the Department of Optoelectronics of the Saint Petersburg State Electrotechnical University named after V.I. Ulyanov (Lenin). At present, he is Director of the mega-faculty of Photonics, Professor at the Faculty of Laser Photonics and Optoelectronics at ITMO University

CONTENTS

VOLUME 27 NUMBER 1 2019

LIGHT & ENGINEERING
(SVETOTEKHNIKA)

CONTENTS

VOLUME 27 NUMBER 2 2019

LIGHT & ENGINEERING
(SVETOTEKHNIKA)

CONTENTS

VOLUME 27 NUMBER 3 2019

LIGHT & ENGINEERING
(SVETOTEKHNIKA)

CONTENTS

VOLUME 27 NUMBER 4 2019

LIGHT & ENGINEERING

CONTENTS

VOLUME 27 NUMBER 5 2019

LIGHT & ENGINEERING

PARTNERS OF LIGHT & ENGINEERING JOURNAL

Editorial Board with big gratitude would like to inform international lighting community about the Journal Partners Institute establishment. The list with our partners and their Logo see below. The description of partner's collaboration you can found at journal site *www.sveto-tekhnika.ru*

Dear authors, co-authors and readers!

Congratulations on the upcoming New Year 2020!

We wish you and our issue as many interesting and versatile publications as possible in such a multifaceted field of knowledge as LIGHT and LIGHTING!

Health and success to you and your loved ones!

Editorial Board of the Journal